Planar polarization of a mono-ciliated epithelium : the zebrafish floor-plate

Antoine Donati

Sorbonne Université
Ecole doctorale Complexité du vivant
Laboratoire de Biologie du Développement

Planar polarization of a mono-ciliated epithelium: the Zebrafish floor-plate

Antoine DONATI

Thèse de doctorat de Biologie du Développement

Dirigée par Christine VESQUE

Présentée et soutenue publiquement le 05 juillet 2019

Devant un jury composé de :

Dr Christine VESQUE	Chargée de Recherche	Directrice de thèse
Dr Hitoyoshi YASUO	Directeur de Recherche	Examinateur
Dr Patrick BLADER	Directeur de Recherche	Examinateur
Dr Nicolas DAVID	Chargé de Recherche	Rapporteur
Dr Juliette AZIMZADEH	Chargée de Recherche	Rapporteur
Dr Sylvie SCHNEIDER-MAUNOURY	Directrice de Recherche	Examinateur
Dr Tsuyoshi MOMOSE	Chargé de Recherche	Invité

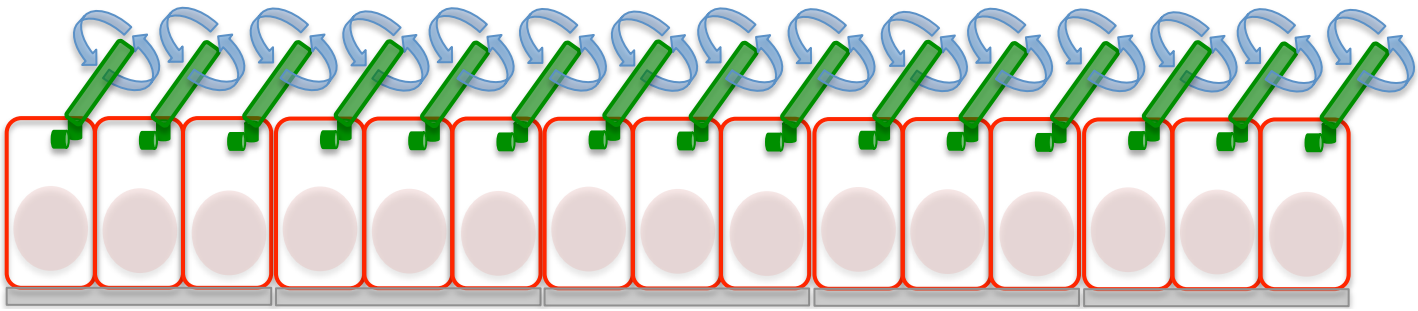

'Polarity is in my mind the essential problem. We have to explain why one part of a cell becomes different from another part.'

Sydney Brenner (1994)

REMERCIEMENTS

Je voudrais remercier Christine et Sylvie de m'avoir accueilli au sein du laboratoire, soutenu et encouragé pendant ces 4 années.
Christine, merci pour ces longues et passionnantes discussions, merci d'avoir su me pousser à avancer tout en me laissant la liberté de poursuivre mes idées. Merci pour ton optimisme à toute épreuve !
Sylvie, merci pour tes conseils et ton aide ; ton énergie et ton enthousiasme sont contagieux !
Je remercie Alexis pour son aide technique, mais surtout pour nos nombreuses discussions sur la gastronomie, la botanique et le Docteur, pour les soirées crêpes, la confiture de coing et pour m'avoir appris à préparer du ragoût de queue de bœuf au chaudron (une compétence rare parmi les végétariens).
Un grand merci à tous les autres membres du laboratoire Schneider-Maunoury : Inès et François ; Abraham pour avoir tenté de m'apprendre la différence entre soy et estoy, et bien sûr pour les massages ; Isabelle pour ses sourires et ses charlottes au chocolat (ainsi que pour le génotypage !) ; Alice ; Diego pour les discussions sur la linguistique comparée et la politique espagnole. Et Martin pour les chocolats PR !
Merci aux membres de l'équipe Breau : Marie pour avoir partagé sa bonne humeur et son expertise en imagerie ; Girish pour les Gulab Jamun ; Pauline pour son soutien à la cause végétarienne ; Marion ; Karen pour les conseils de postdoc ; Melina pour les discussions passionnantes sur R, et bien sûr pour ses incroyables chocolats ; Pénélope pour m'avoir fait découvrir la natation synchronisée et le roi de la nuit.
Merci à Teresa pour son aide dans l'analyse de mes données.
Merci à Jean-Francois et France de la plateforme d'imagerie pour leur aide. Merci à Alex, Stéphane et Edouard de l'animalerie aquatique : Alex pour toutes ses recommandations de voyages que je n'ai pas pu faire, étant en thèse ; Stéphane pour les discussions sur S.J.Gould et la théorie des cordes ; Edouard pour ses discussions sur le sens de la pratique et la beauté des mouvements de maître Noro ;
Merci à tous ces poissons-zèbre que j'ai maltraités au nom de la Science sans leur consentement pendant 4 ans !

Merci aux membres de l'équipe Haumaître : Cécile, Mélanie, Thassadite, Aline et Mandana, ainsi qu'aux membres de l'équipe Umbhauer-Rioux : Sylvia pour m'avoir conforté dans ma haine de Monsanto et pour avoir partagé ses châtaignes ; Pierrebruno ; Laura ; Jennifer pour ses discussions sur le yoga, la spiritualité Masaï et le tofu.

Un grand merci aux gens du laboratoire Houliston/Momose de Villefranche-sur-mer pour m'avoir accueilli et initié à ce merveilleux organisme qu'est Clytia. Merci en particulier à Tsuyoshi pour son enthousiasme et sa jovialité : merci de t'être autant investi dans notre projet collaboratif, qui m'a beaucoup apporté pendant ma thèse. Travailler avec toi fut vraiment un plaisir !

Merci aux membres de mon comité de thèse : Marika Kapsimali, Marie-Hélène Verlhac et Alice Meunier pour leurs commentaires constructifs et leurs encouragements.

Merci aux membres de mon jury de thèse, Juliette Azimzadeh, Nicolas David, Hitoyoshi Yasuo et Patrick Blader d'avoir accepté de se pencher sur mon travail.

Enfin merci à mes amis de longue date : Claire, Marie, Lihui, Michael, Yvon, Aurélien, Nicolas, Jean-Noël, Ivan, Elie, Ali, avec lesquels j'ai passé tant de bons moments ces dernières années, à Paris ou ailleurs. Merci à ma famille, en particulier à ma mère qui supporte mon sale caractère depuis toujours dans la bonne-humeur !

INTRODUCTION

Cell polarity, the asymmetric localization of molecules and cellular structures, is a widely conserved characteristic of living things that could have evolved to restrict senescence to one daughter cell during division by enabling the differential segregation of damaged material (Macara 2008[1]). In metazoan, polarization relies on several conserved protein complexes and leads to the asymmetric localization of proteins, lipids, mRNAs and organelles within cells (Schenkelaars 2016[2], Salinas-Saavedra 2018[3]). This structural polarization is critical for the morphological polarization that allows neurons to transmit information, immune cells to migrate and interact with their target cells or embryonic cells to move relative to each other during morphogenesis.

The importance of cell polarization is particularly obvious in epithelia, layers of tightly packed cells at the interface between the inside of an organism and its environnement. Epithelial cells display two types of polarity : apico-basal polarity, perpendicular to the plane of the epithelium, allows the directional transport of molecules across epithelia. In contrast, planar cell polarity (PCP) refers to the coordinated polarization of cells within the plane of the epithelium. Thus, in many epithelia, cellular structures such as cilia and centrosome are oriented in a given direction. The coordinated orientation of motile cilia allow some epithelia to generate a directional movement of fluids ; for example ependymal cells propel the cerebro-spinal fluid posteriorly in the central canal of the spinal cord, which is critical for brain development and homeostasis (Zappate 2012[4]).

During my PhD, I used the Zebrafish floor-plate as a model system to investigate the mechanisms leading to ciliated epithlelia planar polarization. The floor-plate is a simple epithelium located at the most ventral part of the neural tube. The coordinated posterior positioning and tilting of motile cilia in floor-plate cells is critical for proper anterior to posterior CSF circulation in the spinal cord, and zebrafish, with its many available genetic tools and rapidly developing transparent embryo is a model of choice to adress the dynamics of cell polarization with live-imaging techniques.

To introduce my PhD work, I will first review the mechanisms involved in non-planar cell polarization. I will then give an overview of planar cell polarity (PCP) and the connections that exist between PCP and the proteins involved in non-planar cell

polarization. Finally we will see that cilia and centrosomes are tightly linked to cell polarization and polarity proteins.

I- Mechanisms of cell polarity initiation and maintenance

Cells polarize in response to extracellular cues, like cell-cell contact, cell-extracellular matrix contact or receptor activation. This triggers the asymmetric repartition and activation of several key conserved molecules : the PAR, Scribble and Crumbs complexes, small GTPases of the Rho familly which in turn reorganize cell components. In this section I will illustrate how polarity is initiated and then maintained using polarization of the C.elegans zygote as a single cell example and apico-basal polarization in epithelia as an example of cell polarization within a tissue.

A) Polarization of the C.elegans zygote leads to asymmetric division

1) Par complex discovery through C. Elegans zygote asymmetric division

The Par proteins were first described in C.elegans zygote, where their inactivation leads to polarization defects and a symmetric first division [Kemphues 1988[5]]. Since then, they have been shown to be conserved across metazoans and play a role in a variety of polarization processes [Goldstein 2007[6]]. In many cases, they cooperate with small GTPases of the Rho family.

There are 6 Par proteins in C.elegans, all of which are conserved in metazoan, with the exception of Par2 which is nematod specific. Par3 and Par6 are scaffold proteins, Par1 and Par4 kinases and Par5 a member of the family of 14-3-3 proteins. In addition, Pkc-3

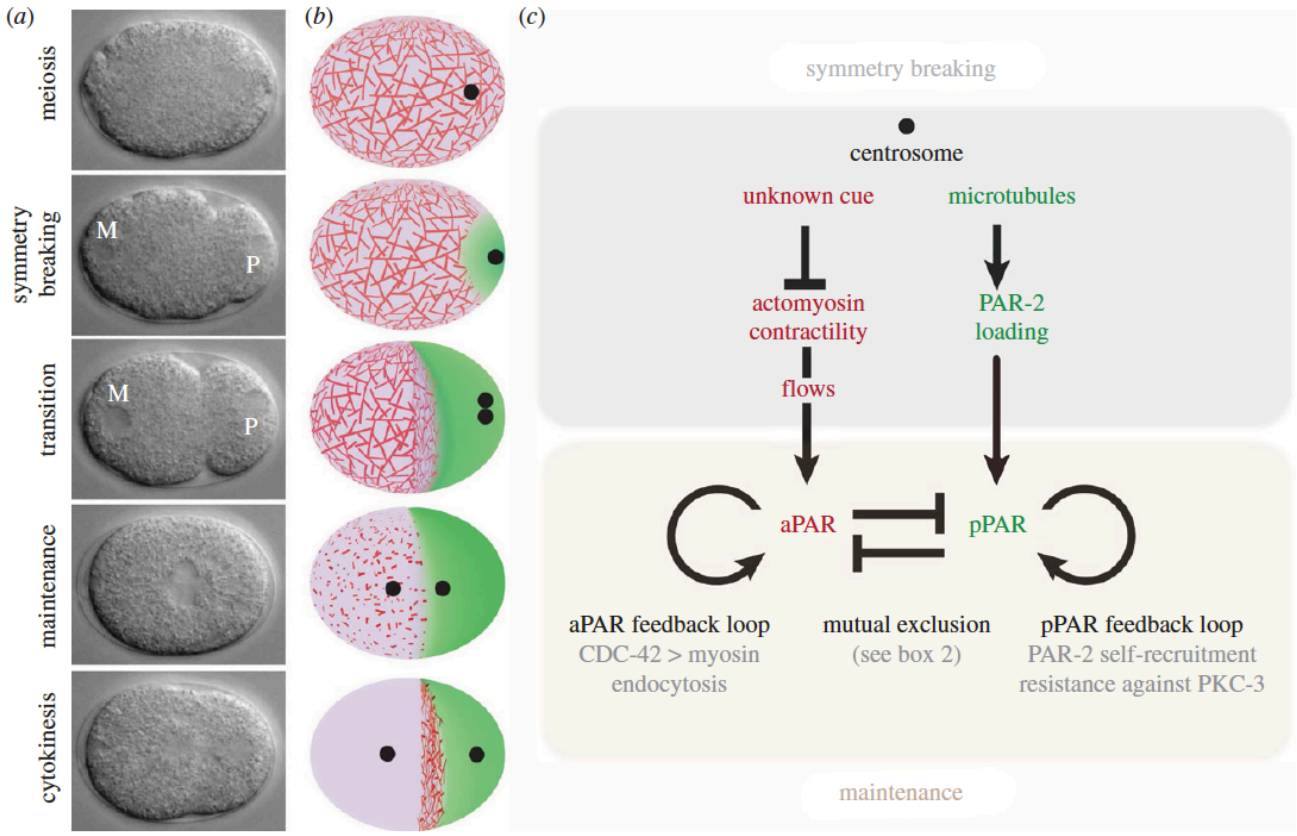

Figure 1 Overview of C.elegans zygote polarization

(a) First asymmetric division of C.elegans zygote. M and P are the male and female pronuclei respectively

(b) Schematic distribution of the cortical actin network (red filaments), aPARs (pink) and pPARs (green). The black dot corresponds to the sperm centrosome.

(c) Two parallel pathways breaking zygotic symmetry downstream of the sperm centrosome. Asymmetry is maintained through mutual exclusion and positive feedback loops.

Adapted from Motegi et al. 2013

(aPKC in vertebrates) is a kinase that has been shown to interact genetically and physically with Par proteins [Tabuse 1998[7]].

2) Polarization initiation in C.elegans zygote

In the C.elegans zygote, the model system where polarization is best understood, fertilization leads to the formation of two separate cortical domains : an anterior cortical domain with Par3, Par6 and aPKC (which are therefore refered to as anterior Pars or aPARs) and a posterior domain composed of Par1 and Par2 (posterior Pars, or pPARs) (Figure 1). Par3, Par6 and aPKC are initially localized uniformly at the zygote cortex, whereas Par2 and Par1 are excluded from the cortex. Following sperm entry, an asymmetric contraction of the acto-myosin network at the cell cortex carries the aPARs to the anterior cortex [Munro 2004[8]]. This asymmetric contraction is driven by a still uncharacterized cue coming from the sperm centrosome. Indeed, at polarity onset, ECT-2, a RhoGEF (Guanine nucleotide Exchange Factor), clears away from the posterior cortex adjacent to the sperm centrosome and this step requires a functional centrosome (Motegi and Sugimoto, 2006[9]). Another candidate mechanism would involve the sperm supplied CYK-4, a RhoGAP (GTPase Activating Protein), which functions by inactivating Rho at the posterior cortex [Jenkins 2006[10]]. These two mechanisms lead to posterior Rho inactivation and therefore lower level of Rho-mediated actomyosin contraction at the posterior cortex. This asymmetric cortical contraction results in an anterior-directed cortical flow that transport aPARs to the anterior side by advection.

However, the repositioning of aPARs to the anterior cortex is not entirely passive since anterior myosin movements occur more slowly in par3 mutants suggesting that Par3 amplifies myosin activity through positive feedback [Munro 2004[8]]. In addition, it was recently shown that Par3 forms large oligomers to promote the localization of the aPARs by advection [Dickinson 2017[11]].

Another mechanism contributing to polarity establishment in the C.elegans zygote is Par2 stabilization at the posterior cortex by centrosomal microtubules : these microtubules protect Par2 against aPKC phosphorylation, which would otherwise trigger its release from the cell cortex (Motegi 2011[12]).

3) Polarisation maintenance in C. elegans embryo

After polarization initiation, asymmetric Par cortical domains must be maintained in order to recruit the downstream effectors that will lead to the zygote first asymmetric division (both in size and in fate). Par domains maintenance is mediated by RhoGTPase signaling and through reciprocal inhibitory interactions between aPARs and pPARs.

At the onset of the maintenance phase, Polo kinase phosphorylates the Par3 oligomerization domain to inhibit its clustering. This results in a reduced association of Par6/aPKC with Par3, leading to the formation of a diffusible complex of Cdc42, Par6 and active aPKC that can exclude the pPARs [Rodriguez 2017[13]]. Indeed aPKC phosphorylates a domain within Par2 that has been shown to mediate its cortical localization [Hao 2006[14]], thereby keeping Par2 off the anterior cortex. In addition, aPKC activity excludes Par1 and Chin-1 (a Cdc42GAP) from the anterior cortex [Sailer 2015[15]]. It is also possible that Par1 and Par5 inhibit Par3 cortical localization at the posterior cortex via a mechanism that operates in Drosophila follicular epithelium and oocyte polarization, whereby Par1 phosphorylates Par3 to create a binding site for Par5, which disrupts the Par3/Par6/aPKC complex [Benton and StJohnston 2003[16]].

B) Initiation and maintenance of polarity within a tissue : epithelia apico-basal polarization

In addition to the Par proteins, two other complexes have been shown to have a role in AB polarity : the Crumbs complex, composed of Crumbs, Pals1 and Patj, and the Scribble complex, composed of Scribble, Dlg (Discs-large) and Lgl (Lethal giant larvae). Proteins of the Crumbs complex localize on the apical side of epithelial cells along with Par6 and aPKC, whereas the Scribble complex localizes basolaterally. Par3 localizes at the interface of these two regions, at the level of cell-cell junctions.

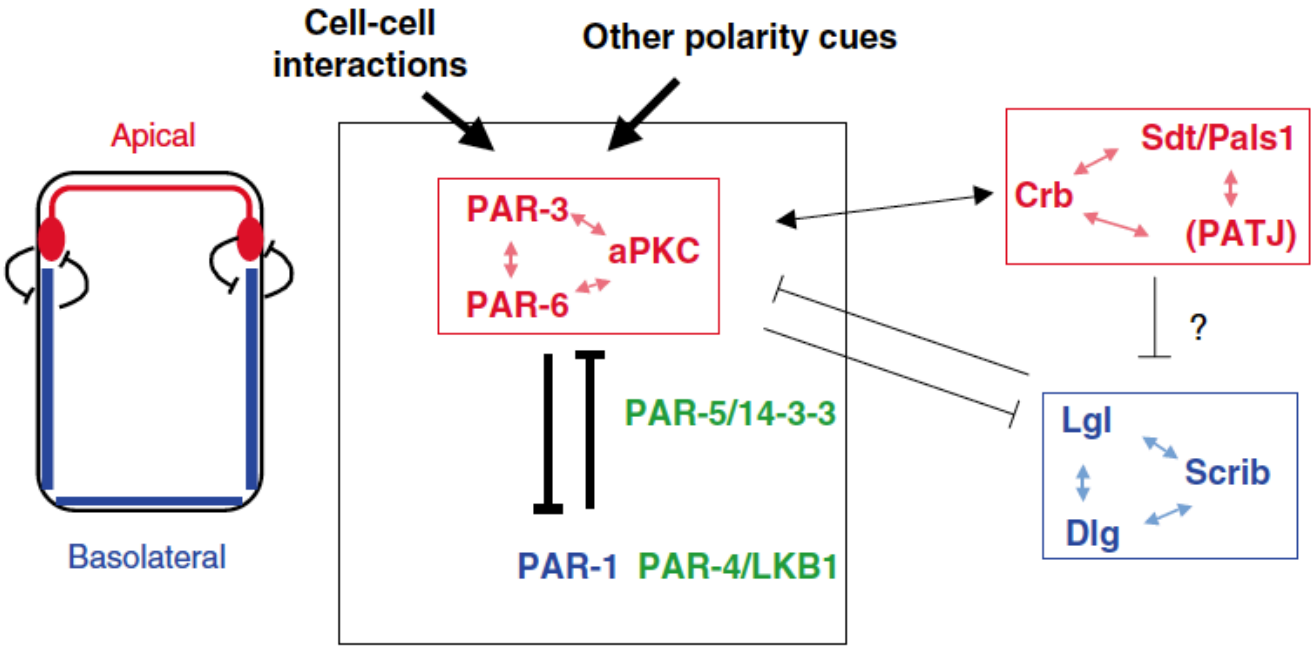

Figure 2 Interactions of polarity modules in apico-basal polarity

Schematic showing the interactions between the apical PAR and Crumbs complexes (red) and the basolateral Scribble complex (blue). Par1 also assumes a baso-lateral localization and antagonizes the apical Par complex.
Adapted form Suzuki et al. 2006

1) Apico-basal polarity initiation

Epithelial or endothelial cell polarity initiation rely on the initial interaction between cell-cell adhesion molecules of adjacent cells such as cadherins, nectins and JAMs. These proteins both establish physical intercellular connections and trigger the development of apico-basal polarity by recruiting polarity proteins at cell-cell contacts. Initial cell-cell contacts form patches and are therefore called « spot-like adherens junctions (AJ)» : they contain adherens molecules but no polarity proteins. The Par complex is then recruited to these junctions and promotes the formation of distinct apical and baso-lateral domains. A crucial actor in these initial steps is Par3, which can be recruited to nascent AJ via its interactions with JAM-A, JAM-B, JAM-C (Ebnet 2001[17], Ebnet 2003[18]) or Nectin-1 and Nectin-3 (Takekuni 2003[19]). Importantly, cell-cell adhesion molecules not only recruit polarity proteins but can activate them via RhoGTPases. E-cadherins and nectins activate Cdc42 and Rac1 (Fukuhara 2004[20], Yamada 2007[21]) which in turn activate the Par-aPKC complex (Yamanaka 2003[22]).
Interaction of epithelial cells with the extra-cellular matrix (ECM) via integrins is also crucial to initiate apico-basal polarization, although the mechanisms involved and how it regulates polarity proteins localization is not well understood (Manninen 2015[23]).

2) Apico-basal polarity refinement and maintenance by mutual exclusion

The mutual exclusion between polarity proteins first documented in the C.elegans zygote has also been found to play a crucial role in apico-basal polarity maintenance (Figure 2).

In Drosophila, it was shown that Par3 association with Par6 and aPKC is transient and that aPKC phosphorylation of Par3 at serine 980 is required for Par3 localization to adherens junctions [Morais de Sa 2010[24]]. In addition, Crumbs is required to exclude Par3 from the apical domain [Walther and Pichaud 2010[25]]. These results suggest that aPKC and Crumbs cooperate to destabilize Par3 association from the apical cortex and restrict its localization to adherens junctions.

In Drosophila epithelia, apical aPKC phosphorylates Lgl [Hutterer 2004[26]] and Par1 [Jiang 2015[27]] causing them to dissociate from the apical cortex and relocalize basolaterally. In addition, the Scribble complex suppresses apical membrane identity on the basolateral surface by inhibiting Par complex function, while Par complex recruits Crumbs to antagonize Scribble activity at the apical surface [Bilder 2003[28], Tanentzapf and Tepass 2003[29]]. As mentioned above, Par3 phosphorylations by Par1 on serine 151 and 1085 exclude Par3 from the baso-lateral membrane [Benton and StJohnson 2003[16]]. This complex set of interactions and mutual exclusions leads to the establishment of distinct apical and basolateral domains, separated by cell-cell junctions.

We have seen that the mechanisms of polarity protein asymmetric localization have been extensively investigated.. Still, the identification of the downstream effectors of polarity complexes is is far from being complete. For example, it was shown that loss of function of either Crumbs or Scribble complex leads to to the reduction of the surface area of the apical or baso-lateral domains respectively [Bilder 2003[28], Tanentzapf and Tepass 2003[29]] but by unknown mechanisms. However other studies have shown that these proteins polarize cells, mostly via the regulation of cytoskeletal dynamics.

C) Downstream effectors of Polarity proteins and small-GTPases in cell polarization

1) Downstream effectors of Par3 and RhoGTPases in cell/cell junction formation

In epithelial cells, polarity proteins and small GTPases are important for the formation and maturation of cell-cell junctions. Par3 has been shown to control tight junction assembly via its direct interaction with the RacGEF Tiam1 in cultured mammalian epithelial cells which restricts Rac activation to nascent tight junctions [Chen 2005[30]].. Rac can recruit the Arp2/3 activator WAVE2 which functions with WAVE1 to activate Arp2/3 and promote exploratory lamellipodia for adherens junction assembly [Yamazaki 2003[31]].

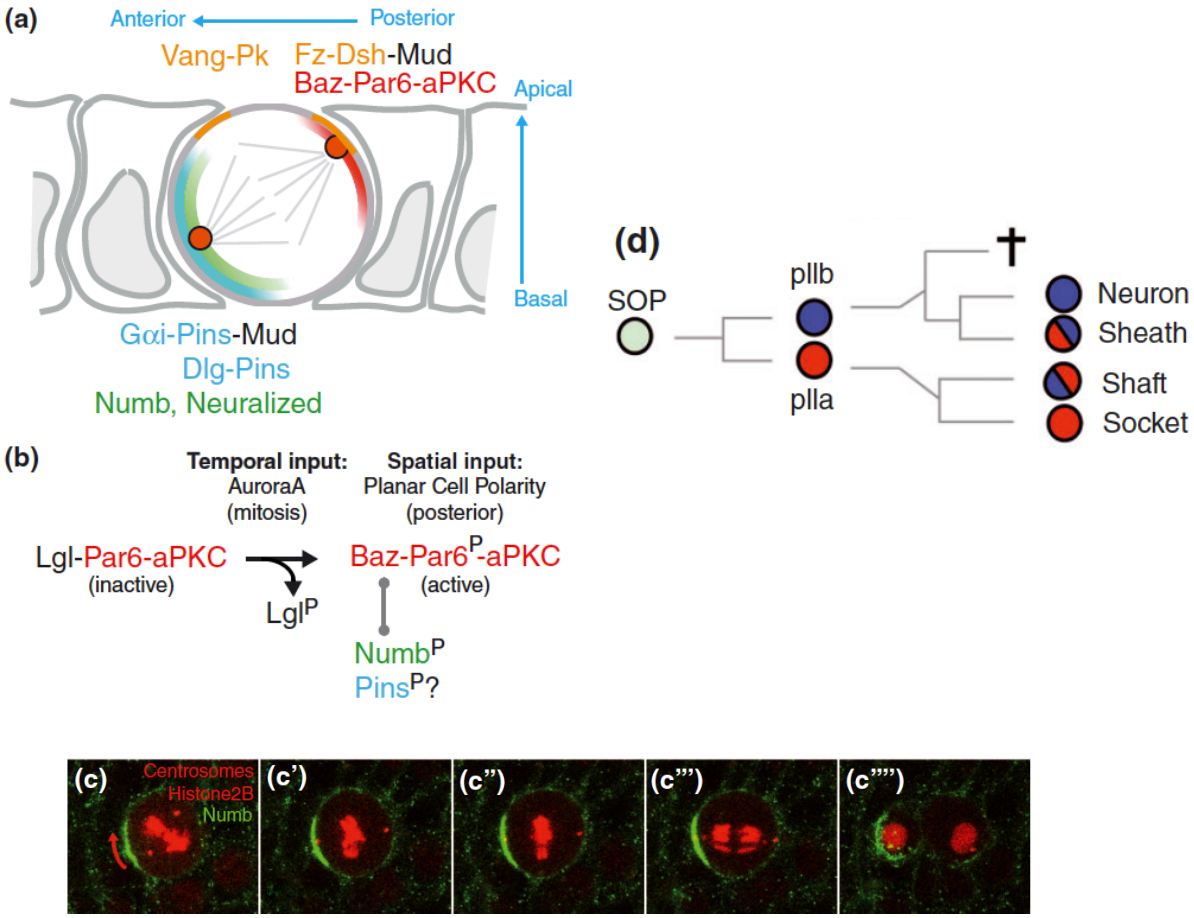

Figure 3 Asymmetric distribution of Numb in SOP

(a) Schematic of a dividing SOP (side view), showing the anterior-basal localization of Numb (green), opposite to the Par domain (red)
(b) In mitosis, AuroraA acitvity activates the Par complex. Baz (Par3) recruits Numb, which is phosphorylated by aPKC and therfore excluded form the posterior-apical cortex
(c) Snapshot from SOP division live-imaging showing Numb asymmetric localization and differential inheritence into the anterior daughter cell. (anterior left)
(d) SOP cell lineage. The daughter cell inheriting Numb (pIIb) will give rise to the neuron and sheath cell of the sensory organ

Adapted from Schweisguth 2015

In the context of Drosophila cellularization, Par3 plays a key role in localizing Cadherin to the apical adherens junctions, in part by coupling it to dynein-mediated microtubule transport [Harris and Peifer 2005[32]].
In the mammary epithelium, Par3 is also required for Cadherin localization, where it targets their exocytosis to the junctional domain via direct binding with the exocyst complex [Ahmed 2017[33]].

2) Polarity proteins cooperate to segregate determinants and orient the spindle during asymmetric cell division

The Par proteins have also important roles in asymmetric cell divisions (ACD). Indeed they are involved both in the asymmetric localization of fate determinants and in spindle orientation, two processes that are crucial in many ACD. Two of the most documented models for ACD are cell divisions of the Drosophila Sensory Organ Precursor (SOP) and of drosophila neuroblast..

a) Asymmetric inheritance of cellular determinants

Within SOP cells, Par6-aPKC complex interacts with and is inhibited by Lgl prior to mitosis [Wirtz-Peitz 2008[34]]. During mitosis, Aurora A phosphorylates Par6 which promotes the dissociation of Lgl from Par6-aPKC and favors the formation of the Par3-Par6-aPKC complex that localizes at the posterior-apical cortex [Bellaïche 2001[35]]. Par3 then recruits Numb, a notch pathway inhibitor [Guo 1996[36]]., promotes its phosphorylation by aPKC and thereby excludes Numb from the posterior cortex [Wirtz-Peitz 2008[34]] (Figure 3a-c). The daughter cell that inherits Numb will divide and give rise to the neuron and sheath cell of the sensory organ, whereas the other cell will give rise to the shaft and socket cells (Figure 3d). Numb functions in this differentiation process by inhibiting the notch pathway.
In Drosophila neuroblasts, asymmetric localization of cell fate determinant relies upon similar mechanisms. The cell determinants Numb, Prospero, Staufen and Miranda colocalize with the Par complex at the apical surface during interphase. During mitosis, Aurora-A induced aPKC activation leads to phosphorylation of Numb, of Partners of Numb and Miranda, thus excluding them from the cortical apical domain [Wirtz-Peitz

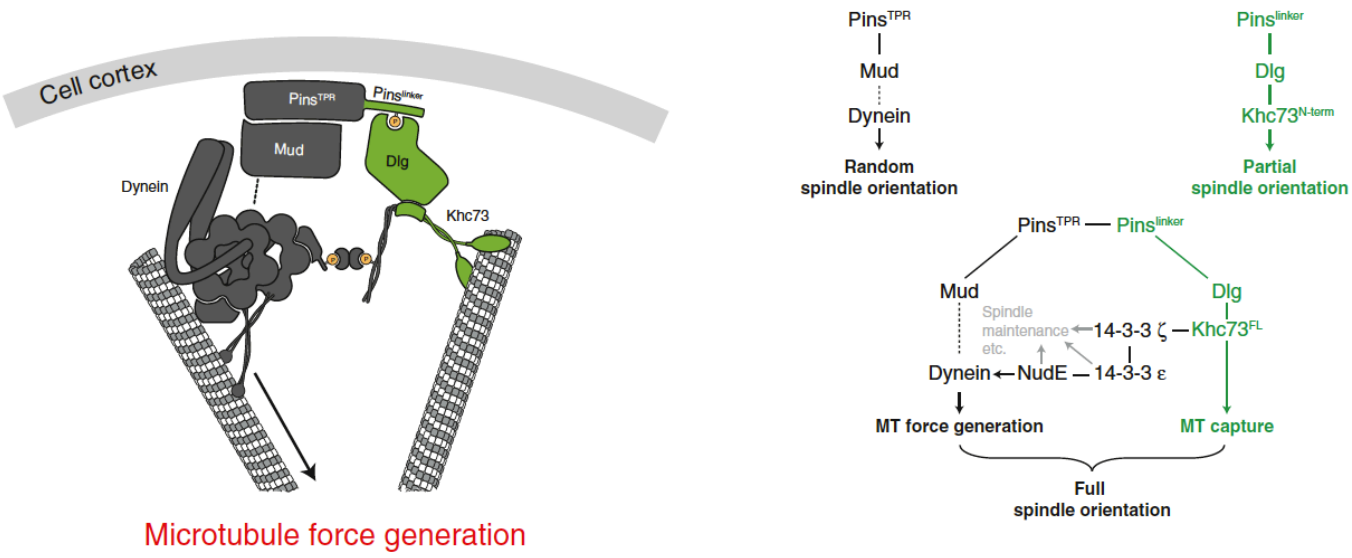

Figure 4 Mechanisms of neuroblast spindle orientation

Schematic showing the cortical localization and interactions of Pins, Mud and Dlg with Dynein and Khc73 at the apical pole of dividing neuroblasts (left) and the two parallel pathways that contribute to proper apico-basal spindle orientation (right)

Adapted from Lu et al. 2013

2008[34],Betschinger 2003[37], Atwood 2009[38], Smith 2007[39]]. In the daughter cell, called the Ganglion Mother Cell (GMC), Numb inhibits Notch activity. This drives GMC differenciation [Spana 1996[40]].

The involvement of polarity protein in asymmetric fate-determinant inheritance could be conserved in vertebrates. For example, in Zebrafish embryo neuroepithelium, neuroblasts divide asymmetrically and the daughter cell that inherits Par3 differentiates into a neuron [Alexandre 2010[41]]. One can assume, that, like in Drosophila, Par3 drives the asymmetric inheritance of Notch regulating factors such as Numb. In addition, in Xenopus neural plate, Par1 regulates neurogenesis by phosphorylating Mind bomb (Mib), an ubiquitin ligase that promotes Notch activity. This triggers Mib degradation, repression of Notch signaling and stimulation of neuronal differenciation [Ossipova 2009[42]].

b) Polarity proteins control spindle apico-basal orientation in Drosophila neuroblasts

As mentionned above, in Drosophila neuroblast, Par3, Par6 and aPKC form an apical cortical complex from late interphase. Par3 interacts with Inscuteable and recruits it to the apical cortex, which in turn recruits Pins and GαiGDP. Pins can recruit Mud, which is essential for spindle orientation [Bowman 2006[43]]. Mud then acts via dynein to orient the spindle, although no dynein apical enrichment has been reported in this system.

In parallel, another pathway contributes to spindle orientation : in artificially polarized S2 cells, Pins can anchor the spindle via its LINKER domain that binds to the polarity protein Dlg in neuroblasts [Bellaïche 2001[35]]. Dlg in turn binds to the kinesin Khc-73, at astral microtubules plus ends. The Pins-Dlg-Khc-73 pathway identified in S2 cells is likely to function in neuroblasts since the loss of Dlg or Khc-73 activity perturbs mitotic spindle orientation in these cells [Siegrist and Doe 2005[44]]. Khc73 links Pins to microtubule plus ends and is also required for Dynein activation and precise positioning of the spindle. [Lu 2013[45]] (Figure 4).

Thus, in neuroblasts, spindle orientation rely on two parallel Pins-dependent pathways : Pins anchors astral microtubules at the cortex via Dlg and Khc73, but also generates pulling forces via Mud-Dynein.

The role of Mud and Dynein in spindle positioning seems to be widely conserved in animals, as it also plays a role in C.elegans first asymmetric division and in vertebrate oriented cell division.

c) Polarity proteins control spindle off-centering in C.elegans zygote

In C.elegans zygote, Par2 and Par3 modulate cortical pulling forces on microtubules on either side of the embryo during both spindle movement to the posterior (the first division is asymmetric in size, with a smaller posterior cell) and a later spindle rocking phase [Grill 2003[46], Labbe 2004[47]]). Par proteins regulate the posterior enrichment of GPR-1/2, the C.elegans Pins orthologue. GPR1/2 binds to Gα proteins. The GPR1/2- Gα complex is necessary to generate a net higher posterior pulling force, and interacts with LIN-5, the C.elegans Mud orthologue [Srinavasan 2003[48]]. These molecules in turn promote the cortical localization of the Dynein-Dynactin complex, which is required for force generation at the cortex [Nguyen-Ngoc 2007[49]]. Although the Dynein-Dynactin complex is not restricted to the posterior side of the zygote and the mechanisms by which GPR1/2 enrichment triggers higher force generation at the posterior cortex is still not clear, a recent paper showed that the tumor suppressor APC (Adenomatous Polyposis Coli) localizes at the anterior cortex in a aPARs dependent manner and reduces force generation by stabilizing microtubule plus ends [Sugioka 2018[50]].

d) Spindle orientation in vertebrates

Studies in embryonic mouse skin progenitors suggest that the spindle orientation mechanisms found in C.elegans and Drosophila are conserved in vertebrates. In dividing skin progenitors, Insc, LGN and NuMA (LGN is the vertebrate ortholog of Pins and NuMA the vertebrate ortholog of Mud) are localized within an apical domain present in a subset of cells that divide along the Apico-Basal (A/B) axis. Integrins and cadherins are essential for the apical localization of aPKC, Par3-LGN-Inscuteable complex and NuMA-dynactin, all of these actors being required for proper spindle orientation [Lechler and Fuchs 2005[51]]. Gαi3 and Dynactin are also localized apically [Williams 2011[52]], and Par3, Insc and Gαi3 cooperate to promote oriented cell division through LGN [Williams 2014[53]].

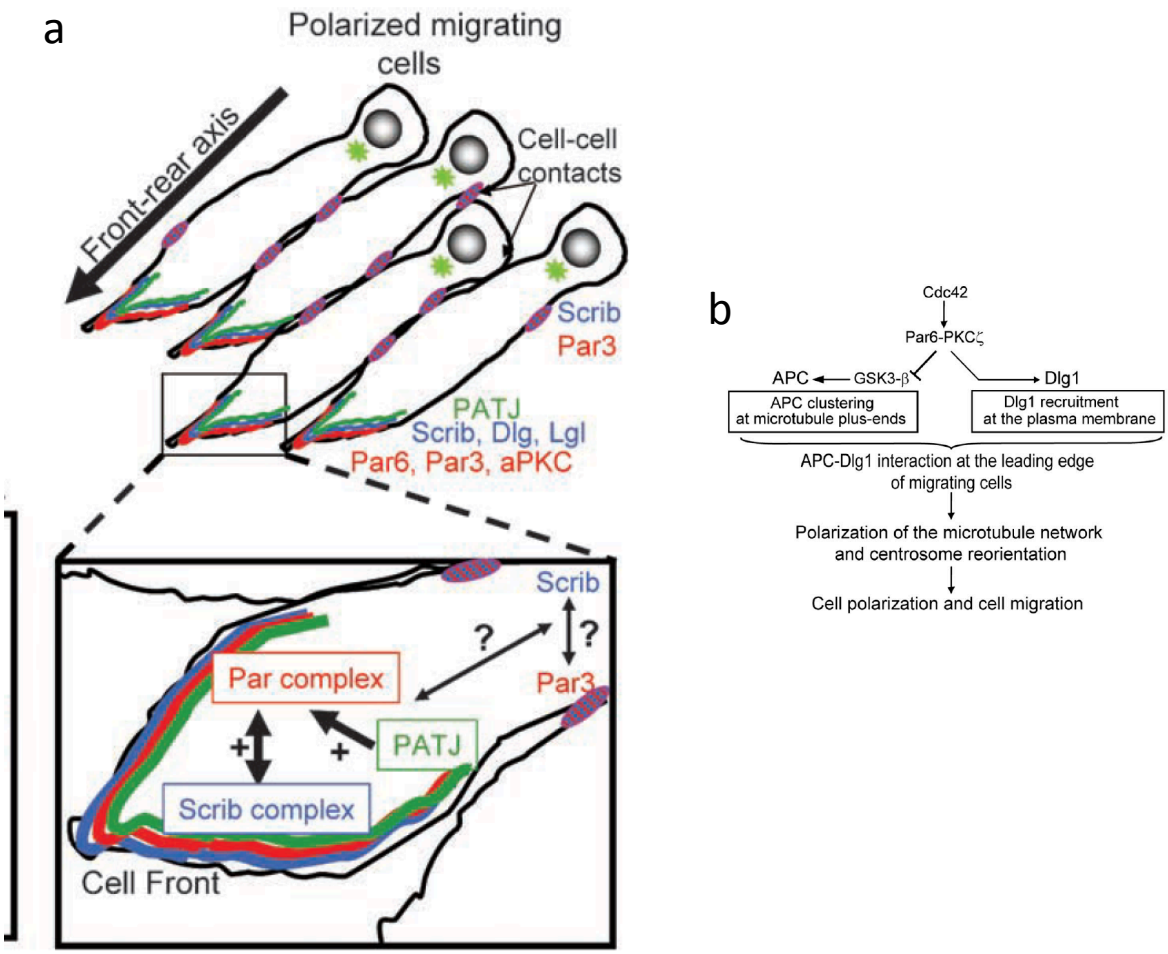

Figure 5 Polarity proteins in cell migration

(a) Polarity proteins colocalize at the leading edge in migrating epithelial cells during wound closure (adapted form Etienne-Manneville 2008)
(b) Cdc42 and polarity proteins regulate cytoskelton polarization during astrocyte migration (adapted from Etienne-Manneville et al. 2005)

3) Functions of Polarity proteins and RhoGTPases during directional migration

During wound induced astrocyte polarization, Cdc42 mediates cytoskeleton polarization, directionnality of membrane protrusions and Golgi and centrosome positioning, whereas Rac1 promotes the outgrowth of protrusions. Cdc42 activates Par6 and aPKC at the leading-edge, where aPKC phosphorylates and inactivates GSK3β. GSK3β promotes the association of APC with microtubule plus ends and allows for the subsequent interaction of APC with Dlg1 at the leading edge, which is required for front-directed polarization of microtubules and allows targeted vesicle transport to the leading edge [Etienne-Manneville 2003[54], 2005[55]] (Figure 5b) .

In migrating cultured epithelial cells (wound assay), polarity proteins localize to the leading edge and regulate front-rear polarization, chemotactic migration and wound-healing (Figure 5a). Scribble is required to localize both Cdc42 and Rac to the leading edge, thereby promoting Golgi apparatus polarization and directional migration [Dow 2007[56]]. As in migrating astrocytes, Cdc42 then activates aPKC which initiates multiple downstream signaling events.
For example, during chemotactic migration of keratinocytes, aPKC and Par3, together with Tiam1, mediate stable front-rear polarization through microtubules stabilization [Pegtel 2007[57]]. In addition, Par3 and aPKC spatially control integrin endocytosis through Numb. aPKC-mediated phosphorylation of Numb prevents integrin endocytosis at the leading edge [Nishimura 2007[58]] and thereby maintains the stimulatory integrin adhesion signal required for polarized migration [Etienne-Manneville 2001[59]].

During collective cell migration of Xenopus neural crest cells, a process described as contact inhibition of locomotion (CIL) takes place [Carmona-Fontaine 2008[60]]. In Xenopus and Zebrafish neural crest cells, Par3 is localized to the cell-cell contact and promotes microtubule catastrophe by inhibiting the RacGEF Trio, which triggers CIL [Moore 2013[61]] (Figure 6).

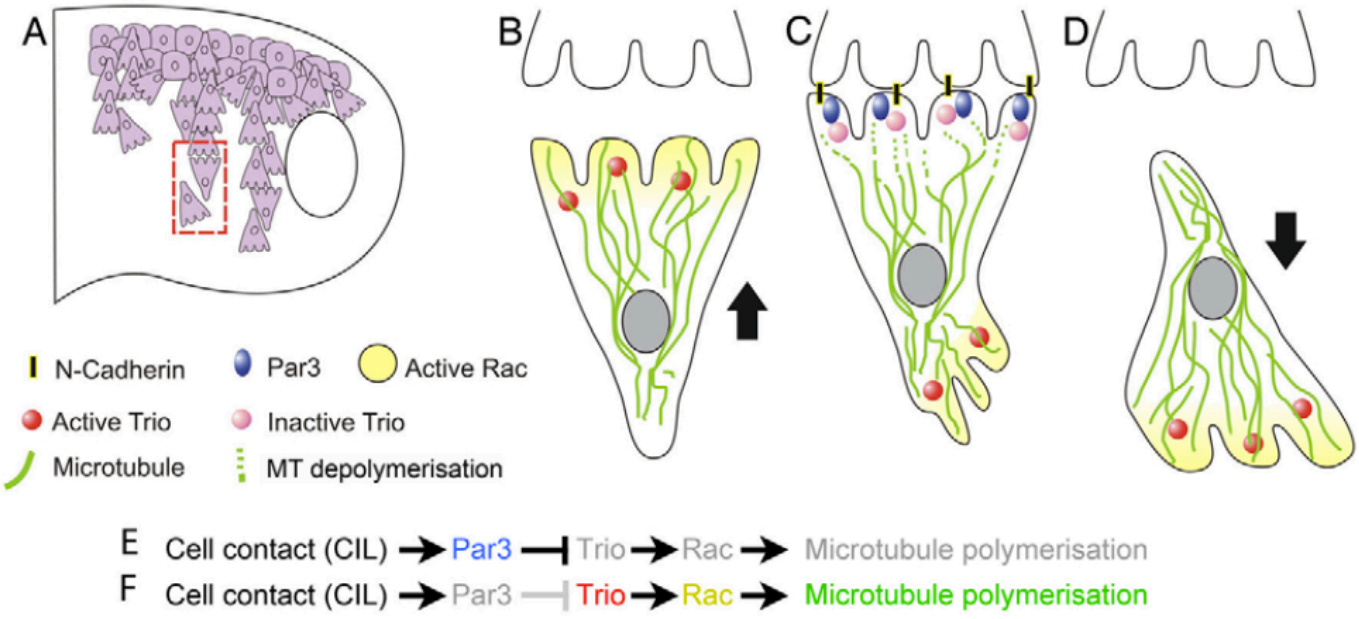

Figure 6 Role of Par3 and Rac in neural-crest cells contact inhibition of locomotion

(A) Xenopus embryo head with ventrally migrating neural-crest cells (purple)
(B-D) Upon contact with another neural-crest cell (C), Par3 localizes to cell-cell contacts where it inhibits Trio and therefore Rac activity, leading to microtubule destabilization and polarity reversal (D)

Adapted from Moore et al. 2013

Interestingly, Par3 interact with microtubules and regulate their dynamics in many polarized cells ; in wound-edge fibroblasts, Par3 localizes to cell-cell contacts where it overlaps with microtubules plus ends and dynein puncta. Microtubules exhibit increased pausing at cell-cell contacts compared to the leading edge and this depends on Par3 and dynein [Schmoranzer 2009[62]]. Although these effects of Par3 on microtubule dynamics seem to be indirect, Par3 can directly regulate microtubule stability and organization in mammalian neurons [Chen 2013[63]].

Thus, polarization is a fundamental characteristic of animal cells and rely on a conserved set of polarity proteins and RhoGTPases that cooperate to regulate cytoskeletal dynamics. This leads to morphological polarization that is crucial for oriented/asymmetric cell division, cell migration and epithelia barrier function. In the following section, we will see how another form of polarity, planar cell polarity, rely on a different set of polarity molecules that orient cells within the plane of the epithelium.

II-Planar cell polarity

In addition to their apico-basal polarity, most epithelia display coordinated asymmetric positioning of cell components within the plane of the epithelium, a form of polarity called planar cell polarity (PCP). Although its morphological manifestations, such as the uniform orientation of hairs or cilia are quite obvious, the underlying molecular mechanisms have only recently begun to be uncovered and remain mysterious. Still, mechanistic insights came from the Drosophila wing model, in which small actin-based hairs (trichomes) point distally. In this system, PCP is controlled by two sets of molecules: the « core » PCP proteins and the Fat-Dachsous-Four-jointed (Ft-Ds-Fj) module. Although the role of Ft-Ds-Fj is not yet clear in other organisms, the role of core PCP components is well established in vertebrates as well. The core PCP module comprises trans-membrane molecules, such as Frizzled (Fz, Fzd in vertebrates), Van Gogh (Vang, Vangl in vertebrates) and Flamingo (Fmi, Celsr in vertebrates), which interact with cytoplasmic molecules such as Prickle (Pk), Disheveled (Dsh, Dvl in vertebrates) and Diego (Dgo, Ankrd6 in vertebrates). One of the key features of core PCP

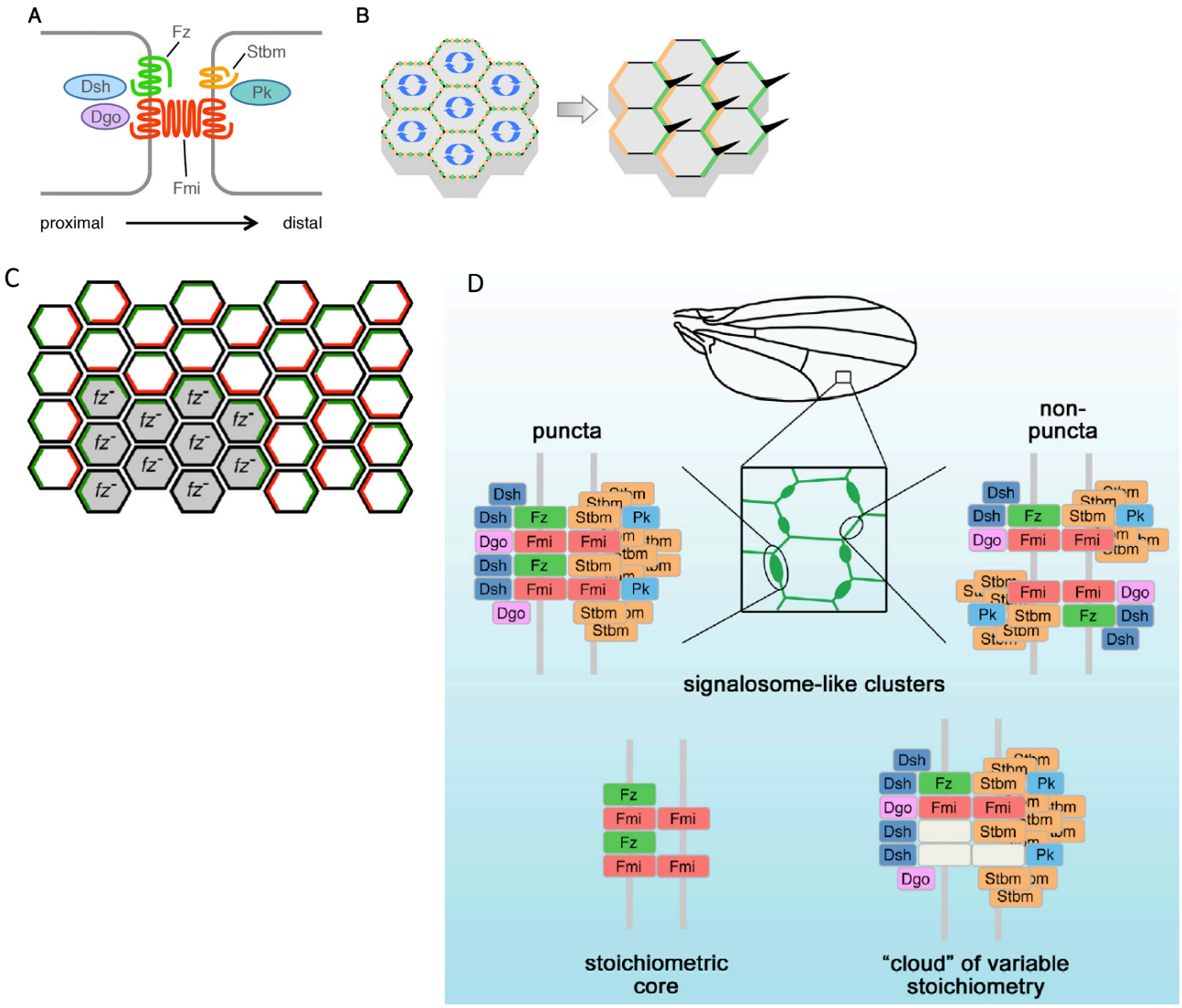

Figure 7 Asymmetric localization of PCP proteins in Drosophila wing

(A) Schematic showing asymmetric localization of Vang/Stbm and Pk on the proximal side and Fz, Dsh and Dgo on the distal side of Drosophila wing cells. Fmi localizes both on proximal and distal cell sides. (adapted form Strutt 2019)

(B) PCP proteins first assume a uniform localization around cells apical junction before being segregated to proximal or distal side, which leads to asymmetric positioning of cellular structure such as the distal trichomes.

(C) Example of the domineering non-autonomy of transmembrane PCP proteins such as Fz: a Fz deficient clone (fz- cells) has Vang localized at its border (green) and triggers the reorientation of PCP of adjacent cells, which all have Fz localized toward the clone (red) and a trichome pointing toward the clone (not shown). (adpated from Strutt 2009)

(D) Assembly of PCP proteins into signalosome-like clusters in Drosophila wing (adapted from Strutt 2016)

proteins is that they form different complexes that localize at opposite sides of epithelial cells. For example in the fly wing, Fmi/Vang/Pk localize on the proximal side whereas Fmi/Fz/Dsh localize on the distal side, next to the trichome (Figure 7A). The presence of Fmi at both cell-cell junctions along the polarity axis defines an "axial" polarization that is tightly linked to the unilateral asymmetric localization of Vang/Pk and Fz/Dsh that define a "vectorial" polarization[64]. Asymmetric localization of PCP proteins have been demonstrated in many planar polarized epithelia, including the vertebrate inner ear[65 66 67 68 69 70], the mammalian epidermis[71 72], brain ventricles [73] and trachea[74] and is required for orientation of cellular structures such as actin hairs or cilia, convergent extension movements and oriented cell divisions in vertebrates.

I will first summarize how this asymmetry is established and amplified, then describe how chemical or mechanical cues can coordinate these asymmetries across tissues , and finally outline the link between PCP components and functional cell polarization.

A) PCP establishment

1) Importance of cell-cell interactions

Cell-cell junctions are crucial for the propagation of asymmetry between adjacent cells. Core PCP components localize at adherens junctions, and the transmembrane proteins Fz, Vang and Fmi establish interactions across neighbooring cells that contribute to PCP propagation within the tissue and explain the domineering non-autonomy of Fz or Vang deficient or over-expressing clones (Figure 7C).

In the Drosophila wing, interaction of Fmi cadherin repeats between adjacent cells promote the formation of Fmi homodimers across apical cell-cell junctions, which in turn recruit Fz and Vang to opposite sides of cell boundaries[75]. Reciprocally, Vang and Fz also influence Fmi stability at cell-cell junctions, and Fmi is diffusely apical rather than apico-laterally enriched in *vang/fz* double mutants[76]. Fmi preferentially binds to Fz rather than Vang and a Fmi-Fz complex is more likely to associate with Fmi molecules in

the adjacent cell that are not bound to Fz[76], thus contributing to the asymmetric exclusive localization of Vang and Fz. In addition, Fz extracellular domain can directly interact with Vang extracellular domain on an adjacent cell, which may constitute a parallel mechanism for PCP propagation[77], but is not required for PCP Vang and Fz asymmetric localization, since Fz and Vang lacking their extracellular domains can still recruit one another between cells[75]. PCP proteins interaction between neighboring cells has recently been shown to involve the clustering of PCP proteins which form signalosome-like structures with a defined stoechiometric Vang-Fz core and a variable stoechiometry of other PCP proteins (Strutt 2016[78]) (Figure7 D).

2) Feedback amplification of asymmetry

Cell-cell interaction alone through Fmi, Fz and Vang is not sufficient for the establishment of a robust PCP pattern. The cytoplasmic core PCP components Dsh, Dgo and Pk are required for locally accumulating the membrane-bound PCP complexes to amplify the asymmetric localization of PCP proteins[79].

Once Fz is recruited by Fmi homodimers, it can recruit Dsh via the binding of its cytoplasmic tail to Dsh DEP (Disheveled, Egl-10, Pleckstrin) domain (which is specifically involved in PCP and not in canonical Wnt/Fz/Dsh signaling). Dgo can in turn be recruited by Dsh PDZ (PSD95, Dlg, ZO1) domain (that is involved both in PCP and in canonical Wnt/Fz/Dsh signaling). In *dsh* mutant cells, the asymmetric enrichment of Fz and global junctional Fmi levels are strongly reduced[80 76 81]. On the other side of the cell, Vang and Pk interact through their C-terminal domains, which also mediate homotypic Vang/Vang and Pk/Pk interactions[82], which facilitates the clustering of Vang and Pk and increases the stability of their junctional localization[83].

Another mechanism to maintain and amplify asymmetric localization of PCP proteins is the mutual exclusion of the Fmi/Vang/Pk and Fmi/Fz/Dsh complexes. The C-terminal regions of Vang and Pk can associate with both Dsh and Dgo[84 85], this could thus prevent Vang and Pk from forming stable complexes on the same side of the cell as Dsh and Dgo, because of competitive binding. It has been proposed that Pk inhibits the association of Dsh with Fmi-Vang by competing for the same binding region of Vang whereas Dgo competes with Pk for binding to Dsh[82 84 85]. More recently, it was shown that in

Drosophila pupal wing, Vang and Pk promote Fz stable junctional localization in neighboring cells, and that Pk destabilizes Fz in the same cell, in a Dsh dependent manner[81]. This could be explained by the fact that Pk interacts with Dsh and blocks the protective function of Dsh on Fz (probably via multimerization into stable complexes) leading to Fz endocytosis by a constitutive mechanism. It could also be that binding of Pk to Dsh-Fz complexes leads to a post-translational modification of Fz or Dsh by an enzyme that is recruited by Pk, resulting in Fz endocytosis. Finally, Fz-dependent Vang phosphorylation by CK1ε in the same cell is required for proper asymmetric localization of core PCP molecules[86].

The positive and negative interactions described above allow PCP protein asymmetric localization and short-range propagation of polarity (Figure7B).

3) Importance of endocytosis in PCP protein localization

In order to establish and maintain a robust asymmetric localization of PCP components, mislocalized or unstable PCP proteins must be removed from the membrane. Therefore, endocytosis and endosomal trafficking are crucial for proper PCP establishment.

For example, Rab5 (a small GTPase that assembles on endosomal membranes and mediates the capture of clathrin-coated vesicles arriving from the plasma membrane[87]) and dynamin (a GTPase involved in clathrin-dependent endocytosis) play a role in PCP components endocytosis [81 88 89]. Inhibiting endocytosis leads to an over-accumulation of Fmi at cell-cell junctions[79]. In addition, Fz may facilitate the feedback amplification of asymmetry described above by promoting Fmi-Vang-Pk endocytosis[76 79].

Less intuitively, ubiquitinylation of Pk can promote Fmi-Vang-Pk endocytosis[90]. Dsh can also trigger Fz and Fmi internalization: for example in Xenopus, Dvl2 (a Dsh ortholog) interacts with the clathrin adaptor AP2 to trigger Fzd4 endocytosis, which is required for proper PCP-dependent convergence-extension processes[91]. Thus cytoplasmic PCP components contribute both to the clustering of their transmembrane protein partners and to their removal from some cell membranes.

Following their endocytosis, PCP proteins can either be degraded or recycled back to the membrane. Indeed, inhibition of lysosomal maturation can lead to intracellular Fmi accumulation[76 79]. In addition Rab4 and Rab11 seem to be able to recycle Fmi back to the membrane[79 76 89]. The recycling back to the membrane of PCP components could be

mediated by AP1 (a clathrin adaptor working in the trans-golgi network and endosomes by recognizing and sorting cargo proteins into specific vesicles) and Arfrp1 (a protein related to the Arf family of small GTPases, which are involved in coat protein assembly during vesicular trafficking[92]) as these molecules have been shown to be required for the trafficking of Vangl2 from the trans-golgi network to the plasma membrane in mammalian cells[93]. In addition, AP1 and Arf1 have been shown to be required for proper Fz trafficking and planar polarization in Drosophila and Zebrafish[94]. More recently, Strutt et al. also found that the retromer complex, a master regulator of endosomal recycling, promotes the junctional localization of Vang and Fmi in the Drosophila wing, further supporting a role of PCP proteins recycling in PCP establishment and maintenance (Strutt 2019[95]).

Finally endocytosis has been shown to have a role in the maintenance of PCP protein asymmetry in proliferative tissues. In the developing mouse epidermis, PCP components are internalized and redistributed during mitoses, which is required for hair follicle planar polarization: upon mitosis, Celsr1 phosphorylation by polo-like kinase 1 promotes its endocytosis along with its associated Fzd[72].

4) Polarized microtubule trafficking and PCP protein asymmetry

Subapical, non-centrosomal microtubule arrays oriented along the polarity axis have been found in many planar polarized epithelia [74 96 97] (Figure 8). These microtubules have been shown to allow the directional trafficking of Fz, Fmi and Dsh comprising vesicles in Drosophila pupal wings [98 99 100], which could serve to amplify asymmetry or provide the initial polarity bias by removing proximal Fmi-Fz-Dsh complexes and transporting them to the distal side. However microtubules don't seem to be required for the maintenance of this asymmetry[101 102], although a recent study showed that they are required for Vangl2 anterior localization maintenance in zebrafish floor-plate cells (Mathewson 2019[103]). Reciprocally, PCP proteins have been shown to be required for microtubule polarization, suggesting the existence of a feedback loop between microtubule orientation and PCP protein asymmetric localization[74 99 104].

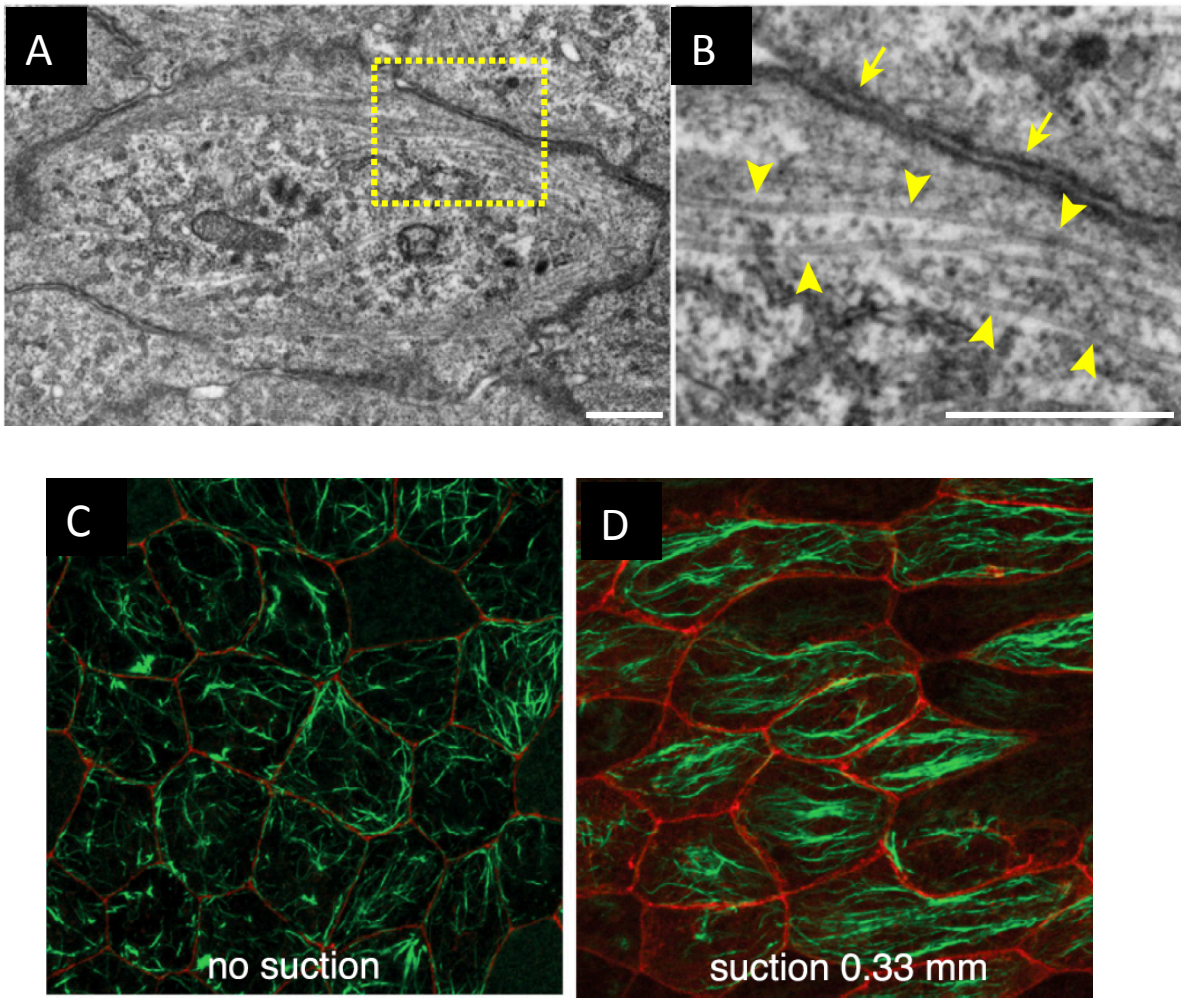

Figure 8 Oriented apical microtubule network in planar polarized tissues

(A) EM image of Drosophila wing cells showing apical microtubules oriented along the proximo-distal axis of the wing (proximal is left, scale bar 500nm)

(B) Close up on the region highlighted in (A). Yellow arrowheads point at proximo-distally oriented microtubules and yellow arrows at cell-cell junctions (scale bar 500nm)

(C) Apical microtubule network (green) in a Xenopus ectodermal explant showing no preferential orientation

(D) Apical microtubule network in a Xenopus ectodermal explant submitted to a right-left oriented succion force: apical microtubule are oriented along the succion axis.

(A)/(B) adpated from Harumoto 2010

(C)/(D) adapted from Chien 2015

5) Ubiquitination and proteasome-mediated degradation regulate PCP

Regulation of PCP protein levels, which is crucial for asymmetry establishment, has been shown to depend on ubiquitin ligases and the proteasome in several systems. It was first shown that the Smurf1 and Smurf2 ubiquitin ligases trigger proteasome-mediated Pk1 degradation and thus play a role in PCP in the mouse neural tube and cochlea [105]. Mice mutated in both Smurf1 and Smurf2 display PCP defects which are associated with a disruption of Pk1 asymmetric localization in the cochlea and the floor-plate. Interestingly, Smurfs can interact directly with Dvl[105], suggesting that Dvl might recruit Smurf to one side of planar polarized cells to trigger local degradation of Pk1 and thus its asymmetric localization. In the Drosophila pupal wing, it was shown that a Cullin-3-Diablo/Kelch ubiquitin ligase regulates Dsh and Fmi levels at cell-cell junctions and is required for PCP establishment[106]. Moreover, in addition to recruiting Pk to the plasma membrane, Vang also promotes its proteasomal degradation, probably via Cullin-1 mediated Pk ubiquitination, which is required for PCP establishment[107] [90]. These mechanisms have been proposed to regulate PCP establishment by controlling the feedback amplification of asymmetry. Finally it was recently shown in Drosophila eye and wing that APC/C (Anaphase Promoting Complex/Cyclosome) can regulate the levels of the Nek2 kinase which phosphorylates Dsh and triggers its proteasome-mediated degradation, thus regulating Dsh levels and allowing proper PCP establishment[108].

B) Cues orienting PCP at the tissue scale

Although the mechanisms described above can account for asymmetry establishment in single cells and local propagation of asymmetry in neighboring cells, global cues are required for PCP coordination and orientation at the tissue scale. Three types of global cues have been proposed: the Fat/Dachsous/Four-jointed (Ft/Ds/Fj) system, Wnt ligands and mechanical forces.

1) The Fat/Dachsous/Four-jointed system

Fat and Dachsous are protocadherins that were first found to regulate the growth of Drosophila imaginal discs via the Hippo pathway[109]. It was later discovered that Ft and Ds have a role in PCP in Drosophila. Like core module components, Ft and Ds are asymmetrically localized in cells of planar polarized epithelia and are required for PCP coordination at tissue scale. In Drosophila wings, Ds is expressed in a decreasing proximo-distal gradient. Conversely, there is a decreasing Disto-proximal gradient of Four-jointed (Fj) expression: Four-jointed is a Golgi-resident kinase that can phosphorylate both Ft and Ds, but with opposing effects. Ft phosphorylation by Fj leads to an increased affinity of Ft for Ds in adjacent cells, whereas Ds phosphorylation by Fj leads to a decreased affinity of Ds for Ft. Thus, the Fj gradient produces a decreasing disto-proximal Ft affinity gradient that is complementary to the Ds gradient[110] (Figure 9A). The interaction of these gradients results in the asymmetric localization of Ft and Ds on opposite sides of epithelial cells[111]. The Ft/Ds can orient sub-apical non-centrosomal microtubules along the polarity axis and it has been shown that the core PCP component Fz can be transported distally in Drosophila wing cells along such microtubules[98]. Indeed, as mentionned previously, Ft/Ds orient apical microtubules along the proximo-distal axis of Drosophila pupal wing, and this is required for Dsh trafficking to the distal side of wing cells[100]. Thus the Ft/Ds/Fj pathway could create a bias of core PCP components localization that would then be amplified by the "feedback amplification of asymmetry" described above. Intriguingly, the relative position of the Ds/Ft and core PCP systems within the cells of planar polarized epithelia varies between tissues in Drosophila. In the wing, cuticular hairs point distally and Vang-Pk localizes proximally, where there is the highest amount of Ds, whereas in the abdomen, cuticular hair point posteriorly and Vang-Pk localize anteriorly away from high Ds. It was shown that Ds can influence PCP in these tissues in the same way thanks to the existence of two different Pk isoforms, Pk and Sple (Spiny Legs)[99 112]. In the wing, the Pk isoform is more abundant and allow the Ds gradient to orient microtubule plus ends with a distal bias (away from high Ds), whereas in the abdomen, the Sple isoform is more abundant and allow Ds to orient microtubules plus ends with a posterior bias (toward high Ds)[99 113] (Figure 9B). Overexpression of Sple in the wing or Pk in the abdomen leads to a spectacular complete polarity reversal[99]. However it was recently shown that these Pk

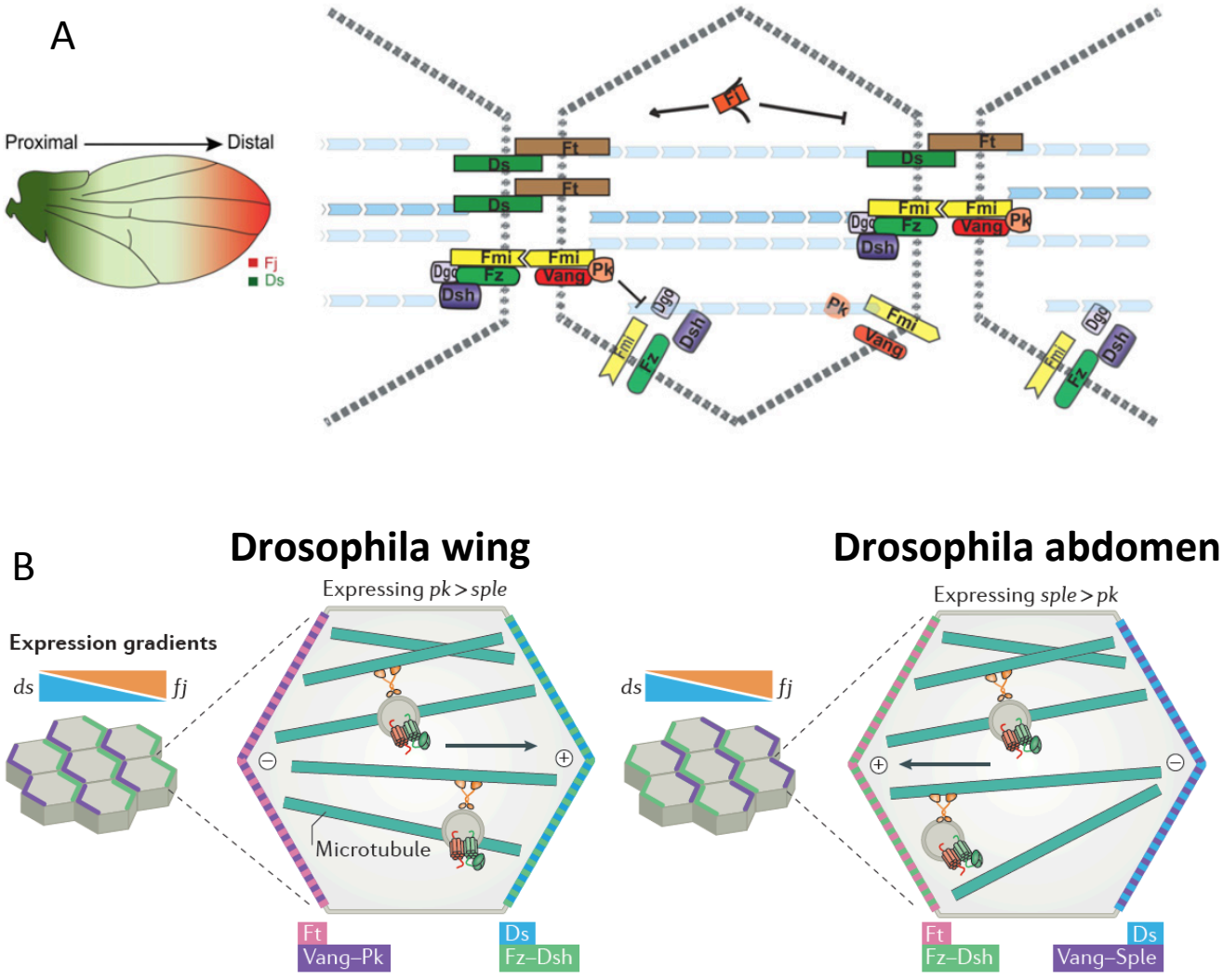

Figure 9 Role of the Fat/Dachsous/Four-jointed system in Drosophila PCP

(A) Fj and Ds opposite gradients in Drosophila wing results in opposite gradients of Ft and Ds (Adapted from Matis 2013)

(B) Asymmetric localization of core PCP proteins relative to Ft and Ds depends on Pk isoforms. In Drosophila wing (left), the pk isoform is more abondant and Vang-Pk localize on the Ft side. In the Drosophila abdomen (right), the sple isoform is more abondant and Vang-Sple localize on the Ds side. (Adapted from Butler 2017)

isoforms control PCP through microtubule polarization only in the proximal wing and the anterior abdomen, whereas in the distal wing and the posterior abdomen they act through a microtubule-polarization-independent mechanism. In addition, the Ds/Ft/Fj system can act independently of the core PCP system[114]. Thus the influence of the Ft/Ds/Fj system as a global polarizing cue upstream of the core PCP remains debated. The role of the Ft/Ds/Fj system in PCP in vertebrate is much less clear, although some studies have shown a role of Fat4 (a Ft orthologue) in PCP-related processes (for example oriented cell divisions in the kidney[115] or in pre-chondrogenic mesenchyme[116]).

2) Wnt

Wnts are secreted glycoproteins that are specific to the metazoan lineage[117]. They are involved in many developmental processes, and their role in primary body axis patterning is conserved across metazoan[118], with higher Wnt expression at the blastopore. Wnt ligands palmitoylation make them hydrophobic and therefore prevent their diffusion in the extracellular space over long distances; rather, they act on target cells at short range, and it was shown in some cases that this involves long membrane protrusions called cytonemes[119]. It has been shown in cultured cells that some Wnt ligands can induce both asymmetric cell fate and orient the mitotic spindle (Figure 10A), which led to the hypothesis that Wnt allowed the emergence of a coupling mechanism between these two processes that are key in metazoan development[117 120]. A potential link with the core PCP pathway came from the fact that Fz are Wnt receptors. In addition, since many Wnt are expressed in a graded fashion, they were good candidates for providing a global cue for PCP orientation. It was first shown that in Zebrafish, Wnt5a and Wnt11 regulate convergence extension (CE, a process that depends on core PCP components in vertebrates, see below) during gastrulation[121 122]. However in this case, the CE defects could be rescued by global expression of Wnt, arguing against the role of a local Wnt source. However a Wnt activity gradient could still be generated by other mechanisms, such as extracellular trapping by Sfrps (Secreted Frizzled Related Proteins).

Indeed, in the mouse inner ear, Wnt5a is expressed in a gradient that is complementary to a gradient of the Wnt inhibitor Sfrp3 (Soluble Frizzled Related Protein 3) and is

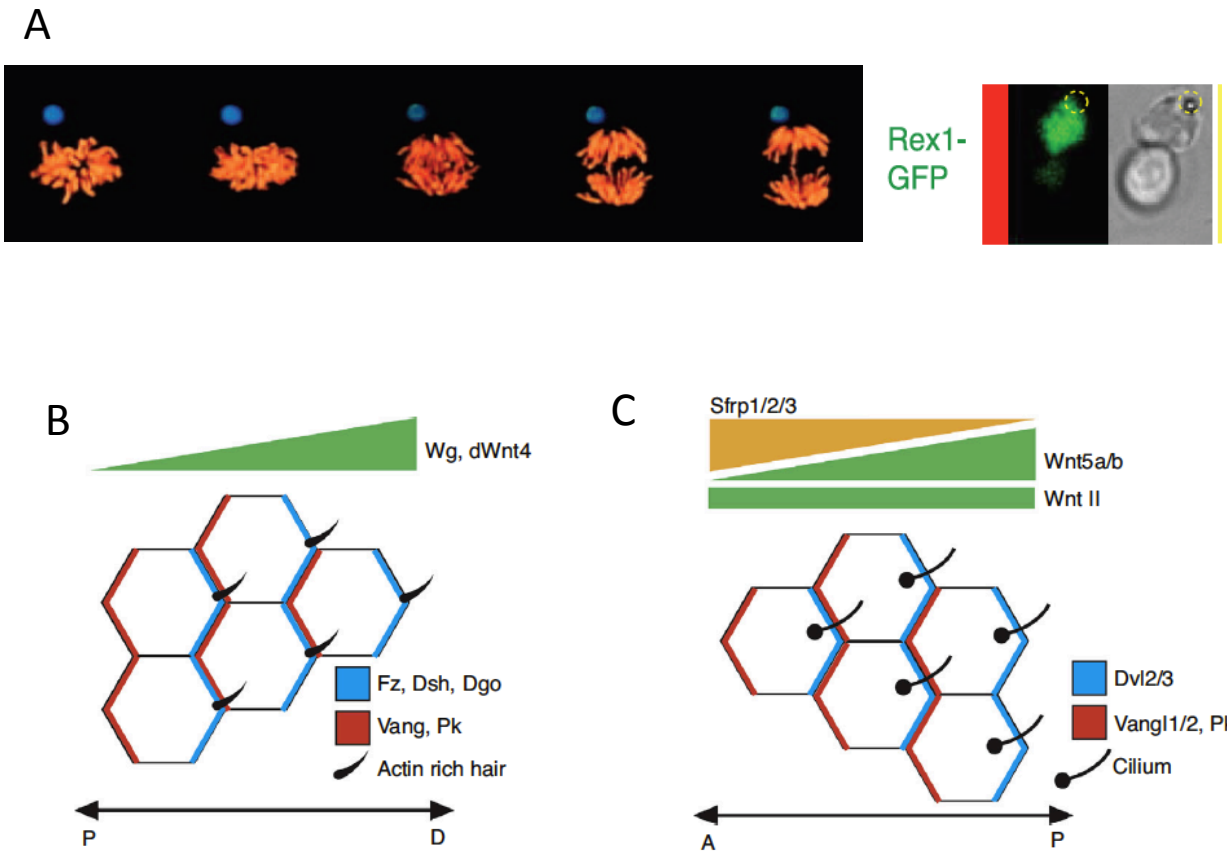

Figure 10 Wnt ligands as directional cues

(A) Wnt3a beads can both orient the axis of division (left, bead: blue dot, orange: DNA) and drive differential gene expression in daughter cells (left; bead: yellow dotted circle). (Adapted from Habib 2013)
(B) Wg and dWnt4 act redundantly to direct PCP in Drosophila wing
(C) Opposing gradients of Wnt ligands and Sfrps direct PCP in the mouse node

(B)/(C) Adapted from Humphries 2018

required for proper cochlea elongation via CE. In addition, Wnt5a cooperates with Vangl2 (a Vang ortholog) to properly orient sensory hair cells in this system[123]. Similarly, in the mouse embryonic node, in which planar polarization is required for left-right axis establishment[124], Wnt5a and Wnt5b are expressed on the posterior side of the node, whereas the Wnt inhibitor Sfrp1,2 and 5 are expressed on its anterior side (Figure 10C). In this system it was shown that both Wnt ligands and their inhibitors are required for core PCP components asymmetric localization, and that uniform expression of the Wnt ligands or their antagonists can not rescue the absence of these molecules, demonstrating an instructive role of Wnts and their inhibitors for the node antero-posterior planar polarization[125]. It was also shown that in the mouse limb, Wnt5a is expressed in a graded fashion, with more Wnt5a present at the distal part of the limb. This results in higher levels of Vangl2 phosphorylation at the distal part of the limb, which translates into stronger asymmetric localization of Vangl2 in chondrocytes. This planar polarization of chondrocytes is required for proper proximo-distal extension of the limb. Interestingly, this effect of Wnt5a on Vangl2 phosphorylation is mediated by an atypical Wnt receptor called Ror2[126]. An instructive role for Wnt ligands in vertebrate has also been suggested in Xenopus embryo early ectoderm, where Wnt5a, Wnt11 and Wnt11b ectopic expression can direct the asymmetric localization of Pk3 and Vangl2 fluorescent construct and ectopic Wnt11b can redirect the polarization of endogenous Vangl2[127], although it is not known whether endogenous Wnt do play this role or even if they are present in a graded fashion in this system.

Finally, in the Drosophila wing, it was long assumed that Wnt didn't have any effect on PCP because individual Wnt mutants did not present PCP phenotypes until it was found that Wg acts redundantly with Wnt4 to orient PCP towards the pupal wing margin[128]. Wg and Wnt4 form a decreasing gradient from the wing margin, and Wg or Wnt4 mis-expression causes PCP defects that are reminiscent of Fz loss of function, which suggests that Wg negatively regulates Fz, perhaps by competing with Vang for Fz binding (Figure 10B). Indeed, Wg can prevent Fz binding to Vang in cultured Drosophila cells[128].

All these studies suggest that Wnt proteins can have an instructive role on global PCP both in vertebrates and Drosophila.

3) Mechanical forces

Mechanical forces generated during morphogenesis have been proposed either to reorient PCP or to initiate it. It was first shown that in the Drosophila wing, anisotropic forces exerted by the wing hinge leads to a pattern of cell elongation, cell divisions and cell rearrangements that results in proximo-distal wing elongation which reorients PCP from its initial wing-edge-pointing state to a proximo-distal orientation[129] (Figure 11A). Interestingly, these forces might be transduced by Ds, since mutations in this gene leads to PCP defects due to a modified epithelial dynamics[129]. In the Drosophila thorax, Ds has also been shown to affect epithelial dynamics by recruiting the myosin Dachs to promote asymmetry of junctional tension[130].

In the mouse skin, it was also shown that forces (probably originating from anisotropic growth of different parts of the embryo) can reorient the global PCP field. In this system, force relaxation through cell rearrangement creates new cell-cell junctions where Celsr1 (a Fmi ortholog) is slow to accumulate, which results in the global alignment of Celsr1 enriched cell-cell interfaces[64] .

Similarly, it was shown that in Xenopus embryo larval skin, a planar axis arises during gastrulation, with the appearance of an oriented apical microtubule network and more stable PCP protein accumulation at cell/cell junctions that are perpendicular to the antero-posterior strain experienced by cells during gastrulation. This mechanical strain is sufficient to define the planar axis, since exogenous strain applied on skin explants have similar effects on cell elongation, apical microtubule polarization and stable PCP protein accumulation at junctions orthogonal to the applied strain[104]. In this system, there seems to be a feedback relationship between apical microtubules orientation and PCP proteins asymmetric enrichment, since Fzd3 or Celsr1 morpholino (MO) mediated knock-down prevents apical microtubule alignment and nocodazol (a microtubule depolymerizing drug) prevents stable PCP accumulation at cell/cell junctions orthogonal to the polarization axis. Together with the observation that applied strain is sufficient to polarize the apical microtubule network, this suggests a model where mechanical strain initially creates a microtubule orientation bias that allows the initiation of PCP components asymmetric positioning that will reinforce their own asymmetry (by the feedback amplification mechanisms described earlier) and microtubule orientation[104], which is reminiscent of the mechanism proposed in some

A

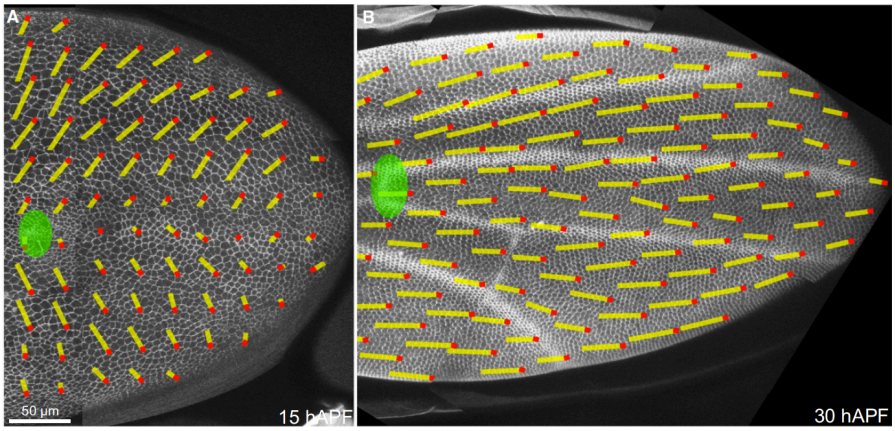

B

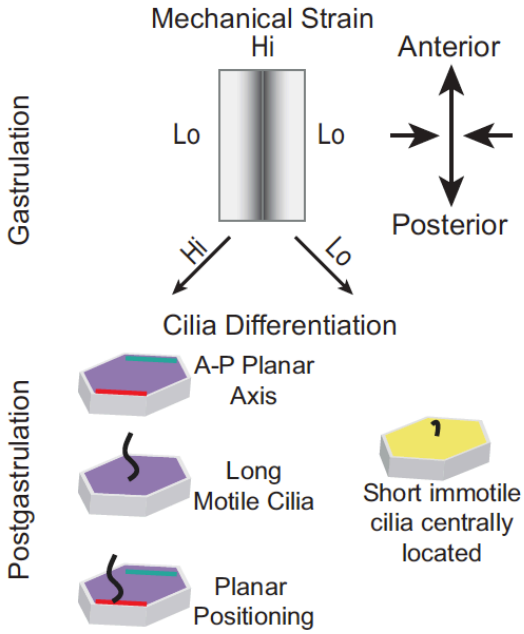

Figure 11 Mechanical forces in planar polarity

(A) Reorientation of wing cells polarity axis during wing growth. Cells express Vang-GFP. Green dot: anterior crossvein. Yellow bars and red dots represent the polarity of local groups of cells (Adapted from Aigouy 2010)
(B) Mechanical stress applied on Xenopus left/right organizer directs PCP protein localization and cilia off-centering and growth (adapted from Chien 2018)

systems for the relationship between the Ds/Ft/Fj system and the core PCP system via apical microtubule orientation. Another study from the same group recently showed that strain can also establish a polarization axis in the Xenopus embryo left-right organizer (LRO): applied strain on LRO explants can both trigger PCP protein enrichment at cell/cell junction orthogonal to the applied strain and direct cilia asymmetric positioning and length[131] (Figure 11B). However directly testing the role of mechanical forces in an intact embryo remains technically challenging; it will be important to identify the endogenous force generators and to test their effect on PCP establishment in vivo.

C) Functional planar polarization

Once the asymmetric localization of PCP protein is established, how is it transduced to functionally polarize cells? The best mechanistic insights come from the asymmetric positioning of actin-based hairs (trichomes) in Drosophila wing cells, but the importance of PCP proteins has also been shown in various other processes, for example oriented cell divisions in Drosophila and vertebrates, convergence extension, axon guidance and cilia-beating orientation in vertebrates, although in these cases, the mechanisms that link PCP proteins to the cytoskeleton to functionally polarize cells are not as clear.

1) Asymmetric trichome positioning

In Drosophila wing, each cell grows an actin-based hair (trichome) that points distally. It has been shown that the proximal Vang-Pk complexes can recruit the proteins Inturned, Fuzzy and Fritz[132 133], which in turn activate Multiple-wing-hairs (Mwh), an actin regulator that inhibits trichome growth[133 134]. Interestingly, Mwh initially accumulates proximally, thus restricting trichome initiation to the distal part of the cell, but it also later accumulates within the trichome itself, probably to promote the fusion of actin bundles and inhibit the formation of extra hairs[134 135] (Figure 12).

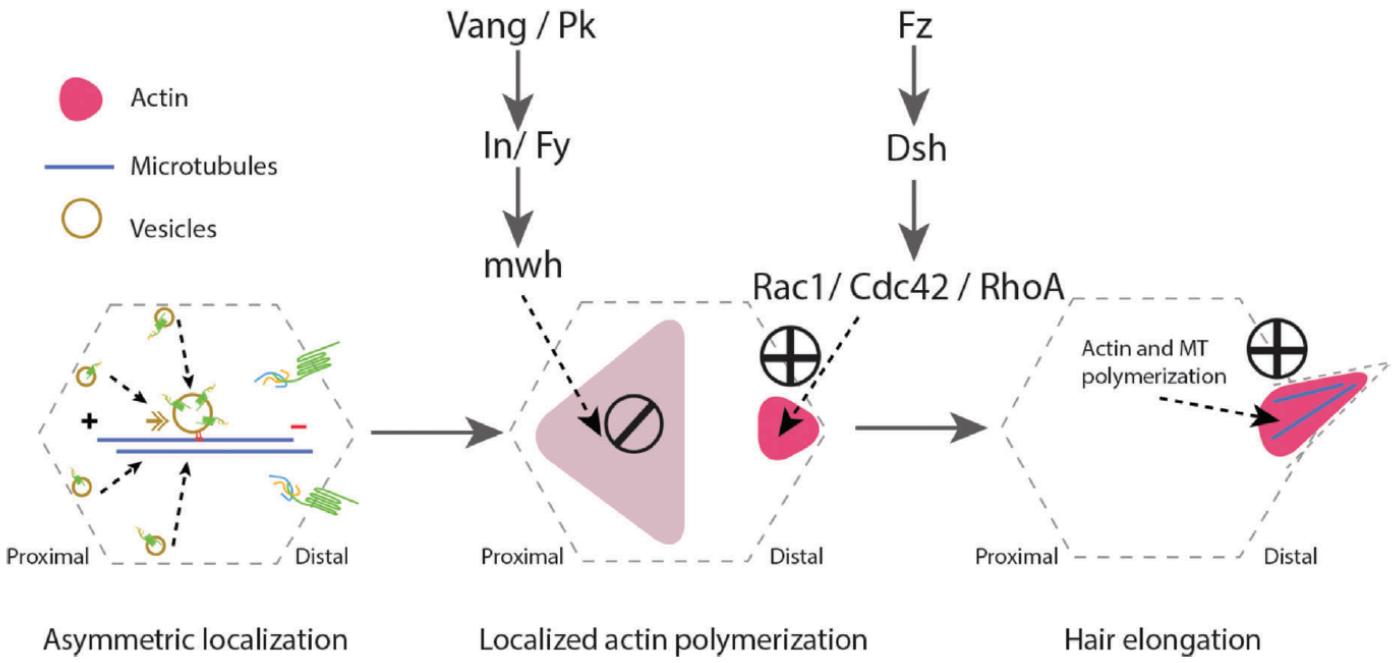

Figure 12 PCP proteins regulate actin dynamics in Drosophila wing cells

Vang/Pk inhibit actin dynamics via mwh on the proximal side while Fz/Dsh promote actin polymerization and trichome growth via RhoGTPases on the distal side.

Adapted from Carvajal-Gonzalez 2016

2) Oriented cell division

Studies in the Drosophila SOP (cf part I, Figure 3) have shown that PCP proteins orient its division along the antero-posterior axis. Disrupting PCP protein in this system randomizes the orientation of mitosis[136] [137]. PCP proteins break the symmetry of PAR complex components in interphase[138], which is required for proper asymmetric division[139]. Fz and Dsh have been shown to orient the spindle via Mud/NuMA both in Drosophila SOP and in Zebrafish[140]. In addition, in SOP, Strabismus orients the spindle by promoting Pins anterior localization[141]. Since Pins also recruits Mud at the anterior cortex, there is a redundancy between Vang and Fz for spindle orientation[137]: Mud is both anterior and posterior and pull on the spindle from both sides to orient it along the anterior-posterior axis. Interestingly, the Ft/Ds/Fj system has also been shown to orient cell division in Drosophila wing and thorax by controlling the asymmetric localization of the atypical myosin Dachs which controls cell shape[142] [130]. In Zebrafish Wnt11, Dvl and Vangl2 have been shown to orient mitotic spindle along the animal-vegetal axis during gastrulation[143], which contributes (although weakly) to axis elongation. Finally the PCP pathway-mediated division orientation is important for organ elongation, for example in the chick limb cartilage[144] and in the mouse forestomach (Matsuyama 2009[145]).

3) Convergence and extension

The first studies on PCP proteins in vertebrates demonstrated that they are involved in convergence extension movements[146], which together with oriented cell division contributes to tissue elongation during morphogenesis, for example during gastrulation, neurulation and elongated organ morphogenesis. Similar to what has been shown in static epithelia, PCP proteins adopt asymmetric localizations in cells undergoing convergence and extension. For example, Pk localizes anteriorly and Dvl posteriorly in presomitic mesodermal cells undergoing convergent-extension during gastrulation in Zebrafish[147], and Pk localizes anteriorly in Xenopus neural plate cells during convergence and extension[148]. The asymmetric localization of PCP proteins is probably important for their function in convergence and extension since both loss and gain of function disrupt their function in this process[149]. The mechanisms linking PCP proteins to cell rearrangements are not yet clear, but some studies have pointed to a link with

acto-myosin contraction at specific cell-cell junctions, allowing cell intercalation and thus convergence and extension. In the mouse neural plate, Celsr1 and Dvl cooperate with the formin DAAM1 and the PDZ-RhoGEF at cell-cell junctions orthogonal to the axis of elongation (in this case, the antero-posterior axis) to up-regulate Rho kinase that activates myosin and leads to the contraction of these junctions that allow cell rearrangement and convergence extension[150]. These acto-myosin contractions also promote apical constriction, and together this allows the proper bending of the neural plate to form the neural tube: this could explain the neural tube closure defects seen in PCP mutants, where the neural tube fail to close from the hindbrain to its posterior end, a defect called craniorachischisis and also found in humans[150]. Similarly, in Xenopus embryo mesenchymal cells undergoing convergence extension during gastrulation, Fritz and Dvl are required to position septins at cell-cell junctions orthogonal to the axis of tissue elongation. Septins restrict acto-myosin contraction at these junctions, leading to cell rearrangement and convergence and extension[151]. (PCP also regulate apical constriction in this system, and Vangl2 is required for proper apical constriction during blastopore formation[152].). A recent study by the same group showed that during Xenopus embryo dorsal ectoderm extension, convergence-extension depends on alternative acto-myosin contraction in neighboring cells within an optimal frequency range; these acto-myosin oscillations depend on the PCP protein Pk2 (Shindo 2019[153]).
Other studies also suggest a role for polarized cell protrusion that would exert traction forces on neighboring cells during convergent-extension (Shih 1992, Keller 2000). However, evidence for the involvement of these protrusions in the embryo and their link to PCP proteins is scarce. It has for example been shown that polarized cell protrusions perpendicular to tissue extension in Keller explants depend on Dvl activity (Wallingford 2000).

It is interesting to note that PCP proteins (Vangl2, Pk and Dvl) are also required for another form of cell rearrangement in Xenopus, radial cell intercalation, which plays a key role in the ectoderm during gastrulation and neurulation[154]. Finally, PCP proteins are also involved in convergence and extension during vertebrate organogenesis: for example, Xenopus embryo kidney tubules elongation depends on a myosin-mediated rosette-based mechanism, and Wnt9b perturbation or a dominant negative form of Dvl

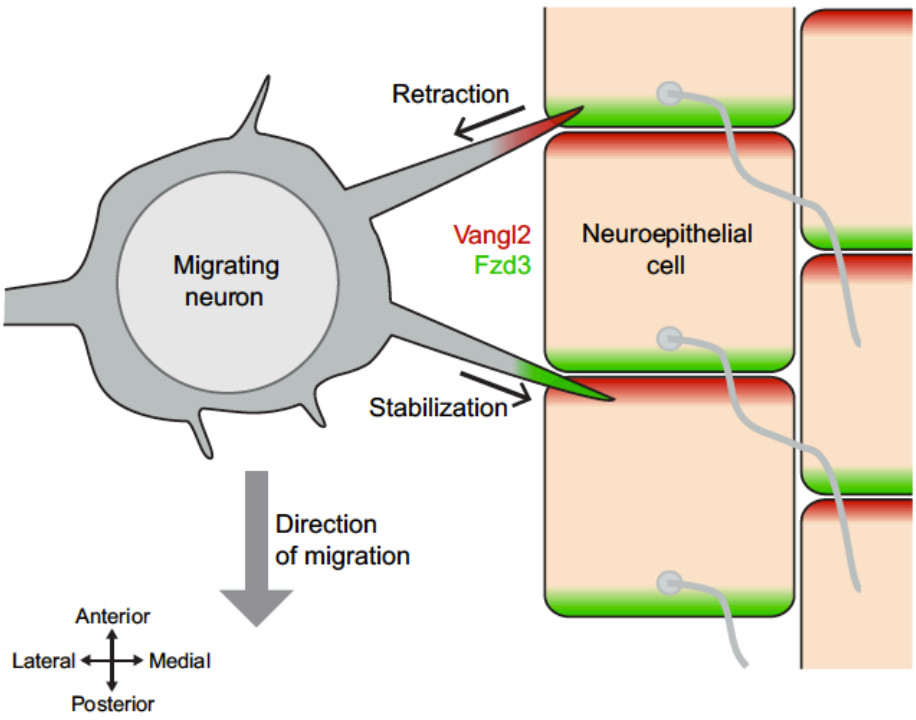

Figure 13 Role of PCP proteins in FBMN migration

Within migrating FBMN (Facial BranchioMotor Neurons), Vangl2 (red) antagonizes Fzd3 (green) and destabilizes filopodia. In contrast, Vangl2 in neuroepithelial cells such as floor-plate cells stabilizes FBMN filopodia.

Adapted from Davey 2017

that specifically affects the PCP pathway and not the Wnt canonical pathway (Xdd1) disrupt rosette topology and orientation, leading to tubule elongation defects[155].

4) Axon guidance and neuronal migration

Commissural axons of the dorsal neural tube first project ventrally, guided by molecules secreted by the floor-plate, and then cross the midline and turn to migrate anteriorly. In the hindbrain, this second turning step depends on PCP proteins such as Fz3, Vangl2 and Celsr3[156 157], and a cell-autonomous requirement has been demonstrated for Celsr3[158]. Fz3 and Vangl2 localize at the tip of growth-cone filopodia and Vangl2 seems to regulate Fz3 endocytosis that is more likely to happen at higher Wnt5a ligand concentration[158], which in the embryo would correspond to the anterior side. However it is still unknown how Wnt, Fz and Vangl have an impact on the cytoskeleton to trigger axon turning.

PCP proteins are also involved in neuron migration, and this has been mainly demonstrated through the study of Zebrafish facial branchiomotor neurons (FBMNs) that are born in the 4th rhombomere of the hindbrain and then migrate posteriorly along the floor-plate to reach the 6th and 7th rhombomeres[159]. Although the role of Wnt ligands is not yet clear, in zebrafish this migration depends on Vangl2[149 160], Pk1[161], Fzd3[162], Dvl [163]and Celsr1,2,3[162]. Similar results have been obtained in mouse, although not for Dvl. Interestingly, in Zebrafish, Vangl2 and Fzd3 are required in the migratory environment (the floor-plate) and Vangl2 and Fzd3 are also required within FBMNs, where Vangl2 localizes transiently at the tip of FBMN filopodia, but with opposite impact on FBMN migration (Figure 13). Within FBMNs, Vangl2 antagonizes Fz3 and destabilizes filopodia, whereas in floor-plate cells, Vangl2 antagonizes Fz3 and stabilizes filopodia[163]. The interactions between FBMN Vangl2 and floor-plate Fz3 destabilize filopodia whereas interactions between FBMN Fz3 and floor-plate Vangl2 stabilize them. Together with the anterior localization of Vangl2 and posterior localization of Fz3 in floor-plate cells, these interactions favors posterior filopodia dynamics within FBMN and therefore direct their migration towards the more posterior rhombomeres.

5) Cilia and centrosome positioning and orientation

One major evolutionary conserved output of PCP is the asymmetric/oriented positioning of centrosomes and the cilia that are often associated with them[164]. The links between PCP and centrosome/cilia positioning will be discussed in detail in the next chapter.

D) Roles of PAR, Crumbs and Scribble complexes in PCP

Since PCP proteins are localized at apical cell-cell junctions in epithelia, it seems obvious that apico-basal polarization, in which the PAR, Crumbs and Scribble complexes are involved, is a prerequisite for PCP protein asymmetric localization and PCP establishment. However, several studies have shown that it is not only a permissive requirement: in the Drosophila eye, which displays a striking planar polarization of ommatidial cells, the Crumbs complex member Patj binds to Fz and limits its action, probably via aPKC, in some ommatidial cells and not in others. Interestingly, Bazooka (Baz, a Par3 ortholog) antagonizes the action of Patj and aPKC[165]. Moreover, in Drosophila wing, Baz overexpression doesn't affect apico-basal polarization but leads to a failure to restrict Fmi to the proximal and distal membranes, and Baz interacts directly with one of the two Fmi isoforms present in the wing[166]. Finally, in mouse neural tube cells, Scribble1, a member of the Scribble complex, is required for Par3 and Vangl2 apical localization, although Scribble1 mutants don't display severe apico-basal polarization defects[167].

In addition, and more intriguingly, several components of the apico-basal polarity complexes (the Par, Crumbs and Scribble complexes) have been shown to be downstream effectors of PCP proteins. In Drosophila SOP, PCP proteins are required for the asymmetric localization of Par proteins along the antero-posterior axis[138]. It has been shown recently that Meru, a RASSF9/RASSF10 orthologue, is recruited to the posterior cortex by Fz/Dsh and recruits Baz[168]. In addition, in Drosophila SOP, Vang colocalizes at the anterior cortex with the Scribble-complex-member Dlg, and Vang and Dlg recruit Pins to orient cell division[141 35]. Interestingly, in some ommatidial cells, Baz

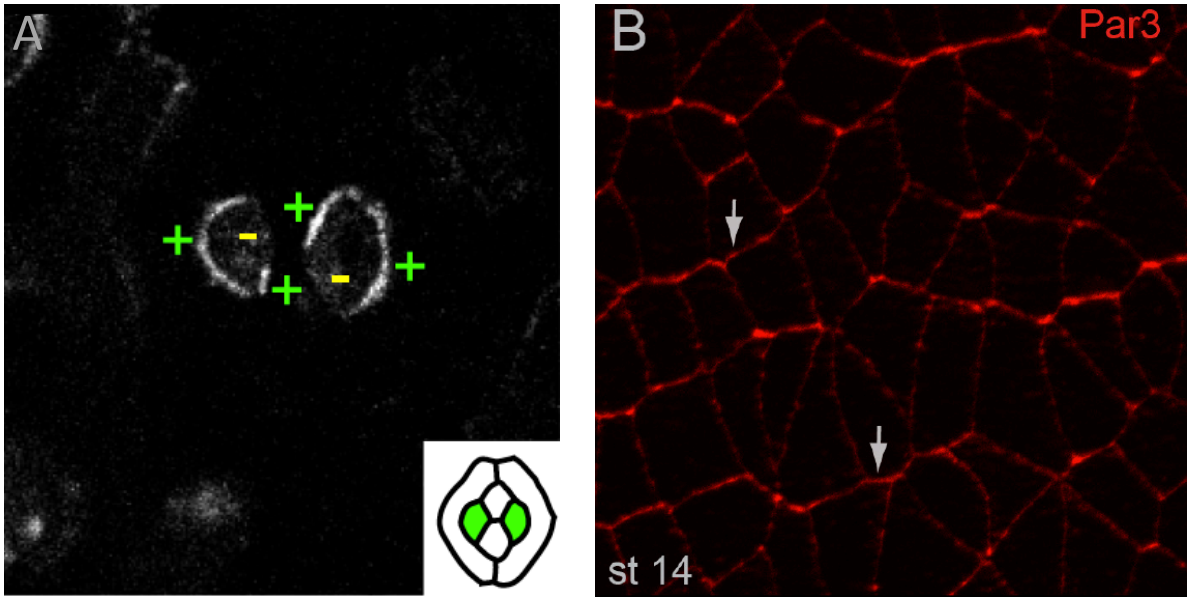

Figure 14 Par3 planar polarization in Drosophila and Xenopus

(A) Par3 asymmetric planar polarization in cells of the Drosophila ommatidia mosaically expressing Par3-GFP (green « + » correspond to Par3-positive cell-cell contacts and yellow « - » to Par3-negative cell-cell contacts) (adapted form Aigouy 2016)
(B) Par3 planar polarization in Xenopus embryo neural plate visualized by immunostaining against endogenous Par3. Arrows point at Par3 enrichment on medio-lateral membranes. Whether Par3 assumes an asymmetric localization in this system is unknown (adapted from Chuykin 2018)

displays an asymmetric localization that depends on Fmi, but this time Baz colocalizes with Vang and partially with Dlg[169] (Figure 14A). Thus, the relationship between the asymmetric localization of PCP proteins and the asymmetric localization of Par, Crumbs and Scribble complexes components seems to be cell-type dependent. Interestingly, Par3 is also planar polarized downstream of Vangl2 in Xenopus embryo neural plate (Chuykin 2018[170]) (Figure 14B), although in this case it is not known whether it is anteriorly or posteriorly enriched. Reciprocally, Par3 interacts with Pk3 and is required for Vangl2 planar polarization.

Finally, Scribble has also been involved in PCP. Scribble binds to Vang in Drosophila eye and wing and likely acts as one of its effectors in PCP establishment[171]. In mice, Scribble1 mutants (*circletail*) display craniorachischisis[172] and mild PCP defects in the cochlea[173] and Scribble1 genetically interacts with Vangl2: Vangl2/Scribble1 double heterozygous mutants display PCP defects in the cochlea that closely resemble those seen in Vangl2 homozygous mice[173].

Reciprocally, some PCP proteins have been involved in other forms of polarization: for example, Pk1 is required for epiblast apico-basal polarity in mice (Tao 2009[174])

We have seen in this part that PCP establishment is similar to other forms of polarization described earlier, as it requires a polarization cue and rely on positive and negative interactions between its components. PCP relies on a specific subset of molecules that have very few described roles outside of PCP. However it is now beginning to emerge that other polarity proteins, such as the proteins of the PAR/Scribble/Crumbs complexes interact with PCP proteins and also have a role in PCP. In the following section, we will see that a widely conserved role shared by PCP proteins and other polarity proteins is to position centrosomes, basal bodies and cilia.

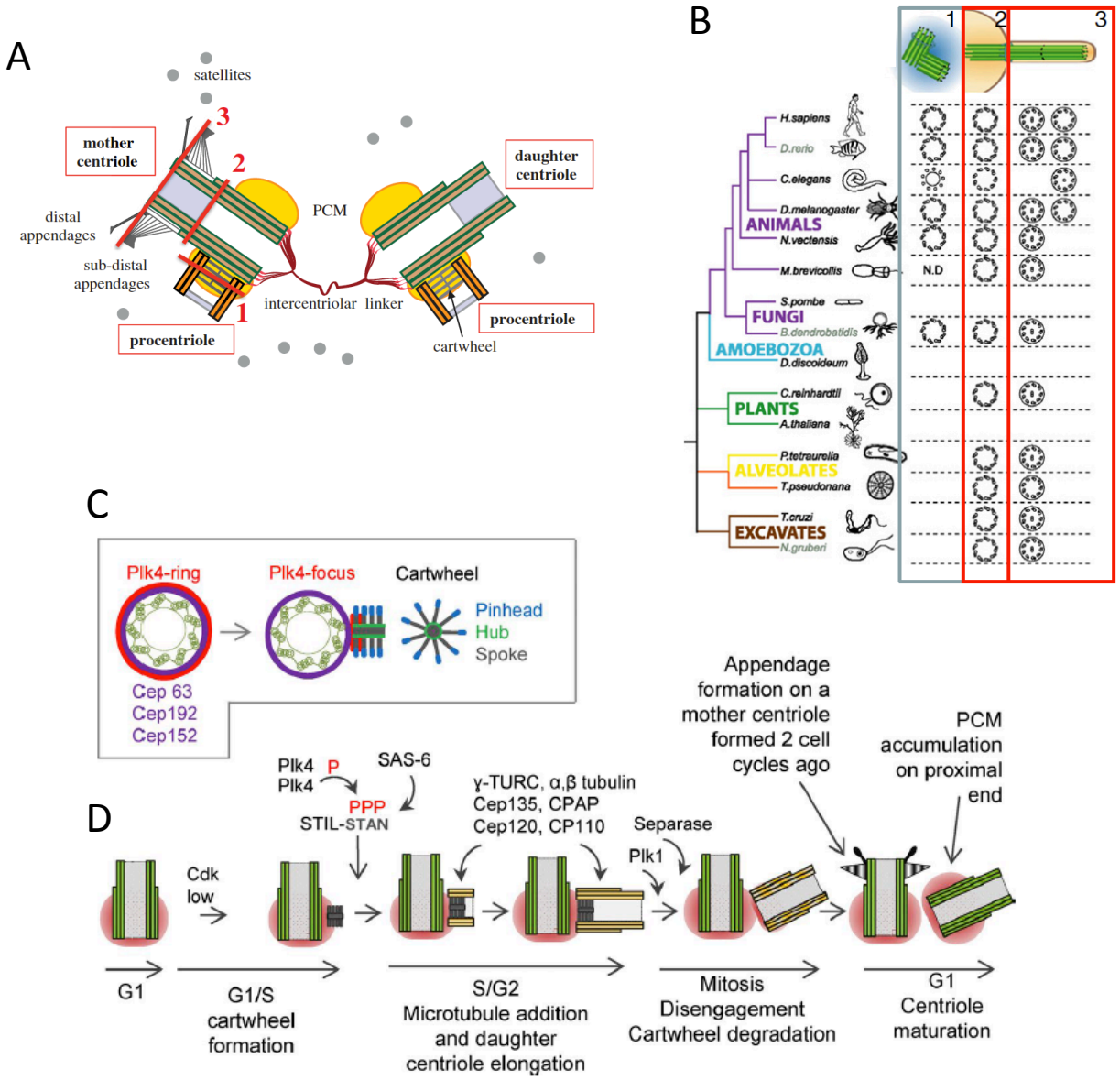

Figure 15 Centriole structure, evolution and duplication

(A) Schematic showing mother and daughter centrioles with some associated peri-centriolar matrix (PCM) (adapted from Bornens 2014)

(B) Eukaryote phylogenetic tree showing the presence or absence of centrosome (green rectangle), basal bodies (middle red rectangle) and axoneme (right red rectangle) (adapted from Bettencourt-Dias 2013)

(C) Localization of Plk4 during centriole duplication

(D) Molecules involved in centriole duplication during the cell cycle

(C) and (D) adapted from Loncarek 2018

III- Links between centrosomes, cilia and cell polarity

A) Structure and function of centrioles, centrosomes and cilia

1) Organisation and composition of Centrioles

Centrioles are microtubule based structures found in most eukaryotic cells, although they are absent in angiosperms, some fungi (including yeast), Amoebozoa and Alveolates[175] (Figure 15B). They usually have a nine-fold symmetry, with 9 microtubule triplets arranged in a circular fashion, but other atypical structures have evolved, mostly in insects[176]. Centrioles are usually found by pair in eukaryotic cells, with one centriole, the « daughter » centriole having been formed in close proximity to the other, the « mother » centriole, born during the previous S phase of the cell cycle[177] (Figure 15A). This « canonical » centriole formation pathway relies upon a conserved set of proteins. In human cells, the PLK4 kinase is recruited to the side of a pre-existing centriole via CEP152 and CEP192[178]. PLK4 in turn recruits SAS6 and STIL, which form a central "cartwheel" structure with a 9-fold symmetry[179]. Finally, these proteins recruit CPAP to the outer edge of the cartwheel, where it helps assemble centriolar microtubules and controls centriole length[180] (Figure 15C,D). Centriole can also form de novo, naturally in some parthenogenetic insects but also in human cells after centriole laser ablation and this process is controlled by the same molecules as in the canonical pathway[181].
In many cells, the mother centriole docks to the membrane (the apical membrane in epithelial cells) to nucleate a cilium. This centriole is then called a basal body (see next section).

2) Organisation and composition of Centrosomes

In Metazoan, in some Fungi, brown algae and Plasmodiophorids, centrioles can recruit many proteins like microtubule organizers and nucleators, cell cycle regulators, and signaling molecules, which constitute a peri-centriolar matrix (PCM). Together, centrioles and PCM are called the centrosome, and this structure is the major microtubule-organizing center (MTOC) of proliferating animal cells. Although some PCM is present in interphasic cells, much more PCM is usually recruited around centriole before mitosis (Palazzo 2000). The kinase Plk1 plays a crucial role in this centrosome maturation, by phosphorylating Pericentrin, which then recruits more PCM proteins[182]. Plk1 also phosphorylates Nek9, which in turn phosphorylates Nedd1, which then recruits γ-tubulin, which can nucleate microtubules[183].

Although the role of centrioles as cilia nucleators is well established in eukaryotes, the other roles of centrioles and centrosomes are less clear.

It was initially thought that centrioles were required for mitotic spindle formation, but it does not seem to be the case, as centriole-independent pathways for spindle formation exists. In the chromatin pathway, spindle microtubules are nucleated close to the chromatin[184]. It has even been shown that bipolar spindle can form in vitro from Xenopus egg extract around DNA-coated beads (Heald 1996). In the Augmin pathway, microtubules can be nucleated from pre-existing microtubules to form the spindle[185]. Finally in the acentriolar MTOC pathway, PCM proteins can form aggregates without centriole that nucleate and organize microtubules[186].

3) Current knowledge on the ancestral function of centrioles

Centriole seem to be required for some cell division events but not for others. For example, Drosophila early embryos require centrioles for cell divisions during the syncytial stage of development[187], but a loss of centriole after this stage doesn't affect embryonic development, and normal adult flies are formed, although they lack mechano-sensory and chemo-sensory cilia and therefore die rapidly because they can not fly and feed properly[188]. However, in these flies, mitotic spindle assembly is slow and around 30% of the asymmetric division of larval neuroblasts are abnormal, with either

misoriented spindle or failure to undergo cytokinesis[188]. Supporting a role for centrioles in Drosophila mitosis, it was shown that wing disc epithelial cells lacking centrioles exhibit slow spindle assembly, chromosome missegregation, DNA damage, misoriented division and apoptosis, and that different mechanisms can buffer the effects of centriole loss, for example via alternative microtubule nucleation pathways[189]. In addition, centrosomes are required in Drosophila male germ stem cells to properly orient the spindle, via a "centrosome orientation checkpoint"[190]. The comparison between two planarians further supports a role of centrioles/centrosomes in oriented cell divisions: the planarian *Schmidtea mediterranea* has lost many genes involved in PCM formation, and thus don't have centrosomes. In addition, cells in this species don't have centriole, with the notable exception of the ventral multiciliated cells that allow gliding motility. Early development of this species appears "anarchic" and does not rely on oriented divisions. In contrast, the closely related planarian species *Macrostomum liguano* do have centrioles and display highly stereotypical early development, a situation which correlates with a precise pattern of oriented cell divisions[191].

Interestingly, all of the 5 mice mutants that lack centrioles dye at mid-gastrulation because of the induction of massive apoptosis. This shows that murine cells, like drosophila cells, can divide without centrioles and centrosomes for several days. Furthermore, no DNA damage, multi-polar spindles or mis-segregation was evident and cell cycle length was not grossly changed contrary to some results obtained in vertebrate cell lines. This reinforces the fact that centrioles are not required for cell division and chromosome segregation. Nevertheless a 10 minutes lenghtening of prometaphase stage was observed, and was sufficient to trigger p53 expression revealing a novel "pro-metaphase checkpoint" in mice that is absent in drosophila. Mice lacking both centrioles and p53 survive longer during embryogenesis but lack cilia[192] and present strong phenotypes linked to deficient Hedgehog signaling, as seen in other ciliary mutants. Centrioles are thus required in these animals models to template a cilia (which is consistent with the fact that all organisms with ciliated cells also have centrioles). Finally, conditional removal of SAS4 function in mice cortical progenitors (Insolera 2014[193]) led to their progressive detachment from the ventricular surface. The detached cells were not impaired in their proliferative capacities, nor in their neurogenic properties but their cleavage orientation plane was completely randomized, reinforcing previous observations on the need for centrioles for oriented cell division.

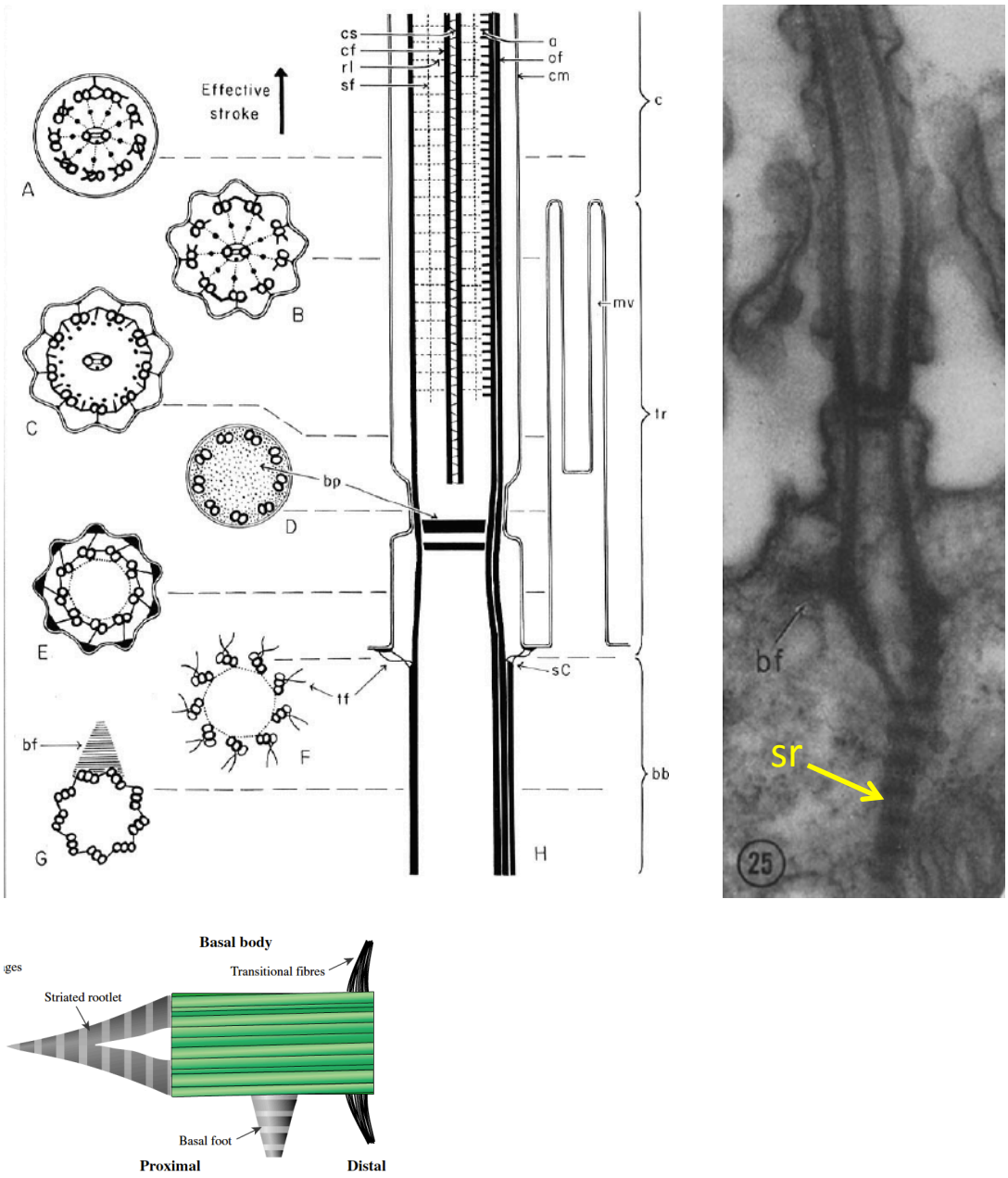

Figure 16 Structure of basal-bodies and cilia

(A) Schematic showing a basal body (bb) and associated axoneme (tr and c) with transverse sections at different levels, revealing microtubule doublets and triplets (bf: basal-foot). (from Gibbons 1961)

(B) EM image from a motile cilia of the mussel Anodonta cataracta, showing the basal-foot (bf) and the striated rootlet(sr, yellow arrow) (from Gibbons 1961)

(C) Schematic of a basal body and its appendages (from Dawe 2007)

The important role of centrioles and centrosomes in normal vertebrate development is supported by their link with various diseases. Although many tumor cells have abnormal number of centrioles, it is not yet clear whether this is a cause or consequence of the transformation process, as somatic cells can efficiently cluster or inactivate extra-centrosomes to ensure proper chromosome segregation[194]. However centrosome amplification can trigger tumorigenesis in fly[195] and a recent study in mice showed that abnormal centrosome number is sufficient to trigger tumorigenesis[196]. Despite centrosome clustering mechanisms, cells with extra-centrosomes display a low level of chromosomal instability that could favor tumor development[197].
There is a much stronger genetic link between centriole assembly pathway defects and microcephaly or dwarfism, as these diseases have been linked to defects in almost all centriole-formation genes in humans[198]. Brain organoïds derived from patients with centriole-formation defects are much smaller than normal, and neural progenitors display premature differentiation[199]. Similar results have been obtained in a mouse mutant lacking centrioles in the brain[200]. In the case of centriole loss, microcephaly can be rescued by p53 depletion, suggesting that p53 dependent apoptosis suppression is a major contributing factor in microcephaly[193].

Thus, it seems that the role of centriole in cilia nucleation is the ancestral role of centrioles, since there is a strong correlation between centriole presence and cilia presence in many species, which is not the case for centriole presence and centrosome presence[175]. Centriole localization at the spindle would have been a way to equally segregate centrioles to daughter cells to ensure proper cilia formation after division and could have later been coopted in some species to properly orient cell division.

4) Cilia and basal-body structure and function

a) Cilia and basal-body structure

Cilia are microtubule-based membrane protrusions found in almost all eukaryotic cells. As the modified centriole at their base, called the basal body (BB) (Figure 16C), nucleates the microtubules within the membrane protrusion (called the axoneme), microtubules within cilia display the same 9-fold symmetry as centrioles, although they

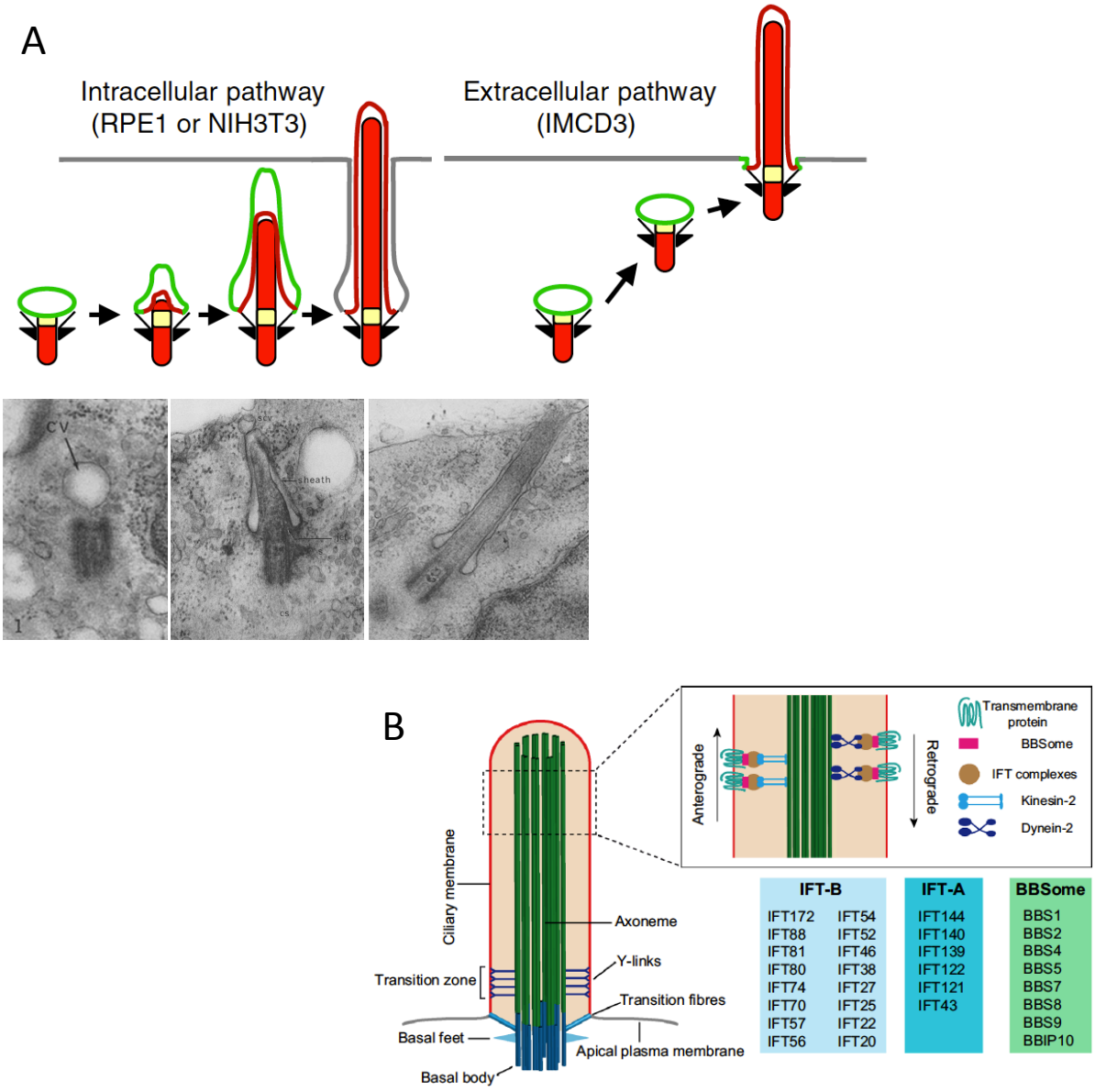

Figure 17 Building a cilium

(A) Schematic showing the two alternative ciliogenesis pathways (from Wu 2018). The micrographs below correspond to different steps of the intracellular pathway as originally described by Sorokin (Sorokin 1962)

(B) Trafficking of proteins in and out the cilium during its genesis or maintenance involves members of the IFT-B, IFT-A and BBSome complexes as well as molecular motors (from Bernabe-Rubio 2017)

are arranged in pairs and not triplets. Some cilia also display a central microtubule pair (Figure 16A).

Cilia can be motile, in which case the movement is powered by dynein arms attached to the axoneme's microtubules, and most motile cilia seem to have a central microtubule pair, although this is not always the case.

BB usually display appendages: distal appendages are required for their tethering to the plasma membrane, whereas the striated rootlet and the basal foot are important for cilia stability by linking the BB to cortical microtubule and actin networks (Figure 16B).

Striated rootlet importance for cilia stability is illustrated by the loss of one of its main components, Rootletin, which leads to photoreceptor degeneration in mouse[201]. Rootletin is also required for cilia integrity and function in sensory neurons of C.elegans [202] and Drosophila[203]. The basal foot is usually localized opposite to the striated rootlet on the basal body. It has been found to be able to nucleate microtubules via γ-tubulin[204], and is required for coordinated ciliary beating in mouse airways[205]

b) Building a cilium

- Centriole membrane docking

In order to form a cilium, the modified mother centriole or BB must first migrate and dock to a membrane: either to the ciliary vesicle for the intracytoplasmic ciliogenesis pathway or to the plasma membrane for the extracytoplasmic pathway (Figure 17A). This step is mediated by distale appendages called transition fibers, which contain two proteins important for basal body docking: ODF2 and Cep164.

- Building and controlling the composition of the axoneme

Once the basal body is docked to the ciliary vesicule or apical membrane, ciliary components must be trafficked from the trans-Golgi network toward the basal body and then progressively imported inside the cilium compartment in order to build the axoneme. Indeed, there is no local translation within cilia, and thus all cilia components must be brought from the cytoplasm. Trafficking of ciliary components from the trans-

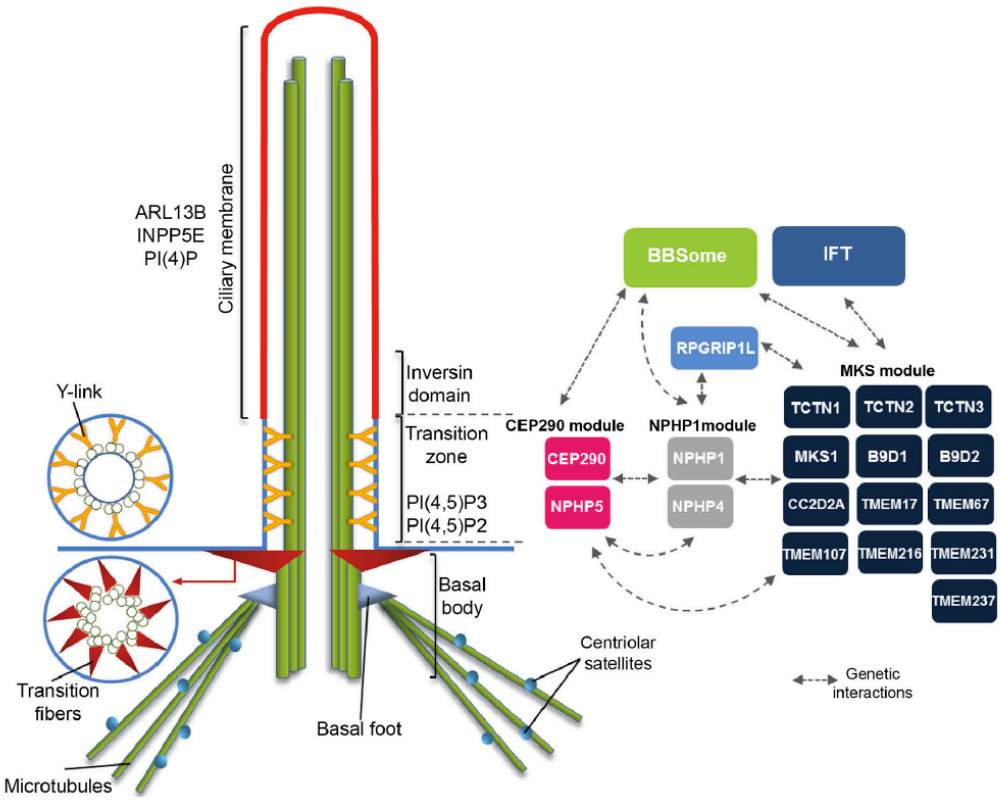

Figure 18 The ciliary transition zone (TZ)
Schematic showing the components of the ciliary gate: the transition fibers and the transition zone. The different modules interacting to build and maintain the TZ are depicted on the right, along with Rpgrip1l, the master regulator of the vertebrate TZ. (from Gonçalvez et Pelletier 2017)

Golgi relies on regulators of polarized vesicle transport such as MyosinVA, Rab8 and the Rab11 [206].

Trafficking of ciliary proteins within the cilium then depends on a set of Intra-flagellar transport (IFT) proteins that were first identified in *Chlamydomonas rheinardii* [207] [208] and are widely conserved (Figure 17B). Indeed, soluble proteins with a molecular weight lower than 100 kDa can enter the cilia by diffusion whereas bigger soluble proteins are part of proteins cargos that are transported via the IFT complex (Nachury 2019). IFT are organized in two main complexes: the IFTB complex, together with kinesin-2 allows the anterograde (from cilium base to cilium tip) transport of ciliary components whereas the IFTA complex, together with Dynein-2, allows the retrograde transport of ciliary components.

The regulation of protein entry and exit into the cilium is important for axoneme building as well as subsequent mature axoneme composition. This regulation is achieved through a ciliary gate, composed of transition fibers, septins and the transition zone (TZ), which is localized in the proximal part of the axoneme, above the BB (Figure 18). The TZ is composed of many proteins including protein modules, such as the NPHP and MKS modules that can be recruited by Cep290/MKS4/NPHP6 and/or Rpgrip1L/MKS5. TZ proteins which interact together and with the IFT and BBS complexes to regulate the protein composition of the cilium[209] (Nachury 2019[210]). In vertebrates and C.elegans, the protein Rpgrip1l is a major regulator of TZ assembly and function, while Cep290/NPHP6 assumes this function in Drosophila.

The TZ also acts as a lipid gate: the exclusion of the phosphatase INPP5E from the TZ leads to its accumulation within the axoneme, where it dephosphorylates the lipids PI(4,5)P3 and PI(4,5)P2, generating PI(4)P. Thus PI(4,5)P3 and PI(4,5)P2 are restricted to the TZ, whereas PI(4)P is present throughout the axoneme.

The trafficking of transmembrane receptors to the axoneme involves their binding to cargo adaptors such as TULP3 used to transport several GPCRs and that can bind IFT-A. The cargos adaptors are recruited thanks to “ciliary targeting sequences” or CTS and since different CTS have been identified to transport various transmembrane proteins such as rhodopsin or PKD2, it is very likely that multiple transport routes to enter the cilia exist depending on the nature of the CTS and its cargo adaptors. Even if a lot of actors have been identified, the mechanisms for these selective entries are far from being elucidated yet (Nachury 2019[210]).

A

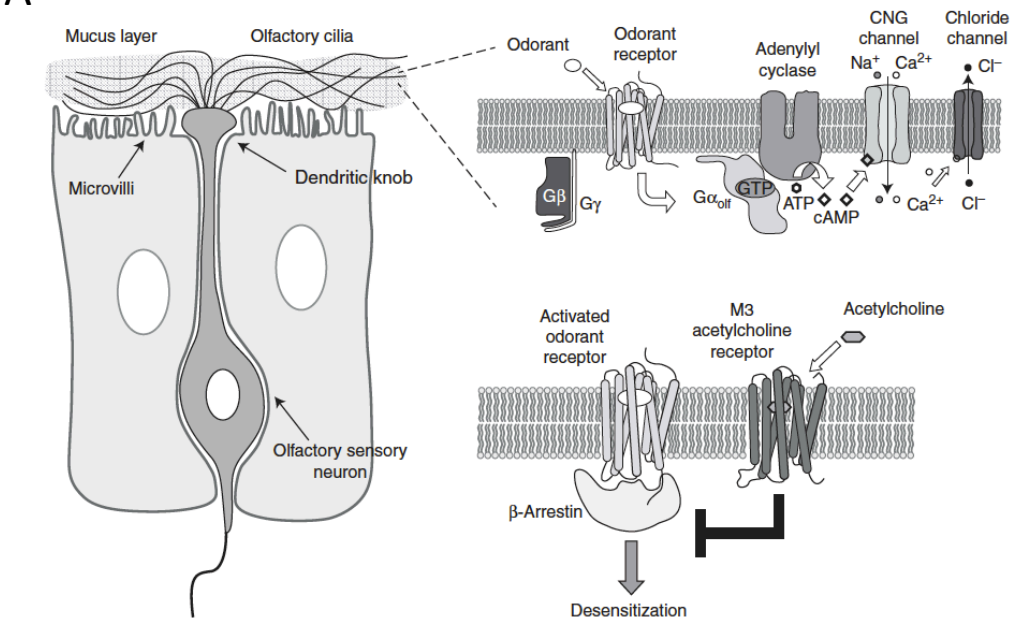

B

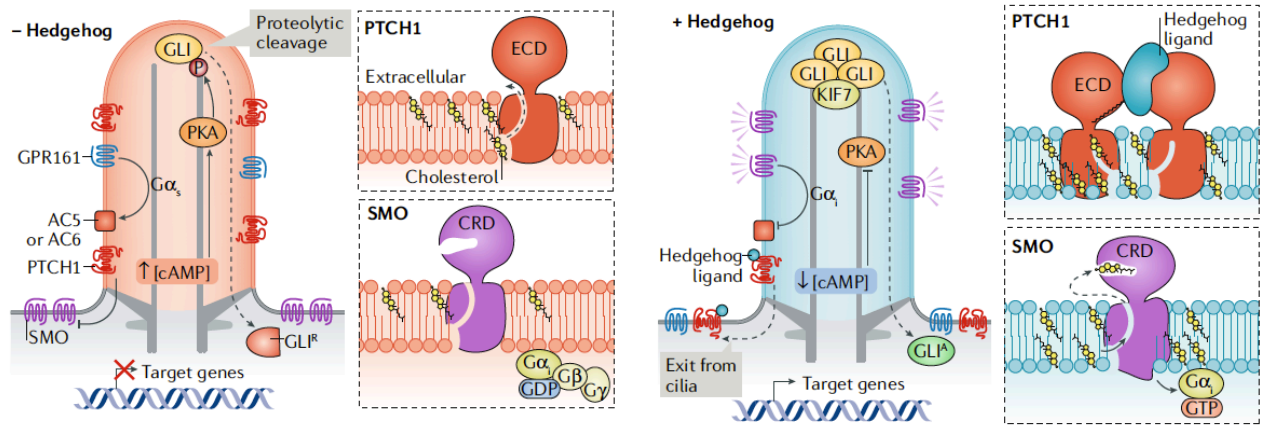

Figure 19 Examples of the importance of cilia in signal detection and transduction
(A) Odorant receptors (which are GPCRs) of olfactory neurons are localized in olfactory cilia, where they detect odorant molecules and trigger cell depolarization (from Mykytyn 2017)
(B) Role of cilia in vertebrate Hedgehog signaling (from Nachury 2019)

c) Ciliary functions:

- Motility functions

Cilia motility is crucial for spermatozoid movement (flagella are long motile cilia), larval movement in many marine species (for example in the Jellyfish Clytia hemisphaerica[211]) or even movement of adult animals, as is the case for ctenophores[212] [212] or flatworms (gliding motility). Ciliated cells also power bodily fluid movement in many cavities, such as in the brain ventricles, the airway or the oviduct[213] (see "centrosome and cilia positioning in epithelia part").

- Sensory functions

Cilia behave as sensory antennas in animals. Modified cilia in the retina allow light perception, and cilia are crucial for hearing, balance and olfaction in vertebrates.
In the case of vision and olfaction, this sensory function of cilia rely on their GPCR content (Mykytyn 2017[214]) (Figure 19A). Indeed, many GPCRs are localized within cilia and their regulated trafficking in and out of this compartment plays a crucial role in signal transduction.
Cilia are also critical for Hedgehog (Hh) signaling in vertebrates (Figure 19B), as many components of the Hh signaling pathway localize within cilia, and IFT mutations as well as TZ mutations lead to characteristic Hh signaling defects, such as polydactyly, neural patterning defects and cranio-facial malformations[215]. In the absence of Hh ligand, the Hh receptor Patched (Ptch) is localized within the ciliary membrane, whereas the transmembrane protein Smoothened (Smo) is excluded from it. Upon Hh stimulation, Ptch exits the cilium whereas Smo enters it, and this leads to the activation of the cilia localized Gli transcription factors which then translocate to the nucleus to activate target gene transcription[216].
Finally, some TRP channels are found enriched in the ciliary proteome from unicellular and pluricellular organisms and signal within the ciliary compartment (Sigg 2017[217]). Since cilia (flagella) from unicellular organisms such Chlamydomonas and Paramecia,

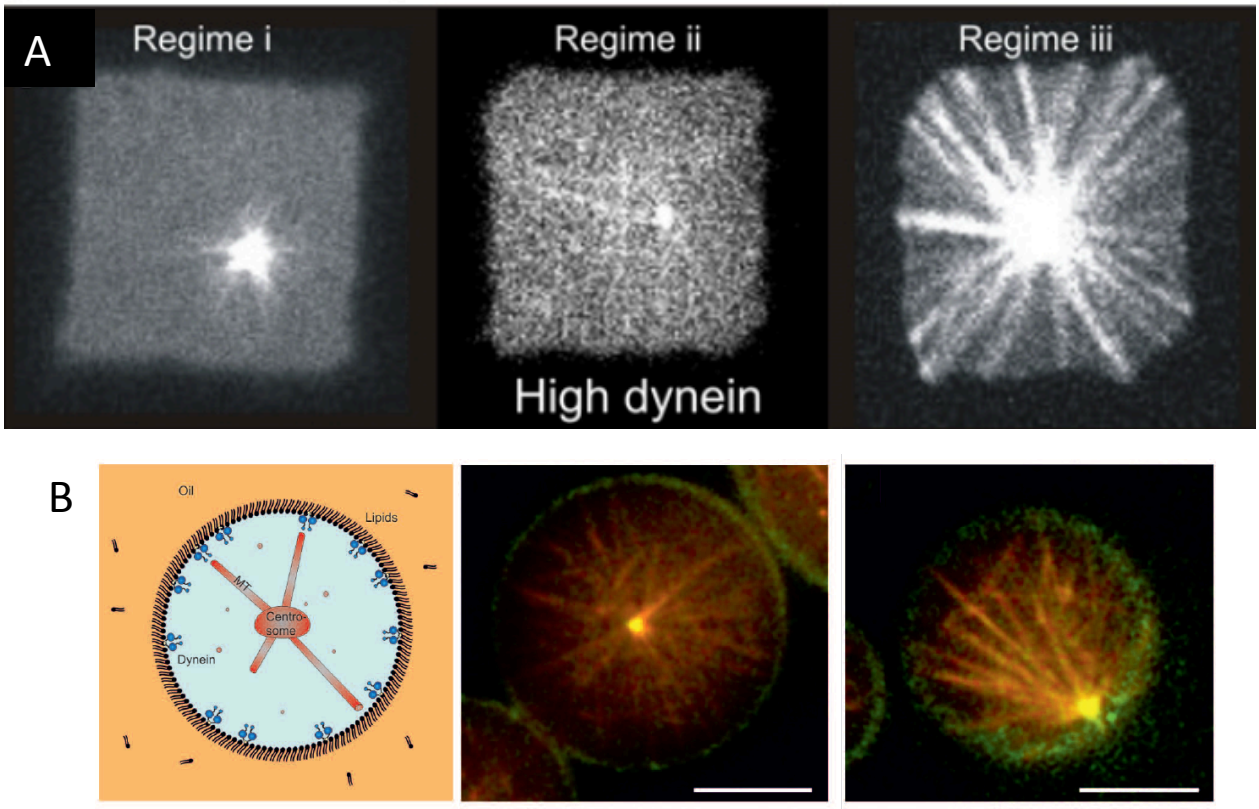

Figure 20 Centrosome positioning in reconstituted systems
(A) Centering of isolated centrosomes in dynein-coated micro-fabricated chambers containing tubulin (from Laan 2012)
(B) Centrosomes isolated in water droplet delimited by lipids and lipid-bound dynein (free to diffuse in the plane of the lipid sheet) can either relocalize to the center of the droplet (middle image) or to the periphery (right image) (Laan 2012)

present both sensory and motility functions, one can wonder which one of this two functions appeared first during the course of evolution.

d) Cilia evolution

Interestingly, cilia might have evolved from a membrane sensory patch formed by polarized transport from the Golgi using specific coat proteins, motors and adaptors. The subsequent gain of motility would have lead to the formation of sensory motile cilia[218]. This hypothesis is supported by the fact that

(a) IFT proteins are homologous to COPI and clathrin vesicle-coating proteins[218]

(b) kinesin-2 and dynein-2, involved in trafficking within the cilium, have cytoplamic equivalents functioning in polarized vesicle transport[219] [220]

(c) Many IFT proteins have extra-ciliary functions (see below): for example, several IFT proteins can localize to spindle poles[221] or the cleavage furrow[222] in dividing cells, suggesting a role in mitosis.

What could be the advantages of signalling from the cilia compartment compared to signaling from the rest of the cell membrane? An interesting hypothesis is that cilia allow to highly concentrate signaling receptors, thus providing increased sensitivity at a precise spot. This local receptor concentration also make it easier to bring together entire signalling modules in close proximity, while at the same time preventing undesired crosstalks with other signaling pathways in the cytoplasm (Nachury 2014[223], 2019[210]).

B) Centrosome positioning in single cells

Centrosome positioning is crucial both during mitosis, to orient the spindle, and in interphasic cells during migration and for proper functioning of immune cells. Indeed, the coupling between centrosomes and the cortex via astral microtubules is crucial to orient cell division. In addition, centrosome coupling to the nucleus and the secretory network (mostly the Golgi apparatus) allows directed vesicular traffic underlying leading edge dynamics in migrating cells and immune synapse formation and effector function in immune cells. Although the detailed mechanisms of centrosome positioning in these cells is not completely understood, it is now clear that PAR complex protein and

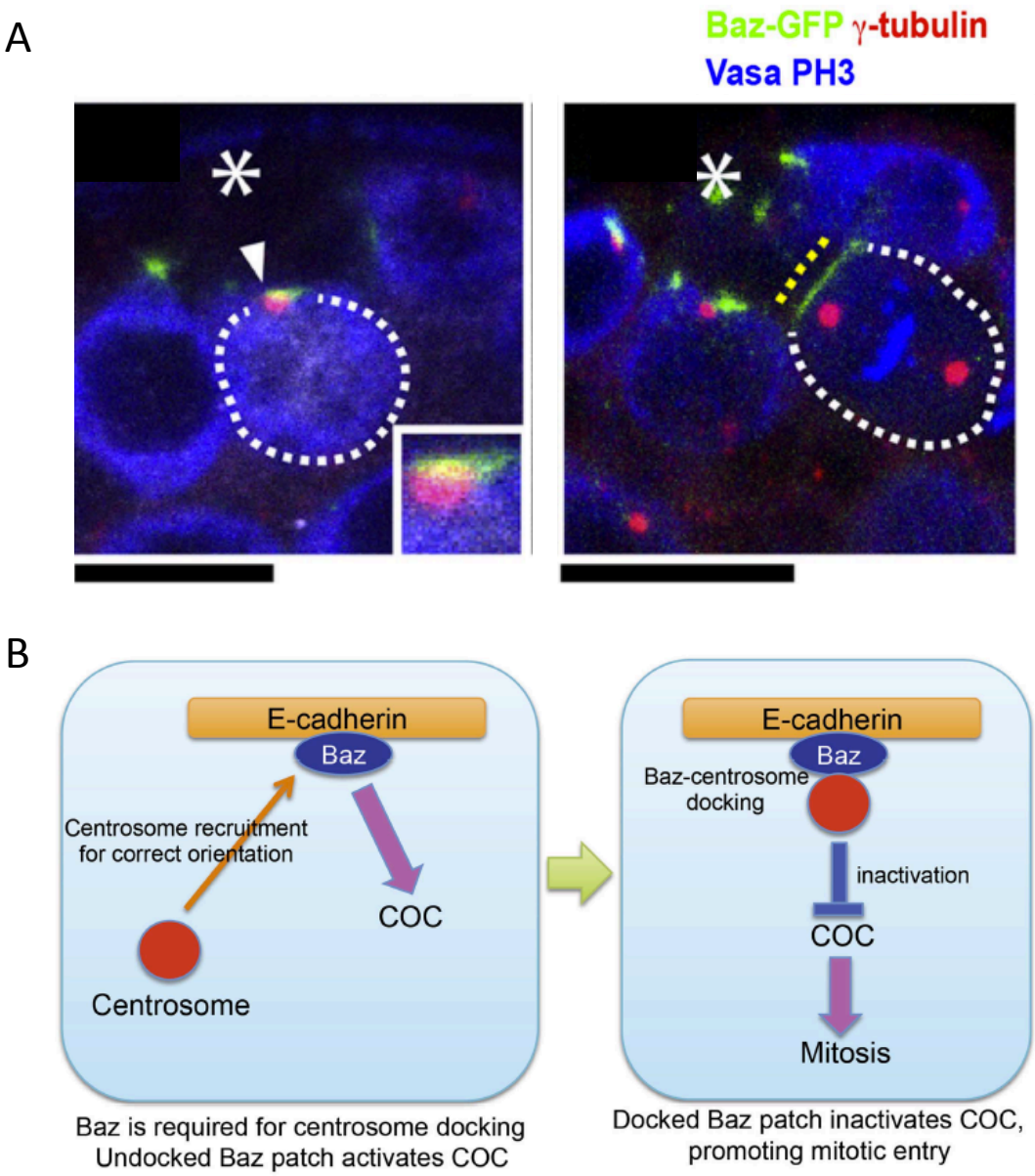

Figure 21 Centriole Orientation Checkpoint (COC) in Drosophila Germ Stem Cells (GSC)

(A) Immunostaining of A GSC before mitotic entry (left) and after mitotic entry (right) showing docking of the centrosome (red) at a Par3 (Baz) patch (green) at the interface between GSC and hub cells (star)

(B) Schematic showing the importance of centrosome docking at Par3 patch downstream of E-cadherin for the COC and proper spindle orientation

(from Inaba 2015)

RhoGTPases are crucial regulators of cytoskeletal remodeling and cytoskeleton-mediated forces that underlie centrosome positioning.

1) Centrosome positioning in dividing cells

It has been shown in vitro that cortically localized dynein can generate pulling forces up to several picoNewtons on microtubules in micro-fabricated chambers[224]. In this system cortical dynein captures microtubule ends, inhibits their growth and triggers catastrophe, leading to pulling forces on microtubules that are transmitted to centrosomes isolated from human cell lines[224]. With uniform repartition of cortical dynein, this leads to the positioning of the centrosome at the center of the micro-fabricated chamber (Figure 20A). Other experiments using water emulsion in lipids showed that cortical dynein can either center or decenter the centrosome, which might depend on the relative size of microtubules and the water droplet[225] (Figure 20B).

Cortical dynein interaction with astral microtubules (emanating from centrosome) is required to asymmetrically position the mitotic spindle in *C.elegans* zygote. In this cell, the posterior cortex is enriched in GPR-1/2 and LIN-5 which interact with dynein, and this results in higher dynein-mediated pulling force exerted on the spindle on the posterior side of the cell[226] [49].

As previously mentioned, centrosome are also required for proper spindle orientation in several systems. In Drosophila male germ stem cells, centrosome docking to a patch of Bazooka (Drosophila Par3) downstream of E-cadherin at the junction between the stem cell and the hub is a checkpoint for proper spindle orientation to ensure that one daughter cell (the stem cell) remains in contact with the hub whereas the other is positioned away from the hub and will therefore differentiate[190] (Figure 21A,B). However the mechanisms that lead to centrosome docking to the Bazooka patch are not known, although Apc2 (Adenomatous polyposis coli 2), which can interact with microtubule (+) ends and β-catenin might be involved (Su 1993[227], Wen 2004[228], Inaba 2010[229]). Bazooka also plays a key role in Drosophila neuroblast oriented cell division by recruiting Insc to the apical cortex which then recruits the Gα/Pins/Mud complex that can interact with astral microtubules to orient the spindle along the apico-basal axis[230] [231] [232].

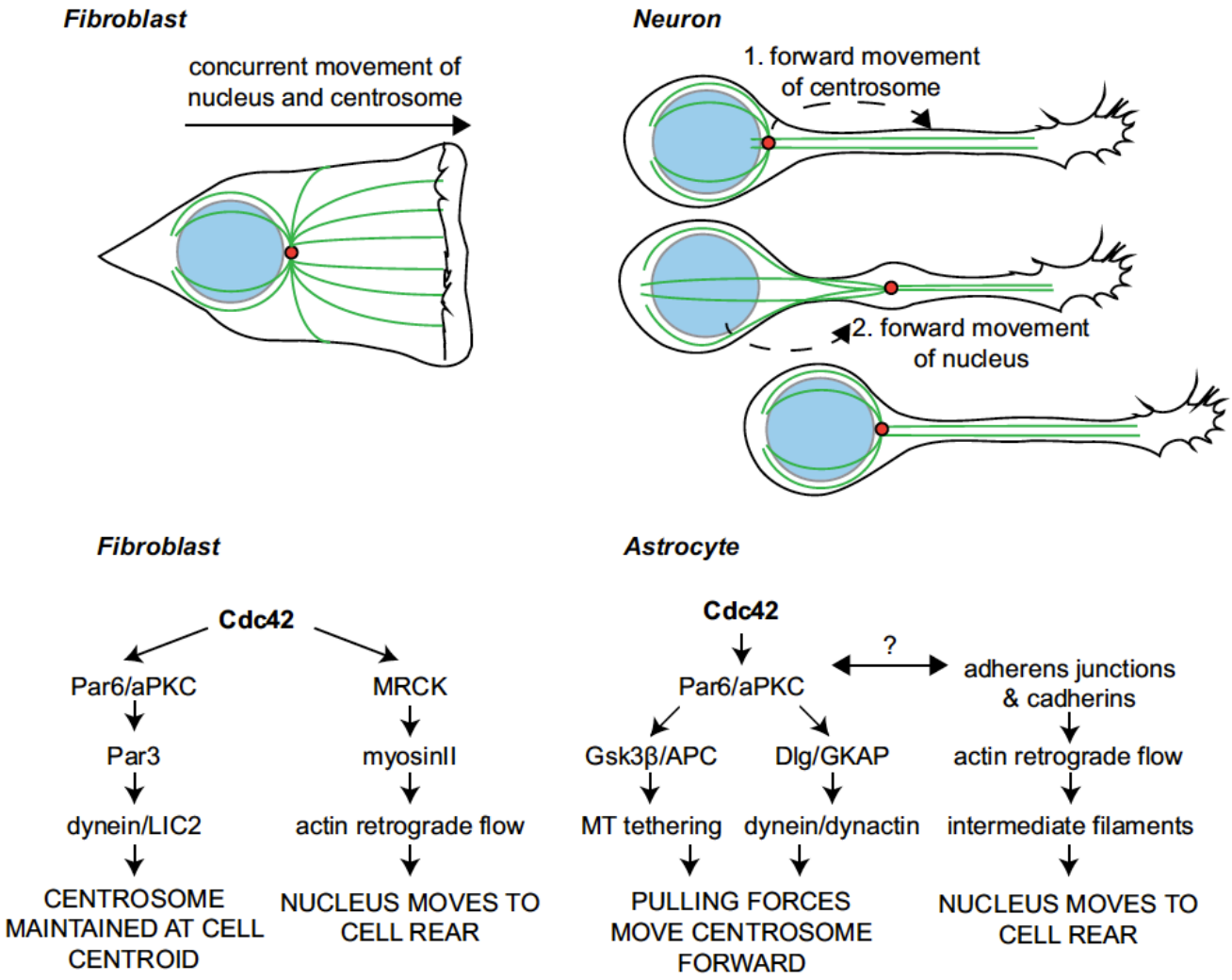

Figure 22 Centrosome positioning in migrating cells

The top schematics outline the position of the centrosome between the nucleus and the leading edge
Bottom: Roles of Cdc42, polarity proteins and molecular motors in migrating fibrobasts and astrocytes migration
(from Barker 2015)

2) Centrosome positioning in migrating cells

Centrosome and Golgi polarization during cell migration are thought to allow directional vesicular trafficking to the leading edge and thus power cell migration. This is consistent with the fact that in most migrating cells, the centrosome is positioned between the nucleus and the leading edge (Figure 22). However the centrosome has also been found behind the nucleus in some migrating cells, for example in T lymphocytes[233].

Cell migration has been most extensively studied using fibroblasts, astrocytes and neurons, which all have a centrosome positioned between the nucleus and the leading edge. However, the modes of migration and the mechanisms of centrosome positioning differ between these cell types. In fibroblasts, the migration speed is almost constant, a large lamellipod is formed at the leading edge and centrosome positioning is the consequence of a rearward nuclear movement coupled to mechanisms maintaining the centrosome at the cell center[234]. In contrast, astrocyte and neuron migration proceeds through neurite extension followed by centrosome migration into the neurite and forward nucleus movement in a saltatory fashion. The centrosome is actively positioned to the leading process[235] while the nucleus is maintained at the rear of the cell by actin retrograde flow[236]. However, microtubules, the PAR complex and Cdc42 play crucial roles in both types of migration, as outlined below (Figure 22).

A common method for studying cell migration is to create a wound in a cell-culture monolayer, which is then invaded by migrating cells. Using this method, it was shown that in astrocytes, wounding activates integrins at the leading edge which leads to the activation and polarized recruitment of Cdc42 which in turn recruits and activates a cytoplasmic Par6/aPKC complex[59]. Localized aPKC activation have been proposed to activate dynein at the leading edge, that would exert pulling forces on the centrosome[59]. The Par6-aPKC complex at the leading edge also triggers GSK3β phosphorylation, which leads to an increase association of APC with microtubule plus ends at the leading edge that are required for centrosome positioning[54]. Finally, the Par6/aPKC complex also triggers Dlg1 accumulation at microtubule plus ends where it has been proposed to interact with APC to anchor microtubules to the cortex[55]. Together with the fact that Dlg1 can recruit dynein to microtubule via its interaction with GKAP[237], this strongly supports a model where microtubule anchoring at the cortex and dynein mediated

forces pull on the centrosome to position it in front of the nucleus during astrocyte migration.

In neurons, the situation is different since Par6 and aPKC localize to the centrosome. Par6 is required for centrosome positioning and the formation of a microtubule cage extending from the centrosome around the nucleus[238]. Par6 also regulates acto-myosin contraction in front of the centrosome which is required for centrosome positioning, probably by pulling it forward[239].

Finally in migrating fibroblasts, Cdc42 activation also leads to Par6 and aPKC recruitment to the leading edge[234], but Par6 and aPKC act through Par3. Par3 and dynein localize to cell-cell contacts where dynein exerts microtubule-based pulling forces on the centrosome to maintain it at the cell center[62]. Par3 interacts with the LIC2 (Light Intermediate Chain 2) dynein subunit and could tether microtubules to cell-cell contacts, allowing pulling forces generation on the centrosome[62]. Cdc42 also activates MRCK (Myosin Regulatory Chain Kinase) which phosphorylates and activates myosin II[234]. This triggers a retrograde actin flow, and together with the coupling of actin with the nucleus through LINC complexes[240], this triggers a rearward nucleus movement.

3) Centriole positioning at the immune synapse

Migrating lymphocytes position their centrosome at their back, in the uropod. Upon contact with an antigen-presenting cell, the centrosome is relocalized from the uropod to the site of cell contact that matures into a so-called “immune synapse” (IS), with central zone enriched in T-cell receptors (TCR) (Figure 23A). In CD8+ T lymphocytes (TL), centrosome relocalization to the synapse is crucial both in naïve TL, to relocate TCR to the synapse, and in activated TL to bring cytolytic granules toward the immune synapse for efficient target cell killing[241].

Upon encounter with a target cell, CD8+TL undergo a precise remodeling leading to their polarization toward the target cell and IS formation. Actin filaments accumulate at the contact site within the first 30s of cell-cell contact: at this point the contact between the lymphocyte and the target cell is interdigitated. Then, within 1min after encounter, actin depletion at the center of the IS occurs, whereas actin at the periphery of the synapse persists, and the contact between the 2 cells become straighter. At the same time, within 2 min after synapse formation, TCR accumulate at the center of the synapse.

A

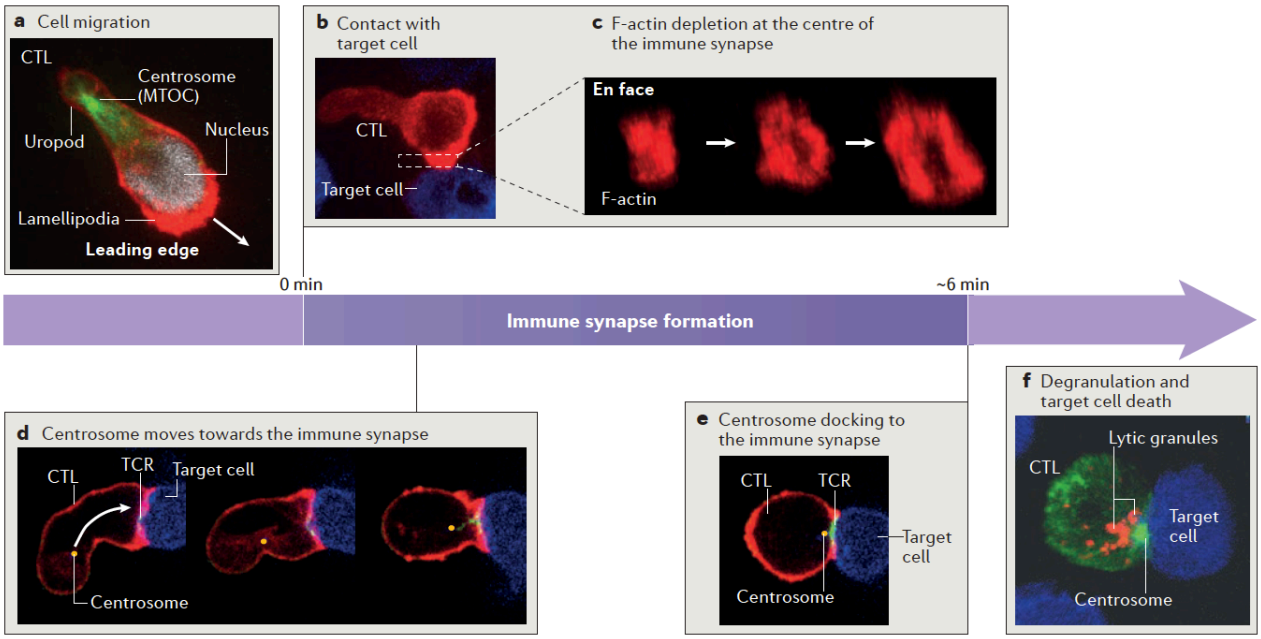

B

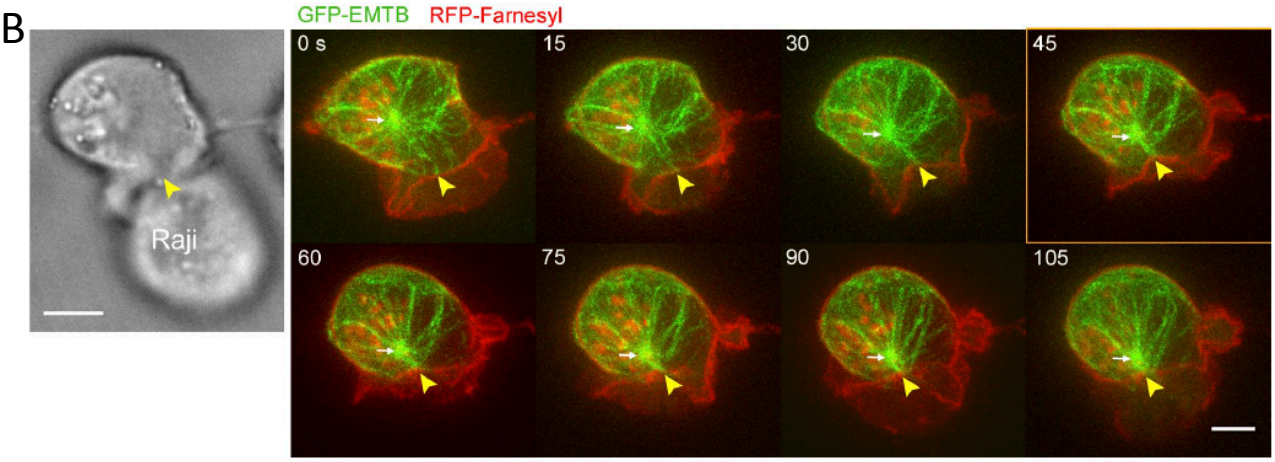

Figure 23 Centrosome positioning during immune cells migration and immune synapse (IS) formation

(A) (a) During migration, centrosome of cytotoxic T lymphocytes is localized at the rear, in the uropod. After contact with the target cell and actin depletion at the center of the IS (b,c), the centrosome relocalizes to the IS in a few minutes (d,e), where it delivers lytic granules (f) (from de la Roche 2016)

(B) Time-lapse immaging of Jurkat immune cells in contact with its target cell (membranes are labelled in red), showing the reorganization of the microtubule network (green) during centrosome migration to the IS. Yellow arrow point at the center of the IS which is linked to the centrosome by a bundle of « pioneer » microtubules and bent due to the mechanical forces exerted to bring the centrosome to the IS (from Yi 2013)

Finally, between 2 min and 6 min after encounter, the centrosome moves from the uropod to the synapse, bringing a second pool of TCR and cytolytic granules[242].

The molecular mechanisms leading to centrosome repositioning at the IS depend on TCR activation. Upon TCR activation, PLCγ (Phospholipase C) is recruited at the IS[243], where it leads to the local accumulation of DAG (Diacyglycerol). DAG is required for centrosome movement to the IS[244], via its role in dynein localization at the IS[244] and activation of PKCθ (Protein Kinase C)[245] which inhibit myosin activation at the synapse, thereby restricting it to areas behind the centrosome where it pushes it toward the IS[246]. In Th(helper) lymphocytes, PKCζ has also been involved in centrosome movement to the IS[247]. Centrosome polarization has also been shown to depend on another member of the PAR complex, Par1b, in Jurkat T cells (immortalized human T lymphocytes). Upon TCR activation, Par1b is phosphorylated and excluded from the IS, and a dominant-negative form of Par1b blocks centrosome polarization[248]. Interestingly, Par3 also plays an important role in B lymphocytes IS, where it promotes BCR (B cell receptor) gathering and centrosome polarization at the IS by facilitating local dynein recruitment[249].

Centrosome relocalization to the IS in Jurkat cells takes place in two phases, one rapid polarization phase (centrosome average speed of 3.3µm/min) and a slower docking phase within the last 2µm to the IS (centrosome average speed of 0.9µm/min)[250]. In this system, centrosome movement to the IS depends on pioneer microtubules extending from the centrosome to the center of the IS and their dynein-dependent capture and depolymerization at the IS that exert pulling forces on the centrosome[250] (Figure 23B).

Together, this shows that, as is the case for cell migration, dynein, microtubule and PAR proteins play keys roles in centrosome positioning in immune cells.

C) Centrosome and cilia positioning in epithelia

1) Centriole apical docking

In most epithelia, centrosomes are positioned at the apical surface, which is a prerequisite for extracytoplasmic ciliogenesis. Centrosome movement toward the apical surface and docking to the apical membrane rely on actin and microtubule dynamics.

In quail oviduct multiciliated cells, treatment with cytochalasin D[251] (which prevents actin polymerization) or with taxol[252] (which stabilizes microtubules) inhibits centrioles migration to the apical surface, whereas colchicine and nocodazole[253] (two drugs that inhibit microtubule polymerization) don't have any effect on this process, suggesting that microtubule dynamics as well as actin network are required for centriole movement to the apical membrane. Supporting a role of actin, an immuno-detection of myosin II isoforms performed in quail oviduct produced a signal next to centrioles at a stage that precedes their movement toward the apical surface. Once centrioles had accomplished their apical movement, the myosin antibody concentrated at the basal foot of docked BB (Lemullois 1987 "Immunocytochemical localization of myosin during ciliogenesis of quail oviduct"). Supporting this result, non-muscle myosin II B (NMIIB) is required for centriole migration toward the membrane in cultured RPE1 cells[254]. Finally centriole docking requires RhoA-dependent apical actin enrichment in mammalian cells in culture[255].

In some cultured cells and in some multiciliated cells (like the quail oviduct[256] or the mouse ependyma[257]), basal body docking occurs on intra-cytoplasmic vesicles, which then migrate to the plasma membrane[258] [256]. The formation of this ciliary vesicle depends on distal appendages proteins such as Cep164, Talpid3, members of the exocyst complex (a conserved protein complex involved in tethering secretory vesicles to the plasma membrane) such as Sec10[259] and members of the Rab family such as Rab8 and Rab11. Cep164 can activate Rab8 via its GEF (GTPase exchange factor) Rabin8, and this is crucial for vesicle docking at the mother centriole[260]. Remarkably, taxol or cytochalasin D treatment do not inhibit centriole association with ciliary vesicle, but only the migration of the vesicle-attached centriole toward the apical membrane[251] [252].

Interestingly, some PCP proteins have been involved in centrosome docking and migration to the apical surface. In Xenopus multiciliated cells (MCCs), Dvl and Inturned together with Sec8, an exocyst component, are required to position centrioles apically[261]. Dvl2 and Sec8 localize next to basal bodies in these cells, and Inturned and Dvl knock down lead to a loss of the apical actin network that has been shown to be required for centriole docking in mammalian cells[255]. In addition, mice lacking Celsr2 and Celsr3 also display centriole docking defects[73].

Finally in cells cultured on micro-patterns, microtubules have been shown to promote centriole movement to the membrane in cooperation with myosin activity. In this *in*

vitro system, a stable microtubule bundle seems to "push" the centriole upward and the distal appendage protein Cep164 plays a key role in centriole migration [262].

An attractive hypothesis would be that following ciliary vesicle formation close to the nucleus via the cooperation of distal appendages proteins and vesicular trafficking molecules, the actin and microtubule cytoskeleton, possibly together with molecular motors such as myosins, kinesins or dyneins, would lead to the migration of this vesicle-attached centriole to the apical membrane with which the ciliary vesicle would fuse in a process reminiscent of exocytosis. Ciliary vesicle formation via Cep164 seems to be a prerequisite for centriole migration toward the plasma membrane in cultured cells[262], which suggests that this migration could depend on the ciliary vesicle, perhaps by an interaction with molecular motors moving along microtubules or actin filaments.
Supporting the importance of both microtubules and actin in this process, MACF1, a protein interacting with microtubules and actin, localizes next to basal bodies, probably to subdistal and distal appendages, and is required for centriole apical docking in the mouse retina[263]. Macf1 might be required for vesicle exchange between microtubules and actin microfilaments next to basal bodies, and thus maturation of the ciliary vesicle.

2) Centriole and cilia positioning within the apical surface

Mono-ciliated and multicilated epithelia are important in animals for the movement of whole organisms (for example in many marine organisms larvae, adult ctenophores and planarians) and to create directional fluid flow in body cavities. The importance of directed ciliary beating is underlined by the wide range of diseases caused by motile cilia defects, such as respiratory disorders, hydrocephalus and infertility (Spassky 2017).
Indeed, proper cilia positioning in multiciliated cells (MCC) is important to perform diverse functions (Figure 24A):

- multiciliated cells in the ependyma create an oriented cerebro-spinal fluid (CSF) flow that is crucial for brain homeostasis and has even been shown to be correlated to directional migration of new neurons to the olfactory bulb in mouse[264]

A

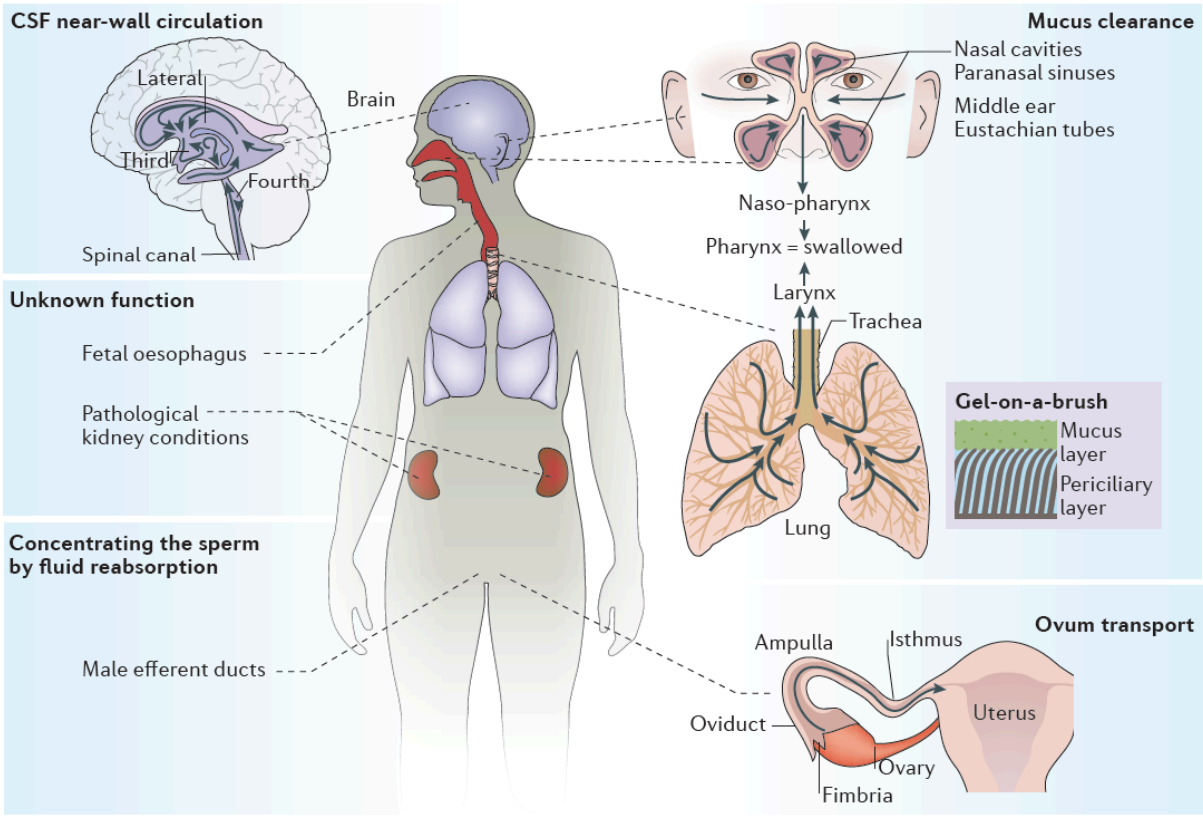

B

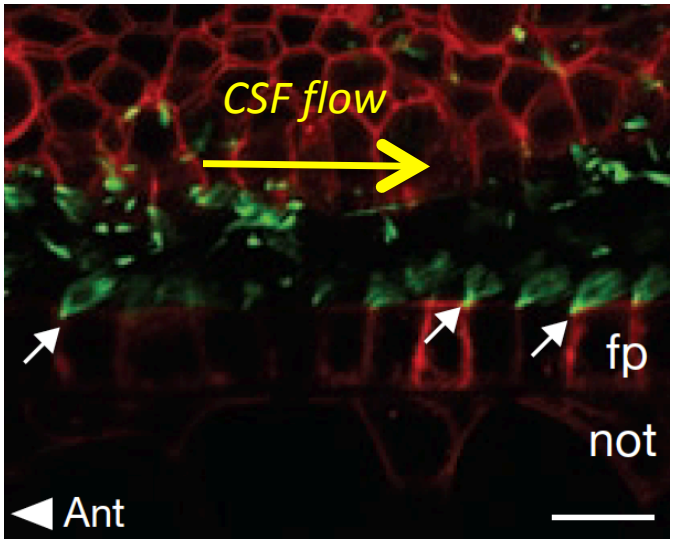

Figure 24 Ciliated epithelia allow the directional flow of bodily fluids

(A) Schematic showing the roles of multi-ciliated cells in various human tissues (from Spassky et Meunier 2017)

(B) Mono-ciliated cells of the zebrafish floor-plate propell the cerebrospinal fluid posteriorly in the central canal of the neural tube (membrane are in red, cilia in green) (from Borovina 2010)

- multiciliated cells of the Xenopus embryo epidermis create a posterior-directed flow that helps keep the surface of the embryo clean
- multiciliated cells of the Planarian Schmidtea mediterranea epidermis allows them to glide on surfaces (Meunier et Azimzadeh 2016[213])
- multiciliated cells in the airway sweep mucus and particles out of the tract
- multiciliated cells in the oviduct transport the female gamete to the uterus

Cilia positioning is also important in monociliated epithelia, to achieve their motility or sensory functions:

- In the vertebrate left-right organizer (Mouse embryonic Node, Xenopus Gastrocoele Roof Plate and Zebrafish Kupffer's vesicle), proper positioning and tilting of cilia allow the creation of a directional flow required for left-right asymmetry establishment.
- Motile mono-cilia in the Zebrafish floor-plate are positioned and tilted posteriorly, which allow proper embryonic CSF circulation[265] (Figure 24B)
- In the mammalian cochlea and Zebrafish neuromast, the off-centering of a non-motile cilium (called the kinocilium) allow correct patterning and orientation of actin-based microvilli to properly detect sound or water directional movement respectively.

In all these tissues, basal bodies/cilia orientation and positioning can be subdivided in two types of polarization:

-**Translational polarity** refers to the displacement of basal bodies/cilia or cilia cluster form the center of the cell apical surface towards one side of the cell (BB/cilia "off-centering") (Figure 25A).

-**Rotational polarity** refers to the uniform orientation of basal body appendages or central pair (Figure 25B). In the case of motile cilia, the basal foot is always pointing in the direction of the beating (which corresponds to the direction of fluid flow).
Some epithelial cells display both types of polarity (for example in the mouse ependyma), whereas others only display rotational polarity (for example in the Xenopus

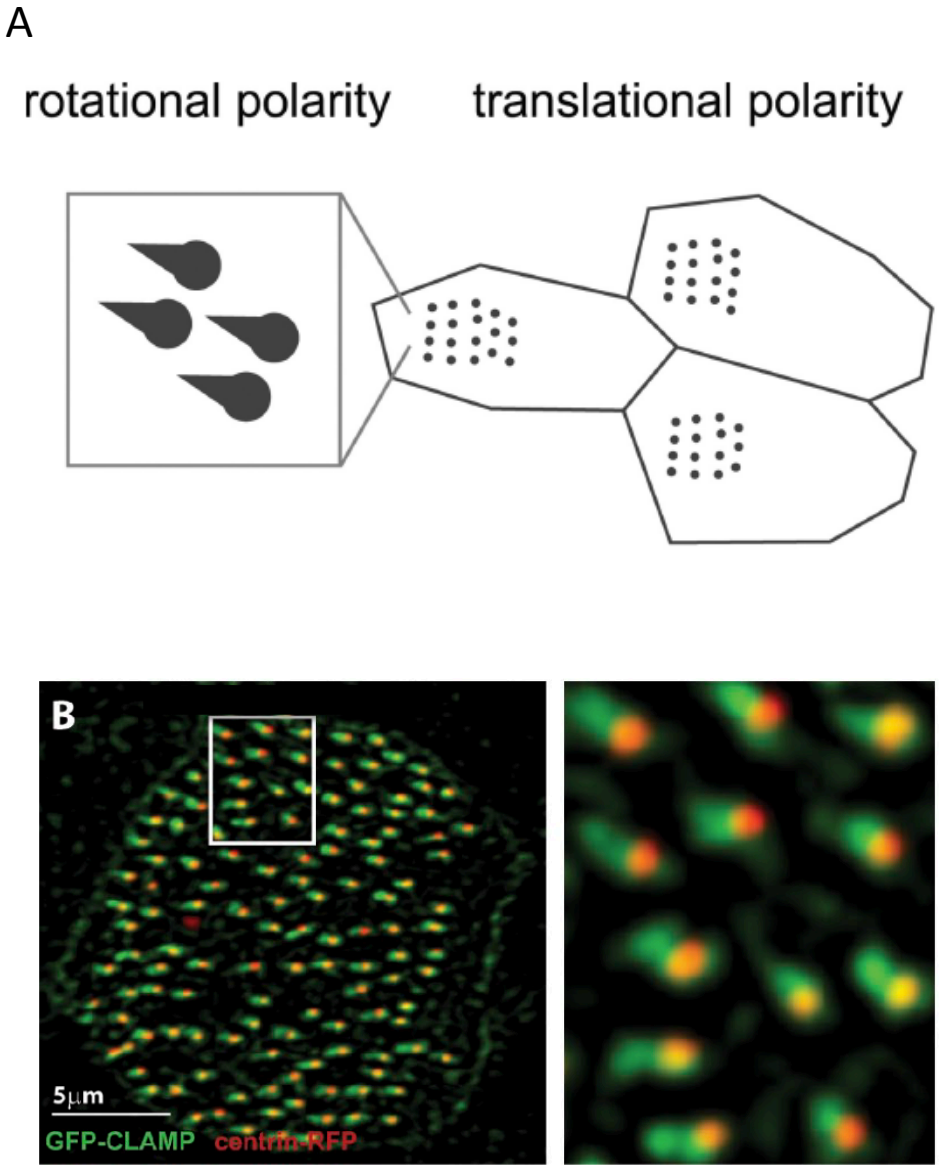

Figure 25 Translational and rotational polarity

(A) Mouse ependymal multi-ciliated cells display both rotational and translational polarity. Dots represent BB and the close-up on the left BB and the triangular-shaped basal-foot

(B) Xenopus embryo ectoderm multi-ciliated cell expressing a rootlet marker (GFP-CLAMP, green) and a BB marker (centrin-RFP) showing rotational polarity but no translational polarity. The image on the right is a close-up of the white rectangle region on the left (from Werner 2011)

embryo epidermis) (Figure 25): One explanation to account for this difference could be the difference in the global organisation of the beating epithelium: in the mouse ependyma, where multi-ciliated cells are adjacent to each other, cilia cluster off-centering allows them to beat without interfering (physically) with cilia of neighboring cells. This is consistent with the fact that multiciliated cells in Xenopus larval epidermis (which do not display translational polarity) are not adjacent due to the presence of other, non-ciliated cells between them, a similar situation as in the respiratory epithelium.

Finally, translational and rotational PCP at the single-cell level are coordinated between cells, giving rise to a "tissue level" PCP.

How are translational and rotational polarities established and coordinated between neighboring cells?
In the following paragraphs, we will see that BB/cilia planar polarization involves PCP proteins, BB/apical cytoskeleton interactions, ciliary proteins and mechanical forces.

a) Conserved role of PCP proteins in BB/cilia planar positioning

The first evidence for a role of PCP proteins in vertebrate ciliated cells PCP came form the study of mouse cochlea, which present planar-polarised ciliated sensory neurons. These neurons display an off-centered cilium at their apical surface that organises a V-shape stair-case of stereocilia (actin-based protrusions) which all point in the same direction (Figure 26A). In Vangl2 mutant mice, cochlea PCP was disrupted, with defects in the coordination of BB translational polarity and/or translational polarization defects (depending on the position of the cells within the cochlea)[266] (Figure 26D). It was then shown that Vangl2 assumes an asymmetric localization in the cochlear cells, that Fzd3 is similarly asymmetrically localized and that this localization depends on Vangl2[68] (Figure 26B).

Later studies performed on the epidermal multiciliated cells (MCC) of Xenopus larvae showed that expression of a mutant form of Dvl that specifically disrupts PCP

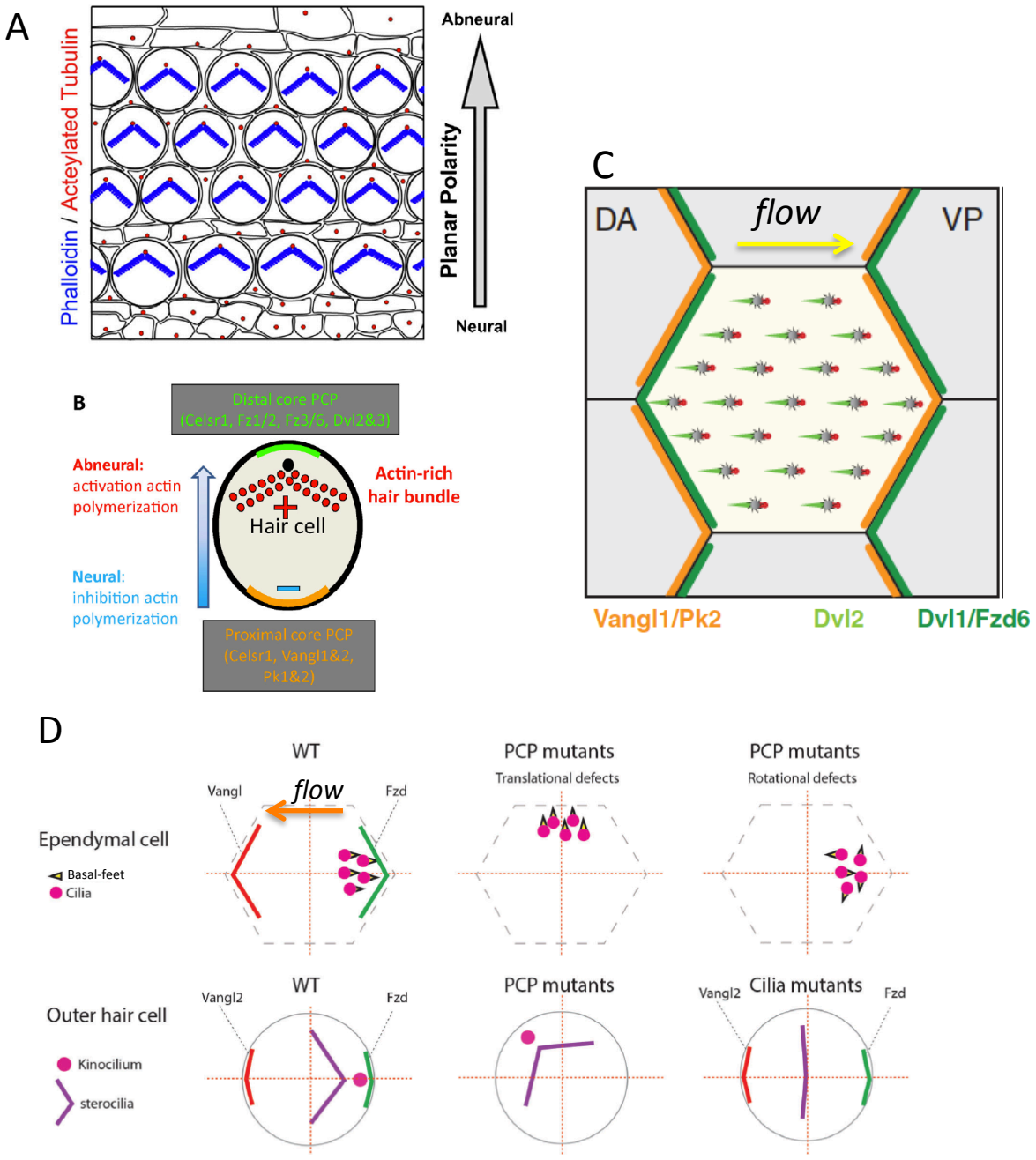

Figure 26 Asymmetric localization of PCP proteins in vertebrate ciliated epithelia

(A) Planar polarization of the mouse cochlea is characterized by the off-centering of the cilium (red) and the associated V-shaped microvilli (blue) (from Ezan 2013)

(B) Asymmetric localization of PCP proteins in mouse cochlea sensory cells (from Ezan 2013)

(C) Asymmetric localization of PCP proteins in Xenopus embryo ectoderm multi-ciliated cells rootlets are in green and basal-feet in pink; DA: Dorso-anterior side/ VP: Ventro-posterior side) (from Meunier 2016)

(D) Asymmetric localization of PCP proteins in mouse ependymal cells and mouse cochlea in wt, PCP and ciliary mutants and associated cilia/BB positioning defects (from Carvajal-Gonzalez 2016)

signaling[267], Xdd1, leads to cell-autonomous rotational polarization defects[261 268]. Similar to what had been shown in Drosophila, it was found that some transmembrane PCP proteins can act non-autonomously in this system: wild-type MCC located at over-expressing or knocked-down clone borders reorient their BB/cilia toward low Vangl2 or high Fzd levels but away from high Vangl2 levels[268].

The subcellular localization of PCP proteins in this system is not fully described, but GFP-Vangl1 and RFP-Pk2 localize at the posterior apical cortex, opposite to Dvl1-GFP and Fzd6-GFP in both MCC and goblet cells, that are part of the ectoderm and probably transmit the PCP information between MCC[83] (Figure 26C). Interestingly, Dvl2 localizes at the cell cortex (with no apparent asymmetry) and at basal bodies rootlet[261], suggesting that the cell-autonomous rotational polarity defects caused by Xdd1 could be due either to a disruption of Dvl action at the cortex or at the ciliary rootlet, or both.

In mouse ependymal MCC, endogenous Vangl2 was found to localize asymmetrically at the posterior side of MCC, opposite to the basal bodies/cilia cluster[269] (Figure 26D). Fzd3 localize at the anterior cortex and Vangl2 and Fzd3 distribution are impaired in Celsr2 and Celsr3 mutants, showing a conserved involvement of atypical cadherins in Vangl2 and Fzd3 asymmetric localization[73]. In addition, Vangl2 and Fzd3 cooperate with Celsr1 to coordinate rotational and translational polarity between cells in radial progenitors (monociliated cells that give rise to ependymal MCC and that display a single primary cilium with translational polarity) and MCC, whereas they cooperate with Celsr2 and Celsr3 to organize multicilia in individual cells (Celsr2 and Fzd3 mutants have abnormally elongated cilia patches, whereas Celsr3 and Vangl2 mutants have patches with defective rotational polarity)[270]. Interestingly, Dvl2 also localizes at basal bodies rootlets in murine ependymal MCC but does not seem to localize at the cortex (Hirota 2010[271]). Introducing a modified version of Dvl2 lacking its PDZ domain (which is required for interaction with Fzd[272]) disrupts rotational but not translational polarization of ependymal cells[271]. This suggests that Dvl2 has a conserved subcellular localization at the rootlet that is required for proper rotational polarization. Interestingly another study also found Dvl1 next to BBs in murine ependymal MCC (Guirao 2010[269]),

Finally in the mouse tracheal MCC, whose cilia beat in the direction of the mouth, PCP proteins are also asymmetrically localized, with Pk2 and Vangl1 at the distal apical cortex, opposite to Fzd6, which localize at the proximal (oral) cortex [74]. Interestingly, Dvl2 is also found next to basal bodies and not at the cortex in this system[74], showing that this localization, and probably its function in rotational polarization, is conserved across tissues in mouse. As in Drosophila, PCP proteins asymmetric localization depends on one another: Vangl1 mutant mice have reduced level of cortical Vangl2, reduced asymmetry of Celsr1 and Fzd6 and complete absence of cortical Pk2[74]. However Pk2, Vangl1 and Fzd6 cortical localization is not affected in Vangl2 mutants, although the cortical crescent orientation is disrupted[74]. Both Vangl1 and Vangl2 mutants display rotational polarization defects in single cells and disruption of rotational polarization coordination between cells[74].

PCP proteins are also required for BB/cilia positioning of motile monocilia, in the vertebrate left-right organizers and in the Zebrafish floor-plate.
Vangl1 and Pk2 localize anteriorly in the mouse node[273] and Vangl1/Vangl2 double mutants display random cilia positioning in the node, leading to left/right patterning defects[70]. Vangl2 MO-mediated knock down also disrupt cilia off-centering in the Xenopus embryo Gastrocoel Roof Plate, and maternal zygotic (MZ) Vangl2 mutant Zebrafish embryos display abnormal flow in Kupffer's vesicle and translational polarity defects in the floor-plate[274]. In the mouse node, knocking out five of the six Dvl alleles (Dvl1-/-; Dvl2-/-; Dvl3+/- mutants) leads to translational polarization defects which impair directional flow in the Node[124]. Intriguingly, in this study, Dvl2-GFP was found to localize at the posterior cortex but not next to basal bodies.

Interestingly, it was shown only recently that in the Drosophila wing, in which PCP have been studied for many years, centrosomes assume an asymmetric distal position, where they localize just beneath trichomes (Figure 27A). This translational polarization was disrupted in Flamingo loss of function and Frizzled over-expression (Figure 27B), and completely reversed when overexpressing the Spiny-legs Prickle isoform[275]. The trichome is not a cilium, but in addition to actin filaments, it contains some acetylated microtubules[275]. The presence of microtubules suggests that trichomes could be highly modified cilia that would have lost the 9 doublets organisation.

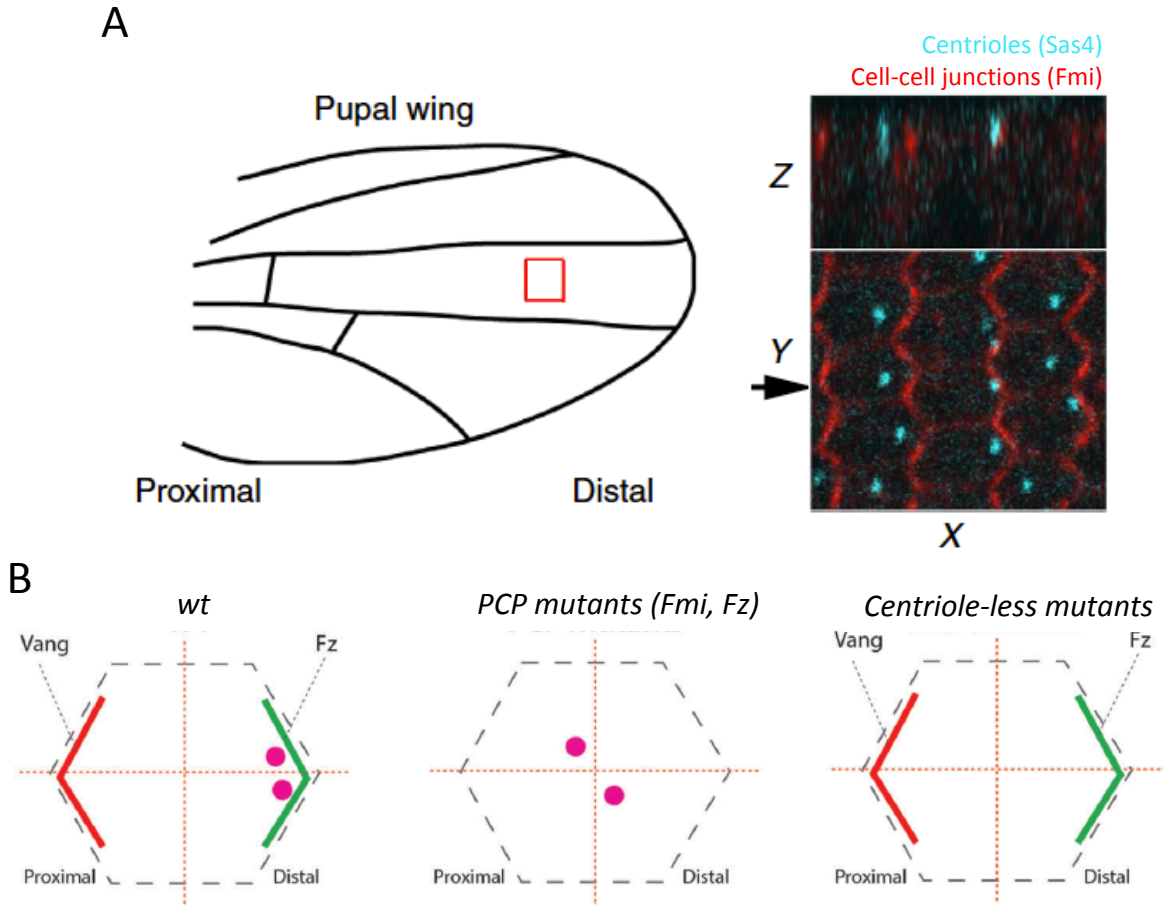

Figure 27 Centriole off-centering downstream of PCP proteins in Drosophila wing

(A) Schematic of a Drosophila wing and immunostaining of wing cells (right) showing centriole off-centering toward the distal side of the wing (blue: centrioles, red: cell-cell junctions) (from Carvajal-Gonzalez 2016)

(B) Relative position of centriole and PCP proteins in wing cells of wt, PCP mutant and centriole-less Drosophila (from Carvajal-Gonzalez 2016)

Finally, PCP proteins are also involved in BB/cilia orientation and positioning in marine larvae ectoderms of Jellyfish: in *Clytia hemisphaerica*, a Vangl orthologue is required for proper translational and rotational polarization and their coordination at the tissue scale to allow aborally-directed swimming, which suggests a very conserved role of PCP proteins in ciliated epithelia planar polarization in Metazoan[276].

Together, these studies argue for a widely conserved role of PCP proteins in the orientation and positioning of cilia in mono and multi-ciliated epithelia.
However the links between PCP proteins and the actin and microtubule cytoskeleton, which are required for BB/cilia orientation (see below) remain largely unknown.

b) Connections between basal bodies and the apical cytoskeleton

Early electron microscopy studies showed that cilia in MCC connect with the apical actin and microtubule networks through their appendages. In quail oviduct MCC, the basal foot is connected to apical microtubules and the rootlet connects both with actin filament at the base of adjacent microvilli and with intermediate filaments deeper in the cytoplasm[277]. Moreover the basal foot has been shown to contain γ-tubulin in human oviduct MCC and can thus nucleate microtubules[204]. In Xenopus MCC, actin is required for proper cilia spacing and microtubules for proper rotational polarization[278] (Figure 28A), probably through the connections between basal body appendages and the cytoskeleton. BB in these cells are also embeded in an intricate microtubule apical network (Figure 28C) that is required for rotational polarization (Figure 28A).
Interestingly, zeta-tubulin localizes at basal feet in these MCC and its MO-mediated knockdown leads to rotational polarization defects and basal bodies spacing defects, although its precise role at the basal foot remains unknown[279]. Further supporting a role for basal feet in MCC planar polarization, the loss of one isoform of Odf2, the one that plays a crucial role in basal feet formation but leaves distal appendages intact, triggers a loss of rotational polarization of MCC in murine trachea that then leads to a coughing/sneezing phenotype[205].
Together, these observations show a crucial role for the basal foot in basal body orientation within the apical surface of MCC.

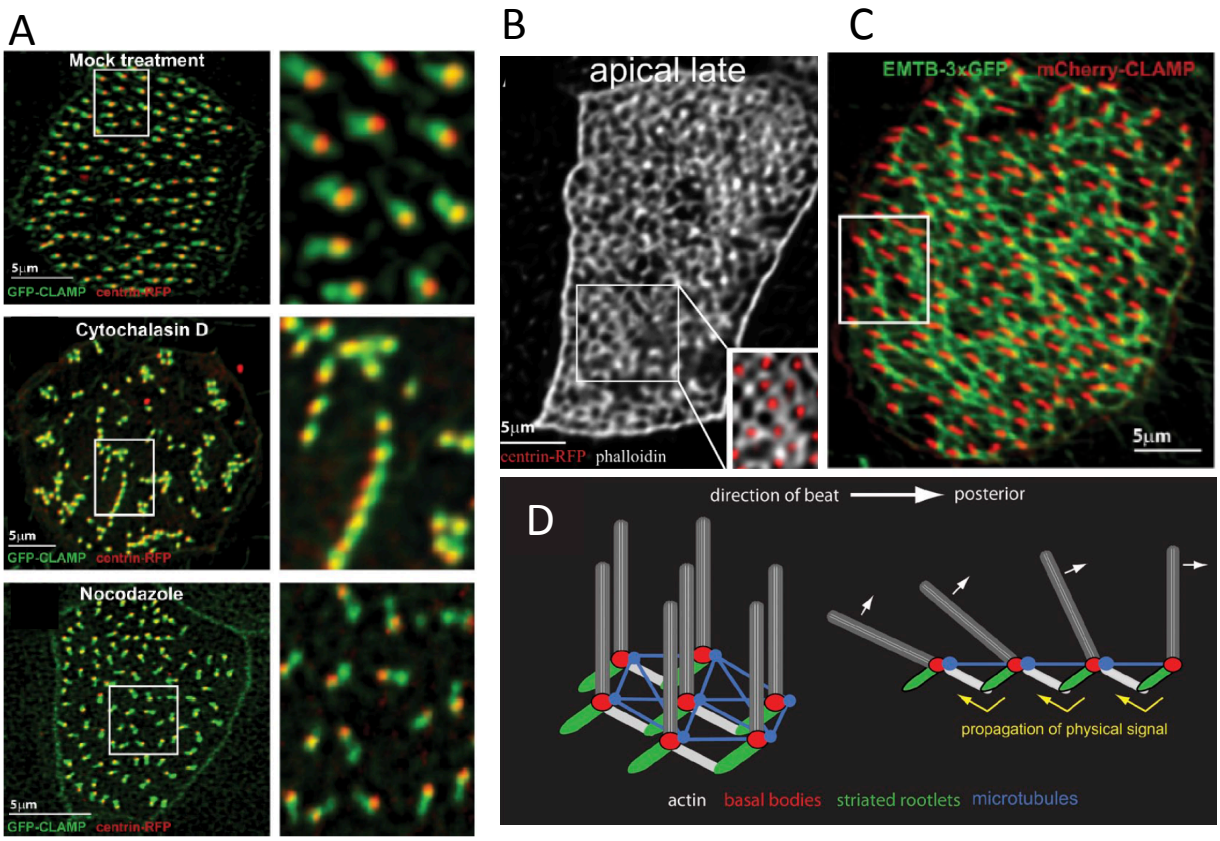

Figure 28 Importance of apical cytoskeleton for BB spacing and orientation in Xenopus multi-ciliated cells (MCC)

(A) Immunostaining showing basal bodies (red) and rootlets (green) of Xenopus embryo ectoderm MCC in control embryos, cytochalasinD-treated embryos (to inhibit actin polymerization) or nocodazol-treated embryos (to depolymerize microtubules). Images on the right are close-ups of left images.

(B) Phalloidin staining revealing the apical actin network of Xenopus MCC

(C) A Xenopus MCC expressing a microtubule marker (green) and a rootlet marker (red) showing the organization of the apical microtubule network

(D) Summary of the links between BB and apical cytoskeleton in Xenopus MCC

(adapted form Werner 2011)

Several proteins localizing at the ciliary rootlet could also be important actors for this process.

CLAMP localizes to rootlets in Xenopus MCC and its depletion leads to rotational polarization defects. However, CLAMP also localizes at the cortex, where it is asymmetrically localized, and it regulates the asymmetric localization of Pk2 and Dvl1[280]. The respective contributions of CLAMP at basal feet and at the cortex are not yet known.
Similarly, Kurly, a protein involved in both cilia motility and planar polarization, localizes to the rootlet in Xenopus MCC and its MO-mediated knock-down leads to impaired rotational polarity and a disruption of Pk2 asymmetric cortical localization[281].
Finally, as mentioned previously, Dvl2 localizes to the ciliary rootlet in Xenopus MCC, mouse ependymal MCC and mouse tracheal MCC and is required for rotational polarization, although it is not yet clear whether this depends on its localization at the rootlet.
Thus, it would be interesting to define the protein domains involved in these differential subcellular localizations (rootlet versus plasma membrane) to perform PCP rescue experiments with specific protein variants only present at rootlets.

Non-muscle myosin II (NMII) (the myosin heavy chains myh10 and myh14, components of NMIIB and NMIIC respectively) also localize close to basal bodies in mouse ependymal MCC, although it is not yet known whether they localize at the basal feet or rootlets[271]. In this system, NMII is required for translational polarity, which consists in the anterior positioning of the motile cilia patch within the apical surface. However the immunostainings performed in this study suggest that NMIIB and NMIIC localize not only at basal bodies but also at the cell cortex. Therefore it is also difficult to conclude on a role of NMII specifically at basal bodies for translational polarization.

Regulation of basal bodies orientation and positioning has been shown to require RhoGTPases in some cell types. In Xenopus MCC, RhoA is active next to apically docked basal bodies and a dominant-negative RhoA disrupts rotational polarization[261]. In the mouse Node and cochlea, Rac is required for translational polarization[124]. However it is

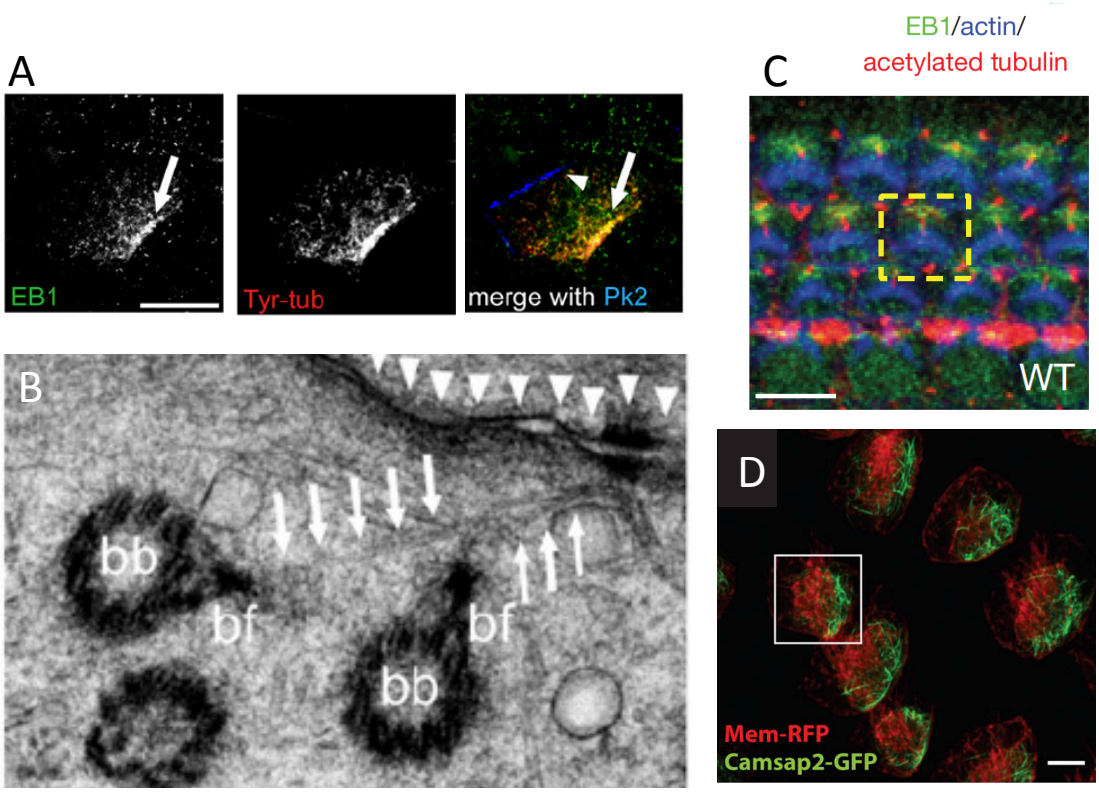

Figure 29 Asymmetric enrichment of microtubule ends in ciliated planar polarized epithelia

(A) Immunostaining of a mouse tracheal multiciliated cell revealing an enrichment of the microtubule (+) end binding protein EB1 (arrow) and Tyrosinated-tubulin opposite to Pk2 (arrowhead) (from Vladar 2012)

(B) EM image showing microtubules (arrows) linking basal-body basal feet (bf) and apical junctions (arrowheads) in mouse tracheal multiciliated cells (from Valdar 2012)

(C) Immunostaining of mouse cochlea showing asymmetric enrichment of EB1 on the same side as the kinocilium (from Ezan 2013)

(D) Xenopus epidermal MCC expressing a membrane marker (red) and a microtubule (-) end marker (green) which is enriched on the posterior side of the cells (from Kim 2018)

not yet clear how these small GTPases are activated and how they act on microtubules or actin filaments to position and orient basal bodies.

Nevertheless, the apical microtubule network is polarized in many ciliated epithelia, which suggests that this network could be important for proper BB/cilia orientation and positioning.

In mouse tracheal MCC, apical microtubules orient parallel to the planar polarization axis and EB1 (a microtubule (+) end binding protein) and Tyrosinated tubulin are enriched on the Fzd/Dvl cortex, toward which basal feet point[74] (Figure 29A,B).

Tyrosinated tubulin is associated with newly synthesized microtubules and can recruits +TIPs (microtubule (+) ends binding proteins)[282]. This suggests that microtubules emanating from basal feet preferentially grow towards this part of the cellular cortex, which is also consistent with electron microscopy data[74].

Similarly in mouse ependymal MCC, EB3 (also a microtubule (+) end binding protein) is enriched on the anterior cortex toward which basal feet point, but this enrichement is clear only at late stages of MCC differentiation, when polarization is already achieved[270].

Thus the role of polarized microtubules linking basal feet and a portion of the cortex in establishing polarity is still uncertain. In mono-ciliated cells, EB1 is enriched on the cortex closer to the kinocilium final position in the mouse cochlea (Figure 29C). The same study also found a weak enrichment of dynein at this cortical site, suggesting a mechanism of microtubule pulling forces at the cortex leading to BB/kinocilium off-centering[283].

Interestingly in the mouse cochlea, BB/kinocilium positioning depends on the mInsc/LGN/Gαi polarity proteins that are involved in oriented cell division (see part I). It was hypothesized that these proteins regulate BB positioning by regulating astral microtubule dynamics[283]. Another study suggested that these proteins are rather required for the creation of an apical “bare zone”, lacking kinocilium, stereocilia and microvilli, that position the BB/kinocilium in an intermediate position, between the cell center and the cell cortex[284], but the connection with microtubule or actin regulation is not clear.

Finally, an asymmetric localization of microtubule (-) ends has also been found in Xenopus embryo ectodermal MCC (Kim 2018[280])(Figure 29D)

However, since in all these studies, the polarization of the MT network is visualized when centrioles/BB or PCP proteins are already polarized, it is difficult to decipher whether microtubule polarity is initiating PCP, concomitant with PCP establishment or a consequence of the PCP process.

c) Role of ciliary proteins in PCP establishment or maintenance

Several proteins first described as localizing to the base of cilia and/or within the axoneme, and important for ciliogenesis or cilia function have been shown to control BB/cilia positioning in the mouse cochlea and ependymal MCC. However it is now becoming clear that most "ciliary" proteins have extraciliary functions[285].

In the mouse cochlea, a first study showed that depletion of BBS6 (Mkks) or BBS4 leads to stereocilia bundle misorientation or flattening[286], although the kinocilium forms normally. Compound heterozygous mice for BBS6 and Vangl2 show stereociliary defects similar to BBS6 homozygous mutants, showing a genetic interaction between BBS6 and Vangl2. In addition Vangl2 was found to localize around basal bodies and within the axoneme in IMCD3 epithelial cells and human respiratory epithelial cells[286]. BBS4 localize at centriolar satellites in HeLa cells and serves as an adaptor for dynein, allowing PCM1 recruitment to the centriole and microtubule anchoring[287]. Thus it could be that BBS4 and BBS6 are important for Vangl2 localization to basal bodies, which could in turn be required for proper kinocilium positioning (although the localization of Vangl2 to basal bodies has only been found in this study). It could also be that BBS4 and BBS6 are required for proper asymmetric cortical localization of Vangl2, or that they regulate the dynamics of microtubules emanating from the basal bodies that could be required to position it within the apical surface. Supporting the first hypothesis, another study showed that BBS8 and Ift20 (an Ift localizing dynamically at the trans-Golgi, at the cilium and along microtubules, required for vesicle trafficking from the trans-Golgi to the base of the cilium[288]) are required for proper Vangl2 asymmetric localization in the cochlea[289].

However two studies showed that in Ift88[290] and Kif3a[291] mutants, which display cochlear PCP defects, asymmetrical localization of PCP proteins is not disrupted. In addition, centriole loss in Drosophila wing does not disrupt asymmetric localization of PCP proteins (Carvajal-Gonzalez 2016[275]) (Figure 27B)

In Ift88 mutant mice, the cochlea is shorter and wider, suggesting a role for Ift88 in cochlea convergence and extension, a process in which PCP proteins are involved[266 65] (see part II). Most stereocilia bundles are V-shaped but their orientation is not coordinated, which is again reminiscent of Vangl2 mutant polarization defects[266]. In addition, 10-15% of hair cells have a central kinocilim, surrounded by stereocilia, indicating defects in kinocilium migration to the cell cortex which are not seen in core PCP mutants. Finally Vangl2 and Fzd3 asymmetric subcellular localization are not affected. This shows that Ift88 act either downstream or in parallel to core PCP components to position the kinocilium at the cortex and to position it at the right place. Interestingly the apical microtubule network emanating from the basal body was disrupted in Ift88 mutants, and Ift88 has been shown to regulate astral microtubule formation in mitotic cells[221] and to control spindle orientation in a PCP and cilia independent manner in Zebrafish[292]. Thus Ift88 effect on BB/cilium positioning in the cochlea could be linked to its ability to regulate the apical microtubule network

In Zebrafish, MZ-Ift88 mutants never form cilia and have no translational polarization defects in the floor-plate[292]. Although this exclude a role for the axoneme in translational polarization, an extraciliary role of Ift88 remains possible since the mutant used can still produce a protein by exon-skipping[293] and BB are still properly docked to the apical membrane.

Kif3a mutant cochlea also display PCP defects. Kif3a is a member of the kinesin II family that allow anterograde transport within cilia. Kif3a mutant cochlea has no kinocilium and display convergence and extension defects[291]. The basal and middle regions of the cochlea have little elongation defects and have mild stereocilia bundle orientation defects. However at the cochlea apex, the extension is more affected and so is the orientation of the stereocilia bundles. In the middle and basal regions of the cochlea, stereocilia bundles are flattened and there is a general loss of correlation between the basal body position and the middle of the stereocilia bundle. The off-centering of the basal body is not affected, but it is localized deeper within the cytoplasm compared to control hair cells. Intriguingly, loss of Kif3a doesn't affect Dvl2 or Fzd3 asymmetric localization but disrupts the asymmetric localization of phosphorylated PAK, a kinase

activated by Rac. Inhibiting Rac or PAK recapitulates the PCP defects seen in Kif3a mutants, although the kinocilium is not affected, suggesting that Kif3a acts through Rac/PAK independently of the axoneme to position the basal body in the cochlea.
Kif3a mutant radial glial cells that are monociliated present a defect in translational polarity, but the potential connection of Kif3a with PCP proteins in that cellular system was not investigated (Mirzadeh, 2010[294]).
Since Kif3a is present at another location, close to the BB, at the subdistal appendages in fibroblast (Kodani, 2013[295]) and this pool could be instrumental in positionning the BB in cochlea.

Finally *Rpgrip1l*, the master-regulator of the ciliary transition zone in vertebrates is also involved in BB/cilia positioning both in mouse and Zebrafish[296]. *Rpgrip1l* mutant mice have convergence-extension and PCP defects in the cochlea, severely affecting kinocilium positionning while leaving stereocilia orientation nearly correct. The disconnection netween kinocilium and stereocilia position is a common feature of ciliopathy mutants in cochlea (Jones 2008[290]) and is different than PCP mutants. In *Rpgrip1l* mutant, approximately 15% of hair cells have shorter kinocilia whereas another 15% completely lack kinocilia. In addition, around 5% of hair cells have misoriented stereocilia bundles and 2.5% a round bundle with a central kinocilium. In Zebrafish, MO-mediated Rpgrip1l knock-down leads to convergent-extension defect as well as translational polarization defects in the floor-plate and this can be rescued by Dvl over-expression. Accordingly, Rpgrip1l was shown to antagonize inversin and nphp4 which target Dvl for proteasome mediated degradation. However the link between Dvl and asymmetric basal body positioning in the Zebrafish floor-plate remains unknown.

Other ciliary proteins such as ALMS1[297] and MKS1[298] are also involved in mouse cochlea PCP, but nothing is yet known about the mechanisms linking these proteins to BB/kinocilium positioning.

Thus, evidence from these examples suggest that ciliary proteins play a role in BB positioning that is independent of their role in axoneme formation and therefore points to their role either on intracytoplasmic transport of PCP components or at the basal

body to organise the microtubule network or connection of the BB with subapical cytoskeletal network.

However, the axonemal function of some ciliary proteins (IFT88, kif3a, pkd1, pkd2) is required to refine PCP or coordinate PCP at tissue level in ependymal MCC rotational polarity most probably through their role as mechanosensors as illustrated below (Guirao, 2010[269] and Ohata, 2015[299]).

d) Role of mechanical forces

Many ciliated epithelia experience fluid flow at their surface, and it has been found that this flow can establish or refine the orientation and position of BB and cilia.
It was first shown that in MCC of Xenopus embryonic epidermis, an initial rotational polarity bias is refined by fluid flow in a second phase. Fluid flow can even reorient cilia polarization, but only when cilia are motile, suggesting a positive feedback mechanism, where flow aligns ciliary beating which then reinforce the flow[300]. A subsequent study in the mouse ependymal MCC[269] showed that fluid flow can establish coordinated rotational polarity in wild-type mice but not in Vangl2 mutants or in Kif3a mutants lacking cilia, suggesting a model where fluid flow initiate a positive feed-back loop that also requires Vangl2. In this system, the mechano-sensitive channels Pkd1 and Pkd2 are very likely to transduce this mechanical signal since they are only expressed along the axonemes of MCC and their mutation triggers a loss of rotational polarization (Ohata, 2015[299]).
More recently, a study exerting forces with a micropipette on Xenopus gastrocoele roof plate explants to mimick mechanical constraints during gastrulation showed that directional mechanical tension can trigger the asymmetric enrichment of core PCP proteins, the asymmetric positioning of BB/cilia and even modulate the length of cilia, although the molecular mechanisms at work in that cellular context are unknown[131].

D) Polarity proteins and ciliogenesis

Many studies have shown an involvement of ciliary proteins in PCP. Reciprocally, many polarity proteins are involved in ciliogenesis.

Some PAR complex members have been found to localize at the cilium base and to be involved in ciliogenesis in many systems. For example in sea urchin larvae, aPKC localizes at the transition zone of ectodermal cilia and regulate their growth[301]. The Par-aPKC complex is also involved in cilia growth in zebrafish photoreceptors through its role in apical and ciliary membrane specification[302]. Par3 is also required for ciliogenesis in cultured epithelial cells via its interaction with kinesin II motors responsible for anterograde trafficking within the cilium[303]. Crumbs protein have also been involved in ciliogenesis[304].

Concerning PCP protein, a role in ciliogenesis is well established for Dvl (see above) and CPLANE (Ciliogenesis and planar polarity effectors, Inturned, Fuzzy and Wdpcp[305]). However the situation is less clear for Vangl. Vangl2 has been found in the axoneme in mouse ependymal MCC but is not required for ciliogenesis in these cells. In the mouse node, ciliogenesis is not affected even in double Vangl1;Vangl2 mutants[70], and in Zebrafish Kupffer's vesicle and floor-plate of MZVangl2 mutants, ciliogenesis is not impaired[274]. However another study using a different Vangl2 mutant (tri^{m209} instead of tritk50f) found a significant decrease in Kupffer's vesicle cilia length and number[306]. MO-mediated knock down of Vang also led to ciliogenesis defects in Clytia hemisphaerica embryos[276]. Because ciliogenesis defects were only observed in morpholinos injected embryos susceptible to off-target effects and with a partially truncated allele (tri^{m209}) which can behave as semi-dominant allele, it is most likely that Vangl1 and Vangl2 are not implicated in ciliogenesis as observed in double-mutants in two different species.

Interestingly, mutations in Pk1 or Pk2 in mouse lead to abnormal cilia: Pk1[307] and Pk2[308] hypomorphic mutant mice display abnormal blebbing of the ciliary membrane in the tracheal and ependymal MCC respectively affecting ciliogenesis but not general apico-basal polarity as in Pk1 null mutants (Tao 2009[174]).

Thus BB/cilia positioning is an important feature of cell polarization. Bringing BBs to the cell surface and controlling their orientation relative to body polarity axis is critical for the function of ciliated cells and rely on polarity proteins, smallGTPases and the

interaction between BB appendages and the cytoskeleton. In some cases the axoneme itself refine cilia polarization. The intricate links between cilia and cell polarization is further illustrated by the fact that some proteins classically described as involved in ciliogenesis have been shown to play a role in cell polarization, and reciprocally, some polarity proteins are involved in ciliogenesis. This suggests that cell polarization mechanisms and cilia coevolved and were always tightly linked in eukaryotic cells.

RESULTS

The general aim of my PhD work was to study the dynamics and mechanisms of planar polarization of cilia in epithelia. As mentioned in the introduction, studies carried out so far on planar polarization in mouse cochlea or ependyma lack a dynamic description with a good temporal resolution. In order to get a better understanding of the dynamics and mechanisms leading to coordinated planar basal body (BB) off-centering, we decided to investigate this polarization process in the zebrafish floor-plate (FP). The zebrafish FP consists of three rows of monociliated epithelial cells at the most ventral side of the neural tube. The posterior position of motile cilia in FP cells ensures the establishment of a directional, anterior to posterior cerebro-spinal fluid flow in the neural tube central canal of the neural tube. In addition, zebrafish is a convenient model system with a transparent, fast and externally developing embryo and powerful genetic tools, allowing us to investigate the dynamics of subcellular structure such as BBs in live-imaging with a high temporal resolution.

I first described BB movements within the apical surface of medial FP cells as the FP polarizes during somitogenesis using a live-imaging approach. I found that BBs have a highly motile behavior at early stages (beginning of somitogenesis), that their movements become less dynamic and their residence time at the posterior membrane increases as development proceeds. I then investigated the role of the polarity protein Par3 in this process and found that Par3 forms patches at transverse membranes next to posterior BBs. Mosaic injection of Par3-RFP revealed that Par3 becomes posteriorly enriched before BB/posterior membrane contact. Strikingly, at early stages, BBs touch the membrane exclusively at the level of these discrete Par3 patches. In many cases, I also observed membrane invaginations between BBs and Par3 patches, suggesting the existence of mechanical forces between these two structures. Investigating the requirement for Par3 in FP polarization, I found that Par3 over-expression disrupts FP polarization, suggesting that the posteriorly enriched Par3 distribution is crucial for proper polarization. I finally assessed whether Par3 could behave as a downstream effector of the PCP pathway by analyzing its distribution in the core PCP mutant vangl2. Indeed, Vangl2 protein is localized anteriorly in FP cells and is required for BB posterior positioning. I showed that in *vangl2* mutants, polarization defects correlate with a mis-localization of Par3.

Together, these results suggest that Par3 acts downstream of core PCP proteins to position FP BBs posteriorly. These results are presented in the first part of the result section as a manuscript soon to be submitted for publication.
To complement this study and understand the mechanisms downstream of PCP and Par3 in BB polarization, I investigated a potential role of acto-myosin and microtubules. Different drug treatments to inhibit acto-myosin contractions had no effect on FP polarization. Microtubules were posteriorly enriched in FP cells, suggesting that microtubule dynamics could contribute to BB posterior positioning. I am currently performing experiments to study their role. My preliminary results on the role of the cytoskeleton in BB polarization are described in Part 3 of the Results section.

Ciliated epithelia also display a second form of planar polarity called « rotational polarity » which refers to the orientation of ciliary beating and is correlated with the orientation of BB appendages (rootlet and basal foot). Whether FP cilia display rotational polarity was not known at the beginning of my PhD due to the lack of BB appendages markers. During my PhD I described rotational polarization in FP cells. I found that Non-Muscle-Myosin IIB localizes as a discrete dot on the posterior side of FP BBs and that myosin light chain was phosphorylated at this site, thus identifying the first marker of BB rotational polarity in the FP. I found that this asymmetric localization was highly disrupted in *vangl2* mutants and moderately affected in *dvl2* mutants (another PCP mutant). These results are presented in Part 2 of the Results section.

Ciliary proteins themselves have been found to play a role in ciliated epithelia PCP, and our laboratory previously showed that the ciliary protein Rpgrip1l is required for FP BB planar off-centering. In a second part of my PhD I set out to determine whether this PCP function of ciliary proteins is an ancestral feature of Metazoan by investigating the role of the only Rpgrip1l ortholog in the PCP of the ciliated ectoderm of the jellyfish *Clytia hemisphaerica* larva in collaboration with Tsuyoshi Momose (LBD Villefranche-Sur-Mer). We found that Rpgrip1l localized at the base of cilia and preliminary data suggest that Rpgrip1l is required for the rotational polarization of

these cells, suggesting that its function in PCP is indeed an ancestral feature of Metazoan. These preliminary results are presented in Part 4 of the Results section.

I-Translational polarity in zebrafish floor-plate: Par3 mediates BB posterior attraction

PLANAR POLARIZATION OF CILIA IN THE ZEBRAFISH FLOOR PLATE INVOLVES Par3-MEDIATED POSTERIOR ATTRACTION OF HIGHLY MOTILE BASAL BODIES.

Antoine Donati[1], Sylvie Schneider-Maunoury[1*] and Christine Vesque[1*]

[1] Sorbonne Université, CNRS UMR7622, INSERM U1156, Institut de Biologie Paris Seine (IBPS) - Developmental Biology Unit, 75005, Paris, France

*co-senior authors, co-corresponding authors.

Keywords: planar cell polarity, cilium, basal body, zebrafish floor plate, Par3, Vangl2.

SUMMARY

To produce a directional flow, ciliated epithelia display a uniform orientation of ciliary beating. Oriented beating requires planar cell polarity (PCP), which leads to planar orientation and asymmetric positioning of the ciliary basal body (BB) along the polarity axis. While the involvement of the PCP pathway in this process is well known, its dynamics and downstream mechanisms remain poorly understood. A major difficulty is to follow the dynamics of BB polarization in vivo or to reproduce it in vitro. Here we took advantage of the polarized mono-ciliated epithelium of the embryonic zebrafish floor plate (FP) to investigate the dynamics and mechanisms of BB polarization. By live-imaging of the FP during the polarization process, we showed that BBs, although bearing a cilium, were highly motile along the antero-posterior axis in both directions. They contacted the anterior and posterior membranes exclusively at the level of apical junctions positive for Par3. At late stages of FP polarization, BBs spent longer periods in contact with the posterior membrane. Par3 was enriched at the posterior membrane of FP cells before BB posterior positioning and FP polarization was disrupted upon Par3 overexpression. In the PCP mutant *Vangl2*, BBs showed faster, poorly oriented movements and this correlated with a reduction of Par3 posterior enrichment. Our data uncover an unexpected motile behavior of ciliated BBs and lead us to propose a conserved function for Par3 in mediating junction-driven attraction forces controlling centriole asymmetric positioning downstream of the PCP pathway.

INTRODUCTION

Cilia are conserved microtubule-based organelles with sensory and motile functions. Motile cilia generate forces sufficient to propel whole organisms or bodily fluids within cavities in animals: in respiratory airways to clear the mucus, in the oviduct to move gametes, in the embryonic laterality organ to establish left-right asymmetry, and in the central nervous system to circulate the nutrient-rich cerebrospinal fluid (Wallingford 2010; Meunier & Azimzadeh, 2016). In order to generate a directional flow, ciliated epithelia display a uniform orientation of ciliary beating, which is a form of planar cell polarity (PCP). Oriented beating of a cilium usually involves two PCP processes: the asymmetric positioning of the cilium basal body along the polarity axis of the cell (translational polarity, in monociliated epithelia and ependymal cells) and its planar orientation (rotational polarity) (Wallingford 2010).

In many vertebrate ciliated tissues such as the mouse cochlea and ependyma, the laterality organ of mouse and zebrafish, the Xenopus larval skin and the zebrafish floor plate, cilium polarity requires the PCP pathway. In these tissues, PCP proteins such as Van Gogh like 2 (Vangl2), Frizzled (Fz3/6), Cadherin EGF LAG seven-pass G-type receptors (Celsr1-3) and Dishevelled (Dvl1-3), localize asymmetrically in ciliated epithelia, and are required for proper cilia/BB positioning (Montcouquiol et al., 2003, Mitchell et al., 2009, Borovina et al., 2010, Mirzadeh et al., 2010, Song et al 2010, Boutin et al., 2012). Outside the PCP pathway, the cellular and molecular mechanisms of BB positioning remain poorly understood. Non-muscle myosin II is required for ependymal translational polarity in murine ependymal multiciliated cells (Hirota et al., 2010) and the murine Myosin Id mutant exhibit defects in both translational and rotational polarity in these cells (Hegan et al., 2015). Translational polarity has been shown to require Rac1 in monociliated cells of the mouse node and cochlea (Hashimoto et al., 2010; Grimsley-Myers et al., 2009) and G protein signalling in cochlear hair cells (Ezan et al., 2013; Tarchini et al., 2013). Ciliary proteins themselves have been involved in planar polarization of cilia in several contexts (Ross et al., 2005; Jones et al., 2008; Mirzadeh et al., 2010; Mahuzier et al., 2012; Ohata et al., 2015). However, the relationships between these different actors and how they impact basal body movement is unclear.

Understanding the mechanisms of cilium polarization would highly benefit from a dynamic analysis of BB movements. A major drawback is the difficulty to follow the dynamics of BB polarization *in vivo* in whole embryos, or to reproduce PCP and cilium polarization *in vitro* in cultured cells. So far, live imaging of cilium polarization has been performed only once in cochlear explants and only confined Brownian motion of centrioles was observed (Lepelletier et al., 2013). In this paper, in order to get a better understanding of the mechanisms leading to BB off-centering in epithelia, we have used the zebrafish embryonic floor-plate (FP) as a convenient system to investigate the dynamics of the polarization process in live embryos. The FP is a simple mono-ciliated epithelium whose posterior-positioned motile cilia allow circulation of the embryonic CSF in an anterior to posterior fashion.

Our results show that planar polarization of BBs and their associated cilia is progressive during somitogenesis and is accompanied by a change in the behavior of the BBs, which are highly motile at early stages and tend to spend an increasing amount of time in contact with the posterior membrane as development proceeds. We found that BBs always contacted membranes at the level of Par3-enriched apical junctions. Par3 became enriched at the posterior apical side of FP cells before BB polarization. Par3 overexpression disrupted FP polarization and its posterior enrichment was disrupted in a *Vangl2* mutants. Thus, we propose that a major role of the PCP pathway in the FP is to drive Par3 asymmetric localization, which in turn attracts the BB at the posterior membrane.

RESULTS

Floor-plate polarization shows temporal progression but no spatial synchronization

Posterior positioning of the BB in the zebrafish FP is visible as soon as 18 hours post-fertilization (hpf) (Mahuzier et al., 2012) and is maintained at least until 72 hpf (Mathewson et al., 2019). From 24 hpf onward, coupled to posterior tilting of cilia, it is instrumental in propelling the CSF in the spinal cord central canal (Borovina et al., 2010, Fame et al., 2016). At late gastrulation stages (10 hpf), ectodermal cells already display a slight posterior bias of centrioles (Sepich et al., 2011). At early somite (s) stages, centrioles have migrated under the apical membrane in several cell types and short cilia are detected with the Arl13b-GFP transgenic line (Borovina et al., 2010).

To define the time-course of FP cell polarization during somitogenesis, we assessed basal-body (BB) position along the antero-posterior (AP) axis on fixed embryos from the 6 s to the 26 s stage (Fig. 1a, b). For each cell we defined a BB polarization index (p.i. in Fig. 1b). BBs already exhibited a posterior bias at 6 s, since 50% of FP cells had a BB in contact with the apical posterior membrane, and 20% of BBs were located within the posterior third. The polarization state did not change significantly until 10 s. While we could find some FP cells with an anterior BB between the 6 s and 14 s stages (Fig. 1a, yellow arrow), it was not the case later. From 10 s onward, there was a progressive increase in FP polarization, mostly due to an increase in the percentage of cells with a BB in contact with the posterior membrane, with a concomitant disappearance of anterior BBs and a reduction of median BBs. The polarization state of the FP was considered complete at 18 s, since no significant difference could be detected between the 18 s and 26 s stages. Interestingly, we did not detect a gradient of polarization index along the A/P axis of the spinal cord (Fig. S1a), and single non-polarized cells were often intermingled among polarized neighbors (Fig. S1b), arguing against the existence of waves of polarization originating from axis extremities.

BBs are highly mobile in FP cells

We then turned to live-imaging to obtain a dynamic view of the polarization process and assess BB motility within the apical surface and potential correlations with cell deformation and cell division. We used time-lapse movies to follow BB movements within the apical surface of individual FP cells at different developmental stages, ranging from 4 s to 21 s. We found that BBs displayed a highly motile behavior, while remaining located in the most apical cortex (Fig. 1c-f) (Supplementary movies S1-S4). They moved both anteriorly and posteriorly (Fig. S1e, first column), and thus not only toward posterior membranes as could be suggested by the analysis on fixed samples.

BB movements seemed independent of cell deformation. Cell deformations along the AP axis were more important at early stages (4-10 s) (Fig. 1c, d), probably as a consequence of convergence-extension movements (compare for example purple lines of graphs in Fig1d and e), but most BB movements were not correlated with cell deformation (see Fig. 1c). At later stages (14-21 s) (Fig. 1e, f), cell deformations were small and did not correlate with BB movements. One possible explanation for the presence of unpolarized cells next to polarized neighbors is that they could either be in mitosis or soon after mitosis, before BB re-localization. To test this hypothesis, we quantified mitoses and followed daughter cells after cell division. Mitoses were rare in FP cells at early stages (6 mitoses / 79 cells for 9 embryos analyzed at 4-8 s) and absent at later stages (118 cells from 15 embryos at 13-21s). In addition, after cytokinesis, the centriole of the posterior daughter cell returned to the posterior membrane in a very short time (14 min in average, n=6), and so did the centriole of the anterior daughter cell that polarized during the movie (22 min in average, n=3) (Fig. S1d) (Supplementary movie S5). Most of the observed unpolarized cells were in interphase. Thus, we concluded that the state of FP cell polarization was neither correlated to the cell shape changes nor to the cell cycle.

FP polarization involves a change in BB behavior

In order to characterize BB behavioral changes during development, we determined the percentage of time that BBs spent in contact with the posterior membrane (Fig.

1g). At early stages, BBs spent in average 44% of their time in contact with the posterior membrane, whereas at later stages (13-21 s) it reached 70%. This was largely due to an increase in the number of cells in which the BB stayed in contact with the posterior membrane during the whole movie (for example in Fig. 1e). This situation will be referred to as “posteriorly docked BB”, although it is not known whether a physical link between BB and the posterior membrane exists. At early stages (4-8s), we did not observe any cell with posteriorly docked BBs (41 cells analyzed, 5 embryos), whereas they made up around a third (34%) of the FP cell population at 13-17s stages (13/38 cells, 6 embryos) and almost half (46%) the FP population at later stages (17-21s, 27/59 cells, 7 embryos). BB behavioral changes during somitogenesis were also characterized by a decrease in the frequency of BB direction changes, as well as an increase in the mean duration of BB/posterior membrane contact events and mean polarization index, suggesting that, as development proceeds, BB movements are less dynamic and more confined to the posterior side of the cell (Fig. S1e, plots of the first line). Posteriorly docked BBs made a significant contribution to these behavioral changes. In order to determine if changes in the behavior of non-posteriorly docked BB contributed to the increase of FP polarization during somitogenesis, we quantified the same parameters, but taking into account only these motile BBs (Fig. S1e, second line): although less drastic, the same trend in BB behavior change was observed.

To further characterize the behavior of non-posteriorly docked BB, we quantified the frequency of contact events between the BB and either the anterior or the posterior membrane (Fig. 1h and i, respectively). First, posterior contacts were more frequent than anterior ones even at 4-8s (compare Fig. 1h and i), confirming that FP cells already have a posterior polarization bias at these early stages. Second, contacts with the anterior membrane were frequently observed at early stages (50% of BBs make at least one anterior contact per hour, see for example at t=70’ in Fig1d), but almost never observed at later stages (only 3/57 cells display one anterior contact). Contact frequency with the posterior membrane was also significantly higher at earlier stages (1.3 contact/h on average) than at later stages (around 0.8 contacts/hour in average within the 13-21s stage window, Fig. 1i). This reduction in the number of contact events could be due to an increase in their duration (Fig. S1e,

plot 2nd column, 2nd line) and to a reduction in BB speed. Indeed, we found that BBs moved faster at earlier stages (FigS1c, median movement speed was around 0.2μm/min at 4-8 s versus 0.1μm/min at 13-21 s). Thus, the observed changes in FP polarization are explained both by an increase in the posteriorly docked BB population and by behavioral changes (reduced speed, less direction changes, longer posterior contact events) in other BBs.

Interestingly, live-imaging revealed the presence of membrane invaginations extending between the BB and transverse membranes (Supplementary movies S6 and S7). At early stages, we could detect such invaginations in 44% of FP cells (taking into account only non-posteriorly docked BBs) (26 cells out of 59 cells from 9 embryos), most of which were linking the posterior membrane and the BB (78%, 25/32 invagination events, Fig. S2a white arrows) (Movie S6), although invaginations from the anterior membrane were also seen (Fig. S2b, white arrow) (Movie S7). These early stage invaginations were most of the time observed on a single time frame (anterior invaginations) or two consecutive timeframes in time-lapse movies with a 5 min time interval between two images (FigS2c). Posterior invaginations were followed by a posterior directed BB movement in 66% of cases (33/50 invaginations), suggesting a causal link between their formation and movement of the BB to the posterior membrane. BB behavior following anterior invaginations did not seem different from BB behavior after posterior invaginations, but these results need to be confirmed as the number of anterior invaginations was very low (we observed only 14 such events, compared to the 50 posterior invagination events) (FigS2d). Membrane invaginations were rarely seen at later stages (after 14s, 9/40 cells, 10 embryos), probably in part because BBs spent a higher fraction of their time associated with the posterior membrane (see Fig. 1 and Fig. S1).

Overall, our dynamic analysis reveals a highly motile behavior of BBs in FP cells at early somite stages. This was unexpected, given that BBs are already anchored to the apical membrane at early somite stages and have grown a cilium that protrudes externally (Fig. 1a) (Borovina et al., 2010). As somitogenesis proceeds, BBs show decreased mobility. They progressively stop shuttling from anterior to posterior cell junctions and their contacts with the posterior membrane last longer. Importantly,

almost half of them still detach from the posterior membrane but only for short periods of time and remain close to the posterior apical junction.

We therefore made the hypothesis that from the 10s stage, the posterior apical junctions become progressively enriched in proteins that can attract the BB.

Posterior enrichment of Par3 precedes BB/posterior membrane contact

In Drosophila, the apical junction protein Par3 modulates centrosome positioning in the male germline and embryonic ectoderm (Inaba et al., 2015, Jiang et al., 2015). In order to test a potential role for Par3 in BB posterior positioning in FP cells, we first assessed Par3 localization by immunostaining (Fig. 2a, b). At the 14 s stage, Par3 localized at apical junctions of FP cells (Fig. 2a). Strikingly, Par3 patches were also detected on transverse membranes (anterior and posterior membranes cannot be distinguished in this experiment) and in close contact with posteriorly docked BBs (white arrows, Fig. 2a). This distribution was confirmed using the BazP1085 antibody (Fig. 2b), which recognizes a conserved Par3 phosphorylation site targeted by Par1 (Krahn et al. 2009). Interestingly, Par3 transversal patches were also present in FP cells in which the BB was not yet in contact with the posterior membrane (Fig. 2a, b, right panels) showing that this enrichment precedes stable BB/posterior membrane contact establishment.

In order to test whether Par3 is asymmetrically enriched in FP cells, we used a mosaic expression approach of Par3-RFP and centrin-GFP fusions in live embryos. Quantification of Par3 expression showed that, among fully polarized (p.i. =1) individual Par3-RFP expressing FP cells, both at early (6-12s, Fig. 2c, left) and late (14-20s, Fig. 2c, right) stages, almost all cells had a Par3-RFP post/ant ratio greater than 1 (Fig. 2d) (29/30 cells out of 20 embryos; 6-12s, mean ratio= 1.42, N=7, n=9; 14-20s mean ratio =1.38, N=13, n=21). To determine whether the enrichment of Par3 at the posterior membrane preceded BB/posterior membrane contact, we made movies of BB movements and quantified Par3-RFP posterior/anterior ratio at each time-point; we found that Par3-RFP was enriched posteriorly before the BB contacts the posterior membrane (Fig. 2e, f) (12/14 cells from 12 embryos) (Supplementary movies S8 and S9). In contrast, BBs of FP cells with weak or no posterior Par3

enrichment tended to remain unpolarized (either making no contact (2/5 cells, 5 embryos) or unstable contacts (3/5 cells, 5 embryos) with the posterior membrane (Fig. 2g) (Supplementary movie S10).

Thus, we show that Par3 forms patches at FP apical transverse membranes and that BBs make contacts with the membrane at these patches. We further show that Par3 is enriched posteriorly before BB/posterior membrane contact. Together, our data strongly suggest that Par3 is a key player in attracting the BB to the posterior membrane, and/or in holding it when it contacts the posterior membrane.

At early stages, BBs contact transverse membranes exclusively at Par3 patches

During the second half of somitogenesis, Par3 tended to form a continuous belt at apical junctions of FP cells, although it was locally enriched, forming patches that associated with centrosomes as described above. In contrast, at the 4 to 8 s stages, Par3 formed small, discrete patches at FP apical transverse membranes, but not at lateral membranes. These patches were roughly aligned with the AP axis of the embryo (Fig. 3a, white arrows). Strikingly, BBs made contacts with anterior and posterior transverse membranes (as described in Fig. 1) exclusively at the level of these patches (58 cells from 18 embryos) as shown in Fig. 3b and Supplementary movie S11. In 33% of these cells (19/58), the discrete Par3 patches stretched toward the BB (for example, Fig. 3b yellow arrows). In about 25% of these stretched patches (5/19) we could detect an underlying membrane digitation originating from either the posterior (Fig. 3c, t=0') or the anterior membrane (Fig. 3c, t=64') and extending toward the BB (Supplementary movie S12). The presence of membrane digitations and their overlap with Par3 patches point to the existence of mechanical forces between BBs and membranes at the level of Par3 patches and suggests that Par3 could be required for local force generation.

Par3 over-expression disrupts BB positioning

To test whether Par3 is required for posterior BB positioning in the FP, we first used a loss of function approach. MO-mediated knock-down of Par3ab (also known as Pard3 or ASIP) did not disrupt FP PCP (Fig. S3a), nor could we see a defect in a MZ-Par3ab mutant (Blasky et al., 2014) (Fig. S3c). However, in both cases, Par3 patches could still be detected in the FP by immunostaining (Fig. S3b, d- g), suggesting that Par3ab loss of function was compensated for by its paralogous genes (Par3aa, Par3ba or Par3bb), which could also be detected by our Par3 antibodies thanks to the high conservation of the epitopes. We thus turned to an over-expression approach to disrupt Par3 posterior enrichment and patch formation. Over-expressed Par3-RFP in the floor-plate localized to apical junctions and did not disrupt apico-basal polarity, as assessed by the presence of the BB at the apical surface and the proper localization of the apical junction protein ZO1 (Fig. S3e). In contrast to MbCherry over-expression taken as a control, Par3-RFP over-expression disrupted BB posterior positioning in the FP (Fig. 3d, MbCherry median p.i.=1, first quartile=0.94; Par3-RFP median p.i.=0.8, first quartile=0.64). Furthermore, mosaic over-expression showed that this effect was cell autonomous, as there was no significant difference in BB positioning between Par3-RFP negative cells in Par3-RFP expressing embryos and MbCherry negative cells in MbCherry expressing embryos (Fig. 3d MbCherry median p.i.=1, first quartile=0.84; Par3-RFP median p.i.=1, first quartile= 0.83).

These results strongly suggest that Par3 posterior enrichment and patch formation are required for proper BB positioning in the FP.

Par3 clustering and localization is disrupted in the *vangl2* mutant FP

Vangl2, a core PCP protein, has been shown to be involved in PCP in the zebrafish FP (Borovina et al., 2010) but the downstream mechanisms linking Vangl2 to centrosome posterior positioning are unknown. We thus analyzed the dynamics of FP polarization in the *vangl2*^{m209} (initially called *tri*^{m209}) mutant (Solnica-Krezel et al., 1996). At 18 s, the BB of *vangl2*$^{m209/m209}$ FP cells was mispositioned at the center of the apical cell surface, while *vangl2*$^{m209/+}$ embryos had normally polarized BBs as

judged by immunostaining (median p.i.=0.6 versus 1 for wt or *vangl2*$^{m209/+}$) (Fig. 4a, FP polarization plot). Live-imaging of *vangl2*$^{m209/m209}$ FP revealed that BBs maintained a high motility at late stages. In addition, most *vangl2*$^{m209/m209}$ BBs made at least one contact with either transverse or lateral membranes (70%, 17/25) (Fig. 4a, right image, white arrows), suggesting that force generators are still present in these mutants but more dispersed around the cell periphery.

To test whether Vangl2 could impact Par3 function in this process, we looked at phospho-Par3 localization in the *vangl2* mutant. Phospho-Par3 localized at apical junctions in *vangl2*$^{m209/m209}$ as in controls (Fig. 4b). Automatic detection of Par3 patches along the transverse apical junctions revealed that in wt, 90% of FP cells had a at least a major phospho-Par3 patch (Fig. 4a lower left panel, yellow arrows), with 39% of cells also having smaller secondary patches (Fig. 4c, N=7, n=186). In *vangl2*$^{m209/m209}$ embryos, the number of FP cells with at least one phospho-Par3 patch was unchanged (around 90% of cells) but the number of cells with more than one patch was increased (54% of cells, N=7, n=129). In addition, the prominence of phospho-Par3 patches fluorescence intensity was decreased in *vangl2*$^{m209/m209}$ embryos as compared to controls (see Fig. 4d for prominence definition and quantification). Similar results were obtained with the antibody against total Par3, although the changes in prominence were not statistically significant in this case. Thus, Par3 forms more numerous, less phosphorylated and smaller patches in *Vangl2* mutants, showing a role for Vangl2 in Par3 clustering and phosphorylation level within patches.

To analyze BB behavior in *vangl2* mutants and test whether Par3 posterior enrichment was affected in *vangl2*$^{m209/m209}$ FP cells, we made time-lapse movies of embryos mosaically injected with Par3-RFP (Fig. 4e, f) (Supplementary movies S13 and S14). In *vangl2* mutants, FP cells displayed motile BBs that contacted the membrane at the level of Par3 patches, but the distribution of the patches was very different. Compared to control embryos (*vangl2*$^{+/+}$ and *vangl2*$^{m209/+}$), *vangl2*$^{m209/m209}$ embryos at 4-8s displayed more cells with an anterior Par3 patch (82% vs 67%) and less cells with a posterior patch (65% vs 87%). In addition, lateral Par3 patches were much more common in *vangl2* mutants (70% vs 20%, *vangl2*$^{m209/m209}$: N=7, n=17; controls : N=16, n=45, Fig. 4g). These results show that Vangl2 is required for proper

positioning of Par3 patches at early stages. Interestingly, live-imaging of these embryos also revealed that, despite being mislocalized, Par3 patches could still attract the BB in Vangl2 mutants (Fig. 4e, f) independently of their position, whether laterally (Fig. 4e) or posteriorly (Fig. 4f). These observations show that Par3 distribution along apical junctions is disrupted in *vangl2* mutants, leading to a fragmentation of Par3 patches into more numerous and less intense clusters that extend to lateral membrane.

DISCUSSION

In this paper we have analyzed the dynamics of BB posterior positioning in the embryonic zebrafish FP. We show that, quite unexpectedly, BBs are highly mobile and are able to contact, and bounce off, apical junctions several times per hour. FP polarization correlates with slowing down of BBs. At the level of individual cells, BBs settle down posteriorly at the level of junctions enriched in Par3, and we show that Par3 asymmetry is important for BB posterior localization. In the PCP mutant *Vangl2*, BBs show poorly oriented movements and this correlates with a loss of Par3 posterior enrichment. We discuss here the implications of our dynamic study on the understanding of the mechanisms of cilium polarization downstream of the PCP pathway. Our data highlight Par3 as a critical player in centriole positioning in this system.

Analysis of fixed samples showed that posterior positioning of BBs within the apical surface of FP cells progressed regularly within the 8 hour-time frame of our study and was complete at the 18 s stage. Surprisingly, live imaging revealed that, during this time frame, BBs underwent active antero-posterior movements under the apical surface, in both directions. This contrasts with the situation in the mouse cochlea, where live-imaging of explants had suggested very slow and regular movements of the BBs to the lateral cortex of inner hair cells (estimated speed of 10-50 nm/h, undetectable in movies) (Lepelletier et al., 2013). The BB speed measured in our experiments (mean speed of 0.1 μm/min at late stages of polarization) is closer to that of the second phase of centrosome migration toward the immune-synapse in T cells, when the centrosome approaches the actin rich cortex that faces the target cell (1 μm/min) (Yi et al., 2013). This suggests that BB movements in FP cells could rely on mechanisms similar to those found in T lymphocytes, where end-on capture-shrinkage of microtubules by dynein at the immune synapse pulls the centrosome. A striking difference between these two processes is the presence of a growing cilium anchored to the distal part of the BB in FP cells. We thus conclude that the presence of a cilium does not hamper BB movement.

The lack of synchronization between adjacent cells and of long-range temporal gradient of BB polarization suggests that the timing of polarization is largely

dependent on cell-intrinsic cues. Cell division did not appear to have a major role in the timing of polarization. Thus, we proposed the maturation of cell junctions as a possible trigger of polarization. Accordingly, we found that Par3 accumulated in patches at the posterior apical junctions of FP cells and that this accumulation preceded BB posterior docking. Interestingly, several recent studies suggest that Par3 could have a widely conserved role in PCP: Par3 is asymmetrically localized within the plane of the epithelium in Drosophila ommatidia (Aigouy et al., 2016), in Xenopus embryo ectoderm (Chuykin et al., 2019) and in the mouse cochlea (Landin Malt et al., 2019). Beside their asymmetric enrichment in polarized tissues, Par3 clusters may be broadly involved in BB/centrioles recruitment. Indeed, In the mouse cochlea, Par3 transiently localizes to the abneural membrane of hair cells and is required for asymmetric BB localization (Landin Malt et al., 2019). Moreover, in Drosophila embryonic ectoderm, Par3 isotropic distribution around apical junctions contributes to epithelium integrity, but in aPKC loss of function mutants, Par3 accumulates as discrete patches that align along the AP axis and recruit centrosomes (Jiang et al., 2015). Centrosome docking at discrete Par3 patches has also been observed in Drosophila germ stem cells and is critical for proper division orientation (Inaba et al., 2015).

Our analysis of the *vangl2* mutant defective in FP polarity brings important insight into the role of Par3 in FP polarization. In *vangl2*$^{m209/m209}$ embryos, BBs showed less oriented movements than in wt embryos. In contrast to the wt situation, BBs contacted both transverse and lateral membranes. Strikingly, in *vangl2* mutants as in wt, BBs always contacted the apical junctions at the level of Par3-positive patches. The altered behavior of BBs in *vangl2*$^{m209/m209}$ embryos correlated with a reduced enrichment of Par3 at the posterior membrane of FP cells. Since Par3 overexpression affected BB polarization, we propose that Par3 posterior enrichment under the control of the PCP pathway is a main actor in BB posterior positioning.

The mechanisms by which Par3 can recruit the BB at the plasma membrane remain unknown. Par3 enrichment could attract the BB to the posterior membrane or, alternatively, could capture or hold it when it contacts the posterior membrane. The observation of membrane invaginations suggests the existence of mechanical forces between Par3-positive patches and BBs. Such membrane invaginations have been

previously observed during cell division in the *C. elegans* zygote (Redemann et al., 2010) and in the *C. intestinalis* embryo epidermal lineage (Negishi et al., 2016), as well as at the immunological synapse in T cells (Yi et al., 2013). In all three cases, the existence of attraction forces between the centriole and the membrane have been proposed. Attraction could involve local microtubule dynamics regulation, since Par3 can interact with Dynein (Schmoranzer et al., 2009) and also with microtubules, directly (Chen et al., 2013) or indirectly via 14-3-3 proteins (Benton et al., 2003). Interestingly, we found that a form of Par3 phosphorylated at two conserved serine residues is enriched at posterior junctions. This phoshorylation site is a target of the Par1 kinase. It plays a role in centrosome recruitment at Par3 patches in Drosophila (Jiang et al., 2015) and in the interaction of Par3 with 14-3-3 proteins and thus with microtubules in other systems (Benton et al., 2003).

Par3 could also act indirectly on microbutules via Rac1, which mediates Par3 function in the mouse cochlea (Landin Malt et al., 2019). In different systems, Par3 regulates the local activity of Rac via the RacGEFs Tiam1 and Trio (Nishimura et al., 2005, Matsuzawa et al., 2016). Par3 can increase microtubule catastrophe rate by inhibiting Trio in neural crest cells (Moore et al., 2013), and Rac1 can regulate microtubule dynamics via CLIP-170 or Stathmin in other systems (Fukata et al., 2002, Wittmann et al., 2004).

Asymmetric centriole positioning is now recognized as a conserved readout of PCP (Carvajal-Gonzalez 2016). It will be interesting to investigate whether Par3 has a conserved role in centriole/BB positioning in metazoans.

MATERIALS AND METHODS

Experimental model and subject details

Wild-type and mutant zebrafish embryos were obtained by natural spawning. To obtain the early stages (4-8s), embryos were collected at 10 am and incubated for 9 h in a 33°C incubator. To obtain later stages (14-20s), embryos were collected at 10 am and incubated for 2 h at 28 °C before being placed overnight in a 24 °C incubator. All our experiments were made in agreement with the european Directive 210/63/EU on the protection of animals used for scientific purposes, and the french application decree 'Décret 2013-118'. The projects of our group have been approved by our local ethical committee 'Comité d'éthique Charles Darwin'. The authorisation number is 2015051912122771 v7 (APAFIS#957). The fish facility has been approved by the French 'Service for animal protection and health' with approval number A-75-05-25.

Method details

mRNA and morpholino injection

mRNAs were synthesized from linearized pCS2 vectors using the mMESSAGE mMACHINE SP6 transcription kit (Ambion). The following amounts of mRNA were injected into one-cell stage embryos: 22pg for Centrin-GFP, 40 pg for mbCherry (membrane Cherry) or Membrane-GFP (Gap43-GFP). For Par3-RFP mosaic expression, mRNAs were injected at the 16 cell stage in a single blastomere, using 50pg for Par3-RFP live-imaging or 150pg Par3-RFP for over-expression experiments (the concentrations for Centrin-GFP and membrane-GFP mRNAs were the same as for one-cell stage injections). Par3-MO was injected at a concentration of 0.3mM at one-cell stage.

Immunostaining

For immunostaining, embryos were fixed in Dent fixative (80% Methanol, 20% DMSO) at 25°C for 2h, blocked in 5% goat serum, 1% bovine serum albumin and 0.3% triton in PBS for 1 h at room temperature and incubated overnight at 4 °C with primary antibodies and 2h at room temperature with secondary antibodies. The yolk

was then removed and the embryo mounted in Vectashield medium on a slide. Imaging was done using a Leica TCS SP5 AOBS upright confocal microscope using a 63X oil lens.

Live imaging.

Embryos were dechorionated manually and mounted in 0.5% low-melting agarose in E3 medium. Movies were recorded at the temperature of the imaging facility room (22 °C) on a Leica TCS SP5 AOBS upright confocal microscope using a 63X (NA 0.9) water immersion lens.

Quantification and statistical analysis

All bar-plots, boxplot and violin plots and statistical tests were generated with R and Rstudio.

Basal-bodies movements

Distance between BB and posterior membrane in FP was measured manually at each time-frame in FIJI. The results were then plotted using python matplotlib and analyzed with a custom python script to extract relevant information such as the frequency of contact with posterior membrane or percentage of total time spent in contact with posterior membrane.

Par3-RFP posterior/anterior ratio

Fluorescence intensity was measured along the anterior-posterior length of isolated labelled FP cells in FIJI. A custom python script was then used to extract the first quarter (cell anterior side) and last quarter (cell posterior side) of fluorescence intensity values, to determine the area under each curve (corresponding to fluorescence intensity), calculate the post/ant ratio and plot it along with the polarization index (see BB movements analysis section).

Par3 peaks quantification

Fluorescence intensity from immunostained embryos was measured along FP cells transverse membranes and exported to Matlab where the findpeaks function was used to detect Par3 peaks and measure their prominence.

Basal-bodies tracking at late stages in wt and Vangl2 mutants

BB detection and tracking was done with the TrackMate plugin in FIJI.

REAGENTS AND RESOURCES

REAGENT or RESOURCE	SOURCE	IDENTIFIER
Antibodies		
Mouse monoclonal IgG2a anti-centrin (clone 20H5)	Merck Millipore	**# 04-1624, RRID:AB_10563501**
Mouse monoclonal IgG1 anti-ZO1 (clone ZO1-1A12)	Invitrogen	RRID: AB_2533147
Mouse monoclonal IgG2b anti-acetylated-tubulin (clone 6-11B-1)	Sigma-Aldrich	#T 6793 RRID: AB_477585
Rabbit polyclonal anti-Par3	Merck Millipore	#07-330RRID:AB_11213581
Rabbit polyclonal anti-phosphorylated-Ser1085-Bazooka	Krahn et al. 2009	N/A
Rabbit polyclonal anti-DsRed	Takara	# 632496,RRID:AB_10013483
Goat anti-mouse IgG1 Alexa633	Molecular probes	# A-21126,RRID:AB_2535768
Goat anti-mouse IgG2a Alexa568	Molecular probes	# A-21134,RRID:AB_2535773
Goat anti-mouse IgG2a Alexa488	Molecular probes	# A-21131, RRID:AB_141618
Goat anti-mouse IgG2b Alexa633	Molecular probes	# A-21146,RRID:AB_2535782
Goat anti-rabbit IgG Alexa568	Molecular probes	# A-11011, RRID:AB_143157
Chemicals, Peptides, and Recombinant Proteins		
Methanol	VWR Chemicals	20847.295
DMSO	Sigma	D2650
Goat serum	Sigma	G6767
Bovine serum albumin	Sigma	A2153
Triton X100	Sigma	T8787
Vectashield	Vector Laboratories	H-1000
Experimental Models: Organisms/Strains		
zebrafish wild-type AB or (TL x AB) hybrid strains	N/A	N/A
Zebrafish Vangm209 mutants	Solnica-Krezel et al., 1996	ZDB-GENO-190204-5
Zebrafish Par3ab fh305 mutants	Blasky et al., 2014	ZDB-FISH-150901-20689
Oligonucleotides		
Par3-MO tcaaaggctcccgtgctctggtgtc	Wei et al., 2004	

Recombinant DNA		
pCS2-Membrane-Cherry	Megason et al. 2009	N/A
pCS2-GFPhumcentrin1	Pouthas et al. 2008	N/A
pCS2+-Par3-RFP	Paula Alexandre, unpublished	N/A
pCS-Gap43-GFP	David Wilkinson, unpublished	N/A
Software and Algorithms		
Fiji/ImageJ	ImageJ	https://imagej.net/Fiji/Downloads
TrackMate	Tinevez et al., 2017	https://imagej.net/TrackMate
MATLAB R2018a	Mathworks	https://www.mathworks.com/downloads/
Python 2.7.13	Python Software Foundation	https://www.python.org/downloads/release/python-2713/
R studio Version 1.1.463	Rstudio	https://www.rstudio.com/
R version 3.3.2	The R Foundation for Statistical Computing	https://cran.r-project.org/bin/macosx/

BIBLIOGRAPHY

Aigouy B, Le Bivic A. The PCP pathway regulates Baz planar distribution in epithelial cells. Sci Rep. 2016 Sep 14;6:33420. doi: 10.1038/srep33420.

Benton R, St Johnston D. Drosophila PAR-1 and 14-3-3 inhibit Bazooka/PAR-3 to establish complementary cortical domains in polarized cells. Cell. 2003 Dec 12;115(6):691-704.

Blasky AJ, Pan L, Moens CB, Appel B. Pard3 regulates contact between neural crest cells and the timing of Schwann cell differentiation but is not essential for neural crest migration or myelination. Dev Dyn. 2014 Dec;243(12):1511-23. doi: 10.1002/dvdy.24172.

Borovina A, Superina S, Voskas D, Ciruna B. Vangl2 directs the posterior tilting and asymmetric localization of motile primary cilia. Nat Cell Biol. 2010 Apr;12(4):407-12. doi: 10.1038/ncb2042.

Boutin C, Goffinet AM, Tissir F. Celsr1-3 cadherins in PCP and brain development. Curr Top Dev Biol. 2012;101:161-83. doi: 10.1016/B978-0-12-394592-1.00010-7.

Carvajal-Gonzalez JM, Mulero-Navarro S, Mlodzik M. Centriole positioning in epithelial cells and its intimate relationship with planar cell polarity. Bioessays. 2016 Dec;38(12):1234-1245. doi: 10.1002/bies.201600154.

Chen S, Chen J, Shi H, Wei M, Castaneda-Castellanos DR, Bultje RS, Pei X, Kriegstein AR, Zhang M, Shi SH. Regulation of microtubule stability and organization by mammalian Par3 in specifying neuronal polarity. Dev Cell. 2013 Jan 14;24(1):26-40. doi: 10.1016/j.devcel.2012.11.014.

Chuykin I, Ossipova O, Sokol SY. Par3 interacts with Prickle3 to generate apical PCP complexes in the vertebrate neural plate. Elife. 2018 Sep 26;7. pii: e37881. doi: 10.7554/eLife.37881.

Ezan J, Lasvaux L, Gezer A, Novakovic A, May-Simera H, Belotti E, Lhoumeau AC, Birnbaumer L, Beer-Hammer S, Borg JP, Le Bivic A, Nürnberg B, Sans N, Montcouquiol M. Primary cilium migration depends on G-protein signalling control of subapical cytoskeleton. Nat Cell Biol. 2013 Sep;15(9):1107-15. doi: 10.1038/ncb2819.

Fame RM, Chang JT, Hong A, Aponte-Santiago NA, Sive H. Directional cerebrospinal fluid movement between brain ventricles in larval zebrafish. Fluids Barriers CNS. 2016 Jun 21;13(1):11. doi: 10.1186/s12987-016-0036-z.

Fukata M, Watanabe T, Noritake J, Nakagawa M, Yamaga M, Kuroda S, Matsuura Y, Iwamatsu A, Perez F, Kaibuchi K. Rac1 and Cdc42 capture microtubules through IQGAP1 and CLIP-170. Cell. 2002 Jun 28;109(7):873-85.

Grimsley-Myers CM, Sipe CW, Géléoc GS, Lu X. The small GTPase Rac1 regulates auditory hair cell morphogenesis. J Neurosci. 2009 Dec 16;29(50):15859-69. doi: 10.1523/JNEUROSCI.3998-09.2009.

Guirao B, Meunier A, Mortaud S, Aguilar A, Corsi JM, Strehl L, Hirota Y, Desoeuvre A, Boutin C, Han YG, Mirzadeh Z, Cremer H, Montcouquiol M, Sawamoto K, Spassky N. Coupling between hydrodynamic forces and planar cell polarity orients mammalian motile cilia. Nat Cell Biol. 2010 Apr;12(4):341-50. doi: 10.1038/ncb2040.

Hashimoto M, Shinohara K, Wang J, Ikeuchi S, Yoshiba S, Meno C, Nonaka S, Takada S, Hatta K, Wynshaw-Boris A, Hamada H. Planar polarization of node cells determines the rotational axis of node cilia. Nat Cell Biol. 2010 Feb;12(2):170-6. doi: 10.1038/ncb2020.

Hegan PS, Ostertag E, Geurts AM, Mooseker MS. Myosin Id is required for planar cell polarity in ciliated tracheal and ependymal epithelial cells. Cytoskeleton (Hoboken). 2015 Oct;72(10):503-16. doi: 10.1002/cm.21259.

Hirota Y, Meunier A, Huang S, Shimozawa T, Yamada O, Kida YS, Inoue M, Ito T, Kato H, Sakaguchi M, Sunabori T, Nakaya MA, Nonaka S, Ogura T, Higuchi H, Okano H, Spassky N, Sawamoto K. Planar polarity of multiciliated ependymal cells involves the anterior migration of basal bodies regulated by non-muscle myosin II. Development. 2010 Sep;137(18):3037-46. doi: 10.1242/dev.050120.

Inaba M, Venkei ZG, Yamashita YM. The polarity protein Baz forms a platform for the centrosome orientation during asymmetric stem cell division in the Drosophila male germline. Elife. 2015 Mar 20;4. doi: 10.7554/eLife.04960.

Jiang T, McKinley RF, McGill MA, Angers S, Harris TJ. A Par-1-Par-3-Centrosome Cell Polarity Pathway and Its Tuning for Isotropic Cell Adhesion. Curr Biol. 2015 Oct 19;25(20):2701-8. doi: 10.1016/j.cub.2015.08.063. Epub 2015 Oct 8.

Jones C, Roper VC, Foucher I, Qian D, Banizs B, Petit C, Yoder BK, Chen P. Ciliary proteins link basal body polarization to planar cell polarity regulation. Nat Genet. 2008 Jan;40(1):69-77.

Landin Malt A, Dailey Z, Holbrook-Rasmussen J, Zheng Y, Hogan A, Du Q, Lu X. Par3 is essential for the establishment of planar cell polarity of inner ear hair cells. Proc Natl Acad Sci U S A. 2019 Mar 12;116(11):4999-5008. doi: 10.1073/pnas.1816333116.

Lepelletier L, de Monvel JB, Buisson J, Desdouets C, Petit C. Auditory hair cell centrioles undergo confined Brownian motion throughout the developmental migration of the kinocilium. Biophys J. 2013 Jul 2;105(1):48-58. doi: 10.1016/j.bpj.2013.05.009.

Mahuzier A1, Gaudé HM, Grampa V, Anselme I, Silbermann F, Leroux-Berger M, Delacour D, Ezan J, Montcouquiol M, Saunier S, Schneider-Maunoury S, Vesque C. Dishevelled stabilization by the ciliopathy protein Rpgrip1l is essential for planar cell polarity. J Cell Biol. 2012 Sep 3;198(5):927-40. doi: 10.1083/jcb.201111009.

Mathewson AW, Berman DG, Moens CB. Microtubules are required for the maintenance of planar cell polarity in monociliated floorplate cells. Dev Biol. 2019 Apr 25. pii: S0012-1606(18)30742-5. doi: 10.1016/j.ydbio.2019.04.007.

Matsuzawa K, Akita H, Watanabe T, Kakeno M, Matsui T, Wang S, Kaibuchi K. PAR3-aPKC regulates Tiam1 by modulating suppressive internal interactions. Mol Biol Cell. 2016 May 1;27(9):1511-23. doi: 10.1091/mbc.E15-09-0670.

Megason SG. In toto imaging of embryogenesis with confocal time-lapse microscopy. Methods Mol Biol. 2009;546:317-32. doi: 10.1007/978-1-60327-977-2_19.

Meunier A, Azimzadeh J. Multiciliated Cells in Animals. Cold Spring Harb Perspect Biol. 2016 Dec 1;8(12). pii: a028233. doi: 10.1101/cshperspect.a028233.

Mirzadeh Z, Han YG, Soriano-Navarro M, García-Verdugo JM, Alvarez-Buylla A. Cilia organize ependymal planar polarity. J Neurosci. 2010 Feb 17;30(7):2600-10. doi: 10.1523/JNEUROSCI.3744-09.2010.

Mitchell B, Stubbs JL, Huisman F, Taborek P, Yu C, Kintner C. The PCP pathway instructs the planar orientation of ciliated cells in the Xenopus larval skin. Curr Biol. 2009 Jun 9;19(11):924-9. doi: 10.1016/j.cub.2009.04.018.

Montcouquiol M, Rachel RA, Lanford PJ, Copeland NG, Jenkins NA, Kelley MW. Identification of Vangl2 and Scrb1 as planar polarity genes in mammals. Nature. 2003 May 8;423(6936):173-7.

Moore R, Theveneau E, Pozzi S, Alexandre P, Richardson J, Merks A, Parsons M, Kashef J, Linker C, Mayor R. Par3 controls neural crest migration by promoting microtubule catastrophe during contact inhibition of locomotion. Development. 2013 Dec;140(23):4763-75. doi: 10.1242/dev.098509.

Negishi T, Miyazaki N, Murata K, Yasuo H, Ueno N. Physical association between a novel plasma-membrane structure and centrosome orients cell division. Elife. 2016 Aug 9;5. pii: e16550. doi: 10.7554/eLife.16550.

Nishimura T, Yamaguchi T, Kato K, Yoshizawa M, Nabeshima Y, Ohno S, Hoshino M, Kaibuchi K. AR-6-PAR-3 mediates Cdc42-induced Rac activation through the Rac GEFs STEF/Tiam1. Nat Cell Biol. 2005 Mar;7(3):270-7.

Ohata S, Herranz-Pérez V, Nakatani J, Boletta A, García-Verdugo JM, Álvarez-Buylla A. Mechanosensory Genes Pkd1 and Pkd2 Contribute to the Planar Polarization of Brain Ventricular Epithelium. J Neurosci. 2015 Aug 5;35(31):11153-68. doi: 10.1523/JNEUROSCI.0686-15.2015.

Pouthas F, Girard P, Lecaudey V, Ly TB, Gilmour D, Boulin C, Pepperkok R, Reynaud EG. In migrating cells, the Golgi complex and the position of the centrosome depend on geometrical constraints of the substratum. J Cell Sci. 2008 Jul 15;121(Pt 14):2406-14. doi: 10.1242/jcs.026849.

Redemann S, Pecreaux J, Goehring NW, Khairy K, Stelzer EH, Hyman AA, Howard J. Membrane invaginations reveal cortical sites that pull on mitotic spindles in one-cell C. elegans embryos. PLoS One. 2010 Aug 20;5(8):e12301. doi: 10.1371/journal.pone.0012301.

Ross AJ, May-Simera H, Eichers ER, Kai M, Hill J, Jagger DJ, Leitch CC, Chapple JP, Munro PM, Fisher S, Tan PL, Phillips HM, Leroux MR, Henderson DJ, Murdoch JN, Copp AJ, Eliot MM, Lupski JR, Kemp DT, Dollfus H, Tada M, Katsanis N, Forge A, Beales PL. Disruption of Bardet-Biedl syndrome ciliary proteins perturbs planar cell polarity in vertebrates. Nat Genet. 2005 Oct;37(10):1135-40.

Schmoranzer J, Fawcett JP, Segura M, Tan S, Vallee RB, Pawson T, Gundersen GG.
Par3 and dynein associate to regulate local microtubule dynamics and centrosome orientation during migration. Curr Biol. 2009 Jul 14;19(13):1065-74. doi: 10.1016/j.cub.2009.05.065.

Sepich DS, Usmani M, Pawlicki S, Solnica-Krezel L. Wnt/PCP signaling controls intracellular position of MTOCs during gastrulation convergence and extension movements. Development. 2011 Feb;138(3):543-52. doi: 10.1242/dev.053959.

Solnica-Krezel L1, Stemple DL, Mountcastle-Shah E, Rangini Z, Neuhauss SC, Malicki J, Schier AF, Stainier DY, Zwartkruis F, Abdelilah S, Driever W. Mutations affecting cell fates and cellular rearrangements during gastrulation in zebrafish. Development. 1996 Dec;123:67-80.

Song H, Hu J, Chen W, Elliott G, Andre P, Gao B, Yang Y. Planar cell polarity breaks bilateral symmetry by controlling ciliary positioning. Nature. 2010 Jul 15;466(7304):378-82. doi: 10.1038/nature09129.

Tarchini B, Jolicoeur C, Cayouette M. A molecular blueprint at the apical surface establishes planar asymmetry in cochlear hair cells. Dev Cell. 2013 Oct 14;27(1):88-102. doi: 10.1016/j.devcel.2013.09.011.

Tinevez JY, Perry N, Schindelin J, Hoopes GM, Reynolds GD, Laplantine E, Bednarek SY, Shorte SL, Eliceiri KW. TrackMate: An open and extensible platform for single-particle tracking. Methods. 2017 Feb 15;115:80-90. doi: 10.1016/j.ymeth.2016.09.016.

Wallingford JB. Planar cell polarity signaling, cilia and polarized ciliary beating. Curr Opin Cell Biol. 2010 Oct;22(5):597-604. doi: 10.1016/j.ceb.2010.07.011.

Wei X, Cheng Y, Luo Y, Shi X, Nelson S, Hyde DR. The zebrafish Pard3 ortholog is required for separation of the eye fields and retinal lamination. Dev Biol. 2004 May 1;269(1):286-301.

Wittmann T, Bokoch GM, Waterman-Storer CM. Regulation of microtubule destabilizing activity of Op18/stathmin downstream of Rac1. J Biol Chem. 2004 Feb 13;279(7):6196-203.

Krahn MP, Egger-Adam D, Wodarz A. PP2A antagonizes phosphorylation of Bazooka by PAR-1 to control apical-basal polarity in dividing embryonic neuroblasts. Dev Cell. 2009 Jun;16(6):901-8. doi: 10.1016/j.devcel.2009.04.011.

Yi J, Wu X, Chung AH, Chen JK, Kapoor TM, Hammer JA. Centrosome repositioning in T cells is biphasic and driven by microtubule end-on capture-shrinkage. J Cell Biol. 2013 Sep 2;202(5):779-92. doi: 10.1083/jcb.201301004.

ACKNOWLEDGEMENTS

We are grateful to the aquatic animal and cell imaging facilities of the IBPS (Institut de Biologie Paris-Seine FR3631, Sorbonne Université, CNRS, Paris, France) for their technical assistance. We thank Teresa Ferraro for sharing her expertise in image analysis, Marie Breau for her help in setting up the live imaging protocol, Isabelle Anselme for participation in genotyping. We thank Paula Alexandre for the kind gift of Par3-RFP construct, Andreas Wodarz for the BazP1085 antibody, Maximilien Furthauer for the *vangl2*^{m209} line. This work was supported by funding from the Agence Nationale pour la Recherche (ANR, project CILIAINTHEBRAIN to SSM) and the Fondation pour la Recherche Médicale (Equipe FRM DEQ20140329544 funding to SSM)**.** A.D was supported by fellowships from the Ecole Normale Supérieure de Cachan and from the Fondation ARC contre le Cancer. The authors declare no competing financial interests.

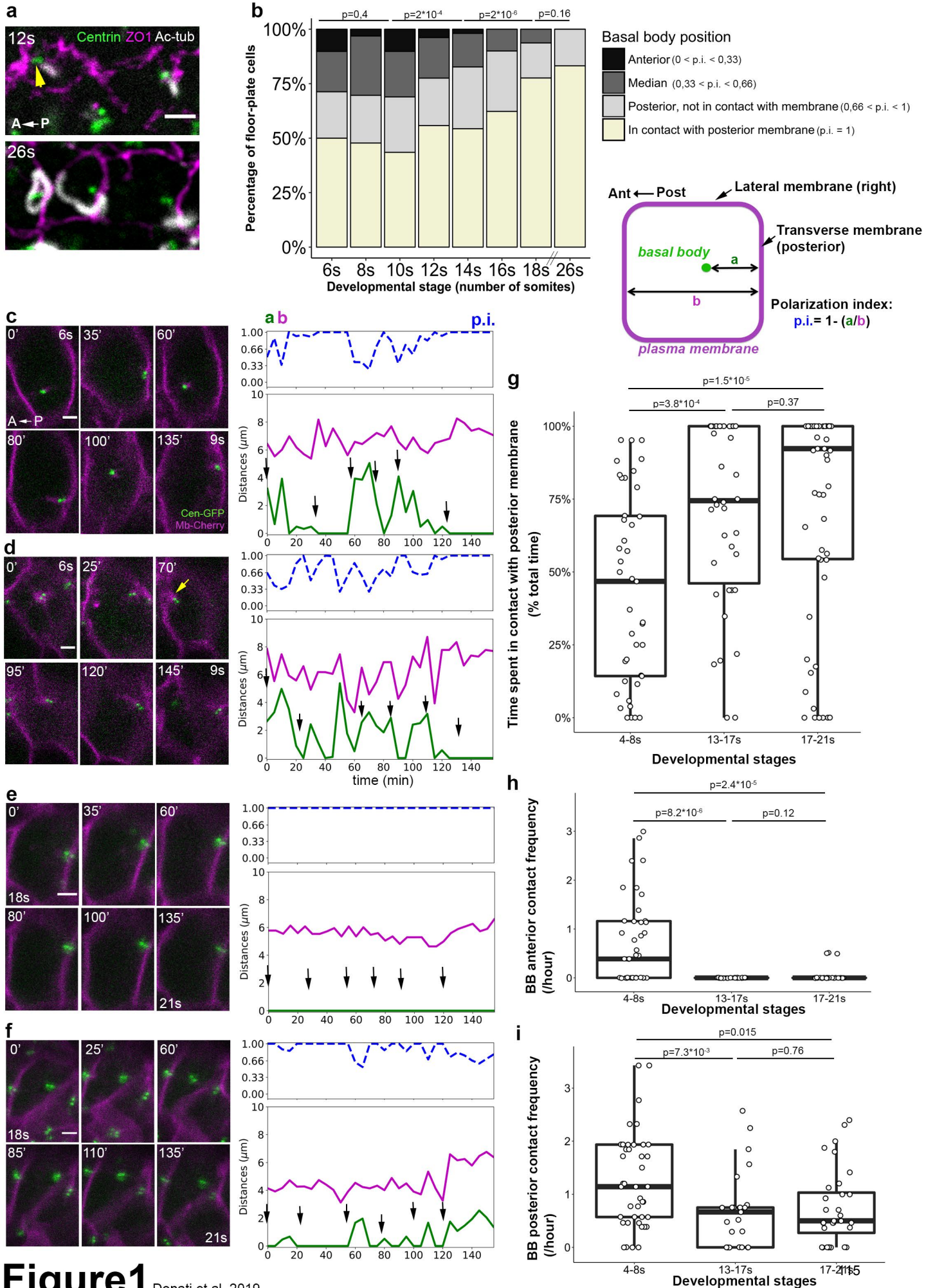

Figure1 Donati et al. 2019

FIGURE LEGENDS

Figure 1 Floor-plate planar polarization involves a change in basal body (BB) motile behavior.

a, b) Time-course of floor-plate polarization between the 6 s and 26 s stages **a)** Dorsal views of the floor-plate of flat-mounted embryos showing immunostaining against Centrin (green, BB), ZO1 (magenta, apical junctions) and Ac-Tub (white, cilia) at 12 s (up) and 26 s (down). Note that cilia are already visible at 12 s but are much longer at 26 s. The yellow arrow points at an anterior BB associated to a cilium. **b)** Quantification of BB position measured from immuno-stained samples as shown in a. BB position along the anterior-posterior axis was quantified using the polarization index (defined as p.i.=1-(a/b) where “a” is the distance between the BB and the posterior membrane and “b” the distance between anterior and posterior membranes, cf scheme in b lower right). Cells were then allocated to different categories depending on their polarization index for each developmental stage (6 s: 7embryos, 108 cells ; 8 s: 14 embryos, 224 cells ; 10 s: 14 embryos, 354 cells ; 12 s: 5 embryos, 156 cells ; 14 s: 9 embryos, 208 cells ; 16 s,: 9 embryos, 220 cells ; 18 s: 5 embryos, 143 cells ; 26 s: 4 embryos, 119 cells). **c-f)** Live imaging of BB movements during the polarization process. Images were taken every 5 minutes; a selection of images is presented here from two early stage embryos (**c, d** movies between the 6 s and 9 s stages; **d** yellow arrow points at an anterior contact event) and two late stage embryos (**e, f.** movies between the 18 s and 21 s stages). The distances between BBs and posterior membranes were then plotted (green curve, “a” in the scheme in Fig1b) along with the distance between the anterior and posterior membranes (magenta curve, “b” in the scheme in Fig1b) and the p.i. (dashed blue curve). Black arrows on the graphs indicate the position of the images displayed on the left. **g)** Quantification of the percentage of total movie time spent by the BB in contact with the posterior membrane. (4-8s: 5 embryos, 41 cells; 13-17s: 6 embryos, 38 cells; 17-21s: 7 embryos, 59 cells). **h, i)** Number of contact events per h between BB and anterior membrane (**h**) or between BB and posterior membrane (**i**) in embryos filmed at different developmental stages: 4 to 8 s (5 embryos, 41 cells), 13 to 17 s (5

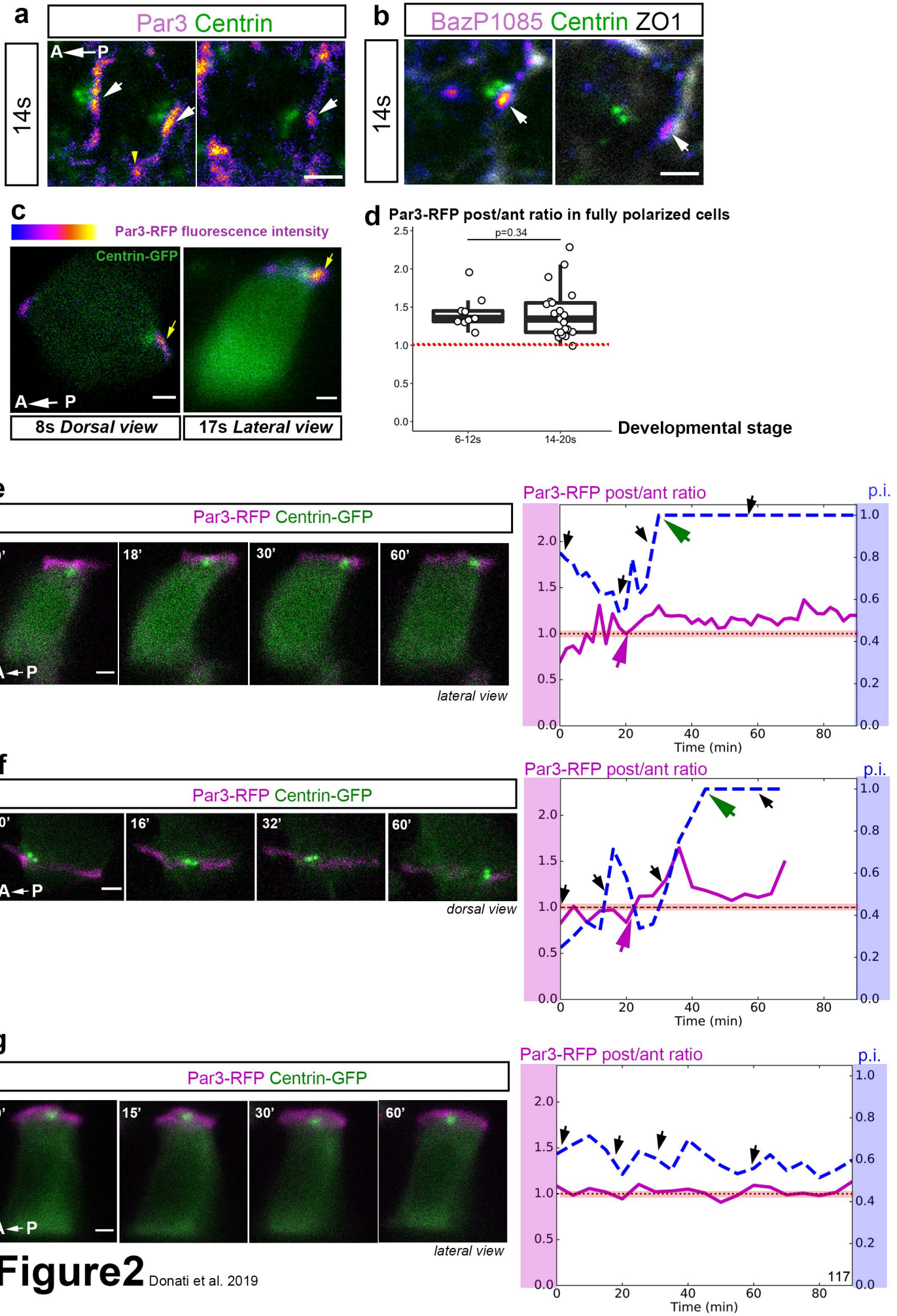

Figure2 Donati et al. 2019

embryos, 25 cells) and 17 to 21 s (7 embryos, 32 cells). Cells with a BB in contact with the posterior membrane during the whole movie (points at 100% in Fig1g) were not plotted here. Statistical significance was assessed using a Wilcoxon test. *Scale bars:* 2 *µ*m.

Figure 2. Par3 forms patches and is asymmetrically localized in FP cells.

a, b) Individual cells from dorsal views of 14 s stage embryos showing IF with a Par3 antibody (a) or an antibody recognizing a phosphorylated form of Par3, BazP1085 (b) in FP cells. Two distinct cells are shown for each antibody. Both total Par3 and its phosphorylated form localize at apical junctions and are enriched at tricellular junctions (yellow arrowhead in a) and in patches at transverse membranes (white arrows), whether the BB is in contact with the posterior membrane (left images) or not (right). **c)** Representative images of isolated FP cells expressing Par3-RFP and Centrin-GFP at early (8 s, left) or late (17 s, right) stages. **d)** Par3-RFP posterior/anterior fluorescence intensity ratio in fully polarized FP cells (such as those displayed in **c**) at early and late stages. The red dotted line indicates a ratio of 1 (corresponding to a symmetric Par3-RFP distribution). **e-g)** Images of time-lapse movies showing individual FP cells from embryos mosaically expressing Par3-RFP (magenta) and centrin-GFP (green) (lateral view). Par3-RFP posterior/anterior fluorescence intensity ratio is plotted on the right plots (magenta curve) along with the polarization index (« p.i. », dashed blue curve). Black arrows on plots indicate the time-points corresponding to the images displayed on the left. **e)** FP cell with Par3 posterior enrichment in an embryo filmed between the 15 s and 17 s stages. Par3 posterior enrichment starts 20 min after the beginning of the movie (magenta arrow), 10 min before BB/posterior membrane contact (green arrow). **f)** FP cell with Par3 posterior enrichment in an embryo filmed between the 8 s and 10 s stages. Par3 posterior enrichment starts 20 min after the beginning of the movie (magenta arrow), 20 min before BB/posterior membrane contact (green arrow). **g)** FP cell with no posterior Par3 enrichment (Par3-RFP post/ant ratio close to 1) with a BB oscillating around the middle of the apical surface, in an embryo filmed between 17 s and 19 s. Scale bars : 2*µ*m.

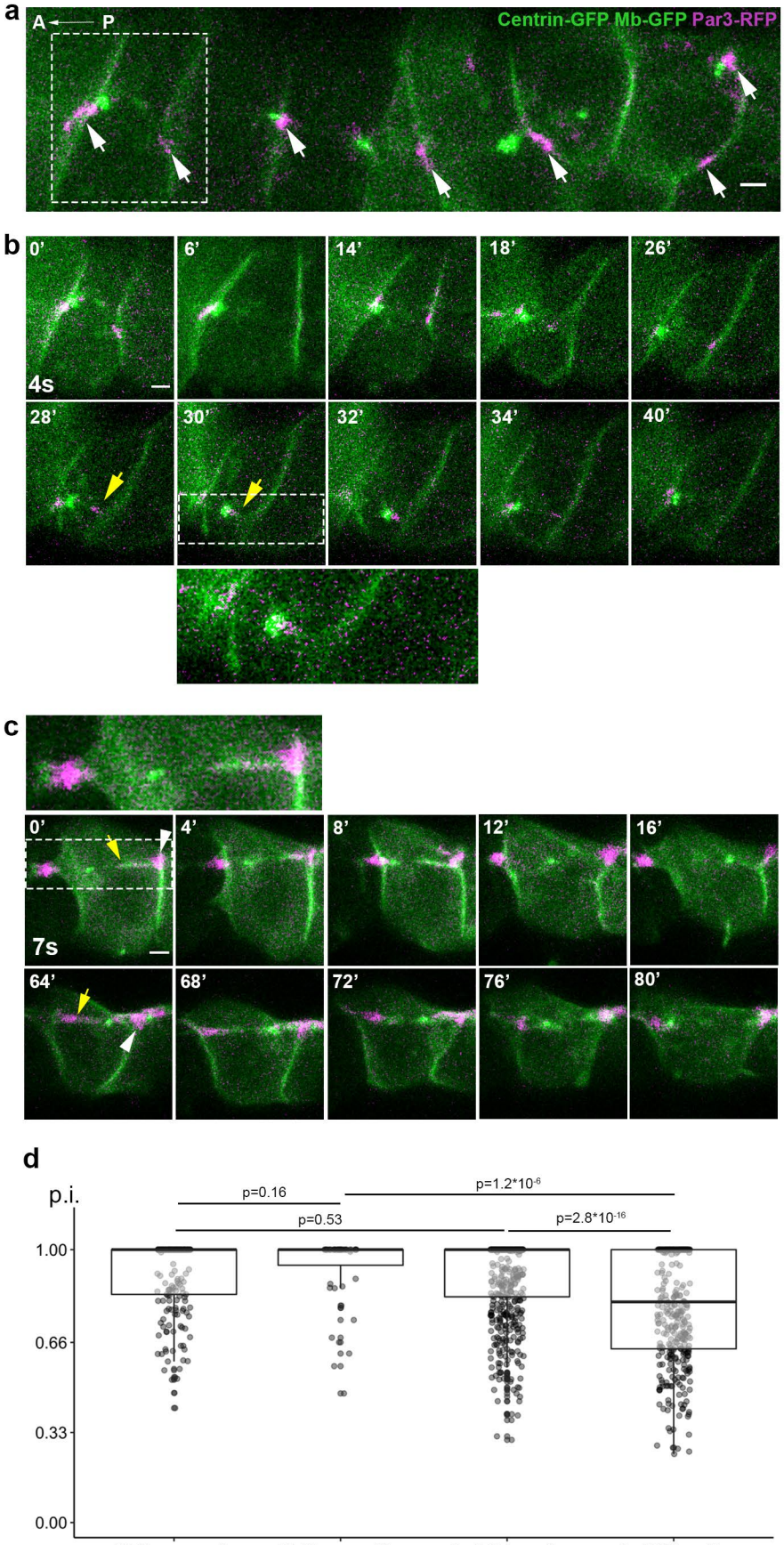

Figure3 Donati et al. 2019

Figure 3. BB/Par3 patches exclusive contacts at early stages and Par3 over-expression

a-c) Images from time lapse movies of embryos mosaically injected with centrin-GFP (green), Membrane-GFP (green) and Par3-RFP (magenta) mRNAs. All pictures are dorsal views of FP cells. **a)** global view of 6 adjacent FP cells at the beginning of the movie shown in **b** ; white arrows point at Par3 patches (aligned along the AP axis) with which BB make contacts during the movie. The dotted frame indicates the position of the cell whose behavior is shown in **b**. **b)** example of a FP cell between the 4 and 5s stages, whose BB is in contact with the anterior Par3 patch at the beginning of the movie but then makes contact with the posterior Par3 patch that stretches in its direction (yellow arrows). A close up of BB and Par3 patches is shown for t=30'. **c)** Example of posterior and anterior membrane invaginations originating from Par3 patches and partially coated with Par3. Yellow arrows point to posterior (t=0') and anterior (t=64') invaginations. White arrowheads point to Par3 patches. Par3 patch deformation is more obvious at t=64' but is also present at t=0'. A close up of BB, Par3 patches and posterior membrane invagination is shown for t=0'. **d)** Polarization index (p.i., cf Fig1) of FP cells from embryos mosaically over-expressing either MbCherry (control) or Par3-RFP. We quantified both the polarization index of MbCherry or Par3-RFP positive cells and the polarization index of MbCherry or Par3-RFP negative cells. Scale bar : 2μm

Fig. 4 Par3 clustering and localization in *vangl2*^{m209} mutant FP

a) Polarization index of *vangl2*$^{m209/m209}$ determined from immunostaining data (wt: 2 embryos, 49 cells; *vangl2*$^{m209/+}$ 3 embryos, 66 cells; *vangl2*$^{m209/m209}$ 5 embryos, 57 cells) **b)** Immunostaining of phoshorylated Par3 (BazP1085 antibody) in *vangl2*$^{+/+}$ and *vangl2*$^{m209/m209}$ mutant embryo FP at 18 s. In each case ZO1 staining was removed in the right image to reveal Par3 patches (yellow arrows). **c)** Quantification of the number of Par3 patches per cell on transverse membranes from immunostaining data as shown in b. **d)** The same method as in c. was used to extract phospho-Par3 patches prominence, defined as the height of Par3 fluorescence peak relative to the highest and nearest valley (local fluorescence minimum) (for each cell, prominence is

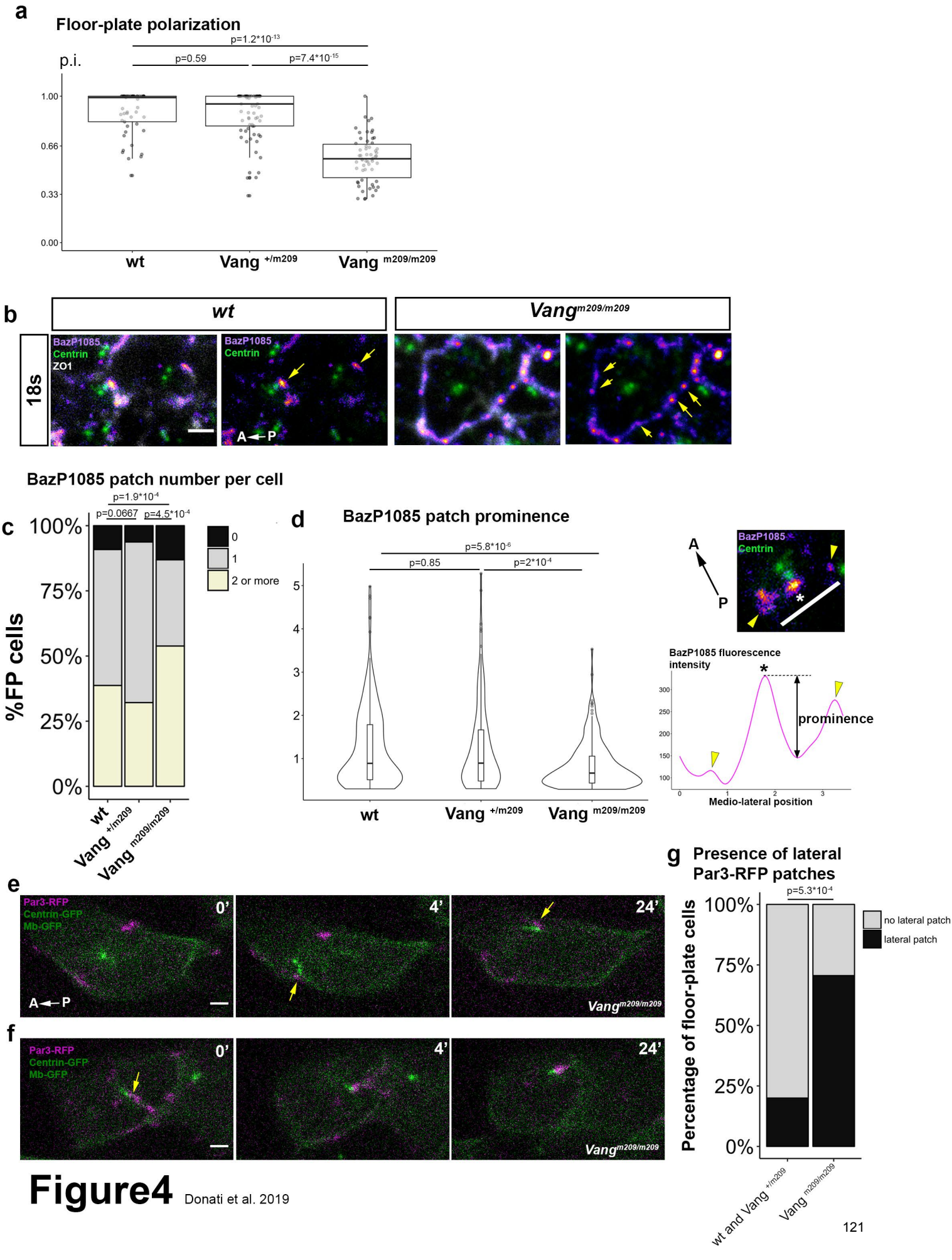

Figure4 Donati et al. 2019

normalized by the lowest Par3 intensity value). Right scheme: yellow arrows: tricellular junctions; white bar: orientation of the fluorescence measurement along the transverse membrane, star: position of Par3 patch. In a-d, *vangl2*$^{+/+}$: N=7, n=186 ; *vangl2*$^{m209/+}$: N=5, n=112 ; *vangl2*$^{m209/m209}$: N=7, n=129. **e, f)** Images from movies of 5s *vangl2*$^{m209/m209}$ embryos mosaically injected with Par3-RFP, Centrin-GFP and Membrane-GFP mRNA at the 16-32 cell stage. Yellow arrows point at contact events between Par3 patches and BBs. **g)** Percentage of cells displaying a lateral Par3-RFP patch in live-imaging experiments such as the one described in e,f. (*vangl2*$^{+/+}$ and *vangl2*$^{m209/+}$: N=16, n=45 ; *vangl2*$^{m209/m209}$: N=7, n=17). Statistical tests: Wilcoxon test for comparison of p.i. and prominence; Fisher test for comparison of patch number and percentage of cells with lateral patches.

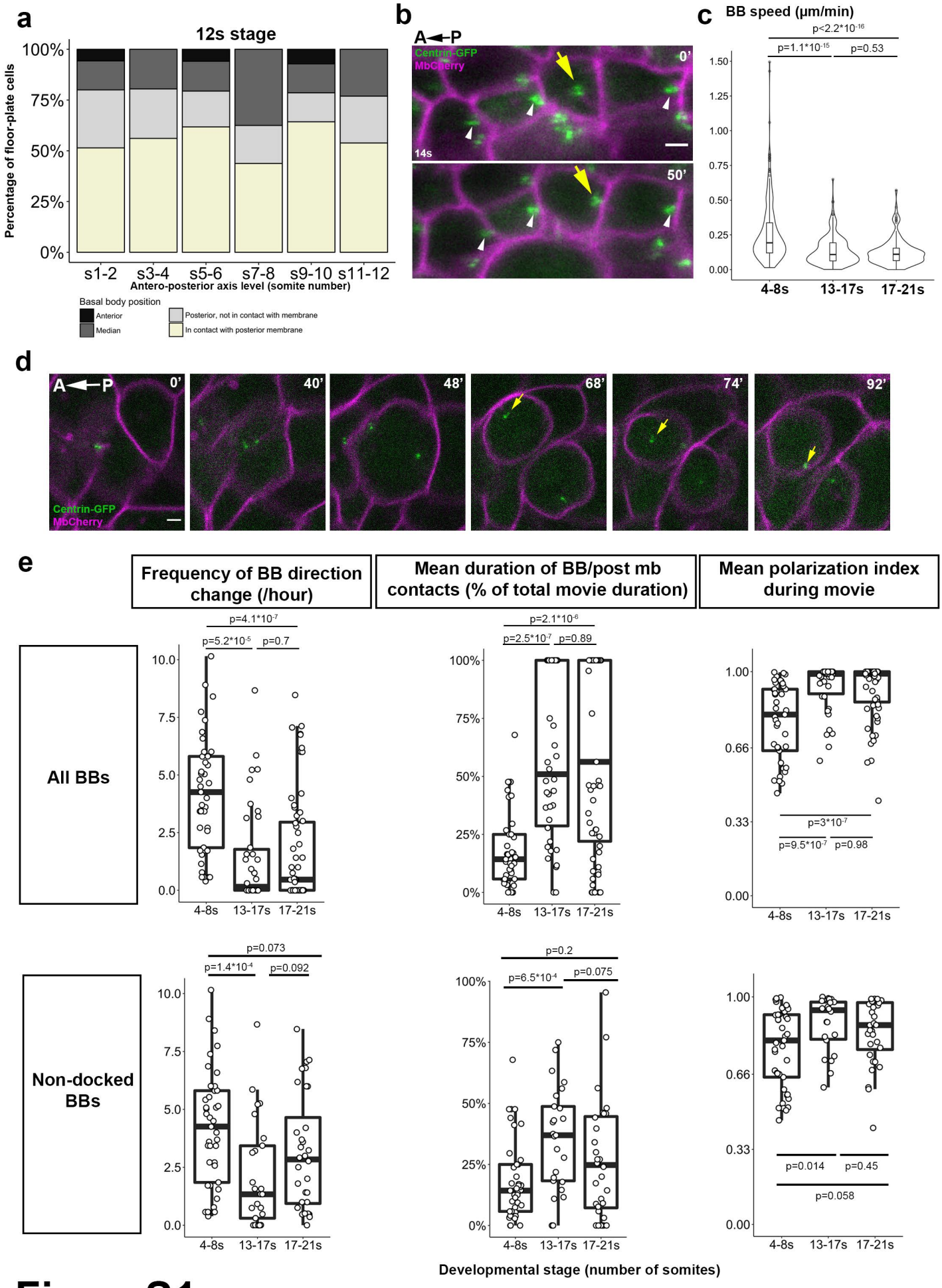

FigureS1 Donati et al. 2019

SUPPLEMENTARY FIGURE LEGENDS

Supplementary Figure S1: Further characterization of FP polarization in space and time.

a Quantification of FP polarization along the AP axis at 12 s. Analysis was performed on fixed immunostained embryos as described in Fig1a. (Wilcoxon test p-values for successive AP axis levels are: 12 s: 0.6095, 0.5514, 0.3596, 0.3668, 0.5487, N=5, n=156 the difference between first and last AP axis levels were also small and non-statistically significant). **b** Still images from FP BB (green) and membrane (magenta) live imaging (dorsal view, start at 14s stage). The yellow arrow points to BB that will move and make contacts with the posterior membrane between 0 and 50 min after the movie started. White arrowheads point at BBs in adjacent cells that stay in contact with the posterior membrane during this time interval. c BB speed measured from live-imaging data at different developmental stages. The speed of each BB movement was calculated by dividing the value of BB/posterior membrane variations (corresponding to green curves in Fig1 c-f) by the total duration of the movement (4-8s: 4 embryos, 38 cells; 13-17s: 6 embryos, 22 cells; 17-21s: 7 embryos, 32 cells). Comparison between stages was done using a Wilcoxon test. **d** Still images from a movie of a 5 s to 7 s stage embryo injected with centrin-GFP (green) and MbCherry (magenta) showing a dividing FP cell. Yellow arrows point at the BB of the anterior daughter cell, which rapidly moves back to the posterior membrane after cytokinesis. **e** Movies described in Fig1 were used to quantify BB direction change frequency, mean duration of BB/posterior membrane contact events as a percentage of total imaging duration and mean polarization index during live-imaging. Plots in the first line take into account the BBs that stay in contact with the posterior membrane 100% of movie duration (posteriorly docked BBs) whereas the second line only represents BBs that are not posteriorly docked. Comparison between stages was done using a Wilcoxon test. Scale bar : 2μm.

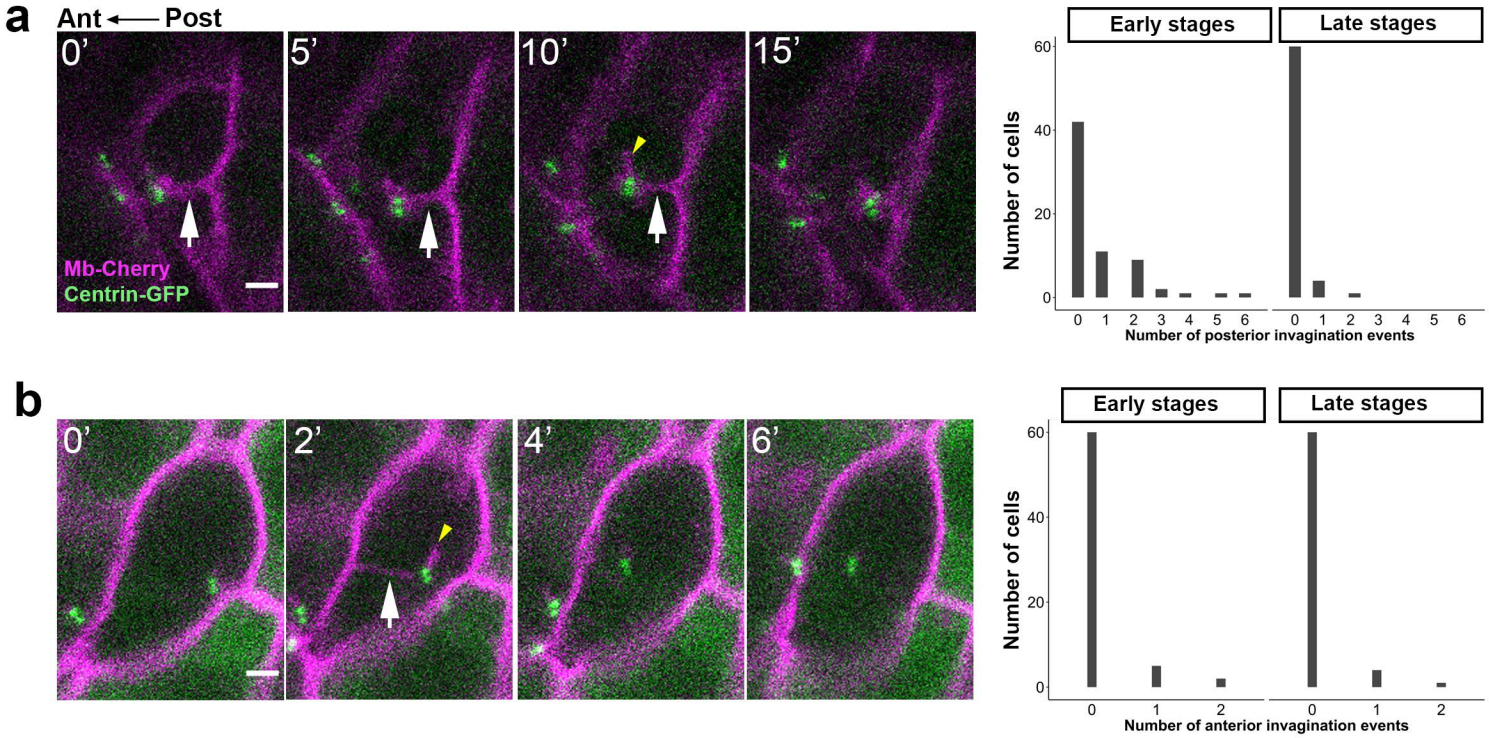

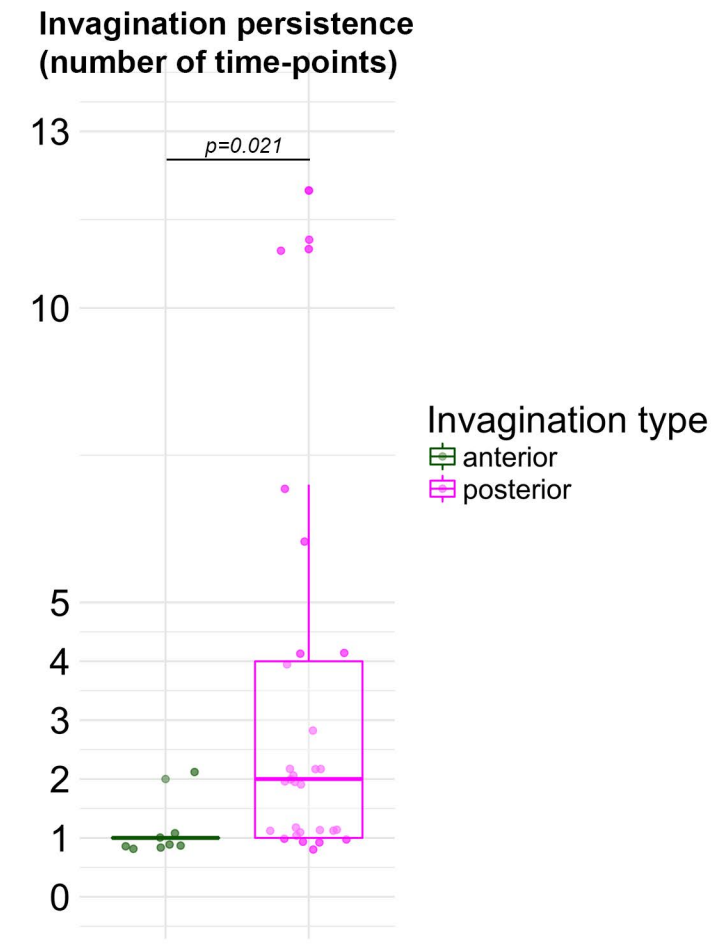

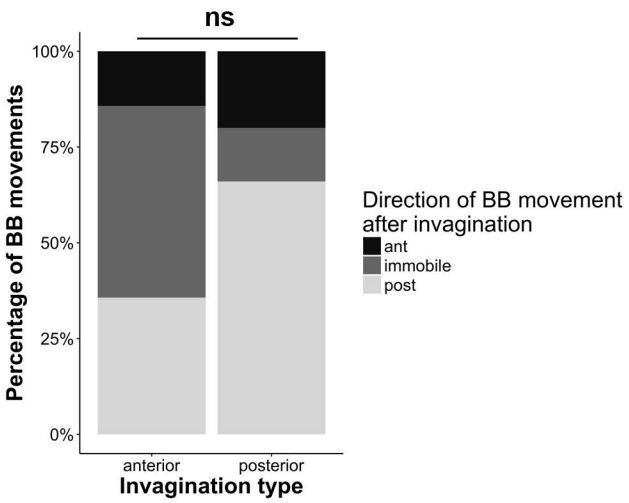

FigureS2 Donati et al. 2019

Supplementary Figure S2: Membrane invaginations link BBs to transverse membranes during FP polarization

a, b) Left : images taken from live-imaging data such as those presented in Fig. 1. Yellow arrows : potential cilia. Time (in minutes) is indicated in the upper-left corner. Right : count of transverse membrane invagination events in FP cells at early (before 14s) and late stages (after14s). a shows a posterior membrane invagination (white arrows); b shows an anterior membrane invagination (white arrow). Short mbCherry-positive digitations, presumably corresponding to cilia, were in some cases associated to the BB opposite the invagination (yellow arrowheads in a and b). These membrane digitations were rare in late stage embryos (6/57 cells out of 10 embryos) compared to early embryos (44/68 cells from 9 embryos), suggesting that Mb-Cherry entry into cilia is less common at later stages, which could reflect a maturation of the ciliary gate. **c)** Number of timepoints where anterior or posterior invaginations were detected in time-lapse movies with a 5 minutes interval between images (10 embryos, 24 cells, Wilcoxon test) d) Behavior of BB immediately after formation of an anterior or posterior invagination: BB either moved anteriorly ('ant'), posteriorly ('post') or did not move ('immobile') (50 posterior and 14 anterior invaginations from 16 embryos, 35 cells, Fisher test).

Supplementary Figure S3: *Par3ab* morphants or mutants have normal FP polarization and Par3 patches

a) FP polarization index (p.i.) in non-injected (NI) and Par3ab morpholino (MO)-injected embryos at 18s stage (NI : N=9, n=171 ; Par3MO : N=16, n=244). **b)** BazP1085 patch prominence (left) and number (right) in NI and Par3ab MO injected embryos at 18s stage (NI : N=4, n=66 ; Par3MO : N=3, n=38). **c)** p.i. of maternal zygotic heterozygous (*MZPar3ab*$^{+/-}$) or homozygous (*MZPar3ab*$^{-/-}$) Par3ab mutants at 18s stage (*MZPar3ab*$^{+/-}$: N=7, n=106 ; *MZPar3ab*$^{-/-}$: N=9, n=152). **d)** Par3 patches prominence (left) and number (right) in maternal zygotic heterozygous (*MZPar3ab*$^{+/-}$) or homozygous (*MZPar3ab*$^{-/-}$) Par3ab mutants at 18s stage (*MZPar3ab*$^{+/-}$: N=3, n=27 ; *MZPar3ab*$^{-/-}$: N=3, n=59). **e)** Immunostaining of FP cells over-expressing Par3-RFP in embryos mosaically injected with Par3-RFP mRNA at the 16 cells stage

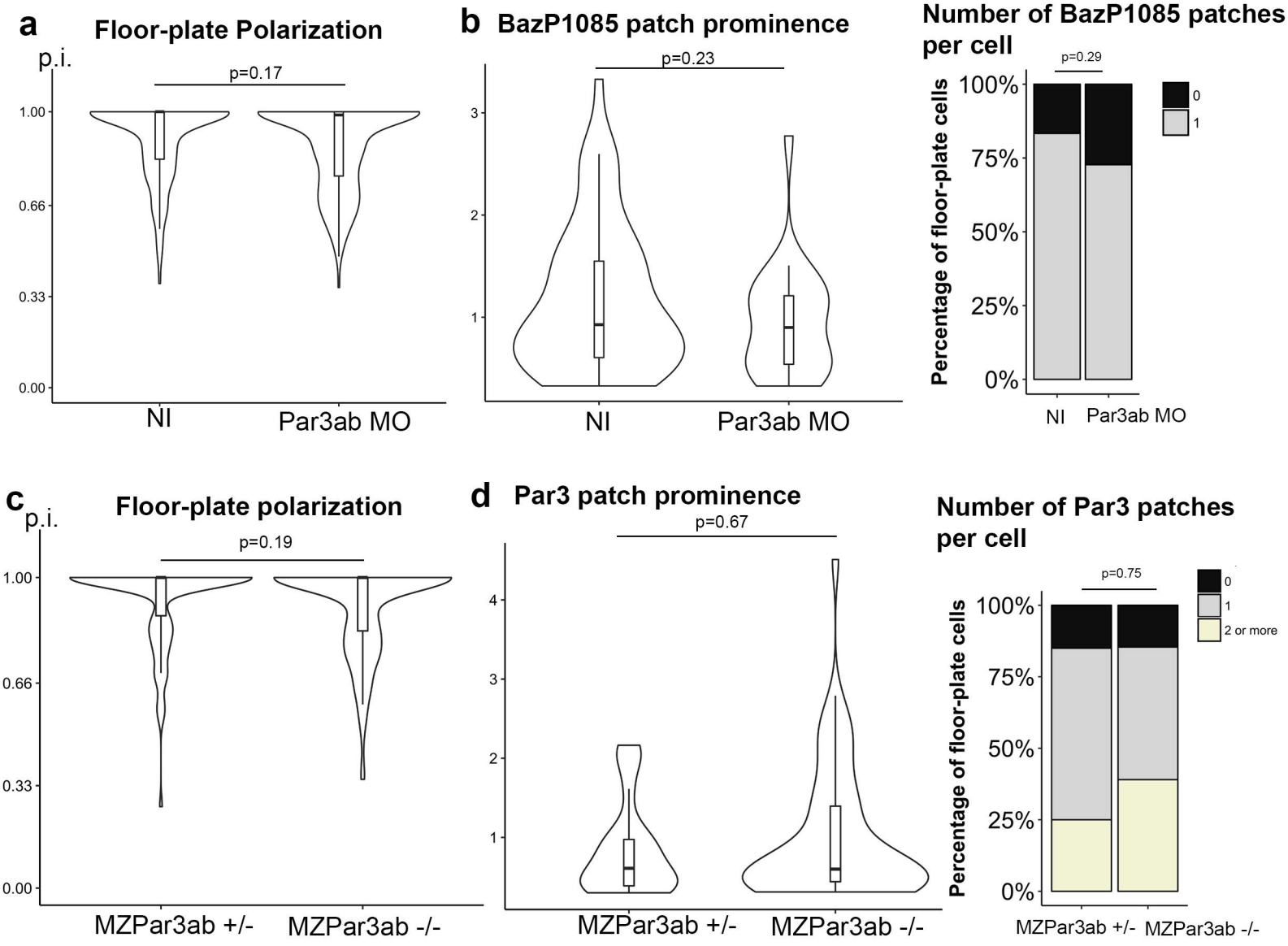

Figure S3 Donati et al.2019

(dorsal view, 18 s stage). Par3 or BazP1085 patches number compared with Fisher's exact test. f) Immunostaining of FP cells not injected (NI) or injected with Par3ab morpholino (Par3abMO) showing the equivalent amount of BazP1085 staining in both conditions. g) Immunostaining of FP cells in MZPar3ab$^{+/-}$ and MZPar3ab$^{-/-}$ showing the equivalent amount of Par3 in both genotypes.

SUPPLEMENTARY MOVIES LEGENDS

Filename: Supplementary movie 1
Description: **Live imaging of a BB bouncing off the posterior membrane in an early-stage FP cell**. wt embryos were injected with Centrin-GFP (green) and membrane-Cherry (magenta) mRNAs at the one-cell stage. White arrows indicate the position of the BB at the first and last time-points. Images were taken every 5 minutes during the 6 s to 9 s stages time-frame. Dorsal view. Corresponds to Fig1c.

Filename: Supplementary movie 2
Description: **Live imaging of a BB bouncing off posterior and anterior membranes in an early-stage FP cell**. wt embryos were injected with Centrin-GFP (green) and membrane-Cherry (magenta) mRNAs at the one-cell stage. White arrows indicate the position of the BB at the first and last time-points. Images were taken every 5 minutes during the 6 s to 9 s stages time-frame. Dorsal view. Corresponds to Fig1d.

Filename: Supplementary movie 3
Description: **Live imaging of a BB staying in contact with the posterior membrane in a late-stage FP cell**. wt embryos were injected with Centrin-GFP (green) and membrane-Cherry (magenta) mRNAs at the one-cell stage. White arrows indicate the position of the BB at the first and last time-points. Images were taken every 5 minutes during the 18 s to 21 s stages time-frame. Dorsal view. Corresponds to Fig1e.

Filename: Supplementary movie 4
Description: **Live imaging of BB bouncing against the posterior membrane in a late-stage FP cell**. wt embryos were injected with Centrin-GFP (green) and membrane-Cherry (magenta) mRNAs at the one-cell stage White arrows indicate the position of the BB at the first and last time-points. Images were taken every 5 minutes during the 18 s to 21 s stages time-frame. Dorsal view. Corresponds to Fig1f.

Filename: Supplementary movie 5

Description: **Live imaging of** the **rapid repolarization of the anterior daughter cell after FP cell division**. wt embryos were injected with Centrin-GFP (green) and membrane-Cherry (magenta) mRNAs at the one-cell stage. White arrows (at the beginning, middle and end of the movie) point at the BB of the anterior daughter cell, which rapidly moves back to the posterior membrane after cytokinesis. Images were taken every 2 minutes during the 5 s to 7 s stages time-frame. Dorsal view. Corresponds to FigS1d.

Filename: Supplementary movie 6
Description: **Live imaging of BB movements in a FP cell displaying a membrane invagination between BB and the posterior membrane** (yellow arrow at t=115 min). wt embryos were injected with Centrin-GFP (green) and membrane-Cherry (magenta) mRNAs at the one-cell stage. White arrows point at the BB. Images were taken every 5 minutes during the 6 s to 9 s stages time-frame. Dorsal view. Corresponds to FigS2a.

Filename: Supplementary movie 7
Description: **Live imaging of BB movements in a FP cell displaying a membrane invagination between BB and the anterior membrane** (yellow arrow at t=18 min). wt embryos were injected with Centrin-GFP (green) and membrane-Cherry (magenta) mRNAs at the one-cell stage. Membrane invaginations between the posterior membrane and BB can also be seen at t=10min, t=26min and t=66min. White arrows point at the BB. Images were taken every 2 minutes during the 8 s to 10 s stages time-frame. Dorsal view. Corresponds to FigS2b.

Filename: Supplementary movie 8
Description: **Live imaging of BB movements and Par3-RFP localization in a polarizing FP cell**. wt embryos mosaically expressing Centrin-GFP (green) and Par3-RFP (magenta). White arrows point at the BB at t=0 and at t=30 min, when the BB touches the posterior membrane. Images were taken every 2 min during the 15 s to 17 s stages time-frame. Lateral view. Corresponds to Fig2e.

Filename: Supplementary movie 9
Description: **Live imaging of BB movements and Par3-RFP localization in a polarizing FP cell**. wt embryos mosaically expressing Centrin-GFP (green) and Par3-RFP (magenta). White arrows point at the BB at t=0 and at t=60 min, when the BB touches the posterior membrane. Images were taken every 4 min during the 8 s to 10 s stages time-frame. Dorsal view. Corresponds to Fig2f.

Filename: Supplementary movie 10
Description: **Live imaging of BB movements and Par3-RFP localization in a non-polarizing FP cell**. wt embryos mosaically expressing Centrin-GFP (green) and Par3-RFP (magenta). White arrows point at the BB at the beginning and end of movie. Images were taken every 5 minutes during the 17 s to 19 s stages time-frame. Lateral view. Corresponds to Fig2f.

Filename: Supplementary movie 11
Description: **Live imaging of BB/Par3 patch contacts in an early-stage FP cell**. wt embryo mosaically expressing Centrin-GFP, Membrane-GFP (green) and Par3-RFP (magenta). White arrows point at the BB at the beginning of the movie, when the BB is in contact with the anterior Par3 patch, at t=30 min when it makes a contact with the posterior Par3 patch and at the end of the movie. Images were taken every 2 min during the 4 s to 5 s stages time-frame. Dorsal view. Corresponds to Fig3b.

Filename: Supplementary movie 12
Description: **Live imaging of membrane invaginations at the level of Par3 patches in early stage FP cells**. wt embryo mosaically expressing Centrin-GFP, Membrane-GFP (green) and Par3-RFP (magenta). White arrows point at the BB at the beginning and at the end of the movie. Yellow arrows at t=0 and t=68 min point at membrane invaginations originating from the posterior and the anterior Par3 patches, respectively. Images were taken every 4 min during the 7 s to 8 s stages time-frame. Dorsal view. Corresponds to Fig3c.

Filename: Supplementary movie 13
Description: **Live imaging of BB/lateral Par3 patch contacts in an early-stage FP cell of a *vangl2*$^{m209/m209}$ mutant**. *vangl2*$^{m209/m209}$ embryo mosaically expressing Centrin-GFP, Membrane-GFP (green) and Par3-RFP (magenta). White arrows point at the BB at the beginning and at the end of the movie. Images were taken every 4 min during the 5 s to 6 s stages time-frame. Dorsal view. Corresponds to Fig4e.

Filename: Supplementary movie 14
Description: **Live imaging of BB/posterior Par3 patch contacts in an early-stage FP cell of a *vangl2*$^{m209/m209}$ mutant**. *vangl2*$^{m209/m209}$ embryo mosaically expressing Centrin-GFP, Membrane-GFP (green) and Par3-RFP (magenta). White arrows point at the BB at the beginning and at the end of the movie. Images were taken every 4 min during the 5 s to 6 s stages time-frame. Dorsal view. Corresponds to Fig4f.

II-Rotational polarity characterization in FP cells

The work presented above mainly focuses on FP translational polarization.
However, previous studies on floor-plate PCP using cilia markers and live-imaging suggested the presence of rotational polarity in FP cells (Borovina 2010[274]).
We found BB appendages markers that allow us to quantify both rotational and translational polarities in the FP and show that they are defective in the PCP Vangl2 $^{m209/m209}$ mutant.

A) Rotational and translational polarity are defective in Vangl2 mutants

In order to characterize Vangl2 $^{m209/m209}$ PCP defects in the floor-plate further, we immunostained wt and Vangl2 $^{m209/m209}$ embryos for Rootletin and Non-Muscle-Myosin-IIB (NMIIB) to assess both translational and rotational polarity. Indeed Rootletin is a known marker of the ciliary rootlet and we found that NMIIB localizes close to BB, opposite to the rootletin staining (cf below, NMIIB part), at the expected position of the basal-foot : thus, these markers are a proxi for BB appendages orientation (rotational polarization) and allow us to quantify both rotational and translational (distance between NMIIB dot and posterior membrane) polarities.

Interestingly, Rootletin and NMIIB staining around the BB were similar in wt and Vangl2 $^{m209/m209}$ embryos, indicating that Vangl2 is not essential for the localization of these proteins next to the BB (Fig 30a). Displaying FP polarization state on a circular plot revealed that Vangl2 $^{m209/m209}$ mutants have both translational and rotational polarity defects (Fig 30b). Rotational polarization was strongly defective (the ratio between variances of wt versus Vangl2 $^{m209/m209}$ mutants was around 10) as well as translational polarity (the median polarization index was 0.9 in wt versus 0.62 in Vangl2 mutants). Interestingly, Vangl2 mutants had slightly shorter rootlets (Fig 30c, median rootlet length was around 2μm in wt versus 1.7μm in Vangl2 mutants) : this could contribute to polarization defects in these mutants.

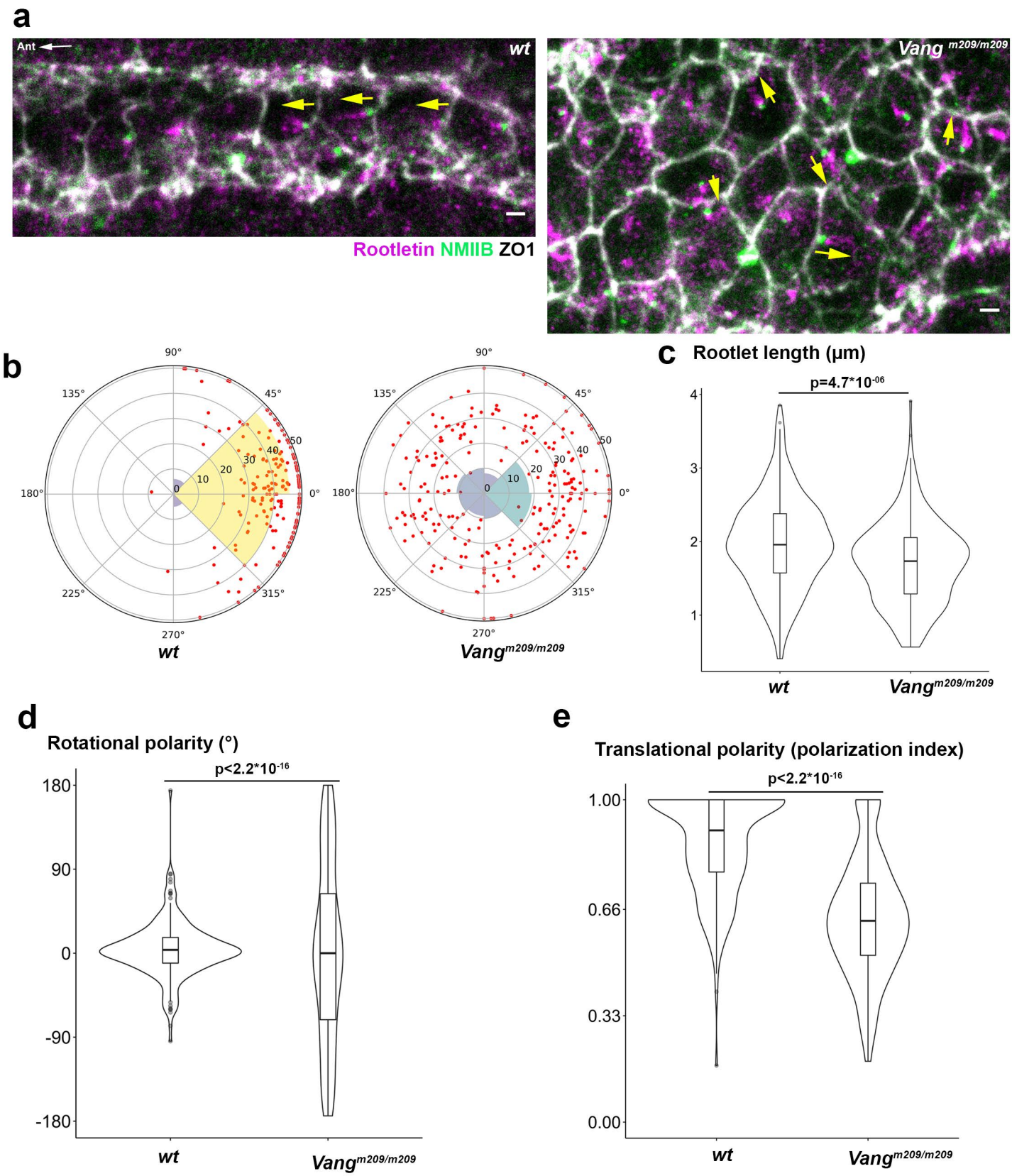

Figure 30 Rotational and translational polarity are defective in Vangl2 mutants

In these experiments, « wt » refers to a mix of Vangl2 +/+ and Vangl2 m209/+ embryos (which have a morphology identical to wt embryos). Vangl2 m209/m209, embryos are identified based on their strong axis extension defects and elongated somites.

a. Immunostaining of 18s wt and Vangl2 m209/m209 embryos stained for Rootletin (ciliary rootlet), NMIIB (BB/Basal-foot) and ZO1 (apical junctions). Rotational polarity was defined as the angle between yellow vectors and the embryo anterio-posterior axis. Scale bar 2µm. Anterior left.

b. Circular plots showing both translational and rotational polarity in wt and Vangl2 m209/m209 FP at 18s. Each red dot is a cell, its position reflects both translational polarity (a polarity index of 0 and 1 correspond to the circle center and edge respectively) and rotational polarity (angles displayed at the periphery of the circle, the embryo's AP axis being vertical, anterior left).

c. Quantification of rootlet length in wt and Vangl2 m209/m209 (Wilcoxon test)

d. Quantification of rotational polarity in wt and Vangl2 m209/m209 (Fisher test)

e. Quantification of translational polarity in wt and Vangl2 m209/m209 (Wilcoxon test)

Since Dvls are important players in PCP and have a role in BB polarization in many systems, we decided to take advantage of a recently generated Dvl2 mutant (Xing 2018[309]) to investigate the role of another PCP protein (Dvl2) in FP PCP.

B) Dvl2 loss of function affects rotational but not translational polarity in FP cells

Rotational and translational polarity plotting on a circular chart suggested that maternal zygotic (MZ) heterozygotes FP polarity was similar to wt FP polarity, whereas MZ-homozygous mutants had a defect in rotational polarity (Fig 31a). We found that significant differences in rootlet orientation (Fig 31b) correlated with a decrease in rootlet length (mean length 2.2μm in wt versus 1.8μm in MZ-Dvl2-/-) (Fig31c). However we could detect no difference in translational polarity (Fig 31d).

Since we find that FP cells BB display oriented appendages and that defects in rootlet length correlates with rotational polarity defects, we wondered if this could be due to a defective link between rootlet and apical cytoskeleton. To test this hypothesis, we investigated the potential presence of « ciliary adhesions » previously described in Xenopus embryonic ectoderm multi-ciliated cells (MCC) that anchor BBs to the apical actin cytoskelton (Antoniades 2014).

C) Paxillin localizes at the base of FP cilia and could be involved in rotational polarization

We find that Paxillin localizes next to FP cells BB (Fig 32a). Co-staining with NMIIB revealed no overlap between the localization of these two molecules. In addition, the polarized localization of paxillin was complementary to that of NMIIB, (Fig 32b) and was obviously polarized at 18s, with the Paxillin to NMIIB vector pointing to the posterior side of the embryo (Fig 32b, yellow arrows).

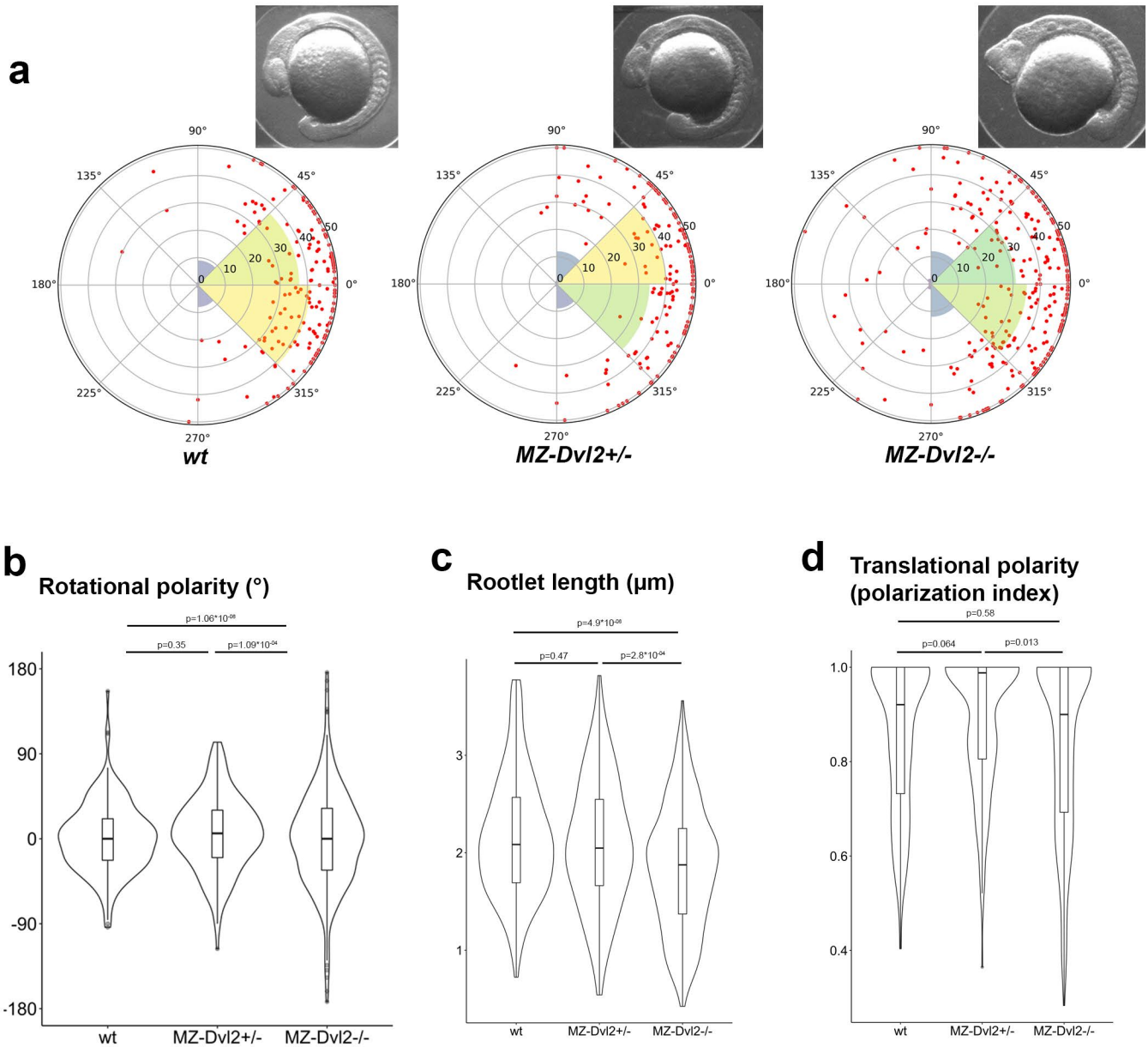

Figure 31 Dvl2 loss of function affects rotational but not translational polarity in FP cells

a. Circular plot showing rotational and translational polarization of FP cells in wt, MZ-Dvl2+/- and MZ-Dvl2-/- embryos at 18s. Upper panel shows the global morphology of the embryo, with no defect in heterozygous but strong body anterior-posterior axis extension defects in homozygous. Each red dot represents a cell : the polarization index is equal to 0 at the center of the circle and to 1 at its edge. Angles represent the angle between the rootlet and the AP axis of the embryo corresponding to the 0°-180° vertical line. (wt : 173 cells from 4 embryos ; MZ-Dvl2+/- : 169 cells from 7 embryos ; MZ-Dvl2-/- : 294 cells from 8 embryos).
b. Quantification and statistical tests comparing rotational polarity in wt and Dvl2 mutants (Fisher test to compare variances)
c. Comparison of rootlet length in wt and Dvl2 mutants (Wilcoxon test)
d. Comparison of polarization index between wt and Dvl2 mutants (Wilcoxon test)

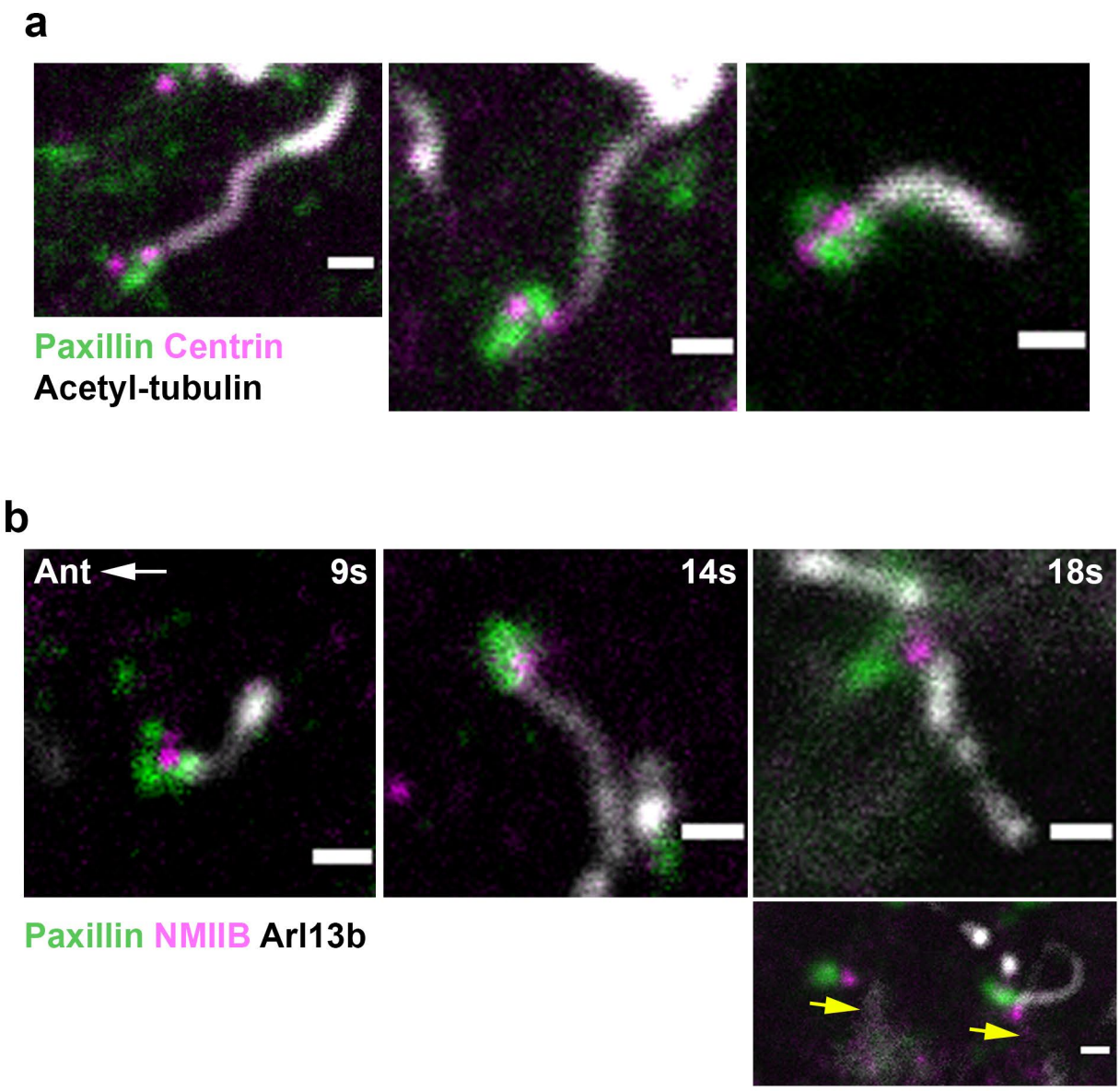

Figure 32 Paxillin localizes at the base of FP cilia

Anterior is left in all pictures
a. Immunostaining of Paxillin, centrin and acetyl-tubulin of FP cells in a 16s stage embryo
b. Immunostaining of Paxillin, NMIIB and Arl13b (a ciliary marker) in 9, 14 and 18s stage embryos.
Scale bars : 1µm

In our system, paxillin is enriched opposite to ciliary beating, on the rootlet side, which could correspond to one of the two pools found in Xenopus MCC at the extremity of the ciliary rootlet.

Since the paxillin pool is present at 9s, long before cilia become motile (24 somites), this anterior patch is probably not induced by mechanical constraints of beating cilia, as proposed for the actin pool surrounding BB of ependyma MCC (Mahuzier, 2018[310]). However ciliary beating could strenghten this paxillin pool. In any case, the presence of Paxillin at the base of FP cells BB suggests the existence of ciliary adhesion in this system, contributing to BB/cilia mechanical stability by linking them to a putative apical actin network : it will therefore be interesting to visualize the actin cytoskeleton in FP cells to assess the presence and organization of such a network.

As mentioned in the introduction, acto-myosin and microtubules are involved in BB/cilia positioning in many systems ; thus we investigated a potential role of these cytoskeletal elements in FP polarization.

III-Zebrafish floor plate cytoskeleton analysis during the polarisation process

A) NMIIB localizes on the posterior side of BB in FP cells

In order to investigate a potential role of acto-myosin in BB positioning, we analysed the distribution of different Non-Muscle Myosin II (NMII) isoforms in the FP using available commercial antibodies. NMIIA was localized at the apical junctions and at the cytokinesis ring. Surprisingly, we found that NMIIB localizes only in a dotted pattern and not at apical junctions in the FP. These dots were seen from the 9s stage and became more intense as development proceeded. They were mostly restrained to FP cells and not detected in other neural tube cells or in notochord cells (Fig 33a). Furthermore the dots were intense in the anterior part of the embryo and became fainter more posteriorly. Closer examination revealed that these NMIIB dots localize

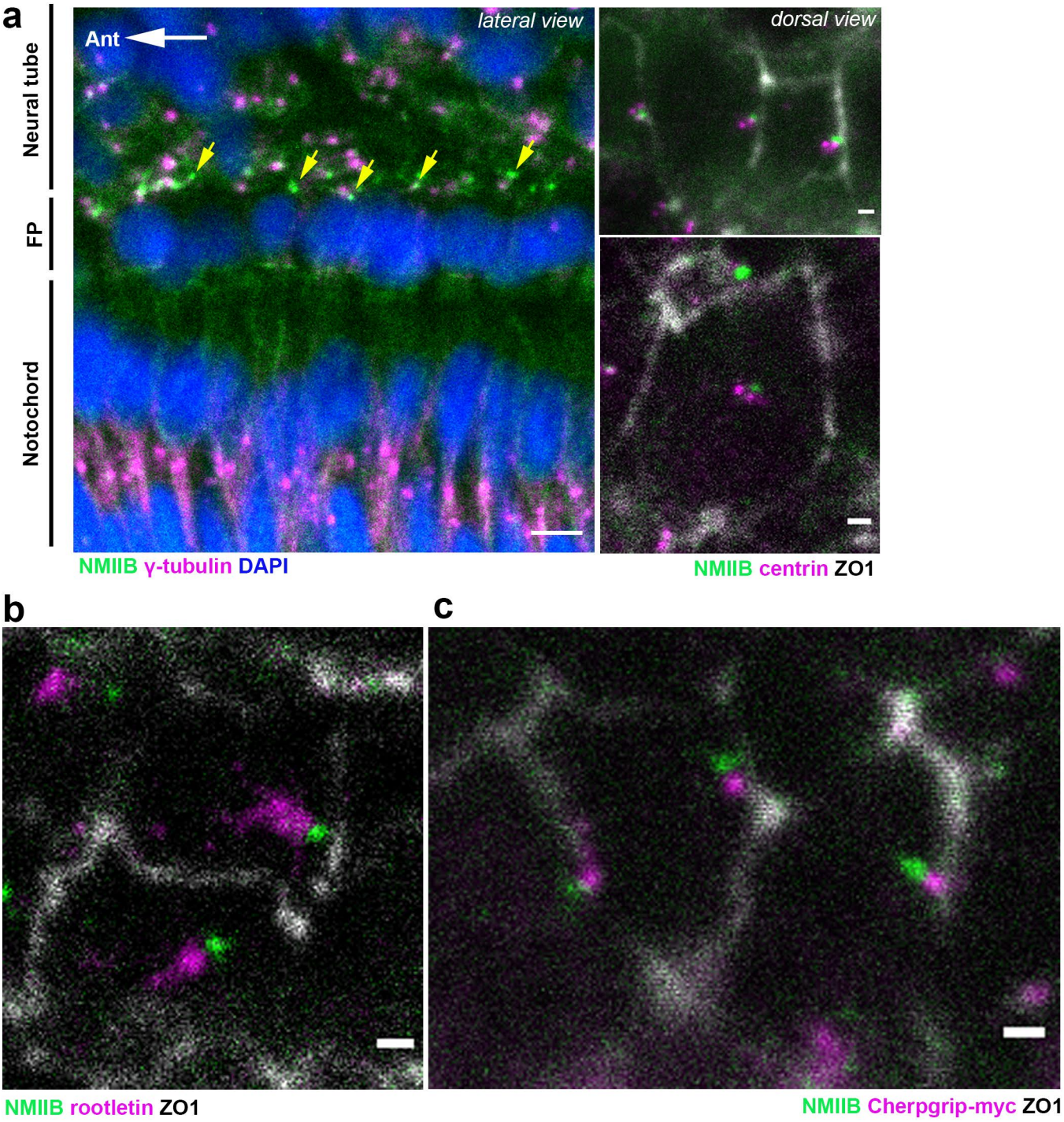

Figure 33 NMIIB localizes on the posterior side of BB in FP cells

Anterior is left in all pictures
a. left : lateral view of a 18s stage embryo immunostained for NMIIB and γ-tubulin. Yellow arrows point at NMIIB dots next to FP cell's BBs. FP :floor-plate. Scale bar : 5µm.
right : dorsal view of 18s stage embryo immunostained for centrin, NMIIB and ZO1. Upper panel shows cells in which the BB is in contact with the posterior membrane. Lower panel shows a FP cell with a median BB.
b. dorsal view of FP cells of a 18s stage embryo immunostained for NMIIB and Rootletin, a ciliary rootlet marker. (Scale bar 1µm)
c. dorsal view of FP cells of a wt embryo injected at the 1 cell stage with Cherpgrip-myc mRNA and immunostained for myc, NMIIB and ZO1 at the 18s stage. (Scale bar 1µm)

close to one of the centriole of FP cells, usually the more posterior one, which corresponds to the mother centriole that forms the BB (Fig 33a, right panel). Importantly, NMIIB localized next to BB even in cells with a median BB (Fig 33a right lower panel), suggesting that it could play an active role in BB posterior positioning.
NMIIB localization did not overlap with the rootlet (Fig 33b) and was distinct from the ciliary transition zone labelled by Rpgrip1l-myc (Fig 33c).
The dynamic increase and posterior orientation of NMII labelling in contact with the mother centriole suggest that this Myosin pool could be localised at the basal foot, a sub-distal appendice of motile cilia that acts as a microtubule polymerisation center.
We could not find other commercial antibodies that would cross-react with zebrafish Myosin IIB but this staining partially overlaps with a phosphorylated Myosin light chain, as described in the following paragraph.

B) Myosin is activated by phosphorylation in the FP but is not required for translational polarity

Myosin can be activated by phosphorylation of its regulatory light chains (MRLC) by the MRCK and ROCK kinases. In the FP, we found that a pool of MRLC phosphorylated at Threonine18 and Serine19 (ppMRLC) localizes at the base of cilia as early as the 10s stage and up to the 18s stage (Fig 34a). In contrast to NMIIB, the localization of this staining was not restrained to FP cells, even if it was stronger in FP cells. To test whether this ppMRLC is associated with NMIIB heavy chain, we did a double immunostaing to assess colocalization at the 18s stage (Fig 34b). Indeed we found that approximately half of the ppMLC pool colocalizes with NMIIB, suggesting that NMIIB could be activated by phosphorylation in FP cells (mean colocalization 50.2%, 6 cells from 2 embryos). To assess a potential role of myosin and its activation by phosphorylation in translational polarity, we treated embryos with Blebbistatin (which inhibits myosin activity) or with ML7 (which inhibits MRLC) or Rockout (which inhibits ROCK) to prevent myosin phosphorylation (Fig 34c). We could not detect a significant effect of any of these drugs on FP translational polarization, suggesting that myosin and its activation are not required for this process.

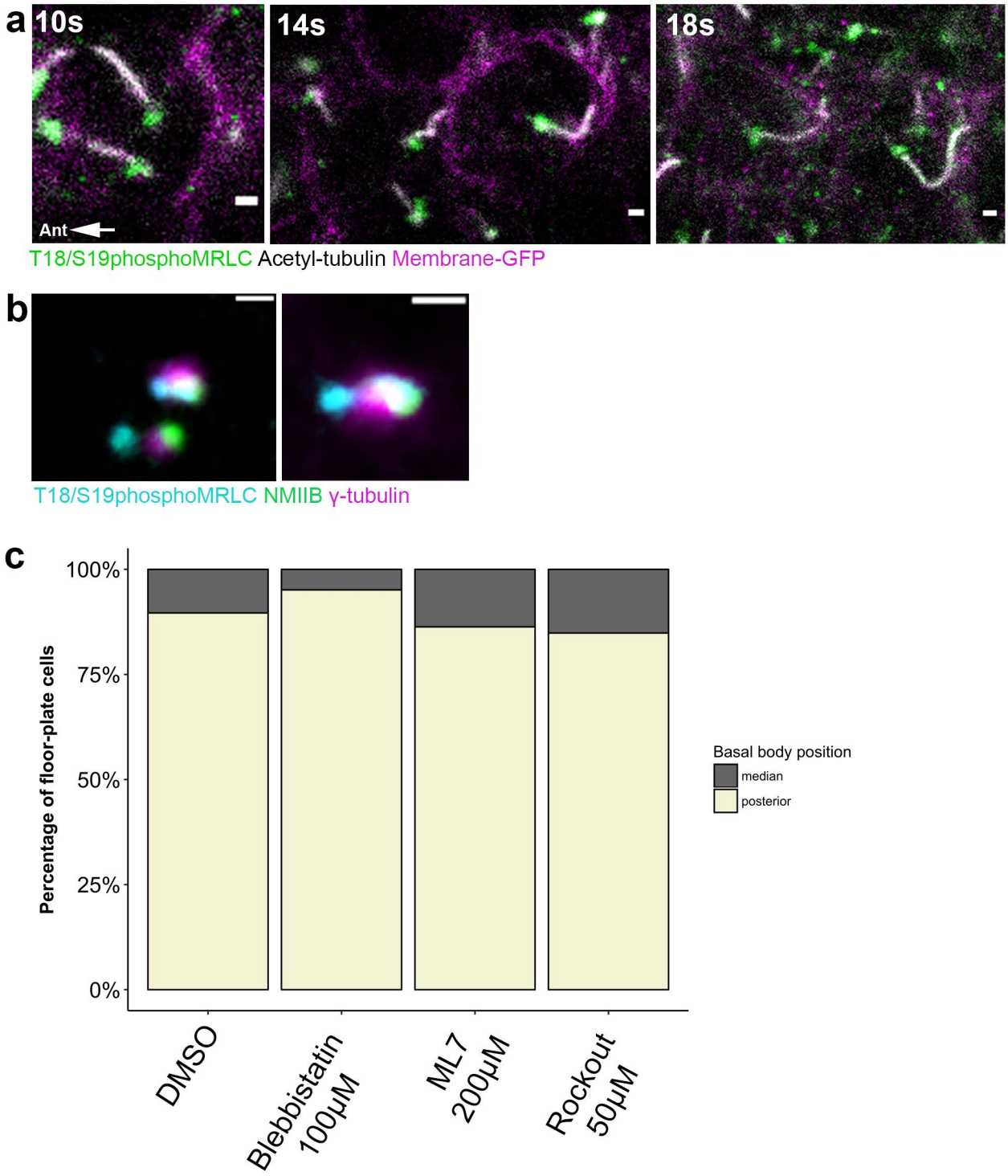

Figure 34 Myosin is activated by phosphorylation in the FP but is not required for translational polarity

a. Immunostaining on wt embryos injected with membrane-GFP mRNA, revealing MRLC phosphorylated on Threonine 18 and Serine 19 (T18/Ser19phosphoMRLC), membrane –GFP and acetylated tubulin (cilia) at 10, 14 and 18s stages.
b. Immunostaining of wt 18s stage embryos showing ppMLC, NMIIB and γ-tubulin. This kind of image was used to assess colocalization between ppMLC and NMIIB.
c. Percentages of FP cells with a median or posterior BB in embryos treated either with DMSO (control), Blebbistatin, ML7 or Rockout. Embryos were exposed to these drugs from the 10s to the 18s stage.

C) Microtubules are posteriorly enriched in FP cells

In order to investigate a potential role of microtubules in BB positioning, we set out to visualize the microtubule network in FP cells. To mosaically label microtubules in the FP, we injected UAS plasmids driving the expression of Doublecortin-GFP (microtubules) or EB3-GFP (microtubule (+) ends) in a Netrin-KAL4 line that we generated, and that expresses the transcriptional activator KalTA4 in FP cells from the 12s stage on.

Both Doublecortin and EB3 local accumulation were seen at the apical posterior side of FP cells, which probably correspond to centrosome/BB (Fig 35a,b,c,d white arrows). In addition, both Doublecortin and EB3 were enriched in a wider region, along the posterior membrane from the apical to the basal side (Fig 35a first panel, lateral view) as well as along the posterior transverse junction (Fig 35a 2nd and third panels, Fig 35c,d). Interestingly in one case, we could detect both a posterior enrichment along the transverse membrane and a medio-apical enrichment that probably corresponds to the BB (Fig 35a second panel, posterior cell) ; this suggests that the posterior microtubule enrichment precedes BB posterior positioning in FP cells, although this result needs to be confirmed by performing time-lapse experiments.

Live-imaging of embryos expressing EB3-GFP also revealed the presence of EB3 comets moving from the posterior apical side (where the BB was probably already positioned given the accumulation of EB3-GFP there) to the anterior apical side (Fig 35b for a lateral view and Fig 35c for a dorsal view, yellow arrowheads point at anterior-directed comets). Preliminary results suggest that EB3 posterior enrichment and anterior-directed comets are also present at earlier stages (Fig 35d). These results show the existence of a dynamic planar microtubule network at the apical side of FP cells, which could be involved in BB posterior positioning.
It will be important to assess microtubule dynamics in non-polarized FP cells at early stages to test for a potential enrichment of microtubule (+) ends at the posterior side before BB posterior positioning.

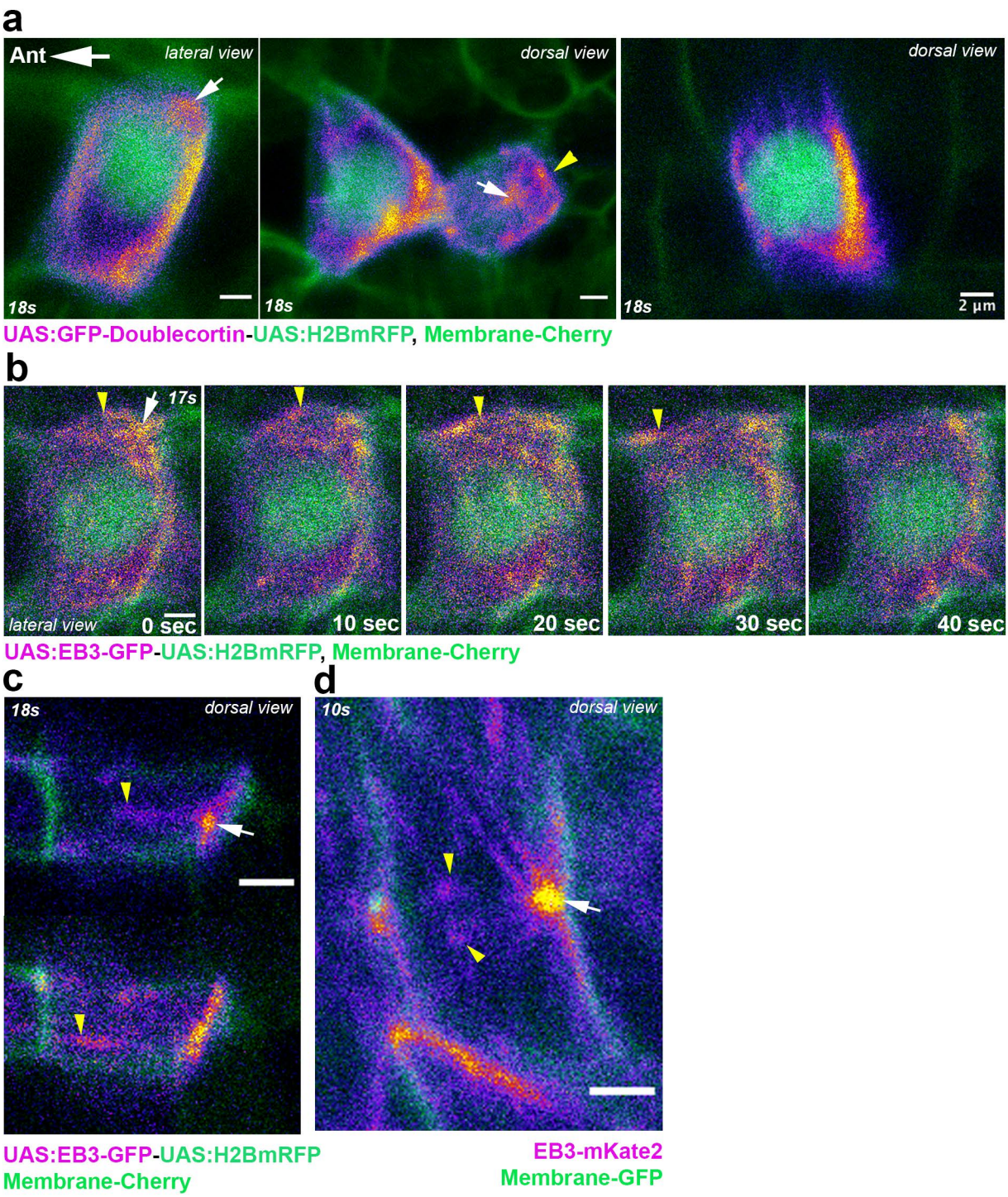

Figure 35 Microtubules are posteriorly enriched in FP cells

a.b.c. Confocal images of live Netrin : KalTA4 transgenic embryos injected at the one-cell stage with plasmids driving the expression of either GFP-Doublecortin (Fig 35a) or EB3-GFP (Fig 35b,c) (microtubules) along with H2BmRFP (nucleus) under the control of UAS sequences and with membrane-cherry mRNA.

a. Still images from live embryos FP cells expressing GFP-Doublecortin, H2B-mRFP and Membrane-Cherry. White arrows : doublecortin accumulation probably corresponding to BB. Yellow arrowhead : Doublecortin enrichment along the posterior transverse membrane.

b. Lateral view of a FP cell expressing EB3-GFP, H2B-mRFP and Membrane-Cherry imaged every 10 secondes at the 17s, revealing anterior-directed EB3 comets within the apical surface (yellow arrowheads). White arrow : probable position of BB (local EB3-GFP accumulation).

c. Dorsal view of a FP cell expressing EB3-GFP, H2B-mRFP and Membrane-Cherry. White arrow : probable location of BB (local EB3 accumulation). Yellow arrowheads : anterior-directed EB3 comets.

d. Dorsal view of a still image from an early stage embryo FP cell expressing EB3-mKate2 and membrane-GFP. White arrow points at the probable location of the BB (strong accumulation of EB3). Yellow arrowheads : anterior-directed EB3 comets.

IV-Are Rpgrip1L and Par3 PCP functions conserved in the cnidarian Clytia hemispherica?

Our lab has previously shown that the transition zone (TZ) protein Rpgrip1l is important both for controlling cilia length and composition and for PCP establishment of mouse cochlea and zebrafish floor-plate (Mahuzier 2012[296]). In vertebrates, Rpgrip1l has a paralogous gene, Rpgrip1, which has a more restricted expression pattern and play a major role in eye development.

In order to determine if the multiple roles of *Rpgrip1l* in ciliogenesis, cilia transduction and PCP is an ancestral feature of metazoans, we investigated the localization and function of the only *Rpgrip1l/Rpgrip1* orthologous gene in the embryo of the jellyfish Clytia hemisphaerica (Fig 36) in collaboration with T. Momose (Laboratoire de Biologie du Développement de Villefranche-sur Mer). Indeed, rpgrip1/1l gene is already present in a subset of unicellulaires organisms such as ciliates and green algae and is conserved both in cnidarians and bilaterians. We made the hypothesis that the rpgrip1/1l cnidarian orthologue could be required to coordinate ciliary beating and/or ciliogenesis.

Indeed, gastrula and later planula of this hydrozoan display a planar polarized ciliated ectoderm that allow their directional swimming (in the aboral direction, Fig 37a, Momose 2012). Planar polarization of this ciliated epithelium depends on PCP proteins such as Vang (Momose 2012[276]), and cilia display both translational and rotational polarity, the later being easily visualized by actin and γ-tubulin that label structures that could correspond to actin bundles and the ciliary rootlet on the aboral side of basal bodies (Fig 37a right panel, Momose 2012)

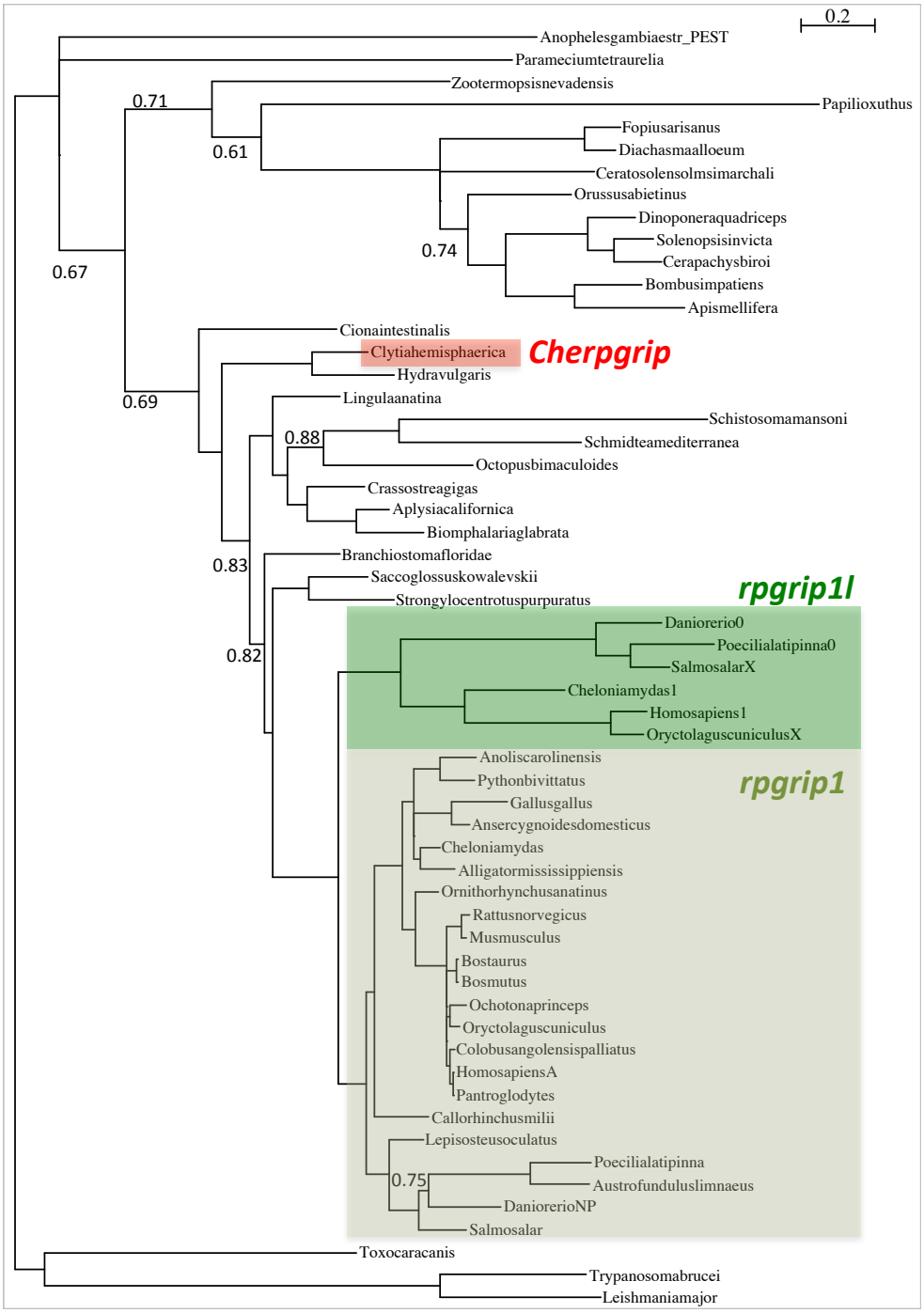

Figure 36 Rpgrip1/1l in Metazoa

Bayesian inference Metazoan phylogenetic tree based on *rpgrip1* and *rpgrip1l* sequences. The *rpgrip1/1l* orthologous gene found in Clytia is highlighted in red (*Cherpgip*). In vertebrate (green shaded rectangles), a duplication gave rise to the two paralogous genes *rpgrip1* and *rpgrip1l*. (Tree generated by Gabriel Krasovec, IBPS)

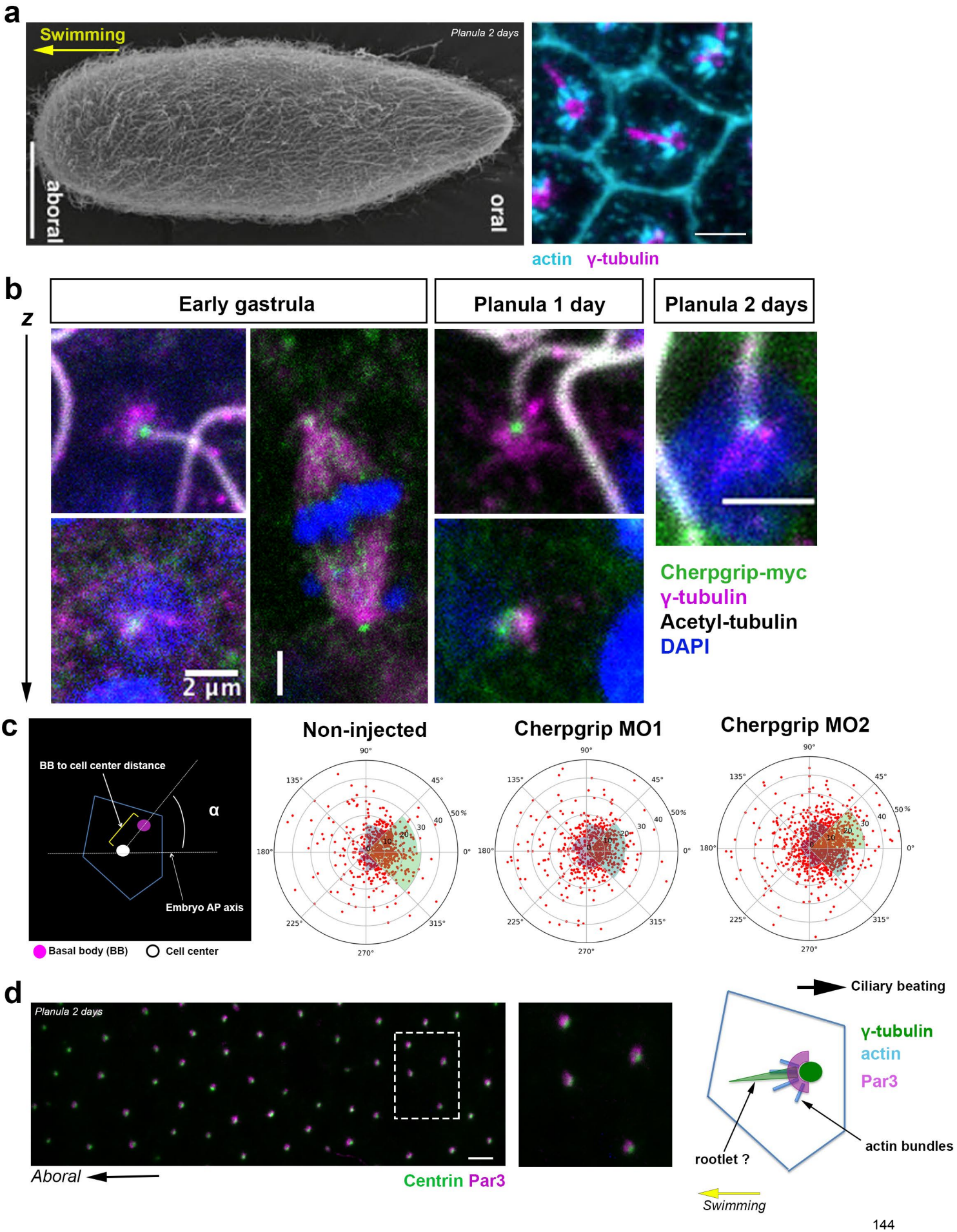
a
Swimming
Planula 2 days
aboral
oral
actin γ-tubulin
b
z
Early gastrula
Planula 1 day
Planula 2 days
2 µm
Cherpgrip-myc
γ-tubulin
Acetyl-tubulin
DAPI
c
BB to cell center distance
α
Embryo AP axis
Basal body (BB)
Cell center
Non-injected
Cherpgrip MO1
Cherpgrip MO2
d
Planula 2 days
Aboral
Centrin Par3
Ciliary beating
γ-tubulin
actin
Par3
actin bundles
rootlet ?
Swimming

Fig 37 Cherpgrip localizes at the base of cilia and is required for rotational polarity in Clytia

a. left : transmission electron microscopy of a 2 days planula (P2) showing the cilia that allow aboral-directed swimming (scale bar : 50μm). Right immunostaining of P2 embryo ciliated ectoderm revealing actin (blue) at the cell cortex and, on the aboral side of BB, an elongated structure labelled with γ-tubulin that could be the ciliary rootlet (scale bar 2μm) attached to the BB. (adapted from Momose 2012)

b. Immunostaining of embryos injected at the one-cell stage with Cherpgrip-myc mRNA at early gastrula (EG), 1 day planulae (P1) and P2. (scale bar 2μm)

c. left : schematic drawing of an ectodermal cell and the relative position of its BB (magenta) with its center of mass (white). The angle **α** (between the embryo AP axis and cell center-BB axis) serve as a proxi for rotational polarity. BB off-centering in each cell was defined as the ratio between the length of the BB/cell-center vector and the radius of the circle with an area equal to that of the cell. Both off-centering and angle α were plotted on circular plots, on the right for control non-injected embryos and on the left for embryos injected with one of two Cherpgrip-targeting MOs. Each red dot represents a cell and the proportion of dotal dots within each 8th of the circle is represented as a colored « piece of cake » (NI : 3 embryos, 682 cells ; MO1 3 embryos 657 cells ; MO2 3 embryos 1095 cells). Statistical significance of rotational polarity variances differences were estimated with a Fisher test (NI/MO1 : ratio of variances 0.59, $p=1.2^{e-11}$; NI/MO2 : ratio of variances 0.78, $p=3.3^{e-04}$).

d. Immunostaining of a P2 planula revealing Par3 staining (magenta) on the aboral side of BBs in ciliated ectodermal cells (scale bar 2μm). The image on the right is a close-up of the region comprised in the dotted-rectangle delimited on the left image. The scheme on the right shows the localization of Par3 relative to BBs, on the same side as actin bundles and potential rootlet.

A) Is Rpgrip1L sub-cellular distribution conserved in cnidarians?

We first cloned C.*hemisphaerica Rpgrip1/1l* (*Cherpgrip*) into a myc-tag vector and then injected Cherpgrip-myc mRNA into zygotes. Immunostaining at later stages of development revealed that Cherpgrip assumes a conserved localization at the base of cilia, distal to the BB (stained by gamma-tubulin) that corresponds to the transition zone (TZ) but we noticed a smaller pool of protein at a more proximal position relative to the BB. (Fig 37b). In in 2 days planulae (P2) we only detected the first TZ pool. Cherpgrip also localized, as its mammalian orthologue, at spindle poles in mitotic cells of the early gastrula ectoderm (Fig 37b, early gastrula, right panel).

B) Assaying Cherpgrip function using morpholinos and Crispr

Since we confirmed that the Cherpgrip protein presents a conserved subcellular localisation at cilia base and centrosomes, we decided to perform loss of function experiments using two different strategies.

Cherpgrip morpholino-mediated knock-down had a small but significant effect on rotational polarity but no effect on translational polarity (Fig 37c). The weak effect could be explained by maternel proteins present in the egg.

In order to confirm these results, we decided to generate a loss of function mutant with CRISPR-Cas9. We succesfuly designed gRNAs that cut the Cherpgrip gene in exon 2 or in exon 10 efficiently (as assessed by a T7 test) and were predicted to induced frameshifts via micro-homology mediated repair. We injected zygotes with gRNAs and Cas9 mRNA and let them develop into polyp for several weeks. After this, polyps were sequenced to test for potential mutations : unfortunatly we could only recover polyps with in-frame insertions or deletions, and these did not have any obvious phenotype. It could be that during polyp growth, cells with out-of-frame repaired Cherpgrip would have been outcompeted by cells with a non-deficient Cherpgrip gene (either not cut or repaired in frame).

C) Is Par3 sub-cellular distribution conserved in cnidarians?

Interestingly, the Par3 immunostaining using Par3-07330 antibody (the same that we used in our Zebrafish study) revealed that Par3 is not localized to cell-cell junctions but rather next to basal bodies in a polarized fashion, on the aboral side (Fig 37d). Although this result needs to be confirmed with other antibodies and Par3 fusion proteins, it suggests that Par3 could have a conserved role in cilia positioning and/or ciliogenesis.

DISCUSSION and PERSPECTIVES

My PhD project aimed at uncovering the mechanisms of asymmetric positioning of cilia within the plane of epithelia, a form of Planar Cell Polarity (PCP). Cilia are sensory organelles protruding from the apical cell surface. Their coordinated oriented beating, which allows the directional flow of fluids within body cavities, depends on the PCP pathway and relies upon proper positioning of cilia and their associated basal body (BB).

In the main part of my PhD, to investigate the mechanisms of cilium planar polarization, I studied the zebrafish embryonic floor plate (FP), a ciliated epithelium in which planar polarized motile cilia allow the directional flow of the cerebrospinal fluid. My work had two main objectives. First, in order to describe the polarization process, I used live imaging to analyze the dynamics of BB posterior positioning in the embryonic zebrafish FP. Second, I investigated the mechanisms involved in BB posterior positioning downstream of the PCP pathway.

An unexpected result from live imaging analysis is that BBs are highly mobile and are able to contact, and bounce off, apical junctions several times per hour. They contact exclusively transverse (anterior or posterior) membranes. Membrane invaginations form between membranes and BBs as they move. I also found that FP polarization correlates with a decrease in BB movements dynamics. At the level of individual cells, BBs settle down posteriorly at Par3-enriched junctions, and my results strongly suggest that Par3 asymmetry is important for BB posterior localization. Membrane invaginations originate from Par3-positive patches at FP transverse membrane. In the PCP mutant *Vangl2*, BBs show poorly oriented movements and this correlates with a loss of Par3 posterior enrichment. I also showed that in Vangl2 mutants, rotational polarity is defective, and found a similar, although weaker effect in another zebrafish PCP mutant, the *dvl2* mutant (Xing 2018[309]).

In the following section I discuss the implications of our dynamic study on the understanding of the mechanisms of cilium polarization downstream of the PCP pathway. Our data highlight Par3 as a critical player in centriole positioning in this system and I discuss its potential link with microtubule-based forces. Indeed, I explored whether acto-myosin network could be implicated in BB polarisation but

although I found that non-muscle-myosin IIB display a polarized localization next to BB in the FP, my loss of function experiments do not support such a role. Finally, I propose several mechanisms that could explain how PCP proteins such as Vangl2 and Dvl2 control Par3 distribution.

A) Par3 asymmetric localization

We found that Par3 is enriched at posterior apical junctions in FP cells from early stages on. Here I outline the possible mechanisms leading to this asymmetric enrichment.

1) Exclusion by Par1 phosphorylation

In the C.elegans zygote, Par3 belongs to the group of « anterior PARs » along with Par6 and aPKC, where it forms an anterior cortical domain, maintained by the antagonistic activity of the Par1 kinase that localizes in a complementary posterior cortical domain. Par3 phosphorylation by Par1 is required for its exclusion from the cortex in several systems such as Drosophila follicular epithelium and oocyte (Benton 2003[16]). A recent study showed that in the Drosophila oocyte, Par3 exclusion from the posterior cortex depends on Par1 and an endocytic mechanism relying on Rab5 and PI(4,5)P2 but also on dynein-mediated vesicular transport and Rab11 (Jouette 2019[311]). Par1-mediated exclusion and dynein-mediated transport of Par3 have also been shown to act redundantly to position Par3 on the apical side of epithelial cells in Drosophila (McKinley 2012[312]). It would therefore be interesting to test a role for Par1 orthologs in Par3 positioning in the FP. We tried to inhibit global Par1 activity with a pharmacological approach (Par1 inhibitor Merck 39621) but Par3 was still phosphorylated on Ser865, the residue that was shown to be a Par1 target in Drosophila (data not shown). This suggests that either our drug treatment was not effective in the embryonic tissue or that another enzyme can phosphorylate this position. Because the global morphology of the treated embryos was totally identical to the untreated controls, we favour the first possibility. Indeed, we noticed the poor solubility of the drug in zebrafish E3 medium. As an Iternative strategy, we are

currently trying a genetic approach by generating Par3-RFP constructs resistant to Par1 phosphorylation (by converting specific serine residues to alanine) to assess whether they will behave as dominant negative constructs.
However, it could also be that Par1 is not required in the FP for Par3 polarization. Remarkably, Kono et al. recently showed that high levels of Par3 overexpression alone in non-polarized cultured Drosophila S2 cells is sufficient to trigger spontaneous Par3 asymmetric localization (Kono 2019[313]).

2) Exclusion by ROCK phosphorylation

During Drosophila germ band extension, filamentous actin, Myosin II and Rho-kinase establish a complementary polarised distribution on A/P membranes while Par3 was enriched on D/V sides (Simões et al, 2010[314]). Rho-kinase negatively controls Par3 recruitment on A/P membrane by phosphorylating Par3 C-ter, preventing its association to membrane PIP2/PIP3. This effect is independent of Myosin II and LIM-kinase, two Rho-kinase identified substrates, but can be reversed by its inhibitor Y-27632.
We tested whether this drug could have an impact on FP PCP and could not find reproducible defects on BB positioning, suggesting that this ROCK-based exclusion mechanism is not active in the FP.

3) Role of PCP proteins: exclusion by Vangl2 and recruitment by Dvl

Par3 is emerging as an important actor in PCP. It has been known for a long time that Par3 plays a role in the asymmetric planar first division of the Drosophila sensory organ precursor (SOP). Par3 assumes an asymmetric cortical localization that is complementary to Vang/Stbm (Bellaïche 2003[141]) and is redundantly directed by Pins and Fz (Bellaiche 2003[141]). Recently, Banerjee et al. found that Par3 posterior localization in dividing SOPs depends on Meru, a RASSF9/RASSF10 homologue which is recruited to the posterior cortex by Frizzled and Dishevelled (Banerjee 2017[315]). More recently, it was shown that PCP proteins can break PAR protein symmetry also in non-dividing cells, before mitosis in SOP (Besson 2015[138]). In

addition, Par3 assumes an asymmetric localization in the plane of the Drosophila ommatidial epithelium that depends on the PCP protein Flamingo (Aigouy 2016[169]).
In vertebrates, Par3 localizes asymmetrically in cochlea sensory hair cells, on the abneural side, where the kinocilium can be found and where several Fz and Dvl proteins localize (Ezan 2013[283]). This asymmetric localization is required for proper kinocilium positioning and in that case Par3 could be recruited by Daple, a protein that interacts with both Par3 and Dishevelled (Landin 2019[316], Siletti 2017[317]). In Xenopus neural plate, Par3 is also planar polarized (although it is not known whether it assumes an asymmetric localization) and interacts with Pk3 to promote its apical localization, thereby contributing to the proper planar polarization of the neural plate and allowing proper neural tube formation (Chuykin 2018[170]). In this system, Par3 enhances the formation of the Vangl2/Pk3 anterior complex in neural plate cells. Interestingly, Vangl2 is in turn required for proper Par3 planar polarization, which is consistent with our findings in the zebrafish FP.
Indeed, we found that in Vangl2 mutants, Par3 patches are mislocalized, even if they still make contact with BBs, strongly suggesting that Vangl2 is required for proper Par3 positioning and therefore proper positioning of a force generator. In FP cells, Vangl2 and Par3 localize at opposite sides, which suggests an exclusion mechanism as described for mutual exclusion of core PCP proteins (cf introduction). Therefore it would be interesting to test if Par3 posterior enrichment is disrupted in Vangl2 mutants by injecting Par3-RFP mosaically and measuring anterior-posterior Par3 ratios, or by using super-resolution microscopy on endogenous Par3.

In most polarized systems, Vangl2 and Par3 assume opposite cortical localization, like for example in the dividing Drosophila SOP (Bellaïche 2003). Intriguingly, Par3 and Vangl2 have also been found on the same side of the cell in Drosophila eye (Aigouy 2016), suggesting that their localization relative to each other must be regulated by unknown, cell-type-dependent mechanisms.

B) Formation and identity of Par3 patches at transverse membranes of FP cells

1) Formation of Par3 patches

We found that in FP cells, Par3, in addition to assuming a posterior enrichment, also forms patches, ie local accumulation, that are more conspicuous at early stages because of the absence of a continuous Par3 localization all around the apical junctions. Such Par3 patches, also called clusters or islands, have been identified in different normal or mutant situations and depend on the ability of Par3 to oligomerize via its CR1 domain (Harris 2017[318]). Such clustering is important for effective transport of PAR proteins to the anterior cortex of the C.elegans zygote by advection via cortical acto-myosin flow (Dickinson 2017[11]). In addition, Par3 asymmetric enrichment is also preceded by patches/islands formation in S2 cells artificially polarizing following Par3 over-expression as mentionned earlier (Kono 2019[313]). Thus, Par3 clustering could be a general requirement for effective asymmetric Par3 localization.
Interestingly, puncta formation has also been observed for core PCP proteins and correlate with the establishment of their asymmetric localization (Strutt 2016[78]). In addition, asymmetry within these puncta is greater than in other junctional regions (Strutt 2011[79], Cho 2015[319]). Core PCP proteins are highly stable within these puncta (Strutt 2011, Chien 2015[104]). These observations led Strutt et al. to hypothesize that the feedback interactions establishing asymmetric localization of PCP proteins act locally at membrane subdomains (Strutt 2016). This could be another shared feature between classical core PCP proteins and Par3.

In addition to the CR1 domain of Par3, cytoskeletal elements seem to play an important role in Par3 clustering: Kono et al. show that myosin inhibition does not affect Par3 islands formation, whereas disrupting actin with latrunculin B lead to changes in islands shape (Kono 2019). Actin is well known for regulating E-Cadherin clusters number, size, mobility and composition turnover and it could be that the

effect of actin on Par3 patch is indirect via E-cadherin since Par3 functions downstream of E-Cadherins in Drosophila male germline stem cells (Inaba 2015[190]).

Interestingly, in Drosophila *aPKC* loss-of-function mutants, Par3 forms planar polarized hyper-clusters along the anterior-posterior axis of the embryonic ectodermal epithelium: this is associated with a failure of apico-basally oriented microtubules to dissociate from apical centrosomes and an abnormal docking of centrosome to Par3 hyper-clusters (Harris 2007[320], Jiang 2015[27]). In this system, actin tends to inhibit Par3 hyper-clustering and antagonizes microtubules that tend to promote it: this balance allows the formation of isotropic adherens junctions and is important for epithelial mechanical stability (Harris 2007). The interaction between Par3 and the centrosome has been proposed to constitute a positive feedback loop, promoting Par3 hyperclustering and recruiting the centrosome at these patches. A similar situtation can be found in Drosophila male germline, where Par3 patches on E-Cadherin-enriched membranes - at the junction between germline stem cells (GSCs) and hub cells - recruits the centrosome from GSCs (Inaba 2015).

In the FP, nothing is known about the mechanisms leading to Par3 patch formation. It will be interesting to test whether it relies on antagonistic distribution of acto-myosin and microtubules and if Par3 clusters correlate with sites of cadherin enrichment.

2) Identity of Par3 patches: are they nascent adherens junctions ?

Par3 is a major player in the formation of apical junctions. It has been shown to be recruited to cell-cell contacts via its interaction with JAM adhesion molecules (Itoh 2001[321], Ebnet 2001[17], Ebnet 2003[18]) or Nectin (Takekuni 2003[19]). Par3 can then regulate tight junction formation by controling Rac activity via Tiam1 (a Rac-GEF) in MDCK cells (Chen 2005[322]). Par3 also regulates both adherens junction and tight junction formation in MDCK cells in part by promoting afadin recruitment via nectin (Ooshio 2007[323]). Afadin is an F-actin binding protein localized at adherens junctions and essential for their formation (Ikeda 1999[324]). In Drosophila embryos, Par3 functions in apical junction formation by promoting the repositioning of apical

Cadherin-catenin clusters at apico-lateral sites for full spot junction assembly, corresponding to the first step of adherens junction formation (McGill 2009[325]). These spot adherens junctions then turn into mature continuous adherens belt as gastrulation procedes (Harris 2012[326]).

Par3 patches have been shown to colocalize with E-cadherin patches at spot adherens junctions during their formation in a wt context (Harris & Peifer 2004[327]) but also colocalize with E-Cadherin and Armadillo (Drosophila beta-catenin) when forming hyper-clusters in *aPKC* loss-of-function mutants (Jiang 2015[27]). Interestingly, in Drosophila male GSCs, Par3 patches forming at the GSC/hub interface are narrower than the full length of cell/cell contact marked by E-Cadh, which thus does not fully colocalize with Par3: however, E-Cadherin is required for Par3 cortical recruitment and patch formation, as a dominant negative E-Cadherin lacking its extracellular domain can trigger the formation of ectopic Par3 patches and loss of E-Cadherin leads to loss of Par3 patches (Inaba 2015[190]). In Drosophila embryos, E-Cadherin also seems to interact, directly or indirectly, with Par3 (Harris 2005[328]).

Thus it is likely that Par3 patches that we observe in the FP at early stages, with which BBs make exclusive contacts, represent nascent apical junctions: in order to confirm this hypothesis, it will be important to investigate whether junctional proteins such as E-Cadherins and alpha/beta/p120 catenins colocalize with Par3 at these patches.
An interesting possibility is that BB recurrent contacts with these spot junctions and potential associated microtubules could contribute to patch maturation and local cortical stiffening (in cooperation with actomyosin, see below): a force between the BB and the patch would then not result in membrane deformation and invagination formation but in the movement of BB toward the « rigid » mature patch.

C) Significance of membrane invaginations between transverse membranes and BBs

We observed membrane invaginations extending mainly from the posterior membrane to the BB in FP cells. Their presence is probably a consequence of the forces that are exerted on the BB during polarization. Indeed, such invaginations have been witnessed in the C.elegans zygote where they correspond to sites of force generation at the cortex that allow asymmetric spindle positioning (Redemann 2010[329]). In this system, invaginations extend from the posterior cortex toward the posterior centrosome and their formation depends on microtubules and dynein, which are required for exerting pulling forces on the spindle (Couwenbergs 2007[330]). However, they are very rare in a wt context (3.4 posterior invaginations per embryo in average); softening the cell cortex by non-muscle myosin II depletion or actin disruption leads to a 10-fold increase in the number of these invaginations (42 posterior invaginations per embryo in average), underlining the influence of cortical tension on their formation. The fact that invaginations are rarely seen at late stages in FP cells compared to early stages could be a consequence of the increase of cortical stiffness during development, as the apical junctions mature and get stronger. Interestingly, it has been proposed that a softer deformable cortex permits a longer association between force generators and microtubules thus providing sustained pulling forces on the microtubules (Kozlowski 2007[331]): in FP cells, the longer life-time of invaginations compared to those seen in C.elegans zygote (medians of 5 min versus 1.8 s respectively) could lead to generation of higher pulling forces that would bring the BB in contact with the posterior membrane. However, the limited time-resolution in our movies probably leads us to over-estimate invagination lifetime. It would be interesting to measure this more precisely by doing live-imaging with higher temporal resolution.

Membrane invaginations have also been seen in immune synapse formation: in around 8% of lymphocyte/target cells pairs in vitro, the centrosome seemed to stay stucked behind the nucleus, and a membrane invagination, composed of the

membrane of both cells, extended from the centrosome to the center of the immune synapse, where the centrosome is normally relocalized (Yi 2013[250]).

Finally, a recent study in *Ciona intestinalis* embryos uncovered membrane invaginations between centrosomes and the posterior apical membrane in epidermal cells prior to the last division (the 11 th division) which is the first to be oriented along the A/P axis. Microtubules are required for the formation of these invaginations, and laser ablation experiments show that they are under tension and could contribute to centrosome positioning to orient cell division along the antero-posterior axis (Negishi 2016[332]) and to properly position the nucleus and centrosome at the posterior pole.

Although evidence is still lacking, this last study suggests the interesting possibility that these invaginations are not only passive manifestations of forces beeing exerted between centrosome/BB and the cell cortex, but could also play an active role in centrosome positioning; indeed, membrane invaginations form between leader and follower cells during collective endothelial cell migration and contribute to the strengthening of adhesion between those cells. Membrane curvature at these invagination sites is sensed by Pacsin2, a protein of the BAR-domain protein family whose members can sense and are recruited to curved membranes (Simunovic 2015[333]). Pacsin2 then inhibits E-Cadherin endocytosis, leading to cell-cell junction strengthening (Dorland 2016[334]).

In the context of centrosome/BB positioning, one can hypothesize that junction reinforcement via BAR-domain proteins-mediated cadherin enrichment at invagination sites could allow the forces exerted between BB and cell-cell junction to bring them together efficiently, instead of leading to membrane invagination formation.

In FP cells, the nature of these protrusions is unknown. In most cases, such as filopodia or cytonemes, membrane invaginations are filled with actin filaments (Yamashita 2018[335]). However in rare cases, membrane invaginations have been found to contain microtubules: this is the case for nanotubes forming between Drosophila male germ stem cells and their niche that mediate BMP signaling (Inaba 2015b[336]). Interestingly, Par3 patches recruiting the centrosome have been found at the exact same cell-cell interface by the same group, as mentionned earlier (Inaba

2015a[190]), supporting the hypothesis that Par3 could contribute to the formation of these invaginations. The situation is less clear in the ascidian embryo, where EB3 comets enter the invaginations but no microtubules were observed using TEM on fixed embryos (Negishi 2016[332]).

Thus, membrane invaginations in FP cells could contribute to BB positioning and are probably a consequence of forces that are exerted between BBs and Par3 patches at transverse membranes. This raises the question of the nature and localization of these potential force generators.

D) Nature and localization of force generators in FP cells

Centrosome/BB positioning in most systems studied so far depend on forces exerted via microtubules, although actin and myosin also play a role in some systems. In the FP, our data do not support a role for acto-myosin in BB positioning. In addition, a recent study showed that maintaining BB at the posterior membrane of FP cells at later stages requires an intact microtubule network (Mathewson 2019[103]). It is therefore likely that forces exerted on the BB are transmited via microtubules in this system. Microtubule dynamics could be regulated at the Par3 patches from which membrane invaginations originate. They could also be exerted from polarized structures in the vicinity of the BB, such as the basal foot or the rootlet (although in this case a cue at the posterior membrane would still be needed to orient the force). Here I discuss some potential mechanisms that could exert forces on BBs via microtubules or actin.

1) Microtubule-dependent force generation

Microtubules could be anchored at the BB and at transverse membranes and then exert forces on the BB either by being depolymerized, generating a pulling force, or by polymerizing, generating a pushing force on the BB. Here I discuss candidate

molecules that could be involved in such microtubule dynamics regulation both next to BB and at posterior apical junctions.

a) Potential regulators of microtubules at BB appendages

- On the rootlet/anterior side of BB

We found that the focal adhesion protein Paxillin localizes in a polarized fashion at the anterior side of the BB in FP cells. Paxillin, along with Vinculin and FAK, has been found at BBs in multi-ciliated cells and serves to anchor the BB to the apical actin network, forming so called 'ciliary adhesions' important for BB migration, docking, and spacing as shown in a morpholino-based knock-down study (Antoniades 2014[337]). It could also be the case in FP cells.

Since paxillin has been documented to stimulate microtubule catastrophes at focal adhesions in migrating fibroblasts, perhaps by serving as a scaffold for microtubule depolymerizing proteins (Efimov 2008[338]), paxillin could help position the BB by stimulating microtubule catastrophe on the anterior side of BBs, only allowing microtubules to grow from the other side of the BB. Coupled to microtubule-based pulling forces on the BB, this would then lead to its off-centering, rather than the centering observed in systems where microtubules are nucleated all around the centrosome (Laan 2012[224]). Live-imaging of FP cells expressing doublecortin-GFP and Paxillin-RFP, tools that are available in our lab, would help us to test this hypothesis.

- On the basal foot/posterior side of BB

Microtubule regulation at the basal-foot could also play a role in BB posterior positioning. We found that at late stages (16-18s), FP cells present a ciliary rootlet that points toward the anterior of the embryo, and thus it is very likely that the basal foot, as observed in many epithelia with motile cilia, would be localized on the other side, between the BB and the posterior membrane.

The basal foot can serve as a microtubule organizing center and gamma-tubulin has indeed been found to localize at the basal foot of oviduct ciliated cells (Hagiwara 2000[339]). Microtubules nucleated at the basal foot can form apico-basal bundles that

contribute to the organization and stabilization of cilia in mouse tracheal epithelial cells (Clare 2014[340]). Microtubules emanating from the basal foot can also extend to the plasma membrane in these same cells (Vladar 2012[74]). Microtubules contribute to ciliated cell rotational polarization (orientation of ciliary beating) in several systems (Werner 2011[278], Vladar 2012) and one can hypothesize that microtubules nucleated at the basal foot play a major role in this process.

In the FP, microtubules nucleated at the basal foot and pointing toward Par3 patches could be captured at the level of patches : microtubule anchoring at the basal foot and patch, coupled to microtubule depolymerization (either at the basal foot or at the patch) could then lead to BB pulling. Here again, live-imaging of FP cells expressing centrosome and microtubule markers will help us to test this hypothesis.

b) Potential regulators of microtubules at Par3 patches

- Microtubule capture at the posterior membrane by dynein

A major regulator of centrosome positioning is the microtubule-associated motor dynein. This minus-end directed motor can exert pulling forces on microtubules that can be transmitted to the centrosome/BB. When linked to the walls of microfabricated chambers containing microtubules and a centrosome, dynein can trigger centrosome centering (Laan 2012). In addition, its activation by micro-beads is sufficient to exert force and to off-center the mitotic spindle in the sea-urchin zygote, leading to the formation of daughter cells with different sizes (Sallé 2018[341]). A less spectacular off-centering of the spindle is also dependent on dynein before the first asymmetric division of the *C. elegans* zygote (Couwenbergs 2007[330]). Dynein-based microtubule pulling can in addition orient the mitotic spindle in Drosophila neuroblasts and SOP.

In the FP, Par3 could directly recruit Dynein to the posterior side. Indeed, Par3 interacts directly with dynein LIC2 (Light Intermediate Chain 2) at cell-cell contacts of migrating fibroblasts in wound-healing assays, which contributes to the maintenance of the centrosome at the cell centroid (Schmoranzer 2009[62]). Par3 also promotes

centrosome movement toward the immunological synapse of B lymphocytes by facilitating local dynein recruitment at the synapse (Reversat 2015[249]).

Alternatively, posterior Par3 could recruit dynein indirectly. During asymmetric and/or oriented cell division, a conserved set of molecules have been shown to recruit dynein to the cortex (see introduction). This depends on the adaptor molecules Mud/NuMA, that can interact with and regulate the dynactin/dynein complex (cf introduction and Morin 2011[342]). NuMA can be recruited by Par3 at the cortex indirectly via Insc and Pins in Drosophila neuroblasts (Schober 1999[343]). In the FP, previous unpublished preliminary results from our lab using a NuMA-GFP fusion protein could only detect NuMA in nuclei of interphasic cells and at spindle poles of dividing cells but not at the transverse membranes. It would still be interesting to investigate further its localization in the FP, especially at early stages to see if it colocalizes with Par3 patches. Alternatively, NuMA could be recruited there via Fz and Dvl, which probably localize at the posterior side of FP cells, opposite to Vangl2. Fzd3a-GFP localizes at the posterior apical side of FP cells, but seems to be present within the apical surface and not at the apical posterior membrane (Mathewson 2019[103]); the localization of endogenous Fzd or Dvl proteins in the FP is still unknown.

- Microtubule capture at the posterior membrane by (+)TIPs

Many microtubule (+) ends interacting proteins (+TIPs) have been shown to regulate microtubule dynamics at the cell cortex, both at cell-cell adhesion sites and at focal adhesions (Akhmanova 2009[344]). For example, APC is recruited at GSC/hub adhesion sites in the Drosophila germline and orients the spindle orthogonal to the junction via anchoring astral microtubules, downstream of E-cadherins (Inaba 2010[229]). Supporting these results, cadherins can stabilize microtubules in cultured cells (Chausovsky 2000[345]) and APC binding to microtubule (+) ends is important for cell polarization of migrating astrocytes (Etienne-Manneville 2005[55]). Another (+)TIP, CLIP-170, is recruited by IQGAP1 downstream of Rac1 and Cdc42 at the cell cortex in migrating cells and is required for directional cell migration (Fukata 2002[346]).

Finally, CLASP1 and CLASP2 can bind to EB1 and regulate microtubule dynamics at the cortex in cultured cells (Mimori-Kiyosue 2005[347]).

These studies underline the ability of microtubules to be captured at cell-cell junctions. Interestingly, EB3 (a (+)TIP) is enriched at the cortex in mouse ependymal multiciliated cells on the side toward which the cilia cluster is off-centered (Boutin 2014[348]), suggesting that microtubule capture at the cortex could play a role in the translational polarization of these cells. In the FP, our preliminary experiments at late FP polarisation-stage showed that EB3 was enriched posteriorly in polarized cells. It is likely that the strong EB3 accumulation I observed corresponds to the BB. One cell seemed to have a median BB and a posterior EB3 enrichment. It will be important to confirm this result, by looking for more unpolarized cells at earlier stages.

In order to exert a pulling force on BB, this microtubule cortical capture by dynein and/or (+)TIPs would need to be coupled to microtubule depolymerization at the BB (cf above) and/or at the cortex, as discussed below.

- <u>Localized microtubule depolymerization by kinesins or Rac1</u>

Microtubule depolymerizing kinesin-13 family proteins are good candidates for triggering microtubule depolymerization at the cortex, as they have been shown to mediate pulling forces on astral microtubules at the ascidian centrosome attracting body (CAB), which allow unequal cell division (Costache 2017[349]). However in the FP, we could only detect kinesin-13 proteins (with Kif2A,B and C antibodies) at the base of cilia, where they have been shown to regulate ciliogenesis (Miyamoto 2015[350]).

Alternatively, Par3 could promote microtubule catastrophe by locally inhibiting Rac1 activity via a RacGEF (Trio) inhibition as shown in neural crest cells, where this mechanism allows contact inhibition of locomotion (Moore 2013[61]). How Rac1 inhibition can increase microtubule catastrophe rate in this system is unknown, but in migrating cells in culture, Rac1 and Pak can inhibit stathmin, a microtubule depolymerization-promoting protein (Wittmann 2003[351]).

2) Acto-myosin–dependent force generation

Actin is involved in BB positioning in several systems. In addition to its role in BB apical docking (Boisvieux-Ulrich 1990[251], Dawe 2006[352], Mahuzier 2018[310]), actin distribution around the BB is required for their proper spacing within the apical surface (Werner 2011[278]) and BB/cilia mechanical stability (Antoniades 2014[337], Mahuzier, 2018). Some evidence suggests that actin and myosin are involved in planar BB positioning.

a) Potential role of Non-muscle-myosin II

Non-muscle myosin II (NMII) is required for asymmetric positioning of BB clusters within mouse ependymal multi-ciliated cells (Hirota 2010[271]). In zebrafish FP cells, I found that NMIIB is localized next to the BB, in a polarized fashion, opposite to the rootlet, at a position where we would expect to find the basal foot.

NMIIB is known to cooperate with NMIIA in cell migration. These two myosins have different properties, which participate in their segregation inside migrating cells (Shutova 2017[353]). NMIIB has a higher duty ratio (fraction of time of the myosin cycle spent attached to actin filaments) (Wang 2003[354]) and is therefore able to exert tension on actin filaments for longer periods of time (Vicente-Manzanares 2009[355]).

In migrating cells NMIIA controls the size of adhesions at the center of the cell and adhesion dissasembly at the rear, whereas NMIIB establishes front-back polarity and centrosome-Golgi-nucleus orientation (Vicente-Manzanares 2007[356]). NMIIA and NMIIB also have important non-redondant roles in apical junction maintenance (Smutny 2010[357]). However, both in migrating cells and at epithelial cell apical junctions, NMIIA and NMIIB have been found to localize at the cell cortex or on cytoplasmic stress fibers, not at the BB. It will thus be important to confirm NMIIB localization in the FP with other antibodies or fusion proteins, and to investigate if this localization indeed corresponds to the basal-foot (for example with ODF2 immunostaining, a basal foot marker).

In contrast to what has been found in mouse ependymal cells, our different drug treatments do not support a role for acto-myosin contraction in FP translational

polarity. Although these results would need further confirmation, for example by disrupting NMIIB function with genetic tools, this suggests that NMIIB is not required for BB positionning in FP cells.

What could be the function of NMIIB at the BB? A first possibility could be that the BB Myosin II pool plays a role in BB apical anchoring, as has been proposed by Lemullois et al. who also found myosin at centrioles and basal feet of quail oviduct BBs (Lemullois 1987). However, in the FP, we reproducibly detect NMIIB at BB only after the 9s stage, while BB are already apically positioned at the 2-3 somites stages (Sepich 2011[101] and our observations).

A second possibility would be that local contraction of actomyosin at the basal foot is responsible for the posterior tilting of FP cilia which is important for them to generate a directional CSF flow. We can test this hypothesis by live-imaging FP cells expressing Mb-Cherry and Arl13b-GFP (ciliary marker) in Blebbistatin-treated embryos.

Finally, a third possibility would be that NMIIB regulates vesicle trafficking between the cytoplasm and the axoneme and therefore cilia molecular composition. Supporting this hypothesis, a study looking for regulators of cilia composition in cultured cells found that depletion of NMIIB (via RNAi against myh10) inhibits Smoothened entry into cilia, a process required for proper hedgehog signaling (Kim 2010[358]). This is also consistent with the timing of apparition of NMIIB at the BB, since we rarely detect it before the 9 s stage, whereas it becomes stronger after this stage, at the same time as Smoothened becomes more strongly enriched in FP cilia (our experiments).

b) A permissive role for the actin network?

Studies in other systems rather point to a permissive role of actin in BB off-centering : local asymmetric depletion of Arp2/3 at immune cells centrosome allow its detachment from the nucleus and migration to the immune synapse (Obino 2016[359]). More recently, a study in the Drosophila wing, where centrioles are off-centered toward the distal part of the wing (at the base of the trichome), showed that actin is required but not sufficient for centriole off-centering and that an unknown pathway,

downstream of PCP proteins and independent of actin, is responsible for this off-centering (Garrido-Jimenez 2018[360]). It will be interesting to test whether in this system local planar polarized accumulation of Par3 is involved in the process similar to what we found in the FP, and whether microtubules are involved.

Interestingly, it has recently been found that centrosomes are actin-organizing centers (Farina 2015[361]) and that actin density around centrosomes can regulate microtubule nucleation (Inoue 2019[362]). This could in part explain the permissive role of actin in centrosome positioning. Thus, in the context of FP polarization, it will be interesting to investigate apical actin network dynamics during polarization with tools such as Lifeact-mCherry to see whether BB movements correlate with apical actin network remodeling. It will also be important to test whether actin-disrupting drugs such as cytochalasinD can prevent BB posterior positioning similar to what is known in the Drosophila wing (Garrido-Jimenez 2018).

Overall, my work suggests the following model for FP polarization: the PCP pathway through Vangl2 and Dvl is required to establish and maintain an asymmetric posterior enrichment of Par3 at nascent adhesion junctions, which likely exerts forces on the BB via microtubules linking the basal foot to the posterior membrane. It will be interesting to test if this mechanism is conserved across metazoan by investigating Par3 localization and function in Ascidian embryos (at the 11th division), Drosophila wing, mouse embryonic node and gastrulating jellyfish embryos (*Clytia hemisphaerica*) since in all these cellular systems, the Wnt-PCP system is active and centrioles are off-centered opposite to Vang/Vangl.

MATERIAL and METHODS

Experimental model and subject details

Zebrafish

Wild-type and mutant zebrafish embryos were obtained by natural spawning. To collect early stages embryos (4-8s), we incubated them from 10 am to for 9 pm in a 33°C incubator. To obtain later stages embryos (14-20s), we incubated them for 2 h at 28 °C before placing them overnight in a 24 °C incubator.
All our experiments were made in agreement with the european Directive 210/63/EU on the protection of animals used for scientific purposes, and the french application decree 'Décret 2013-118'. The projects of our group have been approved by our local ethical committee 'Comité d'éthique Charles Darwin'. The authorisation number is 2015051912122771 v7 (APAFIS#957). The fish facility has been approved by the French 'Service for animal protection and health', with the approval number A-75-05-25.

Clytia hemisphaerica

Wild type laboratory strains of Clytia hemisphaerica Z4B (female) and Z10 (male) were used. All stages are maintained at 19~21 °C in artificial sea water (RedSea salt) dissolved to 37‰ with appropriate water circulation for the jellyfish stage. Artemia salina nauplii larvae (1~4 days after hatching) were used for daily feeding.

Method details

Transgenic line generation

A stable NetKalTA4 was generated by injecting at the 1 cell stage. 15pg of pNetKal4 plasmid along with 20pg of Tol2 mRNA. To build the pNetKal4 plasmid, a 1.4kb fragment from pCS2+Kal4 comprising the KalTA4 promoter was amplified using the Kal4-forward and Kal4-reverse primers, then digested with XhoI and NotI and ligated with a XhoI/NotI-digested netrinTKmCherry Tol2 plasmid.

mRNA injection into zebrafish eggs.

mRNAs were synthesised from linearised pCS2 vectors using the mMESSAGE MACHINE SP6 transcription kit (Ambion). The following amounts of mRNA were injected into one-cell stage embryos: 22pg for Centrin-GFP, 40 pg for mbCherry (membrane Cherry) or Membrane-GFP (Gap43-GFP). For Par3-RFP mosaic expression, mRNAs were injected at the 16 cell stage in a single balstomere, using 50pg for Par3-RFP live-imaging or 150pg Par3-RFP for over-expression experiments (the concentrations for Centrin-GFP and membrane-GFP mRNAs were the same as for one-cell stage injections).

Immunostaining

For immunostaining, embryos were fixed in Dent's fixative (80% Methanol, 20% DMSO) at 25°C for 2h, blocked in 5% goat serum, 1% bovine serum albumin and 0.3% triton in PBS for 1 h at room temperature and incubated overnight at 4 °C with primary antibodies and 2h at room temperature with secondary antibodies. The yolk was removed and the embryo mounted in Vectashield medium on a slide. Imaging was done using a Leica TCS SP5 AOBS upright confocal microscope using a 63X oil lens.

Live imaging.

Embryos were dechorionated manually and mounted in 0.5% low-melting agarose in E3

medium. Movies were recorded at the temperature of the imaging facility room (22 °C) on a Leica TCS SP5 AOBS upright confocal microscope using a 63X (NA 0.9) water immersion lens.

Basal-bodies movements and basal-bodies tracking
Distance between BB and posterior membrane in FP was measured manually at each time-frame. The results were then plotted using python matplotlib and analyzed with a custom python script to extract relevant information such as the frequency of contact with posterior membrane or percentage of total time spent in contact with posterior membrane. BB detection and tracking was done with the TrackMate plugin in FIJI

Par3-RFP posterior/anterior ratio
Fluorescence intensity was measured along the anterior-posterior length of isolated FP cells in FIJI. A custom python script was then used to extract the first quarter (cell anterior side) and last quarter (cell posterior side) of fluorescence intensity values, to determine the area under each curve (corresponding to fluorescence intensity), calculate the post/ant ratio and plot it along with the polarization index (see BB movements analysis section).

Par3 peaks quantification
Fluorescence intensity from immunostained embryos was measured along FP cells transverse membranes and exported to Matlab where the findpeaks function was used to detect Par3 peaks and measure their prominence.

Quantification and statistical analysis
All bar-plots, boxplots and violin plots and statistical tests were generated with R and Rstudio.

Clytia Cherpgrip cloning and Clytia injections of mRNA and Morpholinos
Cherpgrip was amplified by PCR form Clytia cDNA (gift of T.Momose, stage ?): using the CherpgripFOR and CherpgripREV primers and then cloned into a BamHI-digested pCS2+-MT. The Cherpgrip-myc cDNA digested out of pCS2+-MT with BamHI and StuI and cloned into a Clytia-specific pCX3 vector cut by BglII/EcoRV. 140pg of Cherpgrip-MT mRNA was injected into oocytes. Morpholinos (Genetools) were injected at a concentration of 1mM (MO1) or 0.75mM (MO2). After injection, oocytes were fertilized in vitro.

CRISPR/CAS9 in Clytia
gRNAs were bought from IDT, injected in embryos at x concentration along with Cas9 protein (concentration) as described previously (Momose et al. 2018). DNA was extracted form injected and non-injected embryos and gRNA efficiency tested with a T7 endonuclease assay. Efficient gRNAs were then injected along with Cas9 protein in embryos that were raised to the polyp stage and then sequenced to detect potential indels at the cut site.

Clytia immunostaining and embryo polarity analysis
Embryos were fixed either in 4% PFA overnight at 4°C (polarity quantification) or in Dent 2h at room temperature (25°C) (Par3 immunostaining). Following steps were identical to zebrafish embryos immunostaining steps. Cell boundaries and basal-bodies detection were done automatically in FIJI. Cell centroid and BB position were used to determine a BB/cell-center vector, its length and orientation relative to the oral-aboral axis for each cell.

Basal-bodies tracking at late stages in wt and Vangl2 mutants
BB detection and tracking was done with the TrackMate plugin in FIJI.

REAGENT or RESOURCE	SOURCE	IDENTIFIER
Antibodies		
Mouse monoclonal IgG2a anti-centrin (clone 20H5)	Merck Millipore	# 04-1624, RRID:AB_10563501
Mouse monoclonal IgG1 anti-ZO1 (clone ZO1-1A12)	Invitrogen	RRID: AB_2533147
Mouse monoclonal IgG2b anti-acetylated-tubulin (clone 6-B11-1)	Sigma-Aldrich	#T 6793 RRID: AB_477585
Rabbit polyclonal anti-Par3	Merck Millipore	#07-330 RRID:AB_11213581
Rabbit polyclonal anti-phosphorylated-Ser1085-Bazooka	Krahn et al. 2009 (Wodarz lab)	N/A
Rabbit polyclonal anti-DsRed	Takara	# 632496, RRID:AB_10013483
Mouse monoclonal IgG2b anti-Non-Muscle-MyosinIIB (clone A3)	Santa Cruz Biotechnology	sc-376942
Rabbit polyclonal anti-phospho-myosin light chain 2 (Thr18/Ser19)	Cell signaling technology	#3674
Rabbit polyclonal anti-Arl13b	Proteintech	# 17711-1-AP, RRID:AB_2060867
Mouse monoclonal anti-myc (clone 9E10)	Roche	# 11667149001, RRID:AB_390912
Mouse monoclonal IgG1 anti-Paxillin	BD Biosciences	Cat# 610051, RRID:AB_397463
Mouse monoclonal IgG1 anti-Gamma-tubulin	Sigma-Aldrich	# T6557, RRID:AB_477584
Goat anti-mouse IgG1 Alexa633	Molecular probes	# A-21126, RRID:AB_2535768
Goat anti-mouse IgG2a Alexa568	Molecular probes	# A-21134, RRID:AB_2535773
Goat anti-mouse IgG2a Alexa488	Molecular probes	# A-21131, RRID:AB_141618
Goat anti-mouse IgG2b Alexa633	Molecular probes	# A-21146, RRID:AB_2535782
Goat anti-rabbit IgG Alexa568	Molecular probes	# A-11011, RRID:AB_143157
Chemicals, Peptides, and Recombinant Proteins		
Blebbistatin	Sigma-Aldrich	B0560
ML7	Sigma-Aldrich	I2764
Rockout	Calbiochem	#555553
Methanol	VWR Chemicals	20847.295
DMSO	Sigma	D2650
Goat serum	Sigma	G6767
Bovine serum albumin	Sigma	A2153
Triton X100	Sigma	T8787
Vectashield	Vector Laboratories	H-1000
Critical Commercial Assays		

GoTaq flexi	Promega	M8291
InFusion HD cloning kit	Takara	
T7 endonuclease	NEB	M0302S
Deposited Data		
Experimental Models: Organisms/Strains		
zebrafish wild-type AB or (TL x AB) hybrid strains		
Zebrafish Vangm209 mutants	Driever 1996	ZDB-GENO-190204-5
Zebrafish Dvl2 mutants	Xing YY et al . PLoS Genet. 2018	
Zebrafish Par3ab fh305 mutants	Moens lab	ZDB-FISH-150901-20689
Clytia hemisphaerica wt	Cnidarian developmental mechanism lab, LBD Villefranche-sur-mer	
Oligonucleotides		
Kal4-forward	ATGCCTCGAGGCCACCATG	
Kal4-reverse	CGGTTACGTAACCCGGGCCAT	
Cherpgrip-MO1	AGTGTCTCTGGCTCCCATTTCAATC	
Cherpgrip-MO2	ACCAATTTTCATCTTTCTCATACGT	
Par3-MO	tcaaaggctcccgtgctctggtgtc	Wei et al. 2004[363]
CherpgripFOR	TCTTTTTGCAGGATCC GAGTAAGGATTGAAATGGGAGCCAGAGACA	
CherpgripREV	TAAATCGATGGGATCG TTCATACAGACTTTGAAGAGCATCGAGAGC	
tmRNA guide-RNA	ggttggctcattgtcaagga	IDT
adRNA10 guide-RNA	tgatagtttgcgtcatcagt	IDT
adRNA8 guide-RNA	gccaaagagcgtcaaatggttgg	IDT
Recombinant DNA		
pCS2-Membrane-Cherry	Megason et al. 2009	N/A
pCS2-GFPhumcentrin1	Pouthas et al. 2008	N/A
pCS2+-Par3-RFP	Paula Alexandre	N/A
pCS-Gap43-GFP	David Wilkinson	N/A
pT3TS/Tol2	Balciunas et al. 2006	N/A
pCS2+Kal4	Gerety et al. 2013	N/A
pNetrinTKmCherry	Our lab	N/A
pCS2+EB3-mKate2	Strzyz et al. 2015[364]	Addgene #105940
M2: #998 pSKH2B-mRFP:5xUAS:GFP-DCX-5xUAS:memCFP	Distel et al. 2010[365]	N/A

M3: #999 pSKH2B-mRFP:5xUAS:EB3-GFP-5xUAS:memCFP	Distel et al. 2010	N/A
pCS2+MycTag	Dave Turner lab	N/A
pCX3	Tsuyoshi Momose	N/A
Software and Algorithms		
Fiji/ImageJ	ImageJ	https://imagej.net/Fiji/Downloads
TrackMate	Tinevez et al. 2016	https://imagej.net/TrackMate
MATLAB R2018a	Mathworks	https://www.mathworks.com/downloads/
Python 2.7.13	Python Software Foundation	https://www.python.org/downloads/release/python-2713/
R studio Version 1.1.463	Rstudio	https://www.rstudio.com/
R version 3.3.2	The R Foundation for Statistical Computing	https://cran.r-project.org/bin/macosx/

BIBLIOGRAPHY

1. Macara, I. G. & Mili, S. Polarity and Differential Inheritance—Universal Attributes of Life? *Cell* **135**, 801–812 (2008).
2. Schenkelaars, Q., Fierro-Constain, L., Renard, E. & Borchiellini, C. Retracing the path of planar cell polarity. *BMC Evolutionary Biology* **16**, (2016).
3. Salinas-Saavedra, M., Rock, A. Q. & Martindale, M. Q. Germ layer-specific regulation of cell polarity and adhesion gives insight into the evolution of mesoderm. *eLife* **7**, e36740 (2018).
4. Zappaterra, M. W. & Lehtinen, M. K. The cerebrospinal fluid: regulator of neurogenesis, behavior, and beyond. *Cellular and Molecular Life Sciences* **69**, 2863–2878 (2012).
5. Kemphues, K. J., Priess, J. R., Morton, D. G. & Cheng, N. Identification of genes required for cytoplasmic localization in early C. elegans embryos. *Cell* **52**, 311–320 (1988).
6. Goldstein, B. & Macara, I. G. The PAR Proteins: Fundamental Players in Animal Cell Polarization. *Developmental Cell* **13**, 609–622 (2007).
7. Tabuse, Y. *et al.* Atypical protein kinase C cooperates with PAR-3 to establish embryonic polarity in Caenorhabditis elegans. 8
8. Munro, E., Nance, J. & Priess, J. R. Cortical Flows Powered by Asymmetrical Contraction Transport PAR Proteins to Establish and Maintain Anterior-Posterior Polarity in the Early C. elegans Embryo. *Developmental Cell* **7**, 413–424 (2004).
9. Motegi, F. & Sugimoto, A. Sequential functioning of the ECT-2 RhoGEF, RHO-1 and CDC-42 establishes cell polarity in Caenorhabditis elegans embryos. *Nature Cell Biology* **8**, 978–985 (2006).
10. Jenkins, N. CYK-4/GAP Provides a Localized Cue to Initiate Anteroposterior Polarity upon Fertilization. *Science* **313**, 1298–1301 (2006).
11. Dickinson, D. J., Schwager, F., Pintard, L., Gotta, M. & Goldstein, B. A Single-Cell Biochemistry Approach Reveals PAR Complex Dynamics during Cell Polarization. *Developmental Cell* **42**, 416-434.e11 (2017).
12. Motegi, F. *et al.* Microtubules induce self-organization of polarized PAR domains in Caenorhabditis elegans zygotes. *Nature Cell Biology* **13**, 1361–1367 (2011).
13. Rodriguez, J. *et al.* aPKC Cycles between Functionally Distinct PAR Protein Assemblies to Drive Cell Polarity. *Developmental Cell* (2017). doi:10.1016/j.devcel.2017.07.007
14. Hao, Y., Boyd, L. & Seydoux, G. Stabilization of Cell Polarity by the C. elegans RING Protein PAR-2. *Developmental Cell* **10**, 199–208 (2006).
15. Sailer, A., Anneken, A., Li, Y., Lee, S. & Munro, E. Dynamic Opposition of Clustered Proteins Stabilizes Cortical Polarity in the C. elegans Zygote. *Developmental Cell* **35**, 131–142 (2015).
16. Benton, R. & St Johnston, D. Drosophila PAR-1 and 14-3-3 inhibit Bazooka/PAR-3 to establish complementary cortical domains in polarized cells. *Cell* **115**, 691–704 (2003).
17. Ebnet, K. The cell polarity protein ASIP/PAR-3 directly associates with junctional adhesion molecule (JAM). *The EMBO Journal* **20**, 3738–3748 (2001).
18. Ebnet, K. The junctional adhesion molecule (JAM) family members JAM-2 and JAM-3 associate with the cell polarity protein PAR-3: a possible role for JAMs in endothelial cell polarity. *Journal of Cell Science* **116**, 3879–3891 (2003).
19. Takekuni, K. *et al.* Direct Binding of Cell Polarity Protein PAR-3 to Cell-Cell Adhesion Molecule Nectin at Neuroepithelial Cells of Developing Mouse. *Journal of Biological Chemistry* **278**, 5497–5500 (2003).
20. Fukuhara, T. *et al.* Activation of Cdc42 by trans interactions of the cell adhesion molecules nectins through c-Src and Cdc42-GEF FRG. *J Cell Biol* **166**, 393–405 (2004).
21. Yamada, S. & Nelson, W. J. Localized zones of Rho and Rac activities drive initiation and expansion of epithelial cell–cell adhesion. *J Cell Biol* **178**, 517–527 (2007).
22. Yamanaka, T. *et al.* Mammalian Lgl Forms a Protein Complex with PAR-6 and aPKC Independently of PAR-3 to Regulate Epithelial Cell Polarity. *Current Biology* **13**, 734–743 (2003).
23. Manninen, A. Epithelial polarity – Generating and integrating signals from the ECM with integrins. *Experimental Cell Research* **334**, 337–349 (2015).
24. Morais-de-Sá, E., Mirouse, V. & St Johnston, D. aPKC Phosphorylation of Bazooka Defines the Apical/Lateral Border in Drosophila Epithelial Cells. *Cell* **141**, 509–523 (2010).
25. Walther, R. F. & Pichaud, F. Crumbs/DaPKC-Dependent Apical Exclusion of Bazooka Promotes Photoreceptor Polarity Remodeling. *Current Biology* **20**, 1065–1074 (2010).
26. Hutterer, A., Betschinger, J., Petronczki, M. & Knoblich, J. A. Sequential Roles of Cdc42, Par-6, aPKC, and Lgl in the Establishment of Epithelial Polarity during Drosophila Embryogenesis. *Developmental Cell* **6**, 845–854 (2004).
27. Jiang, T., McKinley, R. F. A., McGill, M. A., Angers, S. & Harris, T. J. C. A Par-1-Par-3-Centrosome Cell Polarity Pathway and Its Tuning for Isotropic Cell Adhesion. *Current Biology* **25**, 2701–2708 (2015).
28. Bilder, D., Schober, M. & Perrimon, N. Integrated activity of PDZ protein complexes regulates epithelial polarity. *Nature Cell Biology* **5**, 53–58 (2003).
29. Tanentzapf, G. & Tepass, U. Interactions between the crumbs, lethal giant larvae and bazooka pathways in epithelial polarization. *Nature Cell Biology* **5**, 46–52 (2003).
30. Chen, X. & Macara, I. G. Par-3 controls tight junction assembly through the Rac exchange factor Tiam1. *Nature Cell Biology* **7**, 262–269 (2005).
31. Yamazaki, D. *et al.* Wave2 is required for directed cell migration and cardiovascular development. *Nature* 452–456 (2003).
32. Harris, T. J. C. & Peifer, M. The positioning and segregation of apical cues during epithelial polarity establishment in *Drosophila*. *The Journal of Cell Biology* **170**, 813–823 (2005).
33. Ahmed, S. M. & Macara, I. G. The Par3 polarity protein is an exocyst receptor essential for mammary cell survival. *Nature Communications* **8**, 14867 (2017).
34. Wirtz-Peitz, F., Nishimura, T. & Knoblich, J. A. Linking Cell Cycle to Asymmetric Division: Aurora-A Phosphorylates the Par Complex to Regulate Numb Localization. *Cell* **135**, 161–173 (2008).
35. Bellaïche, Y. *et al.* The Partner of Inscuteable/Discs-Large Complex Is Required to Establish Planar Polarity during Asymmetric Cell Division in Drosophila. *Cell* **106**, 355–366 (2001).
36. Guo, M., Jan, L. Y. & Jan, Y. N. Control of Daughter Cell Fates during Asymmetric Division: Interaction of Numb and Notch. 15
37. Betschinger, J., Mechtler, K. & Knoblich, J. A. The Par complex directs asymmetric cell division by phosphorylating the cytoskeletal protein Lgl. *Nature* **422**, 326–330 (2003).
38. Atwood, S. X. & Prehoda, K. E. aPKC Phosphorylates Miranda to Polarize Fate Determinants during Neuroblast Asymmetric Cell Division. *Current Biology* **19**, 723–729 (2009).
39. Smith, C. A. *et al.* aPKC-mediated phosphorylation regulates asymmetric membrane localization of the cell fate determinant Numb. *The EMBO Journal* **26**, 468–480 (2007).

40. Spana, E. P. & Doe, C. Q. Numb Antagonizes Notch Signaling to Specify Sibling Neuron Cell Fates. *Neuron* **17**, 21–26 (1996).
41. Alexandre, P., Reugels, A. M., Barker, D., Blanc, E. & Clarke, J. D. W. Neurons derive from the more apical daughter in asymmetric divisions in the zebrafish neural tube. *Nature Neuroscience* **13**, 673–679 (2010).
42. Ossipova, O., Ezan, J. & Sokol, S. Y. PAR-1 Phosphorylates Mind Bomb to Promote Vertebrate Neurogenesis. *Developmental Cell* **17**, 222–233 (2009).
43. Bowman, S. K., Neumüller, R. A., Novatchkova, M., Du, Q. & Knoblich, J. A. The Drosophila NuMA Homolog Mud Regulates Spindle Orientation in Asymmetric Cell Division. *Developmental Cell* **10**, 731–742 (2006).
44. Siegrist, S. E. & Doe, C. Q. Microtubule-Induced Pins/Gαi Cortical Polarity in Drosophila Neuroblasts. *Cell* **123**, 1323–1335 (2005).
45. Lu, M. S. & Prehoda, K. E. A NudE/14-3-3 Pathway Coordinates Dynein and the Kinesin Khc73 to Position the Mitotic Spindle. *Developmental Cell* **26**, 369–380 (2013).
46. Grill, S. W. The Distribution of Active Force Generators Controls Mitotic Spindle Position. *Science* **301**, 518–521 (2003).
47. Labbé, J.-C., McCarthy, E. K. & Goldstein, B. The forces that position a mitotic spindle asymmetrically are tethered until after the time of spindle assembly. *The Journal of Cell Biology* **167**, 245–256 (2004).
48. Srinivasan, D. G., Fisk, R. M., Xu, H. & Heuvel, S. van den. A complex of LIN-5 and GPR proteins regulates G protein signaling and spindle function in C. elegans. *Genes Dev.* **17**, 1225–1239 (2003).
49. Nguyen-Ngoc, T., Afshar, K. & Gönczy, P. Coupling of cortical dynein and Gα proteins mediates spindle positioning in Caenorhabditis elegans. *Nature Cell Biology* **9**, 1294–1302 (2007).
50. Sugioka, K. *et al.* Tumor suppressor APC is an attenuator of spindle-pulling forces during *C. elegans* asymmetric cell division. *Proceedings of the National Academy of Sciences* 201712052 (2018). doi:10.1073/pnas.1712052115
51. Lechler, T. & Fuchs, E. Asymmetric cell divisions promote stratification and differentiation of mammalian skin. *Nature* **437**, 275–280 (2005).
52. Williams, S. E., Beronja, S., Pasolli, H. A. & Fuchs, E. Asymmetric cell divisions promote Notch-dependent epidermal differentiation. *Nature* **470**, 353–358 (2011).
53. Williams, S. E., Ratliff, L. A., Postiglione, M. P., Knoblich, J. A. & Fuchs, E. Par3–mInsc and Gαi3 cooperate to promote oriented epidermal cell divisions through LGN. *Nature Cell Biology* **16**, 758–769 (2014).
54. Etienne-Manneville, S. & Hall, A. Cdc42 regulates GSK-3b and adenomatous polyposis coli to control cell polarity. *Nature* **421**, 748–753 (2003).
55. Etienne-Manneville, S., Manneville, J.-B., Nicholls, S., Ferenczi, M. A. & Hall, A. Cdc42 and Par6–PKCζ regulate the spatially localized association of Dlg1 and APC to control cell polarization. *The Journal of Cell Biology* **170**, 895–901 (2005).
56. Dow, L. E. *et al.* The tumour-suppressor Scribble dictates cell polarity during directed epithelial migration: regulation of Rho GTPase recruitment to the leading edge. *Oncogene* **26**, 2272–2282 (2007).
57. Pegtel, D. M. *et al.* The Par-Tiam1 Complex Controls Persistent Migration by Stabilizing Microtubule-Dependent Front-Rear Polarity. *Current Biology* **17**, 1623–1634 (2007).
58. Nishimura, T. & Kaibuchi, K. Numb Controls Integrin Endocytosis for Directional Cell Migration with aPKC and PAR-3. *Developmental Cell* **13**, 15–28 (2007).
59. Etienne-Manneville, S. & Hall, A. Integrin-Mediated Activation of Cdc42 Controls Cell Polarity in Migrating Astrocytes through PKC□. 10
60. Carmona-Fontaine, C. *et al.* Contact inhibition of locomotion in vivo controls neural crest directional migration. *Nature* **456**, 957–961 (2008).
61. Moore, R. *et al.* Par3 controls neural crest migration by promoting microtubule catastrophe during contact inhibition of locomotion. *Development* **140**, 4763–4775 (2013).
62. Schmoranzer, J. *et al.* Par3 and Dynein Associate to Regulate Local Microtubule Dynamics and Centrosome Orientation during Migration. *Current Biology* **19**, 1065–1074 (2009).
63. Chen, S. *et al.* Regulation of Microtubule Stability and Organization by Mammalian Par3 in Specifying Neuronal Polarity. *Developmental Cell* **24**, 26–40 (2013).
64. Aw, W. Y., Heck, B. W., Joyce, B. & Devenport, D. Transient Tissue-Scale Deformation Coordinates Alignment of Planar Cell Polarity Junctions in the Mammalian Skin. *Current Biology* **26**, 2090–2100 (2016).
65. Wang, J. *et al.* Regulation of polarized extension and planar cell polarity in the cochlea by the vertebrate PCP pathway. *Nature Genetics* **37**, 980–985 (2005).
66. Wang, J. Dishevelled genes mediate a conserved mammalian PCP pathway to regulate convergent extension during neurulation. *Development* **133**, 1767–1778 (2006).
67. Wang, Y. The Role of Frizzled3 and Frizzled6 in Neural Tube Closure and in the Planar Polarity of Inner-Ear Sensory Hair Cells. *Journal of Neuroscience* **26**, 2147–2156 (2006).
68. Montcouquiol, M. Asymmetric Localization of Vangl2 and Fz3 Indicate Novel Mechanisms for Planar Cell Polarity in Mammals. *Journal of Neuroscience* **26**, 5265–5275 (2006).
69. Deans, M. R. *et al.* Asymmetric Distribution of Prickle-Like 2 Reveals an Early Underlying Polarization of Vestibular Sensory Epithelia in the Inner Ear. *Journal of Neuroscience* **27**, 3139–3147 (2007).
70. Song, H. *et al.* Planar cell polarity breaks bilateral symmetry by controlling ciliary positioning. *Nature* **466**, 378–382 (2010).
71. Devenport, D. & Fuchs, E. Planar polarization in embryonic epidermis orchestrates global asymmetric morphogenesis of hair follicles. *Nature Cell Biology* **10**, 1257–1268 (2008).
72. Devenport, D., Oristian, D., Heller, E. & Fuchs, E. Mitotic internalization of planar cell polarity proteins preserves tissue polarity. *Nature Cell Biology* **13**, 893–902 (2011).
73. Tissir, F. *et al.* Lack of cadherins Celsr2 and Celsr3 impairs ependymal ciliogenesis, leading to fatal hydrocephalus. *Nature Neuroscience* **13**, 700–707 (2010).
74. Vladar, E. K., Bayly, R. D., Sangoram, A. M., Scott, M. P. & Axelrod, J. D. Microtubules Enable the Planar Cell Polarity of Airway Cilia. *Current Biology* **22**, 2203–2212 (2012).
75. Chen, W.-S. *et al.* Asymmetric Homotypic Interactions of the Atypical Cadherin Flamingo Mediate Intercellular Polarity Signaling. *Cell* **133**, 1093–1105 (2008).
76. Strutt, H. & Strutt, D. Differential Stability of Flamingo Protein Complexes Underlies the Establishment of Planar Polarity. *Current Biology* **18**, 1555–1564 (2008).
77. Wu, J. & Mlodzik, M. The Frizzled Extracellular Domain Is a Ligand for Van Gogh/Stbm during Nonautonomous Planar Cell Polarity Signaling. *Developmental Cell* **15**, 462–469 (2008).
78. Strutt, H., Gamage, J. & Strutt, D. Robust Asymmetric Localization of Planar Polarity Proteins Is Associated with Organization into Signalosome-like Domains of Variable Stoichiometry. *Cell Reports* **17**, 2660–2671 (2016).
79. Strutt, H., Warrington, S. J. & Strutt, D. Dynamics of Core Planar Polarity Protein Turnover and Stable Assembly into Discrete Membrane Subdomains. *Developmental Cell* **20**, 511–525 (2011).
80. Usui, T. *et al.* Flamingo, a Seven-Pass Transmembrane Cadherin, Regulates Planar Cell Polarity under the Control of Frizzled. *Cell* **98**, 585–595 (1999).
81. Warrington, S. J., Strutt, H., Fisher, K. H. & Strutt, D. A Dual Function for Prickle in Regulating Frizzled Stability during

Feedback-Dependent Amplification of Planar Polarity. *Current Biology* (2017). doi:10.1016/j.cub.2017.08.016
82. Jenny, A. Prickle and Strabismus form a functional complex to generate a correct axis during planar cell polarity signaling. *The EMBO Journal* **22**, 4409–4420 (2003).
83. Butler, M. T. & Wallingford, J. B. Control of vertebrate core planar cell polarity protein localization and dynamics by Prickle 2. *Development* **142**, 3429–3439 (2015).
84. Jenny, A., Reynolds-Kenneally, J., Das, G., Burnett, M. & Mlodzik, M. Diego and Prickle regulate Frizzled planar cell polarity signalling by competing for Dishevelled binding. *Nature Cell Biology* **7**, 691–697 (2005).
85. Das, G. Diego interacts with Prickle and Strabismus/Van Gogh to localize planar cell polarity complexes. *Development* **131**, 4467–4476 (2004).
86. Kelly, L. K., Wu, J., Yanfeng, W. A. & Mlodzik, M. Frizzled-Induced Van Gogh Phosphorylation by CK1ε Promotes Asymmetric Localization of Core PCP Factors in Drosophila. *Cell Reports* **16**, 344–356 (2016).
87. Pfeffer, S. R. Rab GTPases: master regulators that establish the secretory and endocytic pathways. *Molecular Biology of the Cell* **28**, 712–715 (2017).
88. Mottola, G., Classen, A.-K., Gonzalez-Gaitan, M., Eaton, S. & Zerial, M. A novel function for the Rab5 effector Rabenosyn-5 in planar cell polarity. *Development* **137**, 2353–2364 (2010).
89. Classen, A.-K., Anderson, K. I., Marois, E. & Eaton, S. Hexagonal Packing of Drosophila Wing Epithelial Cells by the Planar Cell Polarity Pathway. *Developmental Cell* **9**, 805–817 (2005).
90. Cho, B., Pierre-Louis, G., Sagner, A., Eaton, S. & Axelrod, J. D. Clustering and Negative Feedback by Endocytosis in Planar Cell Polarity Signaling Is Modulated by Ubiquitinylation of Prickle. *PLOS Genetics* **11**, e1005259 (2015).
91. Yu, A. *et al.* Association of Dishevelled with the Clathrin AP-2 Adaptor Is Required for Frizzled Endocytosis and Planar Cell Polarity Signaling. *Developmental Cell* **12**, 129–141 (2007).
92. D'Souza-Schorey, C. & Chavrier, P. ARF proteins: roles in membrane traffic and beyond. *Nature Reviews Molecular Cell Biology* **7**, 347–358 (2006).
93. Guo, Y., Zanetti, G. & Schekman, R. A novel GTP-binding protein–adaptor protein complex responsible for export of Vangl2 from the trans Golgi network. *Elife* **2**, e00160 (2013).
94. Carvajal-Gonzalez, J. M. *et al.* The clathrin adaptor AP-1 complex and Arf1 regulate planar cell polarity in vivo. *Nature Communications* **6**, (2015).
95. Strutt, H. *et al.* Retromer Controls Planar Polarity Protein Levels and Asymmetric Localization at Intercellular Junctions. *Current Biology* (2019). doi:10.1016/j.cub.2018.12.027
96. Eaton, S., Wepf, R. & Simons, K. Roles for Rac1 and Cdc42 in planar polarization and hair outgrowth in the wing of Drosophila. *Journal of Cell Biology* **135**, 1277–1290 (1996).
97. Hannus, M. Planar cell polarization requires Widerborst, a B' regulatory subunit of protein phosphatase A. 11
98. Shimada, Y., Yonemura, S., Ohkura, H., Strutt, D. & Uemura, T. Polarized Transport of Frizzled along the Planar Microtubule Arrays in Drosophila Wing Epithelium. *Developmental Cell* **10**, 209–222 (2006).
99. Olofsson, J., Sharp, K. A., Matis, M., Cho, B. & Axelrod, J. D. Prickle/spiny-legs isoforms control the polarity of the apical microtubule network in planar cell polarity. *Development* **141**, 2866–2874 (2014).
100. Matis, M., Russler-Germain, D. A., Hu, Q., Tomlin, C. J. & Axelrod, J. D. Microtubules provide directional information for core PCP function. *eLife Sciences* **3**, e02893 (2014).
101. Sepich, D. S., Usmani, M., Pawlicki, S. & Solnica-Krezel, L. Wnt/PCP signaling controls intracellular position of MTOCs during gastrulation convergence and extension movements. *Development* **138**, 543–552 (2011).
102. Shi, D. *et al.* Dynamics of planar cell polarity protein Vangl2 in the mouse oviduct epithelium. *Mechanisms of Development* **141**, 78–89 (2016).
103. Mathewson, A. W., Berman, D. G. & Moens, C. B. Microtubules are required for the maintenance of planar cell polarity in monociliated floorplate cells. *Developmental Biology* (2019). doi:10.1016/j.ydbio.2019.04.007
104. Chien, Y.-H., Keller, R., Kintner, C. & Shook, D. R. Mechanical Strain Determines the Axis of Planar Polarity in Ciliated Epithelia. *Current Biology* **25**, 2774–2784 (2015).
105. Narimatsu, M. *et al.* Regulation of Planar Cell Polarity by Smurf Ubiquitin Ligases. *Cell* **137**, 295–307 (2009).
106. Strutt, H., Searle, E., Thomas-MacArthur, V., Brookfield, R. & Strutt, D. A Cul-3-BTB ubiquitylation pathway regulates junctional levels and asymmetry of core planar polarity proteins. *Development* **140**, 1693–1702 (2013).
107. Strutt, H., Thomas-MacArthur, V. & Strutt, D. Strabismus Promotes Recruitment and Degradation of Farnesylated Prickle in Drosophila melanogaster Planar Polarity Specification. *PLoS Genetics* **9**, e1003654 (2013).
108. Weber, U. & Mlodzik, M. APC/CFzr/Cdh1-Dependent Regulation of Planar Cell Polarity Establishment via Nek2 Kinase Acting on Dishevelled. *Developmental Cell* (2016). doi:10.1016/j.devcel.2016.12.006
109. Willecke, M., Hamaratoglu, F., Sansores-Garcia, L., Tao, C. & Halder, G. Boundaries of Dachsous Cadherin activity modulate the Hippo signaling pathway to induce cell proliferation. *Proceedings of the National Academy of Sciences* **105**, 14897–14902 (2008).
110. Hale, R., Brittle, A. L., Fisher, K. H., Monk, N. A. M. & Strutt, D. Cellular interpretation of the long-range gradient of Four-jointed activity in the Drosophila wing. *eLife Sciences* **4**, e05789 (2015).
111. Brittle, A., Thomas, C. & Strutt, D. Planar Polarity Specification through Asymmetric Subcellular Localization of Fat and Dachsous. *Current Biology* **22**, 907–914 (2012).
112. Ayukawa, T. *et al.* Dachsous-Dependent Asymmetric Localization of Spiny-Legs Determines Planar Cell Polarity Orientation in Drosophila. *Cell Reports* **8**, 610–621 (2014).
113. Harumoto, T. *et al.* Atypical Cadherins Dachsous and Fat Control Dynamics of Noncentrosomal Microtubules in Planar Cell Polarity. *Developmental Cell* **19**, 389–401 (2010).
114. Casal, J., Lawrence, P. A. & Struhl, G. Two separate molecular systems, Dachsous/Fat and Starry night/Frizzled, act independently to confer planar cell polarity. *Development* **133**, 4561–4572 (2006).
115. Saburi, S. *et al.* Loss of Fat4 disrupts PCP signaling and oriented cell division and leads to cystic kidney disease. *Nature Genetics* **40**, 1010–1015 (2008).
116. Mao, Y. *et al.* Dchs1–Fat4 regulation of polarized cell behaviours during skeletal morphogenesis. *Nature Communications* **7**, 11469 (2016).
117. Loh, K. M., van Amerongen, R. & Nusse, R. Generating Cellular Diversity and Spatial Form: Wnt Signaling and the Evolution of Multicellular Animals. *Developmental Cell* **38**, 643–655 (2016).
118. Martindale, M. Q. & Hejnol, A. A Developmental Perspective: Changes in the Position of the Blastopore during Bilaterian Evolution. *Developmental Cell* **17**, 162–174 (2009).
119. Stanganello, E. *et al.* Filopodia-based Wnt transport during vertebrate tissue patterning. *Nature Communications* **6**, 5846 (2015).
120. Habib, S. J. *et al.* A Localized Wnt Signal Orients Asymmetric Stem Cell Division in Vitro. *Science* **339**, 1445–1448 (2013).
121. Heisenberg, C.-P. *et al.* Silberblick/Wnt11 mediates convergent extension movements during zebra®sh gastrulation. **405**, 6 (2000).
122. Kilian, B. *et al.* The role of Ppt/Wnt5 in regulating cell shape and movement during zebrafish gastrulation. *Mechanisms of Development* **120**, 467–476 (2003).

123. Qian, D. *et al.* Wnt5a functions in planar cell polarity regulation in mice. *Developmental Biology* **306**, 121–133 (2007).
124. Hashimoto, M. *et al.* Planar polarization of node cells determines the rotational axis of node cilia. *Nature Cell Biology* **12**, 170–176 (2010).
125. Minegishi, K. *et al.* A Wnt5 Activity Asymmetry and Intercellular Signaling via PCP Proteins Polarize Node Cells for Left-Right Symmetry Breaking. *Developmental Cell* **40**, 439-452.e4 (2017).
126. Gao, B. *et al.* Wnt Signaling Gradients Establish Planar Cell Polarity by Inducing Vangl2 Phosphorylation through Ror2. *Developmental Cell* **20**, 163–176 (2011).
127. Chu, C.-W. & Sokol, S. Y. Wnt proteins can direct planar cell polarity in vertebrate ectoderm. *eLife* **5**, e16463 (2016).
128. Wu, J., Roman, A.-C., Carvajal-Gonzalez, J. M. & Mlodzik, M. Wg and Wnt4 provide long-range directional input to planar cell polarity orientation in Drosophila. *Nature Cell Biology* **15**, 1045–1055 (2013).
129. Aigouy, B. *et al.* Cell Flow Reorients the Axis of Planar Polarity in the Wing Epithelium of Drosophila. *Cell* **142**, 773–786 (2010).
130. Bosveld, F. *et al.* Mechanical Control of Morphogenesis by Fat/Dachsous/Four-Jointed Planar Cell Polarity Pathway. *Science* **336**, 724–727 (2012).
131. Chien, Y.-H., Srinivasan, S., Keller, R. & Kintner, C. Mechanical Strain Determines Cilia Length, Motility, and Planar Position in the Left-Right Organizer. *Developmental Cell* **45**, 316-330.e4 (2018).
132. Adler, P. N., Zhu, C. & Stone, D. Inturned Localizes to the Proximal Side of Wing Cells under the Instruction of Upstream Planar Polarity Proteins. *Current Biology* **14**, 2046–2051 (2004).
133. Strutt, D. & Warrington, S. J. Planar polarity genes in the Drosophila wing regulate the localisation of the FH3-domain protein Multiple Wing Hairs to control the site of hair production. *Development* **135**, 3103–3111 (2008).
134. Yan, J. *et al.* The multiple-wing-hairs Gene Encodes a Novel GBD-FH3 Domain-Containing Protein That Functions Both Prior to and After Wing Hair Initiation. *Genetics* **180**, 219–228 (2008).
135. Lu, Q., Schafer, D. A. & Adler, P. N. The Drosophila planar polarity gene multiple wing hairs directly regulates the actin cytoskeleton. *Development* **142**, 2478–2486 (2015).
136. Gho, M. Frizzled signalling controls orientation of asymmetric sense organ precursor cell divisions in Drosophila. **393**, 4 (1998).
137. Gomes, J.-E., Corado, M. & Schweisguth, F. Van Gogh and Frizzled Act Redundantly in the Drosophila Sensory Organ Precursor Cell to Orient Its Asymmetric Division. *PLoS ONE* **4**, e4485 (2009).
138. Besson, C. *et al.* Planar Cell Polarity Breaks the Symmetry of PAR Protein Distribution prior to Mitosis in Drosophila Sensory Organ Precursor Cells. *Current Biology* **25**, 1104–1110 (2015).
139. Schweisguth, F. Asymmetric cell division in the *Drosophila* bristle lineage: from the polarization of sensory organ precursor cells to Notch-mediated binary fate decision: Asymmetric cell division in an epithelium. *Wiley Interdisciplinary Reviews: Developmental Biology* **4**, 299–309 (2015).
140. Ségalen, M. *et al.* The Fz-Dsh Planar Cell Polarity Pathway Induces Oriented Cell Division via Mud/NuMA in Drosophila and Zebrafish. *Developmental Cell* **19**, 740–752 (2010).
141. Bellaiche, Y. The planar cell polarity protein Strabismus promotes Pins anterior localization during asymmetric division of sensory organ precursor cells in Drosophila. *Development* **131**, 469–478 (2003).
142. Mao, Y. *et al.* Planar polarization of the atypical myosin Dachs orients cell divisions in Drosophila. *Genes Dev.* **25**, 131–136 (2011).
143. Gong, Y., Mo, C. & Fraser, S. E. Planar cell polarity signalling controls cell division orientation during zebrafish gastrulation. *Nature* **430**, 689–693 (2004).
144. Li, Y., Li, A., Junge, J. & Bronner, M. Planar cell polarity signaling coordinates oriented cell division and cell rearrangement in clonally expanding growth plate cartilage. *eLife Sciences* **6**, e23279 (2017).
145. Matsuyama, M., Aizawa, S. & Shimono, A. Sfrp Controls Apicobasal Polarity and Oriented Cell Division in Developing Gut Epithelium. *PLoS Genetics* **5**, e1000427 (2009).
146. Wallingford, J. B. *et al.* Dishevelled controls cell polarity during Xenopus gastrulation. *Nature* **405**, 81–85 (2000).
147. Yin, C., Kiskowski, M., Pouille, P.-A., Farge, E. & Solnica-Krezel, L. Cooperation of polarized cell intercalations drives convergence and extension of presomitic mesoderm during zebrafish gastrulation. *The Journal of Cell Biology* **180**, 221–232 (2008).
148. Ossipova, O., Kim, K. & Sokol, S. Y. Planar polarization of Vangl2 in the vertebrate neural plate is controlled by Wnt and Myosin II signaling. *Biology Open* **4**, 722–730 (2015).
149. Jessen, J. R. *et al.* Zebrafish trilobite identifies new roles for Strabismus in gastrulation and neuronal movements. *Nature Cell Biology* (2002). doi:10.1038/ncb828
150. Nishimura, T., Honda, H. & Takeichi, M. Planar Cell Polarity Links Axes of Spatial Dynamics in Neural-Tube Closure. *Cell* **149**, 1084–1097 (2012).
151. Shindo, A. & Wallingford, J. B. PCP and Septins Compartmentalize Cortical Actomyosin to Direct Collective Cell Movement. *Science* **343**, 649–652 (2014).
152. Ossipova, O., Chuykin, I., Chu, C.-W. & Sokol, S. Y. Vangl2 cooperates with Rab11 and Myosin V to regulate apical constriction during vertebrate gastrulation. *Development* **142**, 99–107 (2015).
153. Shindo, A., Inoue, Y., Kinoshita, M. & Wallingford, J. B. PCP-dependent transcellular regulation of actomyosin oscillation facilitates convergent extension of vertebrate tissue. *Developmental Biology* **446**, 159–167 (2019).
154. Ossipova, O. *et al.* The involvement of PCP proteins in radial cell intercalations during Xenopus embryonic development. *Developmental Biology* **408**, 316–327 (2015).
155. Lienkamp, S. S. *et al.* Vertebrate kidney tubules elongate using a planar cell polarity–dependent, rosette-based mechanism of convergent extension. *Nature Genetics* **44**, 1382–1387 (2012).
156. Lyuksyutova, A. I. Anterior-Posterior Guidance of Commissural Axons by Wnt-Frizzled Signaling. *Science* **302**, 1984–1988 (2003).
157. Shafer, B., Onishi, K., Lo, C., Colakoglu, G. & Zou, Y. Vangl2 Promotes Wnt/Planar Cell Polarity-like Signaling by Antagonizing Dvl1-Mediated Feedback Inhibition in Growth Cone Guidance. *Developmental Cell* **20**, 177–191 (2011).
158. Onishi, K. *et al.* Antagonistic Functions of Dishevelleds Regulate Frizzled3 Endocytosis via Filopodia Tips in Wnt-Mediated Growth Cone Guidance. *Journal of Neuroscience* **33**, 19071–19085 (2013).
159. Wanner, S. J., Saeger, I., Guthrie, S. & Prince, V. E. Facial motor neuron migration advances. *Current Opinion in Neurobiology* **23**, 943–950 (2013).
160. Bingham, S., Higashijima, S., Okamoto, H. & Chandrasekhar, A. The Zebrafish trilobite Gene Is Essential for Tangential Migration of Branchiomotor Neurons. *Developmental Biology* **242**, 149–160 (2002).
161. Mapp, O. M., Wanner, S. J., Rohrschneider, M. R. & Prince, V. E. Prickle1b mediates interpretation of migratory cues during zebrafish facial branchiomotor neuron migration. *Developmental Dynamics* **239**, 1596–1608
162. Wada, H., Tanaka, H., Nakayama, S., Iwasaki, M. & Okamoto, H. Frizzled3a and Celsr2 function in the neuroepithelium to regulate migration of facial motor neurons in the developing zebrafish hindbrain. *Development* **133**, 4749–4759 (2006).

163. Davey, C. F., Mathewson, A. W. & Moens, C. B. PCP Signaling between Migrating Neurons and their Planar-Polarized Neuroepithelial Environment Controls Filopodial Dynamics and Directional Migration. *PLOS Genetics* **12**, e1005934 (2016).
164. Carvajal-Gonzalez, J. M., Mulero-Navarro, S. & Mlodzik, M. Centriole positioning in epithelial cells and its intimate relationship with planar cell polarity. *BioEssays* **38**, 1234–1245 (2016).
165. Djiane, A., Yogev, S. & Mlodzik, M. The Apical Determinants aPKC and dPatj Regulate Frizzled-Dependent Planar Cell Polarity in the Drosophila Eye. *Cell* **121**, 621–631 (2005).
166. Wasserscheid, I., Thomas, U. & Knust, E. Isoform-specific interaction of Flamingo/Starry Night with excess Bazooka affects planar cell polarity in the Drosophila wing. *Dev. Dyn.* **236**, 1064–1071 (2007).
167. Kharfallah, F. *et al.* Scribble1 plays an important role in the pathogenesis of neural tube defects through its mediating effect of Par-3 and Vangl1/2 localization. *Human Molecular Genetics* (2017). doi:10.1093/hmg/ddx122
168. Banerjee, J. J. *et al.* Meru couples planar cell polarity with apical-basal polarity during asymmetric cell division. *eLife Sciences* **6**, e25014 (2017).
169. Aigouy, B. & Le Bivic, A. The PCP pathway regulates Baz planar distribution in epithelial cells. *Scientific Reports* **6**, 33420 (2016).
170. Chuykin, I., Ossipova, O. & Sokol, S. Y. Par3 interacts with Prickle3 to generate apical PCP complexes in the vertebrate neural plate. *eLife* **7**, e37881 (2018).
171. Courbard, J.-R., Djiane, A., Wu, J. & Mlodzik, M. The apical/basal-polarity determinant Scribble cooperates with the PCP core factor Stbm/Vang and functions as one of its effectors. *Developmental Biology* **333**, 67–77 (2009).
172. Murdoch, J. N. Disruption of scribble (Scrb1) causes severe neural tube defects in the circletail mouse. *Human Molecular Genetics* **12**, 87–98 (2003).
173. Montcouquiol, M. *et al.* Identification of Vangl2 and Scrb1 as planar polarity genes in mammals. **423**, 5 (2003).
174. Tao, H. *et al.* Mouse prickle1, the homolog of a PCP gene, is essential for epiblast apical-basal polarity. *Proceedings of the National Academy of Sciences* **106**, 14426–14431 (2009).
175. Carvalho-Santos, Z., Azimzadeh, J., Pereira-Leal, José. B. & Bettencourt-Dias, M. Tracing the origins of centrioles, cilia, and flagella. *The Journal of Cell Biology* **194**, 165–175 (2011).
176. Ross, L. & Normark, B. B. Evolutionary problems in centrosome and centriole biology. *Journal of Evolutionary Biology* **28**, 995–1004 (2015).
177. Conduit, P. T., Wainman, A. & Raff, J. W. Centrosome function and assembly in animal cells. *Nature Reviews Molecular Cell Biology* **16**, 611–624 (2015).
178. Sonnen, K. F., Gabryjonczyk, A.-M., Anselm, E., Stierhof, Y.-D. & Nigg, E. A. Human Cep192 and Cep152 cooperate in Plk4 recruitment and centriole duplication. *Journal of Cell Science* **126**, 3223–3233 (2013).
179. Kitagawa, D. *et al.* Structural Basis of the 9-Fold Symmetry of Centrioles. *Cell* **144**, 364–375 (2011).
180. Tang, C.-J. C., Fu, R.-H., Wu, K.-S., Hsu, W.-B. & Tang, T. K. CPAP is a cell-cycle regulated protein that controls centriole length. *Nature Cell Biology* **11**, 825–831 (2009).
181. Bettencourt-Dias, M. Q&A: Who needs a centrosome? 7 (2013).
182. Lee, K. & Rhee, K. PLK1 phosphorylation of pericentrin initiates centrosome maturation at the onset of mitosis. *The Journal of Cell Biology* **195**, 1093–1101 (2011).
183. Sdelci, S. *et al.* Nek9 Phosphorylation of NEDD1/GCP-WD Contributes to Plk1 Control of γ-Tubulin Recruitment to the Mitotic Centrosome. *Current Biology* **22**, 1516–1523 (2012).
184. Gruss, O. J. & Vernos, I. The mechanism of spindle assembly: functions of Ran and its target TPX2. *The Journal of Cell Biology* **166**, 949–955 (2004).
185. Goshima, G., Mayer, M., Zhang, N., Stuurman, N. & Vale, R. D. Augmin: a protein complex required for centrosome-independent microtubule generation within the spindle. *The Journal of Cell Biology* **181**, 421–429 (2008).
186. Schuh, M. & Ellenberg, J. Self-Organization of MTOCs Replaces Centrosome Function during Acentrosomal Spindle Assembly in Live Mouse Oocytes. *Cell* **130**, 484–498 (2007).
187. Varmark, H. *et al.* Asterless Is a Centriolar Protein Required for Centrosome Function and Embryo Development in Drosophila. *Current Biology* **17**, 1735–1745 (2007).
188. Basto, R. *et al.* Flies without Centrioles. *Cell* **125**, 1375–1386 (2006).
189. Poulton, J. S., Cuningham, J. C. & Peifer, M. Acentrosomal Drosophila Epithelial Cells Exhibit Abnormal Cell Division, Leading to Cell Death and Compensatory Proliferation. *Developmental Cell* **30**, 731–745 (2014).
190. Inaba, M., Venkei, Z. G. & Yamashita, Y. M. The polarity protein Baz forms a platform for the centrosome orientation during asymmetric stem cell division in the Drosophila male germline. *Elife* **4**, e04960 (2015).
191. Azimzadeh, J., Wong, M. L., Downhour, D. M., Alvarado, A. S. & Marshall, W. F. Centrosome Loss in the Evolution of Planarians. *Science* **335**, 461–463 (2012).
192. Bazzi, H. & Anderson, K. V. Acentriolar mitosis activates a p53-dependent apoptosis pathway in the mouse embryo. *Proceedings of the National Academy of Sciences* **111**, E1491–E1500 (2014).
193. Insolera, R., Bazzi, H., Shao, W., Anderson, K. V. & Shi, S.-H. Cortical neurogenesis in the absence of centrioles. *Nature Neuroscience* **17**, 1528–1535 (2014).
194. Quintyne, N. Spindle Multipolarity Is Prevented by Centrosomal Clustering. *Science* **307**, 124–127 (2005).
195. Basto, R. *et al.* Centrosome Amplification Can Initiate Tumorigenesis in Flies. *Cell* **133**, 1032–1042 (2008).
196. Levine, M. S. *et al.* Centrosome Amplification Is Sufficient to Promote Spontaneous Tumorigenesis in Mammals. *Developmental Cell* **40**, 313-322.e5 (2017).
197. Ganem, N. J., Godinho, S. A. & Pellman, D. A mechanism linking extra centrosomes to chromosomal instability. *Nature* **460**, 278–282 (2009).
198. Thornton, G. K. & Woods, C. G. Primary microcephaly: do all roads lead to Rome? *Trends in Genetics* **25**, 501–510 (2009).
199. Lancaster, M. A. *et al.* Cerebral organoids model human brain development and microcephaly. *Nature* **501**, 373–379 (2013).
200. Buchman, J. J. *et al.* Cdk5rap2 Interacts with Pericentrin to Maintain the Neural Progenitor Pool in the Developing Neocortex. *Neuron* **66**, 386–402 (2010).
201. Yang, J. *et al.* Rootletin, a novel coiled-coil protein, is a structural component of the ciliary rootlet. *The Journal of Cell Biology* **159**, 431–440 (2002).
202. Mohan, S., Timbers, T. A., Kennedy, J., Blacque, O. E. & Leroux, M. R. Striated Rootlet and Nonfilamentous Forms of Rootletin Maintain Ciliary Function. *Current Biology* **23**, 2016–2022 (2013).
203. Styczynska-Soczka, K. & Jarman, A. P. The Drosophila homologue of Rootletin is required for mechanosensory function and ciliary rootlet formation in chordotonal sensory neurons. *Cilia* **4**, (2015).
204. Hagiwara, H., Kano, A., Aoki, T., Ohwada, N. & Takata, K. Localization of γ-tubulin to the basal foot associated with the basal body extending a cilium. 3
205. Kunimoto, K. *et al.* Coordinated Ciliary Beating Requires Odf2-Mediated Polarization of Basal Bodies via Basal Feet. *Cell* **148**, 189–200 (2012).
206. Yoshimura, S., Egerer, J., Fuchs, E., Haas, A. K. & Barr, F. A. Functional dissection of Rab GTPases involved in primary cilium formation. *The Journal of Cell Biology* **178**, 363–369 (2007).

207. Kozminski, K. G., Johnson, K. A., Forscher, P. & Rosenbaum, J. L. A motility in the eukaryotic flagellum unrelated to flagellar beating. *Proceedings of the National Academy of Sciences* **90**, 5519–5523 (1993).
208. Pazour, G. J. *et al. Chlamydomonas IFT* 88 and Its Mouse Homologue, Polycystic Kidney Disease Gene *Tg* 737, Are Required for Assembly of Cilia and Flagella. *The Journal of Cell Biology* **151**, 709–718 (2000).
209. Gonçalves, J. & Pelletier, and L. The Ciliary Transition Zone: Finding the Pieces and Assembling the Gate. *Moleucles and Cells* **40**, 243–253 (2017).
210. Nachury, M. V. & Mick, D. U. Establishing and regulating the composition of cilia for signal transduction. *Nature Reviews Molecular Cell Biology* (2019). doi:10.1038/s41580-019-0116-4
211. Houliston, E., Momose, T. & Manuel, M. Clytia hemisphaerica: a jellyfish cousin joins the laboratory. *Trends in Genetics* **26**, 159–167 (2010).
212. TAMM, S. L. & TAMM, S. Development of macrociliary cells in Beroe. 16
213. Meunier, A. & Azimzadeh, J. Multiciliated Cells in Animals. *Cold Spring Harb Perspect Biol* **8**, a028233 (2016).
214. Mykytyn, K. & Askwith, C. G-Protein-Coupled Receptor Signaling in Cilia. *Cold Spring Harbor Perspectives in Biology* a028183 (2017). doi:10.1101/cshperspect.a028183
215. Reiter, J. F. & Leroux, M. R. Genes and molecular pathways underpinning ciliopathies. *Nature Reviews Molecular Cell Biology* **18**, 533–547 (2017).
216. Goetz, S. C., Ocbina, P. J. R. & Anderson, K. V. The Primary Cilium as a Hedgehog Signal Transduction Machine. in *Methods in Cell Biology* **94**, 199–222 (Elsevier, 2009).
217. Sigg, M. A. *et al.* Evolutionary Proteomics Uncovers Ancient Associations of Cilia with Signaling Pathways. *Developmental Cell* **43**, 744-762.e11 (2017).
218. Jékely, G. & Arendt, D. Evolution of intraflagellar transport from coated vesicles and autogenous origin of the eukaryotic cilium. *BioEssays* **28**, 191–198 (2006).
219. Wickstead, B. & Gull, K. A "Holistic" Kinesin Phylogeny Reveals New Kinesin Families and Predicts Protein Functions. *Molecular Biology of the Cell* **17**, 1734–1743 (2006).
220. Wickstead, B. & Gull, K. Dyneins Across Eukaryotes: A Comparative Genomic Analysis. *Traffic* **8**, 1708–1721
221. Delaval, B., Bright, A., Lawson, N. D. & Doxsey, S. The cilia protein IFT88 is required for spindle orientation in mitosis. *Nature Cell Biology* **13**, 461–468 (2011).
222. Wood, C. R. *et al.* IFT Proteins Accumulate during Cell Division and Localize to the Cleavage Furrow in Chlamydomonas. *PLoS ONE* **7**, e30729 (2012).
223. Nachury, M. V. How do cilia organize signalling cascades? *Philosophical Transactions of the Royal Society B: Biological Sciences* **369**, 20130465–20130465 (2014).
224. Laan, L. *et al.* Cortical Dynein Controls Microtubule Dynamics to Generate Pulling Forces that Position Microtubule Asters. *Cell* **148**, 502–514 (2012).
225. Laan, L., Roth, S. & Dogterom, M. End-on microtubule-dynein interactions and pulling-based positioning of microtubule organizing centers. *Cell Cycle* **11**, 3750–3757 (2012).
226. Grill, S. W., nczy, P. G., Stelzer, E. H. K. & Hyman, A. A. Polarity controls forces governing asymmetric spindle positioning in the Caenorhabditis elegans embryo. **409**, 4 (2001).
227. Su, L., Vogelstein, B. & Kinzler, K. Association of the APC tumor suppressor protein with catenins. *Science* **262**, 1734–1737 (1993).
228. Wen, Y. *et al.* EB1 and APC bind to mDia to stabilize microtubules downstream of Rho and promote cell migration. *Nature Cell Biology* **6**, 820–830 (2004).
229. Inaba, M., Yuan, H., Salzmann, V., Fuller, M. T. & Yamashita, Y. M. E-Cadherin Is Required for Centrosome and Spindle Orientation in Drosophila Male Germline Stem Cells. *PLoS ONE* **5**, e12473 (2010).
230. Schaefer, M., Shevchenko, A., Shevchenko, A. & Knoblich, J. A. A protein complex containing Inscuteable and the Gα-binding protein Pins orients asymmetric cell divisions in Drosophila. *Current Biology* **10**, 353–362 (2000).
231. Schaefer, M., Petronczki, M., Dorner, D., Forte, M. & Knoblich, J. A. Heterotrimeric G Proteins Direct Two Modes of Asymmetric Cell Division in the Drosophila Nervous System. *Cell* **107**, 183–194 (2001).
232. Yu, F., Morin, X., Cai, Y., Yang, X. & Chia, W. Analysis of partner of inscuteable, a Novel Player of Drosophila Asymmetric Divisions, Reveals Two Distinct Steps in Inscuteable Apical Localization. *Cell* **100**, 399–409 (2000).
233. GUDIMA, G. O., VOROBJEV, I. A. & CHENTSOV, Y. S. Centriolar location during blood cell spreading and motion in vitro: an ultrastructural analysis. 18
234. Gomes, E. R., Jani, S. & Gundersen, G. G. Nuclear Movement Regulated by Cdc42, MRCK, Myosin, and Actin Flow Establishes MTOC Polarization in Migrating Cells. *Cell* **121**, 451–463 (2005).
235. Higginbotham, H., Tanaka, T., Brinkman, B. C. & Gleeson, J. G. GSK3β and PKCζ function in centrosome localization and process stabilization during Slit-mediated neuronal repolarization. *Molecular and Cellular Neuroscience* **32**, 118–132 (2006).
236. Dupin, I., Camand, E. & Etienne-Manneville, S. Classical cadherins control nucleus and centrosome position and cell polarity. *The Journal of Cell Biology* **185**, 779–786 (2009).
237. Manneville, J.-B., Jehanno, M. & Etienne-Manneville, S. Dlg1 binds GKAP to control dynein association with microtubules, centrosome positioning, and cell polarity. *The Journal of Cell Biology* **191**, 585–598 (2010).
238. Solecki, D. J., Model, L., Gaetz, J., Kapoor, T. M. & Hatten, M. E. Par6α signaling controls glial-guided neuronal migration. *Nature Neuroscience* **7**, 1195–1203 (2004).
239. Solecki, D. J. *et al.* Myosin II Motors and F-Actin Dynamics Drive the Coordinated Movement of the Centrosome and Soma during CNS Glial-Guided Neuronal Migration. *Neuron* **63**, 63–80 (2009).
240. Luxton, G. W. G., Gomes, E. R., Folker, E. S., Vintinner, E. & Gundersen, G. G. Linear Arrays of Nuclear Envelope Proteins Harness Retrograde Actin Flow for Nuclear Movement. *Science* **329**, 956–959 (2010).
241. de la Roche, M., Asano, Y. & Griffiths, G. M. Origins of the cytolytic synapse. *Nature Reviews Immunology* **16**, 421–432 (2016).
242. Ritter, A. T. *et al.* Actin Depletion Initiates Events Leading to Granule Secretion at the Immunological Synapse. *Immunity* **42**, 864–876 (2015).
243. Koretzky, G. A., Abtahian, F. & Silverman, M. A. SLP76 and SLP65: complex regulation of signalling in lymphocytes and beyond. *Nature Reviews Immunology* **6**, 67–78 (2006).
244. Quann, E. J., Merino, E., Furuta, T. & Huse, M. Localized diacylglycerol drives the polarization of the microtubule-organizing center in T cells. *Nature Immunology* **10**, 627–635 (2009).
245. Quann, E. J., Liu, X., Altan-Bonnet, G. & Huse, M. A cascade of protein kinase C isozymes promotes cytoskeletal polarization in T cells. *Nature Immunology* **12**, 647–654 (2011).
246. Liu, X., Kapoor, T. M., Chen, J. K. & Huse, M. Diacylglycerol promotes centrosome polarization in T cells via reciprocal localization of dynein and myosin II. *Proceedings of the National Academy of Sciences* **110**, 11976–11981 (2013).
247. Bertrand, F. *et al.* Activation of the Ancestral Polarity Regulator Protein Kinase C at the Immunological Synapse Drives Polarization of Th Cell Secretory Machinery toward APCs. *The Journal of Immunology* **185**, 2887–2894 (2010).
248. Lin, J., Hou, K. K., Piwnica-Worms, H. & Shaw, A. S. The Polarity Protein Par1b/EMK/MARK2 Regulates T Cell Receptor-Induced Microtubule-Organizing Center

Polarization. *The Journal of Immunology* **183**, 1215–1221 (2009).
249. Reversat, A. *et al.* Polarity protein Par3 controls B-cell receptor dynamics and antigen extraction at the immune synapse. *Molecular biology of the cell* **26**, 1273–1285 (2015).
250. Yi, J. *et al.* Centrosome repositioning in T cells is biphasic and driven by microtubule end-on capture-shrinkage. *The Journal of Cell Biology* **202**, 779–792 (2013).
251. Boisvieux-Ulrich, E., Lainé, M.-C. & Sandoz, D. Cytochalasin D inhibits basal body migration and ciliary elongation in quail oviduct epithelium. *Cell and Tissue Research* **259**, 443–454 (1990).
252. BOISVIEUX-ULRICH, E., LAINE, M.-C. & SANDOZ, D. In vitro effects of taxol on ciliogenesis in quail oviduct. 12
253. Boisvieux-Ulrich, E., Lainé, M.-C. & Sandoz, D. In vitro effects of colchicine and nocodazole on ciliogenesis in quail oviduct. *Biology of the Cell* **67**, 67–79
254. Hong, H., Kim, J. & Kim, J. Myosin heavy chain 10 (MYH10) is required for centriole migration during the biogenesis of primary cilia. *Biochemical and Biophysical Research Communications* **461**, 180–185 (2015).
255. Pan, J., You, Y., Huang, T. & Brody, S. L. RhoA-mediated apical actin enrichment is required for ciliogenesis and promoted by Foxj1. *Journal of Cell Science* **120**, 1868–1876 (2007).
256. Lemullois, M., Boisvieux-Ulrich, E., Laine, M.-C., Chailley, B. & Sandoz, D. Development and functions of the cytoskeleton during ciliogenesis in metazoa. *Biology of the Cell* **63**, 195–208
257. Cohen, E., Binet, S. & Meininger, V. Ciliogenesis and centriole formation in the mouse embryonic nervous system. An ultrastructural analysis. *Biology of the Cell* **62**, 165–169
258. Sorokin, S. CENTRIOLES AND THE FORMATION OF RUDIMENTARY CILIA BY FIBROBLASTS AND SMOOTH MUSCLE CELLS. *The Journal of Cell Biology* **15**, 363–377 (1962).
259. Zuo, X., Guo, W. & Lipschutz, J. H. The exocyst protein Sec10 is necessary for primary ciliogenesis and cystogenesis in vitro. *Molecular biology of the cell* **20**, 2522–2529 (2009).
260. Schmidt, K. N. *et al.* Cep164 mediates vesicular docking to the mother centriole during early steps of ciliogenesis. *The Journal of Cell Biology* **199**, 1083–1101 (2012).
261. Park, T. J., Mitchell, B. J., Abitua, P. B., Kintner, C. & Wallingford, J. B. Dishevelled controls apical docking and planar polarization of basal bodies in ciliated epithelial cells. *Nature Genetics* **40**, 871–879 (2008).
262. Pitaval, A. *et al.* Microtubule stabilization drives 3D centrosome migration to initiate primary ciliogenesis. *The Journal of Cell Biology* jcb.201610039 (2017). doi:10.1083/jcb.201610039
263. May-Simera, H. L. *et al.* Loss of MACF1 Abolishes Ciliogenesis and Disrupts Apicobasal Polarity Establishment in the Retina. *Cell Reports* **17**, 1399–1413 (2016).
264. Sawamoto, K. *et al.* New neurons follow the flow of cerebrospinal fluid in the adult brain. *Science* **311**, 629–632 (2006).
265. Kramer-Zucker, A. G. Cilia-driven fluid flow in the zebrafish pronephros, brain and Kupffer's vesicle is required for normal organogenesis. *Development* **132**, 1907–1921 (2005).
266. Montcouquiol, M. *et al.* Identification of Vangl2 and Scrb1 as planar polarity genes in mammals. **423**, 5 (2003).
267. Sokol, S. Y. Analysis of Dishevelled signalling pathways during Xenopus development. *Current Biology* **6**, 1456–1467 (1996).
268. Mitchell, B. *et al.* The PCP Pathway Instructs the Planar Orientation of Ciliated Cells in the Xenopus Larval Skin. *Current Biology* **19**, 924–929 (2009).
269. Guirao, B. *et al.* Coupling between hydrodynamic forces and planar cell polarity orients mammalian motile cilia. *Nature Cell Biology* **12**, 341–350 (2010).
270. Boutin, C. *et al.* A dual role for planar cell polarity genes in ciliated cells. *Proceedings of the National Academy of Sciences* **111**, E3129–E3138 (2014).
271. Hirota, Y. *et al.* Planar polarity of multiciliated ependymal cells involves the anterior migration of basal bodies regulated by non-muscle myosin II. *Development* **137**, 3037–3046 (2010).
272. Gao, C. & Chen, Y.-G. Dishevelled: The hub of Wnt signaling. *Cellular Signalling* **22**, 717–727 (2010).
273. Antic, D. *et al.* Planar Cell Polarity Enables Posterior Localization of Nodal Cilia and Left-Right Axis Determination during Mouse and Xenopus Embryogenesis. *PLoS ONE* **5**, e8999 (2010).
274. Borovina, A., Superina, S., Voskas, D. & Ciruna, B. Vangl2 directs the posterior tilting and asymmetric localization of motile primary cilia. *Nature Cell Biology* **12**, 407–412 (2010).
275. Carvajal-Gonzalez, J. M., Roman, A.-C. & Mlodzik, M. Positioning of centrioles is a conserved readout of Frizzled planar cell polarity signalling. *Nature Communications* **7**, 11135 (2016).
276. Momose, T., Kraus, Y. & Houliston, E. A conserved function for Strabismus in establishing planar cell polarity in the ciliated ectoderm during cnidarian larval development. *Development* **139**, 4374–4382 (2012).
277. Sandoz, D. *et al.* Organization and functions of cytoskeleton in metazoan ciliated cells. *Biology of the Cell* **63**, 183–193
278. Werner, M. E. *et al.* Actin and microtubules drive differential aspects of planar cell polarity in multiciliated cells. *The Journal of Cell Biology* **195**, 19–26 (2011).
279. Turk, E. *et al.* Zeta-Tubulin Is a Member of a Conserved Tubulin Module and Is a Component of the Centriolar Basal Foot in Multiciliated Cells. *Current Biology* **25**, 2177–2183 (2015).
280. Kim, S. K. *et al.* CLAMP/Spef1 regulates planar cell polarity signaling and asymmetric microtubule accumulation in the *Xenopus* ciliated epithelia. *The Journal of Cell Biology* jcb.201706058 (2018). doi:10.1083/jcb.201706058
281. Jaffe, K. M. *et al.* c21orf59/kurly Controls Both Cilia Motility and Polarization. *Cell Reports* **14**, 1841–1849 (2016).
282. Hammond, J. W., Cai, D. & Verhey, K. J. Tubulin modifications and their cellular functions. *Current Opinion in Cell Biology* **20**, 71–76 (2008).
283. Ezan, J. *et al.* Primary cilium migration depends on G-protein signalling control of subapical cytoskeleton. *Nature Cell Biology* **15**, 1107–1115 (2013).
284. Tarchini, B., Jolicoeur, C. & Cayouette, M. A Molecular Blueprint at the Apical Surface Establishes Planar Asymmetry in Cochlear Hair Cells. *Developmental Cell* **27**, 88–102 (2013).
285. Hua, K. & Ferland, R. J. Primary cilia proteins: ciliary and extraciliary sites and functions. *Cellular and Molecular Life Sciences* (2018). doi:10.1007/s00018-017-2740-5
286. Ross, A. J. *et al.* Disruption of Bardet-Biedl syndrome ciliary proteins perturbs planar cell polarity in vertebrates. *Nature Genetics* **37**, 1135–1140 (2005).
287. Kim, J. C. *et al.* The Bardet-Biedl protein BBS4 targets cargo to the pericentriolar region and is required for microtubule anchoring and cell cycle progression. *Nature Genetics* **36**, 462–470 (2004).
288. Follit, J. A., Tuft, R. A., Fogarty, K. E. & Pazour, G. J. The Intraflagellar Transport Protein IFT20 Is Associated with the Golgi Complex and Is Required for Cilia Assembly□V. *Molecular Biology of the Cell* **17**, 12 (2006).
289. May-Simera, H. L. *et al.* Ciliary proteins Bbs8 and Ift20 promote planar cell polarity in the cochlea. *Development* **142**, 555–566 (2015).
290. Jones, C. *et al.* Ciliary proteins link basal body polarization to planar cell polarity regulation. *Nature Genetics* **40**, 69–77 (2008).

291. Sipe, C. W. & Lu, X. Kif3a regulates planar polarization of auditory hair cells through both ciliary and non-ciliary mechanisms. *Development* **138**, 3441–3449 (2011).
292. Borovina, A. & Ciruna, B. IFT88 Plays a Cilia- and PCP-Independent Role in Controlling Oriented Cell Divisions during Vertebrate Embryonic Development. *Cell Reports* **5**, 37–43 (2013).
293. Tsujikawa, M. & Malicki, J. Intraflagellar Transport Genes Are Essential for Differentiation and Survival of Vertebrate Sensory Neurons. *Neuron* **42**, 703–716 (2004).
294. Mirzadeh, Z., Han, Y.-G., Soriano-Navarro, M., Garcia-Verdugo, J. M. & Alvarez-Buylla, A. Cilia Organize Ependymal Planar Polarity. *Journal of Neuroscience* **30**, 2600–2610 (2010).
295. Kodani, A., Sirerol-Piquer, M. S., Seol, A., Garcia-Verdugo, J. M. & Reiter, J. F. Kif3a interacts with Dynactin subunit p150 Glued to organize centriole subdistal appendages. *The EMBO journal* **32**, 597–607 (2013).
296. Mahuzier, A. *et al.* Dishevelled stabilization by the ciliopathy protein Rpgrip1l is essential for planar cell polarity. *The Journal of Cell Biology* **198**, 927–940 (2012).
297. Jagger, D. *et al.* Alstrom Syndrome protein ALMS1 localizes to basal bodies of cochlear hair cells and regulates cilium-dependent planar cell polarity. *Human Molecular Genetics* **20**, 466–481 (2011).
298. Cui, C. *et al.* Disruption of Mks1 localization to the mother centriole causes cilia defects and developmental malformations in Meckel-Gruber syndrome. *Disease Models & Mechanisms* **4**, 43–56 (2011).
299. Ohata, S. *et al.* Mechanosensory Genes Pkd1 and Pkd2 Contribute to the Planar Polarization of Brain Ventricular Epithelium. *Journal of Neuroscience* **35**, 11153–11168 (2015).
300. Mitchell, B., Jacobs, R., Li, J., Chien, S. & Kintner, C. A positive feedback mechanism governs the polarity and motion of motile cilia. *Nature* **447**, 97–101 (2007).
301. Prulière, G., Cosson, J., Chevalier, S., Sardet, C. & Chenevert, J. Atypical protein kinase C controls sea urchin ciliogenesis. *Molecular biology of the cell* **22**, 2042–2053 (2011).
302. Krock, B. L. & Perkins, B. D. The Par-PrkC polarity complex is required for cilia growth in zebrafish photoreceptors. *PloS one* **9**, e104661 (2014).
303. Sfakianos, J. *et al.* Par3 functions in the biogenesis of the primary cilium in polarized epithelial cells. *The Journal of Cell Biology* **179**, 1133–1140 (2007).
304. Bazellières, E., Aksenova, V., Barthélémy-Requin, M., Massey-Harroche, D. & Le Bivic, A. Role of the crumbs proteins in ciliogenesis, cell migration and actin organization. *Seminars in Cell & Developmental Biology* (2017). doi:10.1016/j.semcdb.2017.10.018
305. Adler, P. N. & Wallingford, J. B. From Planar Cell Polarity to Ciliogenesis and Back: The Curious Tale of the PPE and CPLANE proteins. *Trends in Cell Biology* (2017). doi:10.1016/j.tcb.2016.12.001
306. May-Simera, H. L. *et al.* Bbs8, together with the planar cell polarity protein Vangl2, is required to establish left–right asymmetry in zebrafish. *Developmental Biology* **345**, 215–225 (2010).
307. Gibbs, B. C. *et al.* Prickle1 mutation causes planar cell polarity and directional cell migration defects associated with cardiac outflow tract anomalies and other structural birth defects. *Biology Open* **5**, 323–335 (2016).
308. Sowers, L. P., Yin, T., Mahajan, V. B. & Bassuk, A. G. Defective Motile Cilia in *Prickle2* -Deficient Mice. *Journal of Neurogenetics* **28**, 146–152 (2014).
309. Xing, Y.-Y. *et al.* Mutational analysis of dishevelled genes in zebrafish reveals distinct functions in embryonic patterning and gastrulation cell movements. *PLOS Genetics* **14**, e1007551 (2018).
310. Mahuzier, A. *et al.* Ependymal cilia beating induces an actin network to protect centrioles against shear stress. *Nature Communications* **9**, (2018).
311. Jouette, J., Guichet, A. & Claret, S. B. Dynein-mediated transport and membrane trafficking control PAR3 polarised distribution. *eLife* **8**, e40212 (2019).
312. McKinley, R. F. A. & Harris, T. J. C. Displacement of basolateral Bazooka/PAR-3 by regulated transport and dispersion during epithelial polarization in *Drosophila*. *Molecular Biology of the Cell* **23**, 4465–4471 (2012).
313. Kono, K. *et al.* Reconstruction of Par polarity in apolar cells reveals a dynamic process of cortical polarization. *bioRxiv* (2019). doi:10.1101/523589
314. Simões, S. de M. *et al.* Rho-Kinase Directs Bazooka/Par-3 Planar Polarity during Drosophila Axis Elongation. *Developmental Cell* **19**, 377–388 (2010).
315. Banerjee, J. J. *et al.* Meru couples planar cell polarity with apical-basal polarity during asymmetric cell division. *eLife* **6**, (2017).
316. Landin Malt, A. *et al.* Par3 is essential for the establishment of planar cell polarity of inner ear hair cells. *Proceedings of the National Academy of Sciences* 201816333 (2019). doi:10.1073/pnas.1816333116
317. Siletti, K., Tarchini, B. & Hudspeth, A. J. Daple coordinates organ-wide and cell-intrinsic polarity to pattern inner-ear hair bundles. *Proceedings of the National Academy of Sciences* 201716522 (2017). doi:10.1073/pnas.1716522115
318. Harris, T. J. Protein clustering for cell polarity: Par-3 as a paradigm. *F1000Research* **6**, (2017).
319. Cho, B., Pierre-Louis, G., Sagner, A., Eaton, S. & Axelrod, J. D. Clustering and Negative Feedback by Endocytosis in Planar Cell Polarity Signaling Is Modulated by Ubiquitinylation of Prickle. *PLOS Genetics* **11**, e1005259 (2015).
320. Harris, T. J. C. & Peifer, M. aPKC Controls Microtubule Organization to Balance Adherens Junction Symmetry and Planar Polarity during Development. *Developmental Cell* **12**, 727–738 (2007).
321. Itoh, M. *et al.* Junctional adhesion molecule (JAM) binds to PAR-3: a possible mechanism for the recruitment of PAR-3 to tight junctions. *The Journal of Cell Biology* **154**, 491–498 (2001).
322. Chen, X. & Macara, I. G. Par-3 controls tight junction assembly through the Rac exchange factor Tiam1. *Nature Cell Biology* **7**, 262–269 (2005).
323. Ooshio, T. *et al.* Cooperative roles of Par-3 and afadin in the formation of adherens and tight junctions. *Journal of Cell Science* **120**, 2352–2365 (2007).
324. Ikeda, W. *et al.* Afadin: A Key Molecule Essential for Structural Organization of Cell–Cell Junctions of Polarized Epithelia during Embryogenesis. *J Cell Biol* **146**, 1117–1132 (1999).
325. McGill, M. A., McKinley, R. F. A. & Harris, T. J. C. Independent cadherin–catenin and Bazooka clusters interact to assemble adherens junctions. *The Journal of Cell Biology* **185**, 787–796 (2009).
326. Harris, T. J. C. Adherens Junction Assembly and Function in the Drosophila Embryo. in *International Review of Cell and Molecular Biology* **293**, 45–83 (Elsevier, 2012).
327. Harris, T. J. C. & Peifer, M. Adherens junction-dependent and -independent steps in the establishment of epithelial cell polarity in *Drosophila*. *The Journal of Cell Biology* **167**, 135–147 (2004).
328. Harris, T. J. C. & Peifer, M. The positioning and segregation of apical cues during epithelial polarity establishment in Drosophila. *J Cell Biol* **170**, 813–823 (2005).
329. Redemann, S. *et al.* Membrane Invaginations Reveal Cortical Sites that Pull on Mitotic Spindles in One-Cell C. elegans Embryos. *PLoS ONE* **5**, e12301 (2010).
330. Couwenbergs, C. *et al.* Heterotrimeric G protein signaling functions with dynein to promote spindle positioning in *C. elegans*. *J Cell Biol* **179**, 15–22 (2007).

331. Kozlowski, C., Srayko, M. & Nedelec, F. Cortical Microtubule Contacts Position the Spindle in C. elegans Embryos. *Cell* **129**, 499–510 (2007).
332. Negishi, T., Miyazaki, N., Murata, K., Yasuo, H. & Ueno, N. Physical association between a novel plasma-membrane structure and centrosome orients cell division. *eLife* **5**, e16550 (2016).
333. Simunovic, M., Voth, G. A., Callan-Jones, A. & Bassereau, P. When Physics Takes Over: BAR Proteins and Membrane Curvature. *Trends in Cell Biology* **25**, 780–792 (2015).
334. Dorland, Y. L. *et al.* The F-BAR protein pacsin2 inhibits asymmetric VE-cadherin internalization from tensile adherens junctions. *Nature Communications* **7**, 12210 (2016).
335. Yamashita, Y. M., Inaba, M. & Buszczak, M. Specialized Intercellular Communications via Cytonemes and Nanotubes. 26 (2018).
336. Inaba, M., Buszczak, M. & Yamashita, Y. M. Nanotubes mediate niche–stem-cell signalling in the Drosophila testis. *Nature* **523**, 329–332 (2015).
337. Antoniades, I., Stylianou, P. & Skourides, P. A. Making the Connection: Ciliary Adhesion Complexes Anchor Basal Bodies to the Actin Cytoskeleton. *Developmental Cell* **28**, 70–80 (2014).
338. Efimov, A. *et al.* Paxillin-dependent stimulation of microtubule catastrophes at focal adhesion sites. *Journal of Cell Science* 10
339. Hagiwara, H., Aoki, T., Ohwada, N. & Fujimoto, T. Identification of a 195 Kda protein in the striated rootlet: Its expression in ciliated and ciliogenic cells. *Cell Motility and the Cytoskeleton* **45**, 200–210 (2000).
340. Clare, D. K. *et al.* Basal foot MTOC organizes pillar MTs required for coordination of beating cilia. *Nature Communications* **5**, (2014).
341. Sallé, J. *et al.* Asymmetric division through a reduction of microtubule centering forces. *The Journal of Cell Biology* jcb.201807102 (2018). doi:10.1083/jcb.201807102
342. Morin, X. & Bellaïche, Y. Mitotic Spindle Orientation in Asymmetric and Symmetric Cell Divisions during Animal Development. *Developmental Cell* **21**, 102–119 (2011).
343. Schober, M., Schaefer, M. & Knoblich, J. A. Bazooka recruits Inscuteable to orient asymmetric cell divisions in Drosophila neuroblasts. *Nature* **402**, 548–551 (1999).
344. Akhmanova, A., Stehbens, S. J. & Yap, A. S. Touch, Grasp, Deliver and Control: Functional Cross-Talk Between Microtubules and Cell Adhesions. *Traffic* **10**, 268–274 (2009).
345. Chausovsky, A., Bershadsky, A. D. & Borisy, G. G. Cadherin-mediated regulation of microtubule dynamics. *Nature Cell Biology* **2**, 797–804 (2000).
346. Fukata, M. *et al.* Rac1 and Cdc42 capture microtubules through IQGAP1 and CLIP-170. *Cell* **109**, 873–885 (2002).
347. Mimori-Kiyosue, Y. *et al.* CLASP1 and CLASP2 bind to EB1 and regulate microtubule plus-end dynamics at the cell cortex. *The Journal of Cell Biology* **168**, 141–153 (2005).
348. Boutin, C. *et al.* A dual role for planar cell polarity genes in ciliated cells SD. *Proceedings of the National Academy of Sciences* **111**, E3129–E3138 (2014).
349. Costache, V. *et al.* Kif2 localizes to a subdomain of cortical endoplasmic reticulum that drives asymmetric spindle position. *Nature Communications* **8**, (2017).
350. Miyamoto, T. *et al.* The Microtubule-Depolymerizing Activity of a Mitotic Kinesin Protein KIF2A Drives Primary Cilia Disassembly Coupled with Cell Proliferation. *Cell Reports* **10**, 664–673 (2015).
351. Wittmann, T., Bokoch, G. M. & Waterman-Storer, C. M. Regulation of leading edge microtubule and actin dynamics downstream of Rac1. *The Journal of Cell Biology* **161**, 845–851 (2003).
352. Dawe, H. R., Farr, H. & Gull, K. Centriole/basal body morphogenesis and migration during ciliogenesis in animal cells. *Journal of Cell Science* **120**, 7–15 (2006).
353. Shutova, M. S. *et al.* Self-sorting of nonmuscle myosins IIA and IIB polarizes the cytoskeleton and modulates cell motility. *The Journal of Cell Biology* jcb.201705167 (2017). doi:10.1083/jcb.201705167
354. Wang, F. *et al.* Kinetic Mechanism of Non-muscle Myosin IIB: FUNCTIONAL ADAPTATIONS FOR TENSION GENERATION AND MAINTENANCE. *Journal of Biological Chemistry* **278**, 27439–27448 (2003).
355. Vicente-Manzanares, M., Ma, X., Adelstein, R. S. & Horwitz, A. R. Non-muscle myosin II takes centre stage in cell adhesion and migration. *Nature Reviews Molecular Cell Biology* **10**, 778–790 (2009).
356. Vicente-Manzanares, M., Zareno, J., Whitmore, L., Choi, C. K. & Horwitz, A. F. Regulation of protrusion, adhesion dynamics, and polarity by myosins IIA and IIB in migrating cells. *The Journal of Cell Biology* **176**, 573–580 (2007).
357. Smutny, M. *et al.* Myosin II isoforms identify distinct functional modules that support integrity of the epithelial zonula adherens. *Nature Cell Biology* **12**, 696–702 (2010).
358. Kim, J. *et al.* Functional genomic screen for modulators of ciliogenesis and cilium length. *Nature* **464**, 1048–1051 (2010).
359. Obino, D. *et al.* Actin nucleation at the centrosome controls lymphocyte polarity. *Nature Communications* **7**, 10969 (2016).
360. Garrido-Jimenez, S., Roman, A.-C., Alvarez-Barrientos, A. & Maria Carvajal-Gonzalez, J. Centriole planar polarity assessment in *Drosophila* wings. *Development* **145**, dev169326 (2018).
361. Farina, F. *et al.* The centrosome is an actin-organizing centre. *Nature Cell Biology* **18**, 65–75 (2015).
362. Inoue, D. *et al.* Actin filaments regulate microtubule growth at the centrosome. *The EMBO Journal* **0**, e99630
363. Wei, X. *et al.* The zebrafish Pard3 ortholog is required for separation of the eye fields and retinal lamination. *Developmental Biology* **269**, 286–301 (2004).
364. Strzyz, P. J. *et al.* Interkinetic Nuclear Migration Is Centrosome Independent and Ensures Apical Cell Division to Maintain Tissue Integrity. *Developmental Cell* **32**, 203–219 (2015).
365. Distel, M., Hocking, J. C., Volkmann, K. & Köster, R. W. The centrosome neither persistently leads migration nor determines the site of axonogenesis in migrating neurons in vivo. *The Journal of Cell Biology* **191**, 875–890 (2010).

Summary

To produce a directional flow, ciliated epithelia display a uniform orientation of ciliary beating. Oriented beating requires planar cell polarity (PCP), which leads to planar orientation and asymmetric positioning of the ciliary basal body (BB) along the polarity axis. While the involvement of the PCP pathway in this process is well known, its dynamics and downstream mechanisms remain poorly understood. A major difficulty is to follow the dynamics of BB polarization in vivo or to reproduce it in vitro. Here we took advantage of the polarized mono-ciliated epithelium of the embryonic zebrafish floor plate (FP) to investigate the dynamics and mechanisms of BB polarization. By live-imaging of the FP during the polarization process, we showed that BBs, although bearing a cilium, were highly motile along the antero-posterior axis in both directions. They contacted the anterior and posterior membranes exclusively at the level of apical junctions positive for Par3. At late stages of FP polarization, BBs spent longer periods in contact with the posterior membrane. Par3 was enriched at the posterior membrane of FP cells before BB posterior positioning and FP polarization was disrupted upon Par3 overexpression. In the PCP mutant *Vangl2*, BBs showed faster, poorly oriented movements and this correlated with a reduction of Par3 posterior enrichment. Our data uncover an unexpected motile behavior of ciliated BBs and lead us to propose a conserved function for Par3 in mediating junction-driven attraction forces controlling centriole asymmetric positioning downstream of the PCP pathway.

We also investigate the potential role of cytoskeletal elements downstream of Par3.

We found a polarized pool of Non-Muscle-Myosin IIB (NMIIB) that is partially phoshorylated, next to FP cells BBs. However inhibiting myosin activity has no effect on FP polarization.

We also found that the microtubule network is polarized in FP cells, with a posterior enrichment present from early stages on, and could therefore contribute to BB posterior positioning

We also describe for the first time FP cells rotational polarity and show that it is defective in the Vangl2 and Dvl2 PCP mutants.

Finally we find a conserved localization and PCP function for the tranzition-zone protein Rpgrip1l in the jellyfish Clytia hemisphaerica, which suggests that the role of this ciliary protein in PCP is conserved across Metazoan.